UNIVERSITY OF LIVERPOOL

Modulation of Breast Cancer Stem Cell Plasticity and Tumourigenesis: Evidence for Regulatory Roles of Heparan Sulphates

Thesis submitted in accordance with the requirements of the University of Liverpool for the degree of

Doctor in Philosophy

By

Roua Sami Baty

December 2016

Declaration

This thesis is the result of my own work unless otherwise stated, and is based upon results from experimental and theoretical work performed as a PhD student between March 2012 and December 2016 within the Institute of Integrative Biology at the University of Liverpool.

Neither this thesis nor any part of it has been submitted in support of an application for another degree or qualification at this or any other University or Institute of Learning.

Roua Sami Baty
December 2016-12-04

Dedicated to my mum, dad, my lovely husband and little daughters

Acknowledgment

The writing of this dissertation has been one of the most significant academic challenges I have ever had to face. Without the support, patience, and guidance of the following people, this study would not have been completed.

First and foremost, my deep appreciation and thanks goes out to my supervisor Prof. Jerry Turnbull for his continuous support, encouragement, the insightful comments, immense knowledge and patient guidance throughout the PhD project. His guidance helped me in all the time of research and writing of this thesis. I have been extremely lucky to have a supervisor like him who cared so much about my work.

Special thanks to Dr. Dada Pisconti for her time, help, support during the first two years of my project and her endless time and patience in explaining flow cytometry.

I would like to thank Dr. Edwin Yates and Dr. Yasser Ahmed for their supply of the chemically modified heparins and Dr. Scott Guimond for helping me with all my computer problems and Dr. Anastasios Chanalaris for helping me with Taqman PCR analysis. Special mention goes to Miss Hannah Clarke who has been amazing help all this time.

I would like to express my gratitude to all members of Lab B in the Institute of Integrative Biology, particularly the molecular glycobiology group, past and present for their technical know-how, specially, to Dr. Scott Guimond, Dr. Yassir Ahmed, Hannah Clarke, Rachel Ghadiali, Adel AL-Assaf, Emma, Sery and Sarah Taylor for useful, insightful discussions and assistance encouragement throughout the project. I would like also to acknowledge Dr. Helen Wright for her help with apoptosis analysis by flow cytometry and Dr. Thamir Ismail and Dr. Christopher Clarke for their help with CSC characterization experiments. Special thanks to Fatima Makki and Batool Al-marzouq; who have helped with the project, provided me with their assistance throughout my dissertation and supported me in many ways. My research would not have been possible without their helps.

I would like also to thank my friend Dalia, Walaa, Khadejah, Ashwaq, Eman for listening, offering me advice, supporting me through this entire process and for all the emotional support.

Special thanks goes to my best friends Nada and Doha, for helping me get through the difficult times, comraderie, entertainment, unlimited support specially for taking care of my daughters when I need them and caring they provided.

My warmest thanks must be to my family. Words cannot express how grateful I am to my Mum and Dad for all of the sacrifices that you have made on my behalf. Your prayer for me was what sustained me thus far. Also I express my thanks to my brother Hattan and sisters Reham, Haneen and Raghad for supporting me spiritually throughout my work, showing faith in me, caring my kids, and my grandmother for her prayer for me. My grandmother and grandfather unfortunately cannot read this thesis or witness my graduation, but I hope I have made them proud.

I owe thanks to a very special person, my beloved husband, Sami for his continued and unfailing love, unconditional support, contribution and understanding during my pursuit of PhD project that made the completion of thesis possible. You were always around at times I thought that it is impossible to continue. I greatly value his belief in me. I owe thanks to my two little angels Revan and Ailan for abiding my ignorance, the patience they showed during my thesis writing, for being such a good girls always cheering me up and giving me much happiness and keep me hopping. Words would never say how grateful I am to all of you.

.

Abstract

Sub-populations of cancer cells have been identified in tumours, leading to the cancer stem cell (CSC) hypothesis, wherein these sub-populations of cells are crucial in tumour recurrence and chemoresistance. This has given rise to interest in the potential to target these cells for effective new anti-cancer therapies. However, little is yet known about the role of extracellular matrix (ECM) components such as heparan sulphate proteoglycans (HSPGs) in the modulation of CSCs. We hypothesised that targeted modulation of HS in CSCs may lead to altered cell phenotype and reduced metastatic potential. To study HS involvement in CSC homeostasis, an *in vitro* model of CSCs was established, using flow cytometry to detect and isolate a well described breast cancer stem cell (BCSC) subpopulation with the marker phenotype $CD44^{+}/CD24^{-}$ in two breast cancer cell (BCC) lines (MDA-MB-231 and Hs578-T). Characterization of these CSCs demonstrated that they possessed typical properties including higher proliferation, invasion, migration, adhesion, and lower apoptosis and drug sensitivity, compared to non-CSCs from the same lines. They also expressed elevated levels of pro-angiogenic factors and stem cell markers. HS, heparin and modified heparins were then added exogenously to these cells in functional assays. This resulted in significant reductions in the proportion of $CD44^{+}/CD24^{-}$ cells, in a dose responsive and structure-dependent manner. Some of these compounds also reduced the cell proliferation, invasion, migration, adhesion, and chemoresistance of these CSCs, and increased apoptosis, indicating a phenotypc switch towards non-metastatic behaviour. Initial investigation of the mechanisms involved showed altered stem cell and angiogenesis markers including Ang-1, Ang-2, CXCR4 and IL-8. Furthermore, the decrease in the rates of invasion, migration and adhesion strongly correlated with differential inhibition of FGF2/ERK1/2 and IL-6/STAT3 signaling, and other pathways involving AMPKα and mTOR were also implicated in a signaling pathway screen.

The key conclusions from these studies are that $CD44^{+}/CD24^{-}$ cells with CSC properties may be manipulated by targeting their cell surface proteoglycans using HS and heparins with divergent structures. This suggest that HSPGs play an important role in regulating the homeostasis of BCSCs, and further that this class of compounds represent promising novel agents for targetted therapeutic interventions designed to modulate the CSC component in breast cancers.

Table of Contents

List of Figures

List of Tables

Abbreviations

mAB	Monoclonal antibody
ABC	ATP-binding cassette
ABCG2	ATP-binding cassette sub-family G member 2
ALDH	Aldehyde dehydrogenases
AML	Acute myeloid leukemia
Ang-1	Angiopoietin 1
Ang-2	Angiopoietin 2
APC	Allophycocyanin
APS	Ammonium per-sulphate
ATIII	Antithrombin III
ATP	Adenosine triphosphate
BC	Breast cancer
BCA	bicinchoninic acid
BCCs	Breast cancer cells
BCSCs	Breast cancer stem cells
BSA	Bovine Serum Albumin
Cis	Cisplatin
COHH	Control of substances hazardous of assessment
CS	Chondroitin sulphate
CSCs	Cancer stem cells
CXCL12	C-X-C motif chemokine 12
CXCR4	Chemokine receptor type 4
kDa	Kilo dalton
DAPI	4',6-Diamidino-2-Phenylindole, Dihydrochloride
DMEM	Dulbecco's Modified Eagle's medium
DMSO	Dimethyl sulfoxide
DNA	Deoxyribonucleic acid
cDNA	Complementary DNA
DNase	deoxyribonuclease
Dox	Doxorubicin
DS	Dermatan sulphate
DTT	Dithiothreitol
ECM	Extra cellular matrix
EpCAM	Epithelial cell adhesion molecule
ECL	Enhanced chemiluminescence
EDTA	Ethylenediaminetetraacetic acid
EGF	Epidermal growth factor
EMT	Epithelial-mesenchymal transition
ER	Estrogen
ERK1/2	Extracellular Signal-Regulated Kinases 1 and 2
EXTs	Exostoses

EXTL1-3	Exostosin-like-1-3
FACS	Fluorescence-activated cell sorting
FBS	Fetal bovine serum
FGF	Fibroblast growth factor
FGF-2	Fibroblast growth factor 2
FITC	Fluorescein isothiocyanate
GAGs	Glycosaminoglycans
GAPDH	Glyceraldehyde-3-phosphate dehydrogenase
GF	Growth factor
GlcA	Glucuronic acid
GLCE	C5-GlcA epimerase enzyme
GlcN	glucosamine
GlcNA	N-acetylated glucosamine
GlcNS	N-sulfated glucosamine
GPCs	Glypicans
GPC 1-6	Glypicans 1-6
GPI	Glycosyl phosphatidylinositol
GTs	Glycosyltransferases
HA	Hyaluronic acid
HBD	Heparin-binding domains
HBSS	Hank's Balanced Salt Solution
HER2	Human epidermal growth factor receptor 2
HGF	Hepatocyte growth factor
dH_2O	Distilled water
HPSE	Heparanase
HRP	Horse radish peroxidase
HS	Heparan sulphate
HSPGs	Heparan sulphate protoglycans
HS2ST1	HS 2-O- sulphotransferase
HS3ST1-6	3-O-sulphotransferase isoforms 1–6
HS6ST1-3	HS 6-O-sulphotransferase isoforms 1–3
IdoA	Iduronic acid
IgG1	Immunoglobulin G subclasse1
IL-8	Interleukin-8
IL-6	Interleukin-6
IL-12	Interleukin-12
JAK2	Janus kinase 2
KS	Keratan sulphate
MAPK	Mitogen-Activated Protein Kinase
MEM	Minimum Essential Medium Eagle
MTT	3-(4,5-Dimethyl-2-thiazolyl)-2,5- diphenyl-2H-tetrazolium bromide
NDST	N-deacetylase/N-sulfotransferase

NEAA	Non ssential Amino Acids
dNTP	Deoxynucleotide triphosphate
2OST	2-*O*- sulfotransferase
3OST	3-*O*- sulfotransferase
6OST	6-*O*- sulfotransferase
PAGE	Polyacrylamide gel electrophoresis
PAPS	3'-phosphoadenosine-5'-phosphosulfate
PAR-1	Protease-activated receptor
PBS	Phosphate buffered saline
PCR	Polymerase chain reaction
PDGF	Platelet-derived growth factor
PE	Phycoerythrobilin
Pen	Penicillin
PET	Polyethylene terephthalate
PGs	Proteoglycans
PH	potential of hydrogen
PI	Propidium iodide
PIGF	Placenta growth factor
PMH	Porcine mucosal heparin
PMHS	porcine mucosal heparin sulphate
PR	Progestrone
RFU	Relative fluorescence units
RIPA	Radioimmunoprecipitation
RNA	Ribonucleic acid
RNase	Ribonuclease
siRNA	Small interfering RNA
RPM	Revolutions per minute
RPMI	Roswell Park Memorial Institute Medium
RSF	Relative centrifugal force,
RT	Room temperature
SD	Standard deviation
SDCs	Syndecans
SDC1-6	Syndecan1-6
SDS	Sodium dodecyl sulphate
SEM	Standard error of mean
18S rRNA	18S ribosomal RNA
Sulf1/2	Sulphatase 1/2
STAT3	Signal transducer and activator of transcription 3
Strep	Streptomycine
Tam	Tamoxifen
TBS	Tris-buffered saline
TBST	Tris-buffered saline, 0.1% Tween 20
TGF-b	Transforming growth factor-β

Thr	Threonine
TICs	Tumour initiating cells
Tie2	Tyrosine kinase receptor
TMED	Tetramethylethylenediamine
TNBC	Triple-negative breast cancer
Tyr	Tyrosine
UDP	Uridine- 5'-diphosphate
VEGF	Vascular endothelial growth factor
VEGFA	Vascular endothelial growth factor A
VEGFB	Vascular endothelial growth factor B
WB	Western blot
WR	Working reagent
Xg	Time gravity
Xyl	Xylose
XylT	Xylosyltransferase

1 Introduction

1.1 Proteoglycans

Proteoglycans (PGs) are major components of metazoan organism's cell surfaces and extracellular matrix (ECM) (Bernfield et al., 1999, Esko et al., 2009, Perrimon and Bernfield, 2001, Turnbull et al., 2001). PGs are also involved in binding diverse chemokines, cytokines and growth factors (Kjellén and Lindahl, 1991). Moreover, they are involved in regulating fundamental cell processes including cell proliferation, differentiation and migration, and by assisting in maintenance of basement membranes (Iozzo, 2005). PGs are glycoproteins which contain a core protein, found covalently O-linked to the glycosaminoglycan (GAG) polysaccharide chains (Esko et al., 2009, Kjellén and Lindahl, 1991).

1.2 Glycosaminoglycans

Glycosaminoglycans (GAGs) are polysaccharides, consisting mostly of repeating disaccharide units of hexosamine and a hexuronic acid, of which there are two types of GAGs: galactosaminoglycans and glucosaminoglycans (Gandhi and Mancera, 2008, Prydz, 2015). The galactosaminoglycans classified to chondroitin sulphate (CS) and dermatan sulphate (DS), while glucosaminoglycans classified to hyaluronan, keratan sulphate (KS), heparan sulphate (HS) and heparin. Galactosaminoglycans and glucosaminoglycans consisting of the same hexuronic acid subunits, either glucuronic acid (GlcA) or iduronic acid (IdoA). The difference between them is aminosugar, galactosaminoglycans have the galactosamine sugar or glucosaminoglycans have glucosamine sugar (Gandhi and Mancera, 2008). Hyaluronan consists of glucosamine and GlcA (Evanko et al., 2007). Unlike the other GAGs, KS has galactose monosaccharides instead of uronic acid (Funderburgh, 2000). Hyaluronan, also known as hyaluoronic acid (HA) is unique since it is unsulfated and not found attached to a core protein (Chen and Abatangelo, 1999) (Figure 1.1). Of all the GAGs, HS has been the most deeply investigated, often described as a master extrinsic regulator of cellular behaviour.

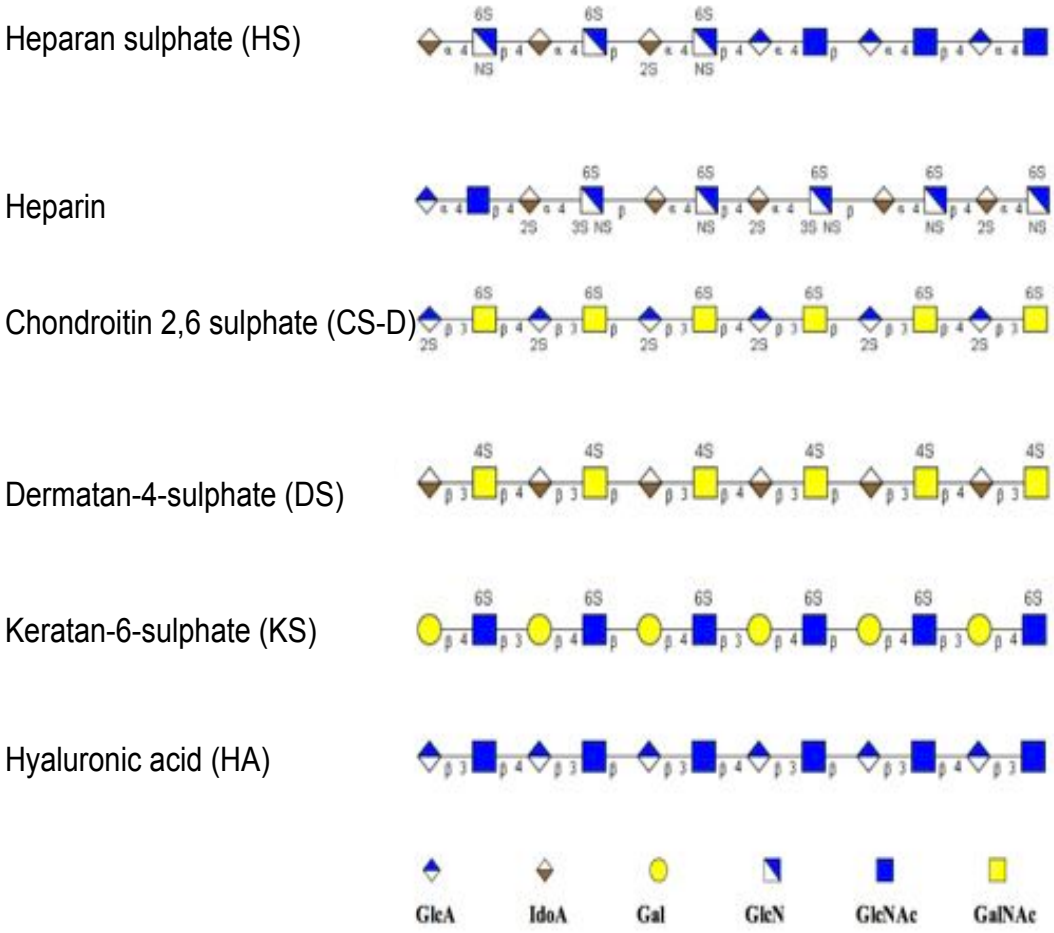

Figure 1.1 Carbohydrate sequences of the six types of GAG chains using monosaccharide symbols. GAGs are repeating disaccharide units of a hexosamine with either uronic acid or galactose. Possible sulphation presence and location (2S, 4S or 6S) is indicated. Sulphate group is lacking in hyaluronan, while uronic acids are replaced by galactose in keratan sulphates. The monosaccharide is illustrated according to the guidelines of the Nomenclature Committee of the Consortium for Functional Glycomics (**http://glycomics.scripps.edu/CFGnomenclature.pdf**).

1.3 Heparan sulphate

Heparan sulphate (HS) is a highly sulphated and negatively charged member of the glycosaminoglycan (GAG) family of polysaccharides found on the ECM and cell surfaces (Gandhi and Mancera, 2008). HS are able to bind and interact with a wide variety of proteins important for tumour development, such as chemokines, enzymes and growth factors. For example, fibroblast growth factors (FGFs), vascular endothelial growth factor (VEGF), hepatocyte growth factor (HGF) and transforming growth factor-β (TGF-b), which are all heparin-binding molecules (Sasisekharan et al., 2002, Turnbull et al., 2001).

1.3.1 HS structure

HS is a linear polysaccharide characterized by α 1-4 linked disaccharide repeating unit backbone of uronic acid (either a D-glucuronic acid, GlcA, or L-iduronic acid, IdoA) covalently linked to D-glucosamine GlcN units, arranged in sulfated (NS) and acetylated (NA) regions (Figure 1.2). The complexity of HS structure derives from the different modification of disaccharide units individually within an oligosaccharide chain. 48 theoretically disaccharide units can form up to 100-200 disaccharide units of complete HS chains. Modification of HSPGs exist at the 6-O (and rarely 3-O) positions of glucosamine, and 2-O position of uronic acids. Therefore, these possible modifications result in fine structural diversity (Sasisekharan et al., 2002). The domain structure of HS chains consisting of NS domains of various length and sulphation, spaced part by NA domains (Turnbull & Gallagher, 1990). Modified regions (NS domains or S-domains) display highly diverse saccharide sequences with specific patterns of *N*- and O-sulphation and of GlcA conversion to IdoA residues. Unmodified regions (NA domains) consist repeating GlcA-GlcNAc disaccharide units. Other parts of HS chains (NA/NS) contain alternating NA/NS glucosamine derivatives (Figure 1.3) (Turnbull et al., 2001).

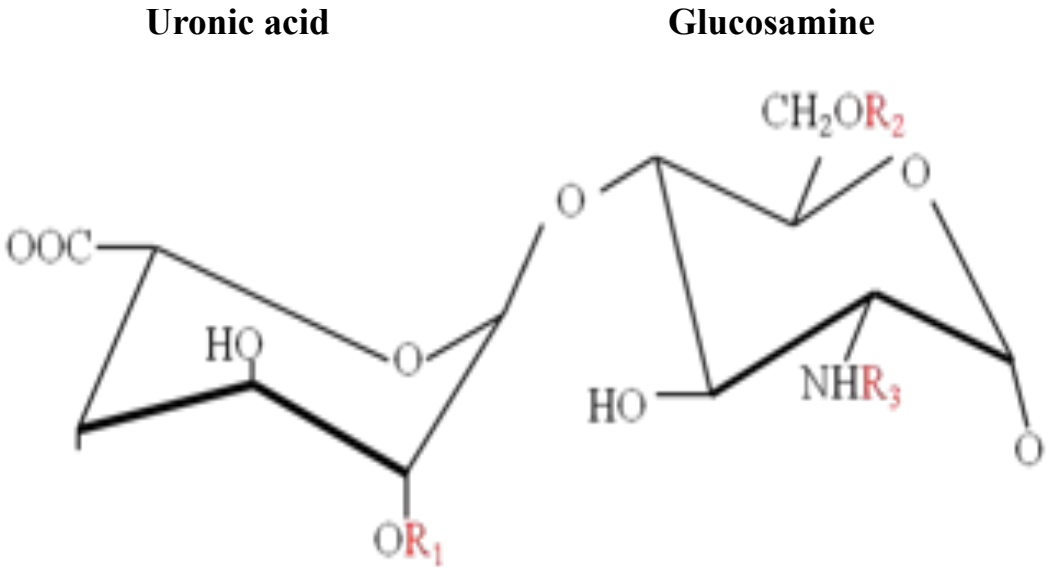

Figure 1.2 Schematic diagram of chemical structure of HS. A disaccharide repeat unit backbone of uronic acid and glucosamine. The configuration of R groups result in the heterogeneity of HS molecular structure. (red; R1 corresponds to O-sulphation at C2 of uronic acid; R2 corresponds to O-sulphation at C6 of glucosamine; R3 corresponds to either SO_3 or acetate).

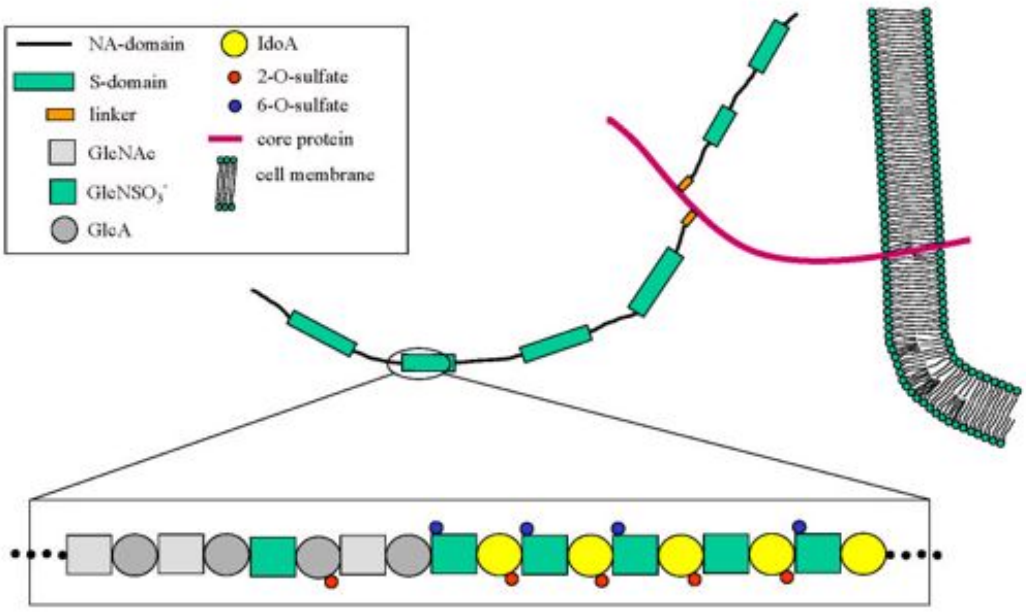

Figure 1.3 Heparan sulphate proteoglycans (HSPGs) overall structure. HS chains are attached to the core protein O-linked through serine residues. Binding sites for ligands are defined by the arrangement of sulphate groups (NS, 2S, 3S, 6S) and uronic acid epimers (GlcA and IdoA). From (Turnbull et al., 2001).

1.3.2 Heparan sulphate proteoglycans

HS chains are usually covalently linked to specific serine residues present in the core proteins to form HS proteoglycans (HSPGs), which are expressed mostly on the mammalian cell surfaces and in the ECM (Turnbull et al., 2001). HSPGs are divided into two main families at the cell surface (syndecans (SDCs) and glypicans (GPCs)), and three major families in the ECM (perlecan, agrin and collagen type XVIII) categorized by their various core proteins (Figure 1.4) (Sarrazin et al., 2011). The syndecan family is composed of four members, ranging from 22-45 kDa in their molecular weights (Bonneh-Barkay et al., 1997, Sarrazin et al., 2011). It was found that syndecans could also contain a CS chain attached to a serine residue near the cell membrane. The syndecans have an extracellular, transmembrane and cytoplasmic domain (Bernfield et al., 1999). Syndecan sub-families differ in their tissue expression patterns and functions. For example, epithelial cells are rich in SDC-1 and are involved leukocyte-endothelial interactions, wound healing and angiogenesis (Stepp et al., 2002), while SDC-2 is the major syndecan of lung, kidney, cartilage, bone, and stomach (Essner et al., 2006). SDC-3 is rich in the neuronal cells and brain (Kaksonen et al., 2002). SDC-4 is expressed through all embryonic development stages and regulates cell migration, adhesion and matrix structure (Couchman et al., 2001).

There are six members in the glypican family; their molecular weights are about 60 kDa. Glypicans are found in various tissues and are involved in biological development and the embryonic central nervous system (Bernfield et al., 1999). The difference between syndecans and glypicans was found in their core proteins as glypican are anchored in the membrane through a glycosylphosphatidylinositol (GPI) anchor, whilst syndecans cross the lipid bilayer with a transmembrane region (Lin, 2004).

Perlecan and agrin are multi-domain HSPGs found in the ECM. Perlecan has a molecular weight of ~400 kDa (Sarrazin et al., 2011) and is found in the connective tissues, lung, kidney and has a vital role in development and homeostatic processes (Handler et al., 1997). Agrin has about 212 kDa molecular weight (Sarrazin et al., 2011) and is widely expressed during development, but is considered mainly as a

neuronal HSPG (Bezakova and Ruegg, 2003, Kröger and Schröder, 2002).

Collagen XVIII has triple-helical domains and some splice variants are interrupted by non-collagenous parts carrying about three HS chains. It is located in the basement membrane of various tissues and has a molecular weight of ~ 150 kDa (Marneros and Olsen, 2005, Sarrazin et al., 2011).

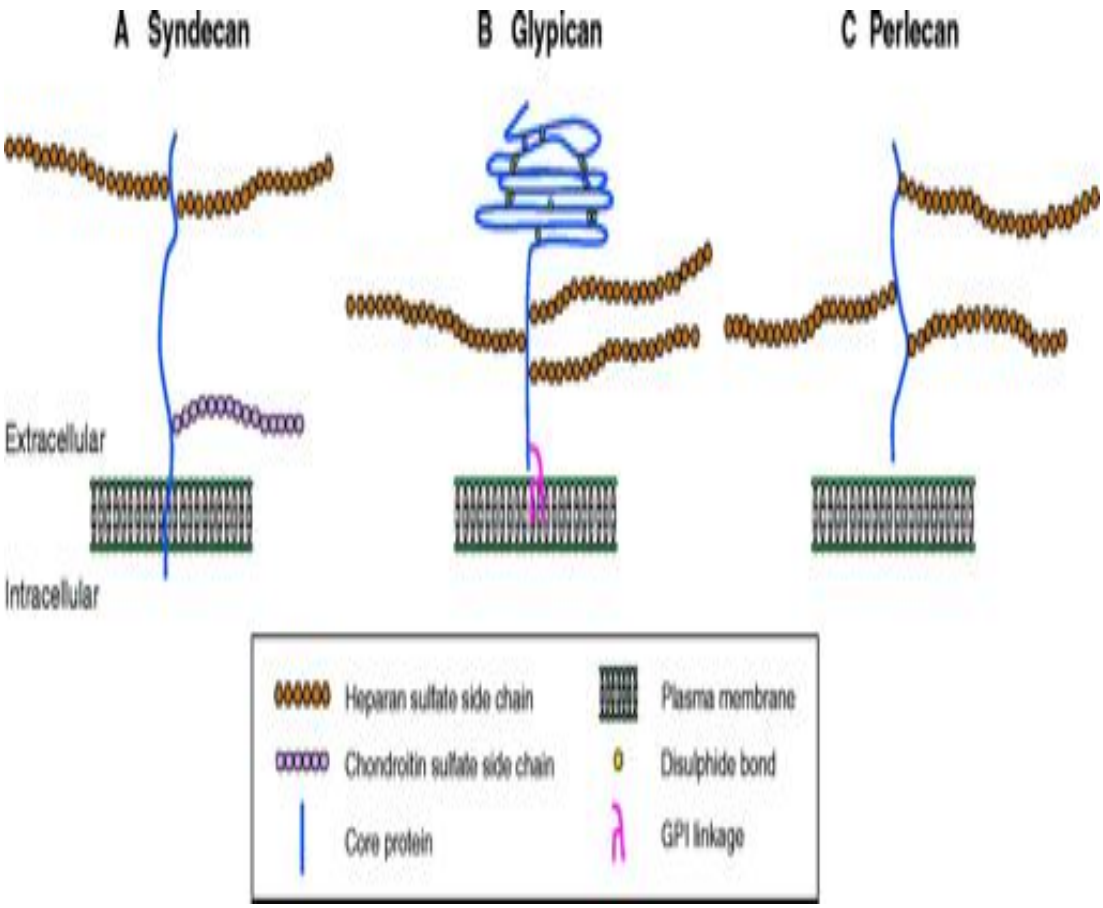

Figure 1.4 Classification of cell surface and ECM HSPGs. (A) Syndecan is transmembrane proteins that contains a short conserved C-terminal cytoplasmic domain. HS and CS side chains are attached to serine residues distal from the extracellular domain. (B) The glypican core proteins are linked to the plasma membrane by a GPI linkage. HS attachment sites in glypican are located adjacent to the plasma membrane. (C) Perlecans are large multidomain proteins and secreted HSPGs that carry HS chains. It found in basement membranes of many tissues. Adapted from (Lin, 2004).

1.3.3 Heparin: a close relative of HS

In 1916, heparin was discovered as an inhibitor of blood coagulation and received increasing attention over the next 20 years when it was first tested as an anticoagulant drug in patients in the mid 1930s (Wardrop and Keeling, 2008). Heparin received its name from the hepatic tissue from which it was first isolated and studied. The difference between heparin and HS is related to both quantitative differences in sulphation, and location of expression (Table 1.1) (Wardrop and Keeling, 2008). HS is expressed on the ECM and cell surfaces of almost all mammalian cells, while heparin is synthesised by mast cells and stored in its granules (Gandhi and Mancera, 2008, Sasisekharan et al., 2002). As described previously, HS and heparin share the same polysaccharide backbone which is a repeating uronic-glucosamine disaccharide. Only the degree of sulphation differ in these two molecules, although the biosynthesis pathway is the same (Gandhi and Mancera, 2008). HS consists of a lower level of sulphation, higher level of acetylated glucosamine and lower level of iduronic acid than heparin (Gandhi and Mancera, 2008). Approximately 85% or more of GlcN residues are N-sulphated and approximately 70% or more of the uronic acid is converted to IdoA in heparin. Consequently, heparin is typically represented by approximately 1.8–2.4 sulfates/disaccharide, compared to heterogenous HS sulphation represented by 0.8-1.8 sulphates/disaccharide (Casu and Lindahl, 2001, Dreyfuss et al., 2009, Rabenstein, 2002). Overall, heparin is very well-studied and understood, and is widely available in large quantities, and is therefore a long standing model or proxy molecule for HS.

Table 1.1 Structural differences and similarities of heparin and heparan sulphate

Property	Heparin	Heparan sulfate
Sulphate versus hexosamine content	1.8-2.4	0.8-1.8
N-sulphate content	>85%	40-60%
α-L-iduronic acid content	>70%	30-50%
Site of synthesis	Intracellular component of mast cells (liver, lungs and skin)	Extracellular component found in the basement membrane and as a ubiquitous component of cell surface
Mass	10-12 kDa	10-70 kDa
Major disaccharide repeating units	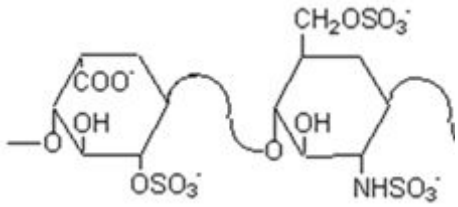	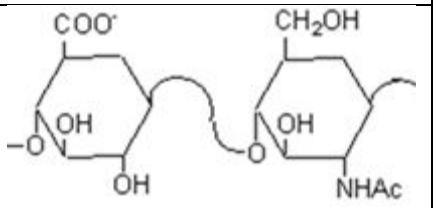
Minor disaccharide repeating units	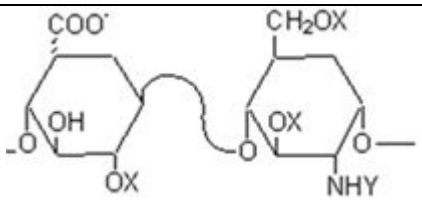	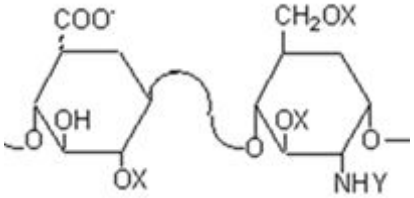

Major and minor disaccharide-repeating units in heparin and heparan sulphate (X= hydrogen (H) or sulphate ($SO3^-$), Y=acetyl (Ac), sulphate ($SO3^-$) or hydrogen (H)) (Gandhi and Mancera, 2008).

1.3.4 HS Biosynthesis

Heparin and HS chains are synthesized by a family of enzymes occurring in the Golgi apparatus. The biosynthetic pathway employs chain initiation, elongation and modification, produced via about eleven different types of membrane bound enzymes, many of which are present in multiple isoforms (Figure 1.5). HS chains are heterogeneous polysaccharides, due to the fact that these membrane bound enzymes do not act to completion (Aikawa et al., 2001, Bernfield et al., 1999).

1.3.4.1 Initiation of heparin/HS chains

The first step of heparin/HS biosynthesis is initiated with the addition of xylose (Xyl) to core protein serine residues; uridine- 5'-diphosphate (UDP)-Xyl is transferred by xylosyltransferase-1/2 to specific acceptor serine residue in the PG core protein, to initiate a tetrasaccharide linkage region. There are two XylT isoforms in mammals, which both have a role in PG biosynthesis. Two Gal residues are then attached by galactosyltransferases-1/2 and GlcA is attached by glucuronyltransferase-1, to complete the ''linkage tetrasaccharide'', - β GlcA-1,3-β Gal-1,3-β Gal-1,4-β Xyl-Ser (Pönighaus et al., 2007).

1.3.4.2 Elongation of heparin/HS chains

HS chain synthesis is determined by addition of the first GlcNAc residue to the tetrasaccharide linker, catalyzed by the action of two heparin/HS dual activity co-polymerase enzymes (GlcNAc transferase II and GlcA transferase II), which are the products of exostosin-like-1/2 related genes (*EXT1* and *EXT2)* (Kim et al., 2001). The HS/heparin chain is then polymerized by the continued alternate addition of GlcA followed by GlcNAc residues, to form heparin/HS chains, consisting about 50-/200 disaccharide units (Busse et al., 2007).

1.3.4.3 Modification of HS/heparin chains

The heparin/HS chain is then modified by various enzymes in the Golgi apparatus membranes (summarised in Table 1.2). After initial polymerization steps, a series of modification reactions are involved to modify *N*-deacetylation and *N*-sulphation of the GlcNAc, epimerization of GlcA to IdoA, and *O*-sulphation at various positions. The first modification step is the replacement of the NAc group of GlcNAc residues with NS group forming N-sulphated glucosamine (GlcNS); this is catalyzed the N-deacetylase/N-sulphotranferases (NDSTs), of which four isoenzymes have been identified (Raman et al., 2005). Next, the epimerization step is mediated by glucuronosyl C5-epimerase, a single enzyme encoded in mammals. C5-epimerase catalyzes the conversion of GlcA monosaccharides to form IdoA residues; this occurs only in regions with Glc-NS residues (Li et al., 1997). Following the epimerization, several sulphotransferase modify the growing NS-domain. 2-*O*-sulfation is added at C2 of IdoA or GlcA residues by 2-*O*- sulphotransferase (2OST). Next, further *O*-sulphation of HS is catalyzed by 6-*O*-sulphotransferase (6OST) at the C6 position of GlcNAc and GlcNS residues. Finally, the 3-*O*-sulphotransferases (3OSTs) act occasionally to add 3-*O*-sulphates at C3 position of GlcNS residues. Importantly, these modification steps are not template-driven and do not occur on all potential sites; thus these enzymatic reactions create regions of variable structure and sulphation, though cell and tissue specific patterns are known to be generated, indicating that these processes must be subject to tight regulatory control by as yet undetermined mechanisms (Turnbull et al., 2001, Whitelock and Iozzo, 2005).

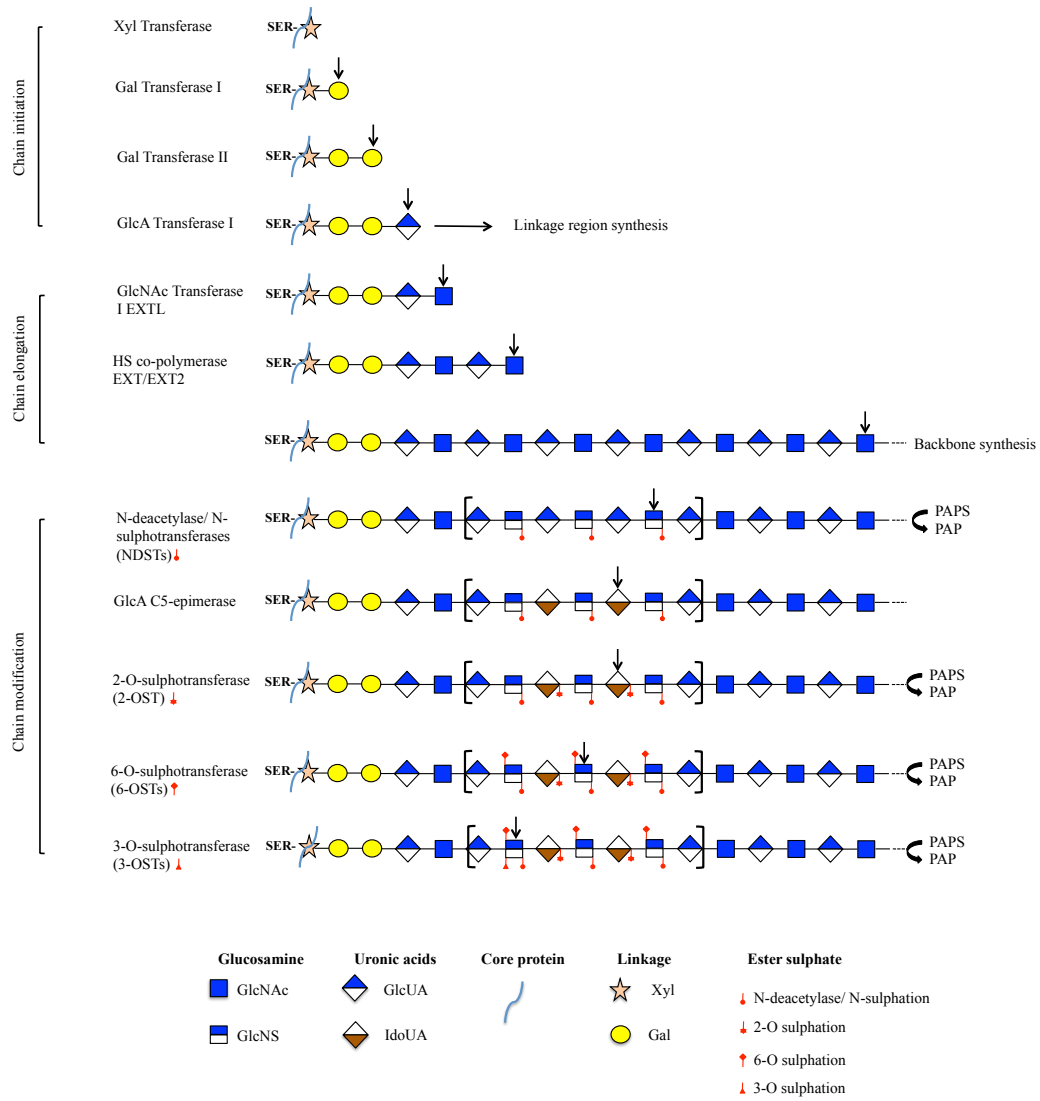

Figure 1.5 The biosynthesis of HS chains. HS chains are initiated by synthesis of a tetrasaccharide linkage attached to serine residues of the core protein, followed by elongation that is achieved through the co-polymerase complex formed by EXT1 and EXT2. The HS chain is then modified sequentially by NDSTs, C5 epimerase, and 2-O, 6-O and 3-O sulphotransferases to generate mature HS. Monosaccharide is represented according to the guidelines of the Nomenclature Committee of the Consortium for Functional Glycomics (**http://glycomics.scripps.edu/CFGnomenclature.pdf**).

Table 1.2 HS biosynthetic enzymes and their respective roles

Enzyme	Name	Function
EXT1	Exostosin1	First step of chain elongation; Alternating addition units of GlcA and GlcNAc to the non-reducing end of the chain (Busse et al., 2007).
EXT2	Exostosin 2	First step of chain elongation; Alternating addition units of GlcA and GlcNAc to the non-reducing end of the chain (Busse et al., 2007).
HS20ST	Heparan sulphate 2-O sulphotransferase	The sulfo group is transferred by HS20ST from 3'-phosphoadenosine 5'-phosphosulfate (PAPS) to the 2-OH position of the uronic acid adjacent to N-sulphated glucosamine (Kreuger and Kjellén, 2012)
HS30ST1-6	Heparan sulphate 3-O sulphotransferases (6 isoforms)	The sulfo group is transferred by HS30ST1-6 PAPS to the 3-OH position of the glucosamine which are N-sulphated (Kreuger and Kjellén, 2012)
HS60ST1-3	Heparan sulphate 6-O sulphotransferases (1-3)	The sulfo group is transferred by HS60ST1-3 from PAPS to the 6-OH position of the glucosamine which is N-sulphated or N-acetylated (Kreuger and Kjellén, 2012)
NDST1-3	N-deactylase/N sulphotransferases 1-3	Replaces acetyl groups with sulphate groups at the N-position of the glucosamine (Kreuger and Kjellén, 2012)
Sulf1	6-O-endosulphatase	Removes 6-O sulphate groups (Turnbull et al., 2001).
Sulf2	6-O-endosulphatase	Removes 6-O sulphate groups (Turnbull et al., 2001).
C-5 epimerase	C-5 epimerase	Conversion of glucuronic (GlcA) acid to iduronic acid (IdoA) (Li et al., 1997)

1.4 Chemically modified heparins

Several attempts have been made to produce and characterize chemically modified heparin derivatives by selective chemical de-sulphation by different groups (Figure 1.6); this work was undertaken with the aim of producing systematically simplified structures of authentic heparin with which to correlate activity relationships and generate potential novel therapeutics.

Methods to produce these saccharides employ different modification of the widely available heparin polysaccharide chain. Compared to heterogeneous HS structures, a relatively homogeneous polysaccharide is produced by carefully controlled addition or removal of the N-acetamido, N-sulfonamido, and O-sulfoxy modifications (Powell et al., 2004, Yates et al., 1996). These saccharides can then be used as mimetics of HS domains. The characterization of chemically modified heparins is normally achieved by nuclear magnetic resonance and disaccharide composition analysis; however characterization of these saccharides are also undertaken by other techniques such as infrared spectroscopy and mass spectrometry (Grant et al., 1989, Yates et al., 1996). Reports of modified heparins that have been characterized have described some of the more accessible modifications of heparin, and used as a marker for the association of biological activities with existence or the absence some groups, in order to establish structure-activity relationships. Several studies have established that there is a relationship between a change in activity or interaction and the modification types (Chen et al., 2009, Guimond et al., 2006, Irie et al., 2002, Yates et al., 2004). Chemically modified heparins were found to be inhibitors of the BACE-1 protease involved in Alzheimer's disease (Patey et al., 2006, Scholefield et al., 2003). Moreover, chemically modified heparin were found to block L and P-selectin-mediated cell adhesion, resulting in prevention of tumour metastasis in human colon and ovarian carcinoma respectively (Chen et al., 2009, Wei et al., 2004). In addition, chemically modified heparin can be used to disrupt the red blood cells resetting in severe and cerebral malaria caused by *Plasmodium falciparum* (Skidmore et al., 2008).

Functionally distinct HS sequences are difficult to define, and the isolation of HS material with a given bioactivity in useful quantities is very difficult. As mentioned before, the closely related polysaccharide heparin is thus usually used as an alternative source of HS, although this approach has several drawbacks. Heparin is homogeneous, highly sulphated and consisting of mostly highly charged sequences, and thus model only some NS-domains. They also possess some non-specific binding activities towards basic proteins, making it difficult to maintain required activity but avoid unwanted side effects. This emphasizes the importance of applying chemically modified heparin derivatives in initial structure-function studies especially into the importance of particular sulfate and acetyl groups (Guimond et al., 2006).

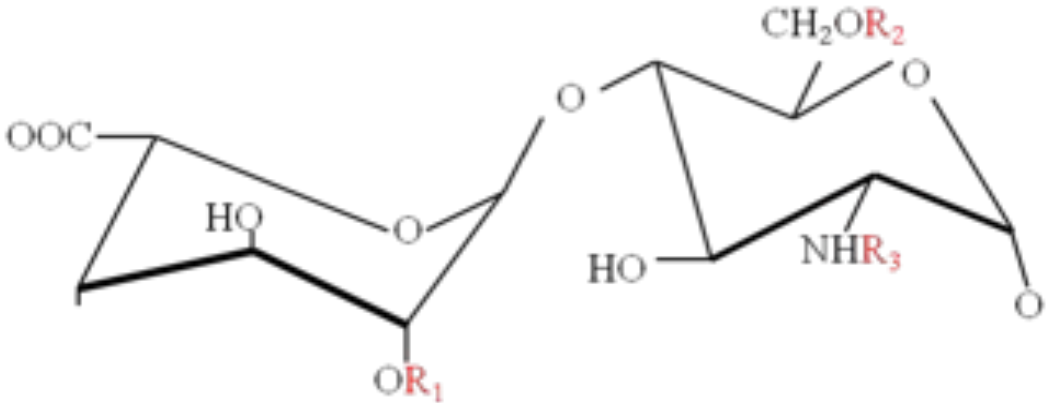

Compound	Name	Symbol	R1	R2	R3
1	*Per-sulphate heparin	PerS H	SO_3	SO_3	SO_3
2	NAc heparin	NAc H	SO_3	SO_3	NAc
3	2 deS-NS hepar n	2 deS-NS H	H	SO_3	SO_3
4	6 deS-NS heparin	6 deS-NS H	SO_3	H	SO_3
5	2 deS-NAc heparin	2 deS-NAc H	H	SO_3	NAc
6	6 deS-NAc heparin	6 deS-NAc H	SO_3	H	NAc
7	2, 6 deS-NS Heparin	2,6 deS-NS H	H	H	SO_3
8	2, 6 deS-NAc Heparin	2,6 deS-NAc H	H	H	NAc
9	Heparin		SO_3	SO_3	SO_3

Figure 1.6 Predominant disaccharide repeat structures of chemically modified heparins (compounds 1-9). The heparin polysaccharide derivatives were prepared from porcine intestinal mucosal heparin (Celsus), as described (Yates et al., 1996). * A disaccharide repeat unit backbone of uronic acid and glucosamine of PerS H consists of anion group ($OSO3^-$), while heparin consists of hydroxyl group.

1.5 HS-protein interactions

Hundreds of HS/heparin-interacting proteins have been identified to, termed the HS interactome (or "heparactome"). These interactions are highly diverse in their nature, as they include growth factors, enzymes, cytokines, enzyme inhibitors and ECM components (Bernfield et al., 1999, Turnbull et al., 2001). HS/heparin protein binding is thought to be mediated principally by anionic binding between the negatively charged sulphate and carboxylic acid groups on HS/heparin chains with basic amino acids, particularly arginine and lysine, on proteins, though hydrophobic interactions and Van der Waals forces have also been implicated in some interactions (Fromm et al., 1995, Rabenstein, 2002).

1.5.1 HS-growth factor interactions

Growth factors (GF) represent a large family of soluble proteins that regulate a wide range of cellular responses, such as, cell growth, proliferation, differentiation, migration and apoptosis. For many of these GFs, signaling is regulated via their binding to HSPGs on cell surface and the ECM (Forsten-Williams et al., 2008). Examples of some of these HS-GF interactions are provided below.

1.5.1.1 HS-FGF complex

The Fibroblast growth factor (FGF) family consists of about 22 members to date, most of which bind to HS. FGFs transmit their signaling depending on their protein receptor specificity, but HS also binds to tyrosine kinase receptors (FGFRs), such as FGFR1, 2 and 4 through heparin-binding sequences (Loo et al., 2001, Ornitz, 2000, Powell et al., 2002), which activate the intracellular signaling pathway responses. The HS-FGF interaction has been extensively studied. FGF activity depends on formation of a HS-FGFR-FGF high affinity complex (Guimond and Turnbull, 1999). The mechanism of interactions between FGF with HS involves basic amino acids on the FGFs interacting with O-sulphate group and carboxylates in the HS chain. However, HS binding with FGF-2 was found to be only 30% ionic (Guimond et al., 1993). The structural determinants of HS interactions with FGF-2 and its receptors have also been studied. The size and sulfation of oligosaccharide chains of

HS/heparin needed to serve as co-receptors when added along with FGF-2 to HS-deficient mouse fibroblasts has been studied, showing that around 12 mers are optimal for activity (Cole et al., 2010, Guimond et al., 2006, Jastrebova et al., 2006). Furthermore, activity is dependent 6-O sulfate in addition to IdoA2S and NS, whereas binding to FGF-2 alone without its receptors requires NS and IdoA2S (Figure 1.7) (Guimond et al., 1993).

1.5.1.2 HS-VEGF complex

The vascular endothelial growth factors (VEGFs) are a family of endothelial cell mitogens. VEGF is identified as a heparin-binding angiogenic growth factor, which regulates angiogenesis via promoting endothelial cell proliferation and migration (Zhao et al., 2012). In addition, VEGF and its receptors play a pivotal role in most aspects of vascular development and function such as tumour angiogenesis regulating tumour growth, invasion and metastasis (Hicklin and Ellis, 2005). As a result of alternate mRNA splicing, the *vegf* gene forms at least six VEGF isoforms. Each isoform has different biological properties due to each having different structures, including the presence or absence of short C-terminal heparin-binding domains (HBDs) (Ruhrberg, 2003). The functions of VEGF are flexible, related to expression of the different isoforms with various affinities for HS, linking it to different signaling receptor complexes.

VEGF-A isoform (VEGF $_{165)}$ is the most potent isoform, and binds with moderate affinity to heparin; it generates a homodimer containing two disulfide linked polypeptides of amino-terminal and disulfide-linked units with two identical 5-residue C-terminal fragment heparin-binding sites (Zhao et al., 2012). The interaction of HS with VEGF regulates the affinity of VEGF165 for its signaling receptors. HS contributes to the strength of VEGF165 interactions via 2-O, 6-O, and N-sulfation groups, with emphasis on the 6-O sulfates. Moreover, it has been shown that an oligosaccharide of about seven monosaccharide residues was sufficient to fully occupy the heparin-binding site of a single $VEGF_{165}$ monomer, suggesting that longer sequences with 2 such sites are required to interact with the homodimer of VEGF (Robinson et al., 2006). Various studies have found that a lack of HS-VEGF binding disrupts VEGF concentration gradients in the ECM and results in

uncharacteristic extracellular localisation of VEGF; this indicates that HS plays a pivotal role for HS in controlling VEGF diffusion (Xu et al., 2011).

A number of other HS-growth factor interactions such as hepatocyte growth factor (HGF), epidermal growth factor (EGF), platelet-derived growth factor (PDGF), and transforming growth factor beta (TGFβ) have been reviewed by Nigam and Bush (Table 1.3) (Nigam and Bush, 2014).

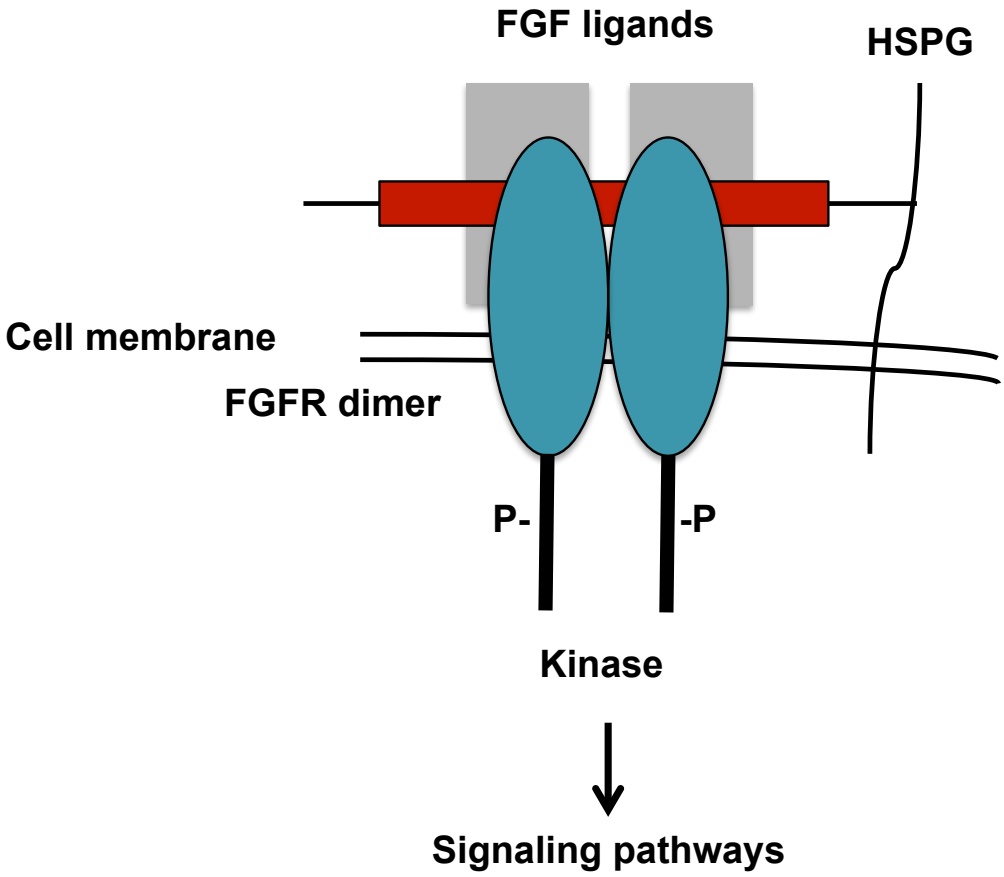

Figure 1.7 Model of interactions between HSPG, FGF and FGFR. Heparin induced dimerization and activation of the FGF receptors. The HS chain of HSPG can bind with FGF molecules for inducing dimerization that required for receptor signaling.

Table 1.3 Summary of the HS selectivity for selected GFs.

Proteins	**Selectivity**
Growth factors:	
Fibroblast growth factors (FGFs) FGF-1 and FGF-2	2-O and 6-O sulfation and NS and IdoA2S required for binding for FGF-2, whereas NS and IdoA2S were sufficient for binding of FGF-2 alone without the receptor (Guimond et al., 1993).
Vascular endothelial growth factor (VEGF)	2-O, 6-O, and N-sulfation, with emphasis on the 6-O sulfates (Robinson et al., 2006), no selective sequence.
The hepatocyte growth factor (HGF)	6-O-sulfated, NS glucosamine and IdoA, the minimal binding sequence 10-12-mer in length (Catlow et al., 2003), no selective sequence.
Transforming growth factor beta (TGF-β) (TGF-β_1 and TGF-β_2)	Heparin and high sulfated HS. Requires high level of N-sulfation for binding; no selective sequence (Nigam and Bush, 2014)
Platelet-derived growth factors (PDGFs)	Six–eight monosaccharide units with N, 2-O, and 6-O-sulfate groups all contribute to the interaction (Feyzi et al., 1997); no selective sequence.
Heparin-binding epidermal growth factor (HB–EGF)	Heparin/ HS optimizes activity (Nigam and Bush, 2014); no selective sequence.

1.6 Stem cells

Stem cells have been recognized as multi-or pluripotent undifferentiated cells with 2 key properties; firstly to be able to divide and multiply in their unspecialized state to generate more stem cells (self-renewal), and the ability to differentiate to give rise to cells with specialized functions. However, in most cases, stem cells do not differentiate directly to specialized cells. They give rise to progenitor cells that have more restricted potential, with a limited capacity to self-renew before differentiating into cell types of the specific tissue of origin (Florio, 2011). Normal stem cells are generally assigned to one of the following two categories depending on their source; embryonic stages are totipotent and pluripotent cells that are a capable of forming every cell in the embryo and placenta; or somatic (adult) stem cells which are more specialized, continuously forming a range of different cell types for their specific tissue compartment (Nemeth and Karpati, 2014, Wagers and Weissman, 2004).

Normal stem cells in mammals exist in a specialized microenvironment of each tissue named 'niches' that are anatomically defined, comprised of components of ECM, and which support stem cell survival. Normal stem cells from different tissues have been shown to be slowly cycling so that only a few times during the lifetime of a mouse, a number of these stem cells enter the cell cycle (Greco and Guo, 2010). In embryonic development, different niche factors can act on embryonic stem cells to change gene expression and promote their differentiation and proliferation for the development of the fetus. In contrast adult stem cell niches maintain these cells in a deactivated state, for example after tissue injury, the surrounding micro-environment can then signal to stem cells to either promote differentiation or self-renewal to form new tissues (Florio, 2011, Greco and Guo, 2010). In different tissues, adult stem cell niches differ in their cellular location, structure and composition. So far, these have been identified in intestine, brain, testis, skin and bone marrow but all tissues and organs may contain stem cell niche populations (Barker, Bartfeld and Clevers, 2010).

1.7 Cancer stem cells (CSCs)

1.7.1 CSCs: definition and characteristics

While embryonic and adult stem cells are an integral part of a healthy organism, cancer stem cells (CSCs), also known as tumour-initiating cells (TICs), may enhance the status of the disease process. The model of stem cells for the regulation of plasticity in adult tissues gave new impetus to study of tumours from several tissues (Florio, 2011). The CSC hypothesis is contrary to previous understanding of a stochastic model that any cell within the tumour is capable of limitless tumour growth, with ability to spread throughout the body, and become tumorigenic. In contrast, the CSCs model predicts that only a subset of tumour cells is tumorigenic and can generate a new tumour (Figure 1.8). These cells are defined as capable of self-renewal and differentiation. An important implication is that CSCs should be targeted to develop effective anti-cancer therapies (Girouard and Murphy, 2011).

Although a small subset (<1%) of cancer cells can extensively proliferate and form new tumours, these components are significant because they can lead to tumour recurrence, chemo/radio-therapy resistance, and metastasis (Han et al., 2013). Stem cell fate depends on controls from intrinsic (gene mutations) and extrinsic (microenvironment alterations), and losses or changes in these factors could contribute to the carcinogenic process (Florio, 2011, Han et al., 2013). Therefore, CSCs can be defined through four main CSC characteristics; self-renewal, differentiation, tumorigenicity and specific surface markers. CSCs subsets are maintained through various generations, indicating a self-renewing capacity. In addition forming tumorigenic daughter CSCs by symmetrical cell division, the pluripotent CSCs can also produce non-tumorigenic bulk populations by asymmetrical cell division. Moreover, a small subset of CSCs have tumorigenic potential when transplanted into animals and the CSCs subset can be separated from the non-stem cells by cell surface markers. Thus, the main two characteristics of CSCs are self-renewal and lineage capacity (Han et al., 2013).

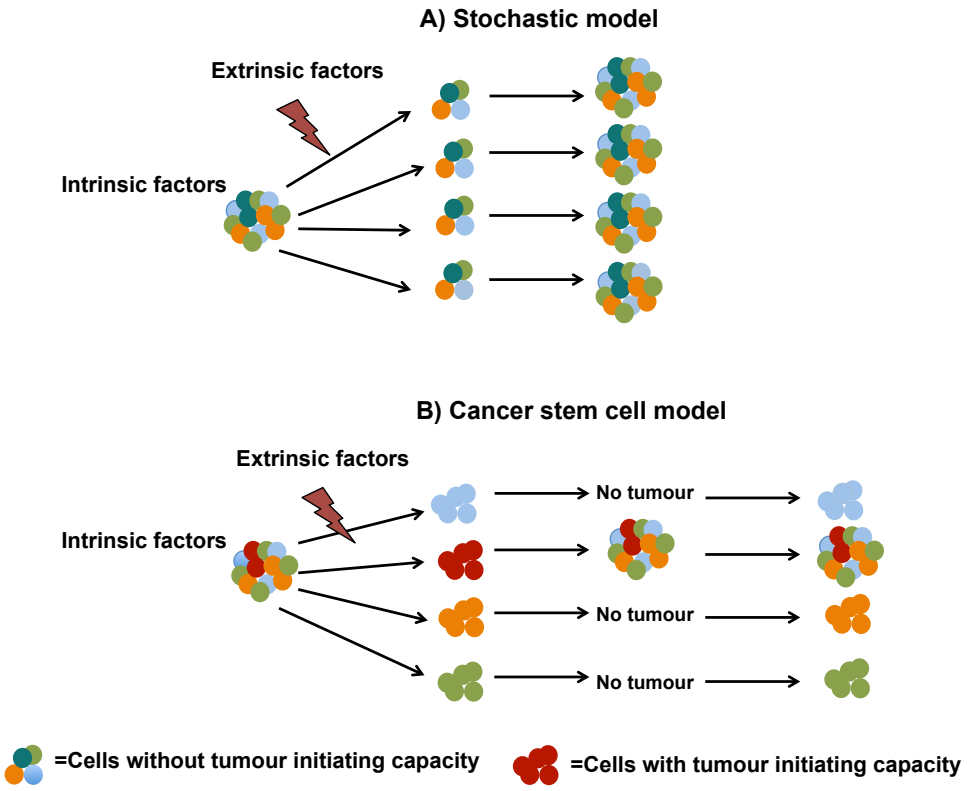

Figure 1.8 Stochastic versus CSC models of carcinogenesis. (A) The stochastic model predicts that every cell within the tumour will be able to randomly become tumorigenic. (B) The CSC model predicts that only a small number of cells, known as CSCs, are able to give rise to new or recurring tumours and produce differentiated tumour cells.

1.7.2 CSCs: isolation and identification

Like somatic stem cells, the first identification of the hierarchy of CSCs was studied in the haematopoietic system. In the 1970s, studies in leukemia demonstrated that a small fraction of tumour cells were able to proliferate widely. These cells are called leukemic stem cells (Bonnet and Dick, 1997, Dick, Gil et al., 2008, Girouard and Murphy, 2011, Wagers and Weissman, 2004). In the 1990s, Lapidot and colleagues isolated leukemic stem cells and found a cell surface phenotype ($CD34^+/CD38^-$) in acute myeloid leukemia (AML) patients (Lapidot et al., 1994). They demonstrated that tumour forming cells were found when injected into non-obese diabetic (NOD)/severe combined immunodeficiency (SCID) mice. In addition, $CD34^+/CD38^-$ cells did not initiate the formation of tumours, as these cells were similar to the phenotype of normal hematopoietic stem cells. Since their recognition in leukemia, CSCs have been identified in a variety of solid tumours such as, liver, prostate,

breast, pancreatic, skin, and colon tumours (Gil et al., 2008, Girouard and Murphy, 2011).

The identification and isolation of CSCs from mass cell lines or tumour tissues via various methods will be important to research on tumour initiation, development, diagnostics and therapeutics. CSC populations can be identified based on multiple *in vitro* assays, such as Hoechst dye exclusion side population cells (SP) (Mannelli and Gallo, 2012), sphere forming assays (Cao et al., 2011), detection of enzymatic activity of aldehyde dehydrogenase-1 (ALDH1) (Sun and Wang, 2010), detection of surface markers (Dou and Gu, 2010), serial colony-forming unit assays (Dou et al., 2007) and migration assays (Biddle et al., 2011). Since normal and CSCs have much in common, the properties of SCs, such as the expression of specific surface markers, have been used to identify and isolate CSCs. Although all these *in vitro* assays are used to demonstrate the CSC phenotype, *in vivo* assays are considered as the gold standard, such as using the animal models for serial transplantation assays, which can enhance the ability of *in vitro* assays to detect CSCs (Han et al., 2013).

1.7.3 CSC markers

CSC populations can be identified and isolated based on the presence or absence of various cell-surface proteins (markers) and cytoprotective enzymes (such as ALDH) either singly or in combination. Some CSCs markers include $CD133^+$ (brain tumour), $CD34^+/CD38^-$ (leukaemia), $CD44^+/CD24^-$, $ALDHI^+$ (breast cancer), and $CD133^+$, EpCAM high $CD44^+$, $ALDHI^+$ (colon cancer) among many others (Kamijo, 2012). Fluorescence-activated cell sorting (FACS), flow cytometry, immunofluorescent staining and polymerase chain reaction (PCR) analysis are used to detect these specific cell surface markers of CSCs and are widely used to identify, isolate and characterize the CSC subpopulation (Mannelli and Gallo, 2012, Pozzi et al., 2015, Qiu et al., 2012).

1.7.3.1 The following markers have been used in the study of breast cancer stem cells (BCSCs): CD44 marker

CD44 is a transmembrane glycoprotein, generally binding to its ligand hyaluronic acid as a receptor, promoting cell division, adhesion, migration and signalling. This binding is normally responsible for regulating cellular signaling and other biological process within cells (Jaggupilli and Elkord, 2012). CD44 contains three major domains, including extracellular (ectodomain), transmembrane and an intracellular domain. The interaction between extra cellular matrix (ECM) glycosaminoglycan hyaluronan and CD44 are currently an exciting area of investigation (Yan et al., 2015). Hyaluronan has been found to be enriched in the SCs niche and has an important role in the behaviour of CD44 in CSCs. The molecular weight of CD44 is around 85-200 KDa, encoded by a single gene, containing 20 exons. The standard isoform, referred to as CD44s, comprising exons 1-5 and 15-20. The variable exons are designated as v1-v10, respectively (Sahlberg et al., 2014).

1.7.3.2 CD24 marker

CD24 is a small cell surface glycoprotein, expressed on the external side of the plasma membrane. It is of considerable importance in cell differentiation and expressed by cells involved in the immune system, such as hematopoietic subpopulations of many B and T lymphocytes and differentiating neuroblasts (Sahlberg et al., 2014). It also expressed on granulocytes and many carcinomas (Ghuwalewala et al., 2016). CD24 has an important role in cell adhesion, invasion and migration as measured by various *in vitro* assays (Keysar and Jimeno, 2010). In addition, it is a determinant of stemness in many types of cancer. The distribution of CD24 in different type of cancer is under dispute, although patients with colorectal cancers expressed CD24 highly and a CD24 positive subset of colon cancer cells have these stem-like properties. In contrast, tumor initiating cells from breast cancer and head-and-neck cancer have been identified based on being CD24 negative (Sahlberg et al., 2014). CD24 consists of a 27 amino-acid, extensive core that is *O*- and *N*-glycosylated. The linkage of the encoded protein to the cell membrane is via a glycosylphosphatidylinositol (GPI) anchor (Ghuwalewala et al., 2016).

1.8 Breast cancer

1.8.1 Normal breast cancer

Breast cancer is one of the most common causes of death through malignant tumours among women worldwide, despite different types of treatment regimens such as chemotherapy, radiotherapy and endocrine therapy (Ghebeh et al., 2013, Prabhakaran et al., 2013, Xu et al., 2012). The main cause of death in most patients suffering from breast cancer which is metastatic, having evolved from the primary tumour (Lobba et al., 2012). Metastasis of breast cancer cells (BCCs) is the spread from the primary tumour to specific organs, depending on a multi-step process including: detachment of metastatic cells from the primary site, migration and intravasation to the blood supply, circulating through the body, adhesion to vasculature, extravasation at the next site via tissue endothelium (Croker et al., 2009, Mellor et al., 2007). This process is parallel to the normal leukocyte mechanism mediated by chemokines (Müller et al., 2001).

Breast cancer is highly heterogeneous and classified into five sub-types based on histopathological parameters such as receptor status (estrogen (ER), progesterone (PR), and/ or human epidermal growth factor receptor 2 (HER2)). These sub-types are: luminal A, luminal B, HER2, basal and normal and summarised in table 1.4. Each of these subtypes has different prognosis and response to treatment (Holliday and Speirs, 2011, Prabhakaran et al., 2013). Basal-like and claudin-low tumors were found to lack the ER, PR and HER2 receptors, and are thus referred to as triple-negative, and are known to be very resistant to existing therapies (Prabhakaran et al., 2013).

Table 1.4 Molecular classification of breast carcinoma

Classification	Immunoprofile	Other characteristics	Example cell lines, adapted from (Neve et al., 2006, Prat et al., 2010)
Luminal A	ER^+, $PR^{+/-}$, $HER2^-$	Cells are more differentiated and can be treated with chemotherapy	MCF-7, T47D, SUM185,
Luminal B	ER^+, $PR^{+/-}$, $HER2^+$	Cells are more differentiated and can be treated with chemotherapy	BT474, ZR-75
HER2	ER^-, PR-, $HER2^+$	Cells are more differentiated and can be treated with hormontherapy	SKBR3, MDA-MB-468
Basal	ER^-, PR^-, $HER2^-$	Cells are less differentiated, low response to chemotherapy	MDA-MB-468
(claudin-low)	ER^-, PR^-, $HER2^-$	Cells are less differentiated, low response to chemotherapy	BT549, MDA-MB-231, Hs578-T, SUM1315

1.8.2 Breast cancer stem cells (BCSCs)

There is a significant base of literature indicating that the heterogeneity of breast cancer tissues may be rooted in the existence of a small subset of CSCs or TICs (Gong et al., 2010), with the ability to self-renew and differentiate to support tumour growth (Girouard and Murphy, 2011). This theory could explain the failure of traditional chemotherapeutic treatments. It has been shown that BCSCs are more resistant to chemotherapy and radiotherapy than normal BCCs due to multiple molecular mechanism (de Beça et al., 2013, Prabhakaran et al., 2013).

Several studies have identified a subpopulation of BCSCs based on cell surface markers enriched in these cells, with the $CD44^+/CD24^{-/low}$ and $ALDH^+$ phenotype the most consistently associated with cells displaying stem-like characteristics (de Beça et al., 2013, Ghebeh et al., 2013, Sun et al., 2013). $CD44^+/CD24^{-/low}$ sub-population

of BCCs was first identified by Al-Hajj and colleagues, who found that as few as about 100-200 BCSCs with the $CD44^{+}/CD24^{-/low}$ phenotype were able to initiate new tumours when introduced into NOD/SCID mice (Al-Hajj et al., 2003). In addition, two other cell surface markers have become a standard combination for identifying human normal mammary gland cells: Ep-CAM (epithelial specific antigen, ESA) and CD49f (α-6-integrin) (Ghebeh et al., 2013). These CSCs have enhanced invasive abilities, chemo/radio resistance and poorer prognosis (Olsson et al., 2011).

1.8.3 Breast cancer cell lines as models of mammary cancer stem cells

Working with CSC sub-populations derived from cell lines has many advantages, as models to further understand the biology of CSCs and therapeutic targets. Triple-negative breast cancer (TNBC) is the most aggressive and lethal subtype of BCC line and is characterised by the absence of HER2, PR and ER receptors. It still poses a major challenge (Holliday and Speirs, 2011). Recently, various studies have also demonstrated that angiogenesis plays a pivotal role in the TNBC pathogenesis (Ribatti et al., 2016, Rugo, 2012), resulting in the development of a number of novel and targeted therapies.

1.9 Resistance of breast cancer to therapeutic

1.9.1 CSCs are controversial

The CSC theory is controversial, due to the existence of small subpopulations, which grow slowly in experiments that involve breaking down a tumour, taking out particular cells and then transplanting them. Existing traditional cancer treatments such as chemotherapy, radiotherapy, and endocrine therapy to treat cancer have been developed and widely used in clinic; these conventional treatments aim to eliminate the tumor and reduce the risk of metastasis, but they are non-targeting and tumour relapse often occurs after therapy, possibly related to the presence of CSCs/TICs (Figure 1.9) (Cojoc et al., 2015). The mechanism of BC resistance to therapies include various factors such as, high capacity for DNA synthesis, slow cell cycle kinetics, the microenvironment properties including hypoxia, anti-apoptosis proteins and multiple drug resistance membrane transporters (*e.g.*, ABC transporters) (Cojoc et al., 2015, Holliday and Speirs, 2011). To achieve cancer remission or cure, targeted therapy will be necessary to develop novel therapies that hit the small

proportion of the tumor (CSCs).

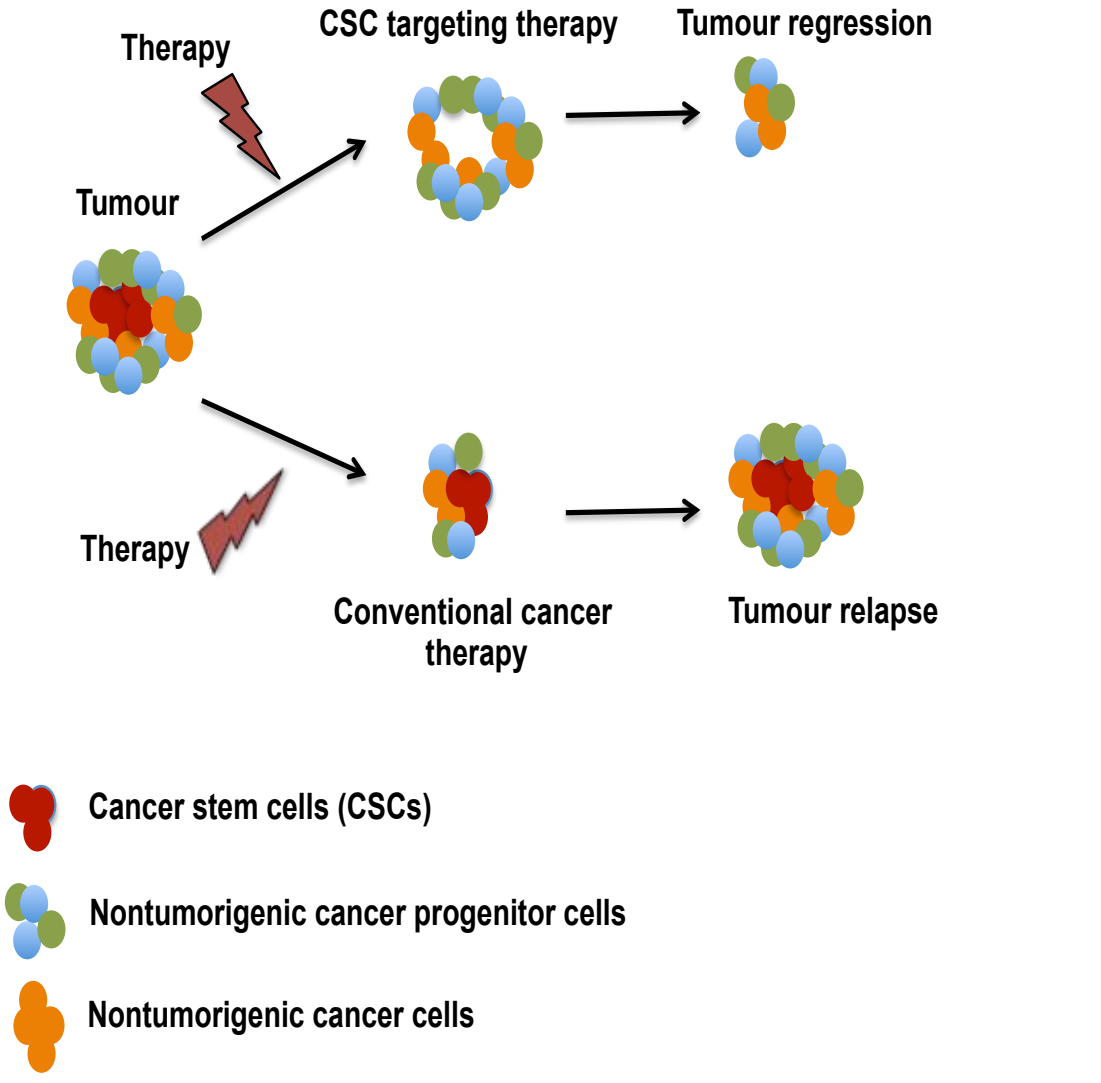

Figure 1.9 Conventional cancer therapies versus CSC targeted therapies. Conventional therapy can diminish tumor burden but are not able to eliminate CSCs, which can later regenerate and regrow the tumour. If the CSCs are eliminated by CSC targeted therapy, there is tumor regression. It will be necessary to develop novel treatments that attack both cell types.

1.9.2 BCSCs therapy

Various types of BC treatments have been developed, including hormone therapy, chemotherapy, radiotherapy and surgery depending on the stage. Hormonal therapy such as Tamoxifin (Tam) and chemotherapy such as doxorubicin (Dox) and cisplatin (Cis) are widely used (Holliday and Speirs, 2011, Prabhakaran et al., 2013). Cisplatin and doxorubicin are chemotherapeutic anti-cancer drug that have been used extensively for the treatment of different types of cancers. Particularly, cisplatin has been used in breast cancer in combination with other chemotherapies resulting in synergistic or additive effects. The exact mechanism of how cisplatin and doxorubicin work are complex, but it is thought that they cause DNA damage by interacting with DNA. Cisplatin forms Pt-DNA, adducts at the 1,2-intrastrand crosslink, resulting in the activation of various signal transduction pathways (Prabhakaran et al., 2013). Doxorubicin interacts with DNA, preventing formation of the DNA double helix. Doxorubicin was found to induce autophagy. Tamoxifen is an estrogen receptor antagonist which blocks the estrogen effect via binding to its receptor as an antagonist. The tamoxifen/estrogen receptor complex stops the genes being switched on by estrogen. In addition, tamoxifen was found to induce autophagy and apoptotic cell death in estrogen-positive BCC lines (Holliday and Speirs, 2011). Thus, the identification of anti drugs that are involved in tumorigenesis and angiogenesis in TNBC, is essential for the development of therapeutic agents targeting this aggressive breast cancer subtype.

1.9.3 Role of HSPGs in breast carcinoma and BCSCs

Several lines of evidence demonstrate that the HSPGs syndecans have pivotal regulatory roles in various type of cancer cell behavior (Lim et al., 2015). For instance, SDC-4 has been reported to modulate cell invasiveness. Moreover, previous work by (Beauvais and Rapraeger, 2003) demonstrated that syndecan-1 promotes cell adhesion and spreading with inhibition of cell invasion.

Emerging evidence suggests that BCSCs are regulated by signal transduction pathways, such as IL-6/JAK2/STAT3 and Wnt pathways (Marotta et al., 2011, Okolicsanyi et al., 2014). HSPGs could have an important role in breast cancer by modulating these pathways. Members of the syndecan family of HSPG core proteins

are reported to have an important role in breast cancer. High expression of syndecan-1 in patients with breast cancer is associated with reduced overall survival of patients with breast cancer (Ibrahim et al., 2013, Okolicsanyi et al., 2014). In addition, (Ibrahim et al., 2013) found that knockdown of syndecan-1 reduced side population (SP) and ALDH1-positive cell pool of triple negative MDA-MB-231 and hormone receptor positive MCF-7 cells detected by flow cytometry technique. Other studies showed that an absence of syndecan-4 in breast cancer correlated with poor prognosis and aggressive breast cancer phenotype (Lendorf et al., 2011). Side chain initiation and modification, with specific HS sulphation profiles have been investigated for a prominent role in breast cancer progression and metastases (Okolicsanyi et al., 2015). It was found that GPCs1-6 have a role in breast tumours. The expression of GPC-1 and GPC-6 appears to be significantly increased in MDA-MB-231 and MCF-7 human BCCs, with moderately expression of glypicans-3 and glypicans-4 in both cell lines (Matsuda et al., 2001). These findings mark HSPGs as prominent contributor to breast cancer and BCSC.

The use of HS-related compounds as antitumor chemotherapeutic agents has been reported in numerous studies. Low anticoagulant chemically modified heparin has a positive effect on P-selectin adhesion reduction in BCCs (Mi et al., 2009). In addition, HS/heparin oligosaccharides were found to inhibit HS-dependent tumor behaviour such as metastasis formation, tumour growth and migration (Mellor et al., 2007). Moreover, GPC-3 has also been tested to inhibit aggressive behaviour on mouse breast cancer cell line LM3 via maintaining adequate levels of protective molecules (Gomes et al., 2013, Peters et al., 2003).

1.10 CSC-targeted mechanisms and implications

The intricate regulation of different signaling pathways has a pivotal role in embryonic and adult stem cells related to self-renewal, proliferation and differentiation; however, the aberrant activation or dysregulation of these signalling pathways may also enhance the formation of CSCs (Han et al., 2013, Karamboulas and Ailles, 2013). Therefore, signaling pathways in the biology of CSCs are increasingly being used to demonstrate mechanisms underlying tumour relapse and drug resistance.

1.10.1 The signal transducer and activator of transcription 3 (STAT3)

Interleukin 6 (IL-6) is an interleukin mediator involved in the regulation of the inflammatory and infection responses (Xie et al., 2012). The serum level of IL-6 is elevated in breast cancer, particularly in advanced metastatic breast cancer patients (Bachelot et al., 2003). Previous studies demonstrated that when the $CD44^{+}/CD24^{-}$ sub-population of T47D human BCCs are exposed to IL-6, it results in promotion of the generation of CSCs by induction of epithelial mesenchymal transition (EMT) (Xie et al., 2012).

The signal transducer and activator of transcription 3 (STAT3) protein is a member of a family of transcriptional factors. STAT3 protein is phosphorylated (pSTAT3) by receptor-associated janus kinase (JAK), dimerizes, and translocates into the cell nucleus (Wei et al., 2014). In particular, full activation of STAT3 protein may occur via tyrosine phosphorylation 705 in response to such ligands as IL-6 or EGF. Additionally, it becomes activated after phosphorylation of serine 727 via MAPK. In view of the important role of STAT3 in regulation of gene expression, STAT3 promotes malignant stem cells of hematopoietic and various solid tumors such as breast and colon CSCs (Aznar et al., 2001, Wei et al., 2014). In addition a number of pieces of evidence have also suggested a role for IL-6/STAT3 signaling pathway in inducing or maintaining a $CD44^{+}/CD24^{-}$ subpopulation of BCCs (Marotta et al., 2011, Xie et al., 2012). Interestingly, (Ibrahim et al., 2013) demonstrated that Syndecan-1 silencing inhibited proinflammatory signaling in the BCC line (MDA-MB-231) by downregulation of such receptors and ligands as IL-6/IL6-R, which was linked to eliminating STAT3 activation. This finding indicates that SDC-1 depletion decreases the SP and CSC sub-population isolated from MDA-MB-231 BCCs through intereference with IL-6/STAT-3 signaling pathways (Figure 1.10).

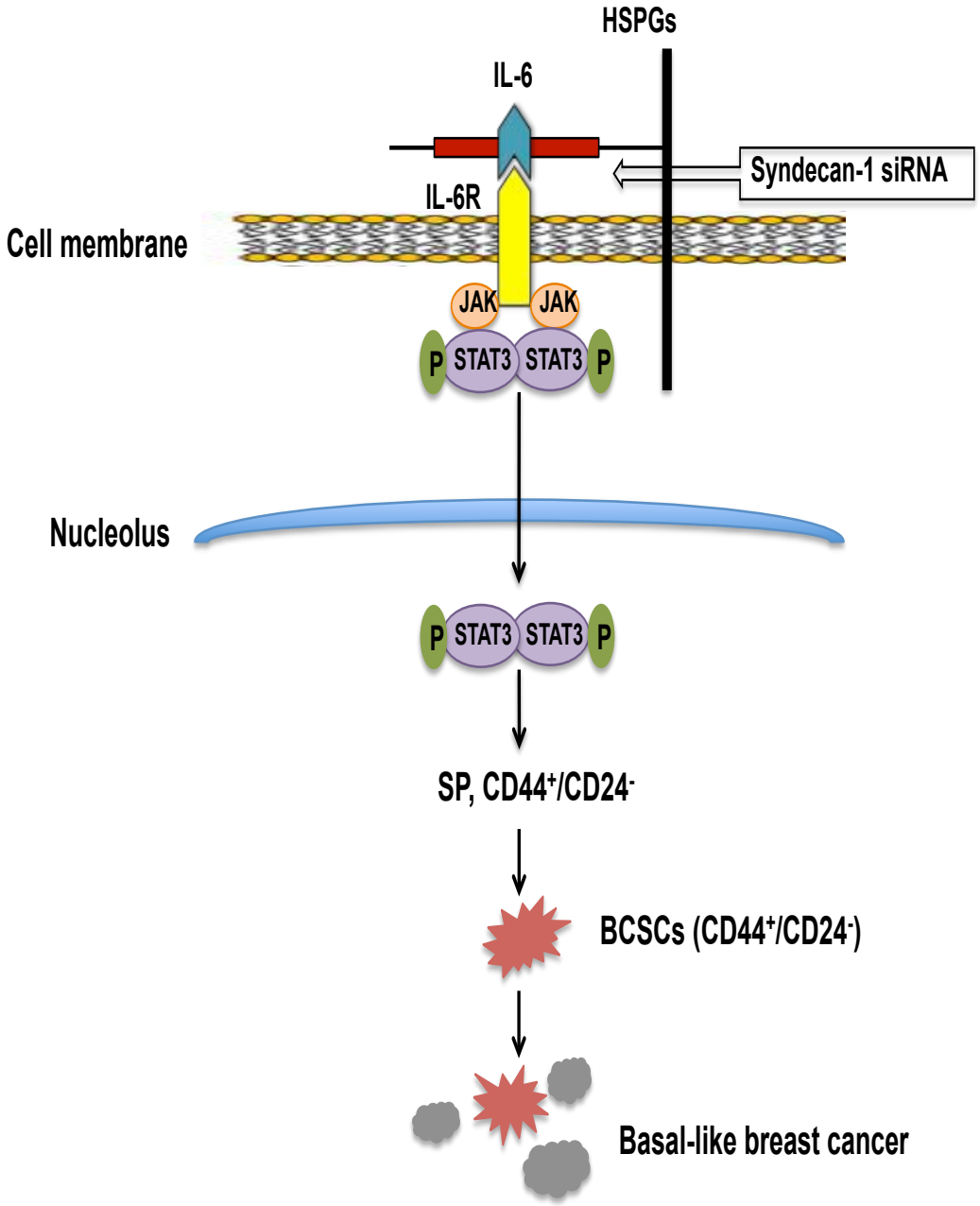

Figure 1.10 Cell surface HSPGs (Syndecan-1) modulates BCSCs properties through the IL-6/STAT3, signaling pathways. siRNA-mediated knockdown of Syndecan-1 results in reduction of IL-6 and IL6-R expression, possibly due to a reduction of JAK activation. The reduction of the expression of IL-6 signaling pathway results in decreased constitutive downstream signaling (STAT3 activation) in human BCCs.

1.10.2 MAP kinase signaling

A family of protein kinases is one of the largest gene families identified in the human genome. Dysregulation and mutation of these proteins play vital roles in human disease. Human protein kinase families are classified as protein-serine/threonine kinases, protein-tyrosine kinases, tyrosine-kinase-like proteins and protein kinase pseudogenes (pseudokinases). Mitogen-activated protein (MAP) is a member of the protein kinase family, consisting of serine and threonine cytoplasmic protein kinases, and has been subjected to conserved function and regulation in eukaryotes. This sub-family includes the p38 kinase family, extracellular signal-regulated kinase (ERK) family and the c-Jun N-terminal kinase family (JNK). MAPK is activated by catalysing the phosphorylation of such substrate proteins as protein kinases, transcription factors and phosphatases, and other functional proteins. In common with all protein kinases, ERK1/2 consist N- and C-terminal extensions that are involved in signaling specificity (Lu and Xu, 2006, Roskoski, 2012). MAPK/ERK signalling pathway is a chain of proteins, located in the cell that induce a signal from a receptor on cell surface to the DNA in the nucleus of the cell. Abnormal regulation of ERK1/2 pathways has been reported in number of breast cancer progression models. In addition, CSCs can be derived from cultured mammary cells following ERK1/2 activation and induction of EMT (Whyte et al., 2009).

FGF signaling is modulated and regulated at multiple levels both extracellular and intracellular. FGF ligands are regulated by binding to cell surface HSPGs or binding to FGFR–HSPG complexes as co-receptor for FGF ligands, enabling dimerization of FGFR intracellular domains and inducing intracellular tyrosine kinase phosphorylation (Guimond and Turnbull, 1999, Lin and Wang, 2010). Then downstream signaling from FGFR–HSPG results in phosphorylation cascade in proteins of the Ras-Raf MAPK pathway. Ras activation induces a further multistep phosphorylation cascade, resulting in the activation of MAPKs such as ERK1/2 (Figure 1.11). Finally, pERK1/2 regulates the transcription of molecules correlating with activities including, proliferation, survival, and transformation (Yashiro and Matsuoka, 2016).

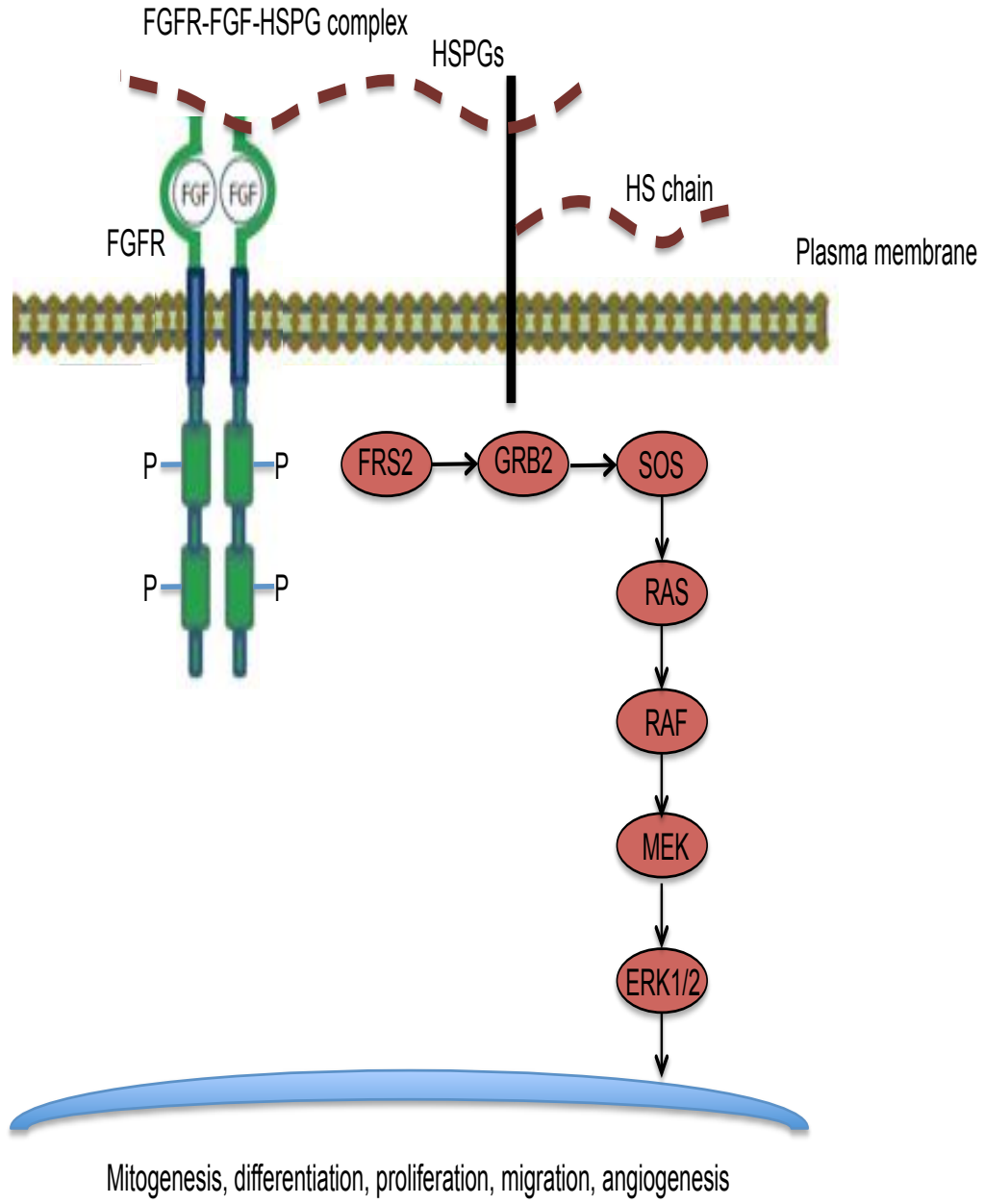

Figure 1.11 The role of HSPGs/ERK1/2 signaling in breast cancer. Cell surface HSPGs associated with FGF ligands form active dimers and activate the FGFR. FGF/FGFR/HSPG complex induces intracellular tyrosine kinase phosphorylation and docking of adapter molecules such as FRS2 protein, which in turn activates SOS and GRB2, which then further activates downstream pathways, including Ras-Raf-MAPK(ERK1/2). HSPG: Heparan sulfate proteoglycan; FGF: Fibroblast growth factor, FGFR: Fibroblast growth factor receptor; FRS2α: FGFR substrate 2α; GRB2: Growth factor receptor-bound 2; SOS: Son of sevenless; GAB1: GRB2-associated binding protein 1.

1.11 Work leading to current studies

Preliminary work from our group demonstrated that non-anticoagulant chemically modified heparin derivatives are required for inhibiting galectin-3-mediated endothelial cancer cell adhesion, angiogenesis and metastasis (Cheng et al., 2015). Moreover, FGF has been studied as a model example for regulation of HS-protein interaction. HS-FGF2 binding signaling is regulated through various FGFR isoforms and there is evidence that HS saccharides are receptor and ligand specific modulators of activity. Taken together, and considering the requirement of HS/FGF/FGFR binding in regulation downstream signaling such as MAPK and STAT3 in various types of cancer, it is likely that HSPGs facilitates FGF signaling and vice versa, in an HS-dependent manner, that is relevant to regulation of CSCs.

This raised a number of questions to be addressed in the current study including; (i) is endogenous HS required for CSC functions?; (ii) do HS structures have a pivotal role in regulation of CSCs?; and (iii) could this information be exploited to synthesize artificial substrates with CSC regulatory properties?

1.12 Project Aims

From the above introduction, it is evident that HS is a highly sulphated polysaccharide found at the cell surface where it is known to interact with a variety of proteins important for tumour development. This interaction invokes changes in intracellular signaling pathways that can regulate cellular processes such as proliferation, differentiation, adhesion and migration. Evidence suggests that different forms of HS, with different degrees and patterns of sulphation, exist at the surface of different cell types where it performs cell type-specific functions. The broad aim of this thesis was to use HS, heparin and chemically modified heparin derivatives to explore possible roles for HS in the regulation of cell fate in cancer stem cells (CSCs).

This will be achievable by:

1. Determining markers (CD44 and CD24) that will allow CSC-like subpopulations to be distinguished in BCC lines.
2. Developing this model system for characterizing differences between cell populations of normal and CSC ($CD44^-/CD24^-$, $CD44^+/CD24^-$, $CD44^-/CD24^+$ and $CD44^+/CD24^+$) sub-populations from BCC lines in terms of metastatic characteristics such as proliferation, invasion, migration, adhesion, apoptotic rates, clonogenic properties.
3. Establishing whether interference with endogenous HS present in CSCs by addition of exogenous HS/heparin/modified heparins can alter the phenotype of CSCs, making them less likely to form tumours and/or more sensitive to chemotherapy.
4. Investigating a potential role and mechanisms of action of exogenous HS/heparin/chemically modified heparins on CSCs via controlling signalling and other molecular pathways.

Overall, this study will explore whether it is possible to regulate cancer cell phenotype by manipulating the stem cell niche via HS glycans, and begin to establish an understanding of the structure-activity relationships and molecular mechanisms involved, hoping ultimately to develop small molecule therapeutics that target CSCs to reduce cancer cell invasion/metastasis.

2 Materials and methods

2.1 Materials

2.1.1 GAGs

Porcine intestinal mucosal heparin (PMH) was purchased from Celsus Laboratories (www.heparin.com, Cat. No. PH-3005, Ohio; USA). Porcine mucosal heparan sulfate (PMHS) and chemically modified heparins (PerS H, NAc H, 2 deS-NS H, 6 deS-NS H, 2 deS-Nac H, 6 deS-NAc H, 2,6 deS-NS H and 2,6 deS-NAc H) were contributed by Dr. Edwin Yates and Dr. Yasser Ahmed, Biochemistry Dept., University of Liverpool, UK.

2.1.2 Antibodies and Dyes

APC-conjugated human CD44 (clone: DB105) # 130-095-177; FITC-conjugated human CD44 (clone: DB105) # 130-095-195; Monoclonal CD24 antibodies human conjugated to FITC (clone: 32D12) # 130-095-952; CD24-FITC, human (clone: 32D12) # 130-099-118; CD24-FITC, human (clone: 32D12) # 130-099-118; CD133/1 (AC133)-PE, human # 130-080-801; FITC-conjugated mouse IgG1 isotype control # 130-092-213; APC-conjugated mouse IgG1 isotype control # 130-092-214 and PE- conjugated mouse IgG1 # 130-092-212 were bought from (MACS Miltenyi Biotec, UK); Annexin V, Alexa Fluor® 488 conjugate # A13201 was from Life technology, (Paisley, UK). Phospho-p44/42 MAPK (Erk1/2) (Thr202/Tyr204) (D13.14.4E) XP Rabbit mAb # 4370; P44/42 MAPK (Erk1/2) Antibody # 9102; Phospho-STAT3 (Tyr705) Antibody # 9131; STAT3 (D3Z2G) Rabbit mAb # 12640; Histone H3 (3H1) Rabbit mAb # 9717; Tubulin (11H10) Rabbit mAb # 2125 were purchase from Cell Signaling Technology, UK). Donkey anti-rabbit IgG-HRP:sc-2313 was acquired from Santa Cruz Biotechnology, UK). DAPI, FluoroPureTM grade was purchased from Life technology (Paisley, UK # 000000010236276001). Propidium iodide (PI) # P4170-10MG was purchased from Sigma (Poole, UK). Precision Plus Protein™ WesternC™ prestained protein standardsv # 161-0376 were purchased from Bio-Rad, UK.

2.1.3 Cell lines

Human BCC lines (MDA-MB-231, Hs578-T, MCF-7-A-1, T47D, and ZR-751-1) were kindly provided by Prof. Philip Rudland and Dr. Roger Barraclough, Biochemistry Dept., University of Liverpool, UK.

2.1.4 Chemotherapeutic regents

All chemotherapeutic agents (cisplatin (Cis), tamoxifen citrate (Tam) and doxorubicin (Dox) were purchased from Sigma-Aldrich (Dorset, UK).

Recombinant Human IL-6 Protein # 206-IL-010 was purchased from R&D Systems (Wiesbaden, Germany). FGF-2 was kindly provided by Prof. David Fernig Biochemistry Dept., University of Liverpool, UK.

2.1.5 Hormone solutions

Hydrocortisone-water soluble 100 mg # H0396 and Insulin from porcine pancreas 10 mg # I5523 were purchased from Sigm-Aldrich, life technology (Dorset, UK).

2.1.6 Reagents

All common chemicals were of analytical grade; a list of chemicals, their suppliers and catalogue numbers shown in Table 2.1.

Table 2.1 Chemicals used and suppliers

Reagents and Solutions	**Suppliers and catalogue number**
Accutase® solution, 100 ml	Sigma-aldrich, Cat. No. A6964
30% Acrylamide/Bis Solution 19:1 500 ml	BIO-RAD, CAT. No.161-0154
Agar ultrapure (Nobel agar) 100 gm	Affymetrix, Cat. No. 10907
Agarose,low gelling temperature 5 g	Sigma-aldrich, Cat. No. A9414
Ammonium Persulfate	BIO-RAD, Cat. No. 161-0700
Bovine Serum Albumin (BSA), 100 g	Sigma, Cat. No. A9647
Cell Lysis Buffer	Cell Signaling Technology, Cat. No. 7018

Complete protease inhibitors cocktail tablets	Roche, Cat, No. 04693116001
Control siRNAs	Santa Cruz Biotechnology, Cat. No. sc-37007
Clarity ™ Western ECL Substrate	BIO-RAD, www.bio-rad.com, Cat. No. 170-5061
Dimethyl sulfoxide (DMSO)	Sigma, Cat. No. D2650-100ML
Distel Ready-to-use spray (1:100), clear unfragranced, 500 ml	Star lab, Cat. No. TM301
Distel concentrate, clear, unfragranced, 5 L container	Star lab, Cat. No. M309
DNase I recombinant, Rnase-free	Roche, Cat. No. 04716728001
Dulbecco's Modified Eagle Medium 1x (DMEM) medium	Gibco by life technologies, CAT. No. 41966-029
Dulbecco's phosphate buffered saline PBS (1x) 500 ml (Cell culture)	Invitrogen / Gibco, No. 14190-094
EDTA	Sigma, Cat. No. E5134
Ethanol	BDH, Cat. No. 1047 EUN1170
Fibronectin from bovin plasma 1 mg	Sigma, Cat. No. F4759
L-glutamine 200 mM	Invitrogen / Gibco, No. 25030-024
Glycine	Fisher Sientific, G/0800/60
Guava Check Kit	Merck Millipore, Cat. No. 4500-0020
Guava ICF Instrument Cleaning Fluid, 100ml	Merck Millipore, Cat. No. 4200-0140
HAEMA – LT-SYS ® Quick-Stain (Diff-Quick)	Labor + Technik, Cat. No. LT-SYS
Hank's Balanced Salt Solution 1x (HBSS)	Invitrogen/ Gibco, No. 24020-091
Heat inactivated fetal bovine serum (FBS) 500 ml	Gibco by life technologies, Cat. No. 10500-064
High Pure RNA Isolation Kit	Roche, Cat. No. 11828665001
Hydrochloric acid	BDH, Cat. No. 450023K
LightCycler® 480 SYBR Green I Master	Roche, Cat. No. 04707516001
MEM Non-essential amino acid solution 100x	Sigma life science, Cat. No. M7145
2-Mercaptoethanol, 100 ml	Sigma, No. M3148-100ML
Methanol, 2.5 L	Thermo Fisher Scientific, No. M/4000/PC17
Minimum essential medium (MEM) 1X	Gibco by life technologies, CAT. No. 31095-029
MTT (3-(4,5-Dimethyl-2-thiazolyl)-2,5-	Sigma, No. M2128

diphenyl-2H-tetrazolium bromide)	
PBS (Dulbecco A Tablet) (Lysis)	OXOID, Cat. No. BR0014G
PathScan® Intracellular Signaling Array Kit (Chemiluminescent Readout)	Cell Signaling Technology, Cat. No. 7323
Pen/ Strep 10.000 units	Invitrogen / Gibco, No. 15140-122
Pierce TM BCA Protein Assay Kit 1 L	Thermo Fisher Scientific, Cat. No. 23227
Ponceau S solution	Sigma Aldrich, Cat. No. P7170-1L
Precision Protein™ StrepTactin-HRP Conjugate 125 µl	BIO-RAD, Cat. No. 1610381
RNaseZap^{TM} 250 ml	Sigma-aldrich, Cat. No. R2020
siRNA Transfection Reagent	Santa Cruz Biotechnology, Cat. No. sc-29528
RPMI 1640 medium (1x) 500 ml	Invitrogen/Gibco, Cat. No. 21875-034
Sodium chloride	Fisher Sientific, Cat. No. S/3160/60
Sodium pyruvate 100 ml	Sigma life science, Cat. No. S8636
Sodium dodecyl sulfate 500 g	Fisher Sientific, No. S/5200/53
Sodium orthovanadate (Na_3OV_4) ≥90% (titration)	Sigma, Cat. No. S6508-10G
TEMED (N,N,N′,N′-Tetramethylethylenediamine)	BIO-RAD, www.bio-rad.com, Cat. No. 161-0800
Transcriptor High Fidelity cDNA Synthesis Kit	Roche, Cat. No. 05081955001
Tris (hydroxymethyl) methylamine	Fisher Sientific, Cat. No. T/P630/60
Trypsin-EDTA solution	Sigma, Cat. No. T3924-100 ml
0.4% Trypsin Blue Solution	Sigma, Cat. No. T8154- 20 ml
10% Tween 20 Solution	BIO-RAD, Cat. No. 161-0781
Water	Deionised obtained from a water purifier or commercial supplier.

2.1.7 Buffers

2.1.7.1 Preparation of Western blot buffers

PBS

1 Tablet was added to 100 ml distilled water (dH_2O) and sterilized by autoclaving at 115°C for 10 min.

1.5 M Tris-HCl pH 8.8

181.65 g Tris base was dissolved in approximately 800 ml of dH_2O. The pH was adjusted to 8.8 with fuming HCL. 200 ml of dH_2O was added to bring the volume to 1 L.

1 M Tris-HCl pH 6.8

60.55 g Tris base was dissolved in 700 ml of dH_2O. The pH was adjusted to 6.8 with fuming HCl and volume adjusted to 1 L with dH_2O and stored at RT.

10X Tris-Glycine Buffer

For 1 L, 30.3 g Tris base and 144.0 g Glycine added to 900 ml dH_2O and stored at RT.

1X SDS-PAGE Running Buffer (1 L)

For protein separation during SDS-polyacrylamide gel electrophoresis: 100 ml 10x Tris-Glycine Buffer and 10 ml 10% SDS was diluted to 1L dH_2O and stored at 4°C.

1X Tris-glycine Transfer Buffer (1 L)

For protein transfer from SDS-PAGE gels to nitrocellulose membrane: 100 ml 10x Tris-Glycine Buffer and 200 ml Methanol were added to 700 ml dH_2O and stored at 4°C.

10X Tris-buffered saline (TBS) 1 L

24.2 g Tris base and 80 g NaCl were added to 800 ml dH_2O. The pH was adjusted to 7.4 with fuming HCl and the volume made to 1 L with dH_2O and stored at RT.

1X Tris-buffered saline with Tween (TBST) 1 L

For washing nitrocellulose membranes for during western blotting: 100 ml 10x TBS and 2 ml Tween-20 were made to 1 L with dH_2O or distilled water and stored at RT.

10X SDS

5 g SDS added to 100 ml dH_2O or distilled water and stored at RT.

2X Loading buffer

Loading sample buffer was used protein extraction and for loading of protein samples onto SDS-polyacrylamide gels for SDS-PAGE and Western Blotting: 4% SDS, 20% glycerol, 10% (v/v) 2-mercaptoethanol and 0.004% (w/v) bromophenol blue in 0.125 M Tris-HCl, pH 6.8.

Blocking buffer (5% BSA)

For 100 ml, 0.5 g of BSA added 100 ml of 1x TBS-T and stored at 4°C.

Preparation of sodium orthovanadate Na_3VO_4 stock solution (100X)

1 mM stock was prepared in dH_2O adjusted to pH 10. Orange colour was observed due to decavanadate. The solution was boiled by heating in a microwave for 5 to 15 sec until translucent. Colourless monovanadate was observed over several hours due to depolymerisation of decavanadate; the solution was placed on ice for 5 min. Then, solution was readjusted to pH 10. The cycles of boiling, cooling and adjusting pH were repeated many times until reaching the point of stabilization at pH 10. Solution was aliquoted and stored at -20°C.

Preparation of cOmplete solution (100X conc.)

One cOmplete tablet was dissolved in 500 µl dH_2O, PH 7. Stock solution was aliquot and stored at -20°C.

Lysis buffers (RIPA buffer)

For 100 ml, 150 mM NaCl, 1.0% IGEPAL, 0.5% sodium deoxycholate, 0.1% SDS and 50 mM Tris-HCl, pH 8.0 were added to the final volume 100 ml of dH_2O into a cylinder Filtered through a 0.45 filter and stored at 4°C.

Immediately prior to lysing cells, 200x 200 mM sodium fluoride (NaF), 100x sodium orthovanadate (Na_3OV_4) and 100x complete protease inhibitor cocktail were combined/250 µl of RIPA lysis buffer to prevent proteolysis and maintain phosphorylation status of proteins.

Stripping buffer (100 ml)

2% SDS (20 ml of 10% SDS), 62.5 mM Tris-HCl pH 6.8 (12.5 ml Tris-HCl pH 6.8, 0.5M), 67.5 ml dH_2O and 100mM β-Mercaptoethanol (700 µl of liquid b-ME) were mixed and sored at RT.

2.1.7.2 Preparation of PathScan buffers and antibodies

Preparation of 1X cell lysis buffer for PathScan assay

1x Cell lysis buffer were thawed, mixed thoroughly and supplemented with complete protease inhibitor cocktail to a final concentration of 1 mM.

1X Array wash buffer

1x Array wash buffer was prepared by diluting of 1 mL of 20x Array wash buffer in 19 ml dH_2O and kept at RT.

1X Detection antibody cocktail

For running 1 slide: 150 µl of 10x Detection antibody cocktail was diluted with 1350 µl of array diluent buffer and kept on ice.

1X HRP-linked streptavidin

For running 1 slide: 150 µl of 10x HRP-linked Streptavidin was diluted with 1350 µl of array diluent buffer and kept on ice.

1X LumiGLO® and peroxide solution

To make 10 ml of 1x LumiGLO® and peroxide solution, 9 ml of dH_2O were combined with 0.5 ml of 20x LumiGLO® and 0.5 ml of 20x Peroxide. 1x LumiGLO® and peroxide solution was Diluted and combined immediately before use.

2.1.7.3 Preparation of fibronectin

Fibronectin stock was prepared by dissolving 1 mg/ml fibronectin in 0.9% PBS and aliquots have been made and saved at -20°C. Immediately, before coating, a final concentration of 15 µg/ml has been made and 2.5 µg/cm^2 of culture cells has been added, 5 µg/well of fibronectin was coated in a 24-well plate.

2.1.7.4 Preparation of hormone solutions

Insulin

Stock: Insulin stock was prepared by dissolving 1 mg/mL insulin in 0.9% PBS + 0.005 m HCl (4.5 µl cHCl in 10 ml), then filter sterilized.

Routine Solution: 5 µg/ml in 0.001m HCl in PBS.

1 mL Stock (1 mg/ml) + 0.18 ml cHCl + 200 ml sterile saline.

Then 5 ml aliquots were prepared in bijou bottles, and stored in -20°C. One aliquot per 500 ml bottle of medium was used.

Hydrocortisone

Stock: 1 mg/ml in 100% Ethanol.

Routine Solution: 5 µg/ml in 25% Ethanol in PBS.

1 ml stock (1mg/ml) + 50 ml Ethanol + 150 ml sterile PBS.

Then, 5 ml aliquots were prepared in bijou bottles and stored in -20^{o}C. One aliquot per 500 ml bottle of medium was used.

2.1.8 Equipment

Equipment used in this study is listed in Table 2.2

Table 2.2 Equipment used and suppliers

Equipment	**Suppliers and catalogue number**
Centrifuge	Centrifuge 5804, Eppendorf, Cat. No. 1T5804 000.013
Analytical balance	Mettler and Toledo, Cat. No. AB54-S
Centrifugal evaporator	Speed Vac SPD121P, ThermoSavant, uk.vwr.com, Cat. No. 195-227
Cover glass	VWR, cat no: 631-0149
Dissecting microscope	Motic, K401, GDC Microscopes (Surrey, UK)
DVC camera	Model. 1310c-FW-OO; digital images recorded using DVC view version 2.2.8 software
Filter syringe	Sterile Minisart® 0.2µm CE, Sartorius stedim biotech, Cat. No. 16534.
Filter Bottle top	Polysulfone Nalgene®, uk.vwr.com, Cat. No. 516-0578 with 0.2 µm, 47 mm I.D. cellulose acetate membrane filters, Nalge Nunc, Fisher Scientific, Cat. No. 13TFDM-309-100Q.
Freeze dryer	Heto PowerDry PL3000,
Gel electrophoresis system • Power Supplies 300V • Mini Trans-Blot Cell Module 1703811 • Mini-PROTEAN Tetra Cell Handcasting accessory kit	Mini-PROTEAN tetra cell system, Bio-Rad

1653370 • Mini-PROTEAN system Casting stand 1658050 • Mini PROTEAN System Glas Plates 1653308 • Supported Nitrocellulose Membrane 162-0094 • Mini-PROTEAN TGX Gels 456-1031	
Heat block	Grant, Cat. No. QBT2
LightCycler® 480 Instrument II 96-well version	Roche, Cat. No. 05015278001
LightCycler® 480 Multiwell Plate 96	Roche, Cat. No. 04729692001
Microcentrifuge	Eppendorf minispin,
PH meter	Jenway, Cat. No. 3505
Plates: • 96 wells Maxisorp: • 96 conical-bottom wells: • 4 wells plate: **Corning® 96 wells TC:** • Corning® BioCoat™ Matrigel® Invasion Chambers with 8.0µm polyethylene terephthalate (PET) Membrane in two 24 Well Plates, 24/Pack, 24/Case. • Corning® Costar® Transwell® cell culture inserts 6.5mm Transwell® with 8.0µm Pore Polycarbonate Membrane Insert, Sterile (Corning, Bedford, USA).	 Nunc, uk.vwr.com, Cat. No. 735-0083 Nunc, uk.vwr.com, Cat. No. 732-0191 Nunc, uk.vwr.com, Cat. No. 734-2176 Corning, www.corning.com, Cat. No. #3595 Corning, www.catalog2.corning.com, Cat. No. #354480) Corning, www.catalog2.corning.com, Cat. No. #3422)
Plate reader	Thermo MultiSKAN EX
Rocker-GYRO	Stuart Scientific www.stuart-equipment.com
Rotator	SB2, Stuart Scientific www.stuart-equipment.com
Summit Balances	Denver Instrument, Cat. No. S-602.

Tubes: • 1.5 mL Micro tubes, Cat. No. 72.690.001 • 0.5 mL Micro, Cat. No. 72.699 • 2.0 mL Crystal clear M/C tubes, Cat. No. E 1420-2000 • CELLSTAR® Centrifuge Tubes, Polypropylene, Sterile, Greiner Bio-One, 15 ml, 188261 • CELLSTAR® Centrifuge Tubes, Polypropylene, Sterile, Greiner Bio-One, 10 ml, 227261	• SARSTEDT, (autoclaved) • StarLab, www.starlabgroup.com VWR, http://us.vwr.com
Vortex	VWR, uk.vwr.com, Galaxy mini
Water bath	Grant JB Series, www.grant.co.uk

2.2 Methods

2.2.1 Cell culture

2.2.1.1 BCC medium

MDA-MB-231 and Hs578-T cell lines: High glucose DMEM medium was supplemented with 10% (Heat inactivated FBS sreum), 1 µg/ml insulin from porcine pancreas, 500 ng/ml hydrocortisone-water soluble, 1% pen/strep and 2 mM/l-glutamine.

T47D and ZR-75-1 cell lines: PRMI-1640 medium was supplemented with 10% (Heat inactivated FBS sreum), 1 µg/ml insulin from porcine pancreas, 500 ng/ml hydrocortisone-water soluble, 1% pen/strep, 2 mM/L-glutamine and 1 mM Sodium Pyruvate (NaP)

MCF-7-A-1 cell line: To make the complete growth medium, the following components were added to the base MEM medium: 0.01 mg/ml human recombinant insulin, 500 ng/ml hydrocortisone-water soluble, 2 mM L-Glutamine, 1% pen/strep, 1% Non ssential Amino Acids (NEAA), heat inactivated FBS to a final concentration of 10%.

2.2.1.2 Routine culture of BCCs

Human BCC lines (MDA-MB-231, Hs578-T, T47D, ZR-75-1 and MCF-7-A) were routinely maintained in standard tissue culture flasks in growth medium supplemented with 10% (Heat inactivated FBS), 1µg/ml insulin from porcine pancreas, 500 ng/ml hydrocortisone-water soluble, 1% pen/strep and 2 mmol/l L-glutamine. All cultures were maintained at 37^{o}C in a humidified atmosphere containing 5% CO_2. Cells were then washed twice with PBS, trypsinized with 0.1% trypsin and 0.1% EDTA and passaged at a ratio of 1:3 three times a week.

2.2.1.3 Freezing cells

It is important for future studies to freeze cells as a seed stock and store them as soon as they become available from sub-culturing. Cryopreservation ensures that there is a back-up of cells if needed at any time or in case of loss of cell supply or contamination. Freezing medium was made by supplementing the cells in normal growth medium, with addition of an equal volume of 40% warm FBS and 10% DMSO. Briefly, medium was removed from the T75 cm^2 culture flask and cells were washed twice with PBS, followed by trypsinisation with 1x trypsin/EDTA for 3-5 min. Once cells were detached, cells were neutralized with equal volumes of growth medium. 90% confluent viable cells were counted in order to achieve a good recovery after freezing, before harvesting the cells by centrifuging at 1000 rpm for 5 min; the supernatant was again discarded and cells were re-suspended and seeded at a concentration of 2×10^6 cells/ml in freezing medium. New cryovials were labeled with the cell line name, cell concentration, passage number and date. Typically a 0.5 ml volume of cells was added in a cryovial, and freezed slowly by placing them at -20°C for 2-3 hrs, then overnight at -80°C. The cells were then transferred to liquid nitrogen if long-term storage was necessary.

2.2.1.4 Thawing frozen Cells

Thawing frozen cells is stressful to the desired cells, so thawing cells with a good and fast technique is crucial way to ensure the viability and functionality of a high proportion of the cells.

The cryovial containing the frozen cells was removed from liquid nitrogen and thawed rapidly (<1 min) in a 37°C water bath by holding and gentle flicking of the cryovial on water bath surface. The outside of the cryovial was dried and wiped with 70% ethanol solution before opening to avoid contamination. The cells were then re-suspended slowly into pre-warmed growth medium and centrifuged at 1000 rpm for 3 min. Medium was removed and cells re-suspended with appropriate medium depending on cell type. And cells were finally transferred to a T75 cm^2 culture flask and incubated at 37°C, 5% CO_2.

2.2.1.5 Cytotoxicity cell culture preparation

2.2.1.5.1 Chemotherapeutic agents preparation

Doxorubicin (Dox): The stock solution of doxorubicin was made by adding 10 mg of doxorubicin to 100 µl of DMSO and suspended in 10 ml of dH_2O to a final concentration 1 mg/ml.

Cisplatin (Cis): The stock solution of cisplatin was made by dissolving this agent in PBS for a final concentration of 100 mM.

Tamoxifen (Tam): The stock solution of tamoxifen citrate was prepared by dissolving tamoxifen in PBS at a concentration of 10 mM.

In order to obtain pharmacologically relevant final concentrations of these chemotherapeutic agents, the stock solutions were diluted in the culture medium to indicated concentrations when inducing apoptosis.

Due to their toxicity, all precautions for handling Tam, Dox, and Cis were taken according the COSHH assessment and material safety data sheet delivered by the manufacturer.

2.2.1.5.2 Cytotoxicity cell culture

Approximately $1x10^5$ cells/ml of isolated cell populations were seeded and placed in 24 well plates containing 2 ml of growth medium and incubated for 24 hrs in a humidified incubator of 5% CO_2. Cells were treated the following day with different concentrations of chemotherapeutic agents (Dox 1, 5, 10 µg/ml, Cis 0.001, 0.01, 0.1,

1, 10 μM and Tam 1, 10, 100, 1000, 10000, 100000 nM; and incubated for different time points 24, 48 and 72 hrs.

2.2.1.5.3 HS/heparins and chemically modified heparin treatments

To examine the effects of HS/ heparin and chemically modified heparins on BCSC apoptosis, $1x10^5$ cells/ml of isolated cells were cultured in 6 well plates and incubated for 24 hrs in a humidified incubator of 5% CO_2. Cells were treated the following day with the optimum concentration of chemotherapeutic agents (Dox; 5 μg/ml, Cis; 0.1 μM, Tam; 10 μM) with or without 10 ng/ml HS/heparin or chemically modified heparin (PerS H, NAc H, 2-deS-NS H and 2,6 deS-NS H) and incubated for 48 hrs, before measurement of apoptosis (see section 2.2.1.5.2). Cells were compared with a negative control that was incubated in the absence of inducing agents.

2.2.2 Flow cytometry

2.2.2.1 Flow cytometric analysis of BCS-like cell surface marker expression

Based on cell surface marker phenotype, cells were grown in monolayer culture in tissue culture flasks at a density of 1×10^6 cells/$75cm^2$ flask in complete medium, cultured for 48 hrs. After the incubation period, cells were washed twice with PBS and harvested with accutase as a replacement for trypsin/EDTA. The resulting detached cells were centrifuged at 300 xg for 5 min. Medium was removed and blocked with PBS containing 5% FBS and incubated on ice for 20 min. After blocking, flurochrome-conjugated monoclonal antibodies against human CD44 (APC, FITC); CD24 (FITC, PE, APC); CD133 PE or their respective isotype controls (FITC, APC and PE-conjugated mouse IgG1 isotype controls) were added to the BCC suspensions at the concentrations recommended by the manufacturer (Table 2.3). A total of 1×10^5 cells/100 μl were incubated with specific antibodies at 4°C in the dark for 30 min. Unbound antibody was washed out with two cycles of washing with PBS + 5% FBS and resuspended in 0.5 ml (per million cells) of PBS + 5% FBS. The cells were then analysed using flow cytometry analysis (FACSCalibur cytometer from Becton Dickinson) and at least 40,000 events per sample were collected. Positive staining was considered based on the negative of an isotype control. Percentages of cells expressing CSC markers (CD44, CD24 and CD133) were

calculated from histograms and dot plots using Flowing Software (version 2.5.0).

2.2.2.2 Role of heparin/HS and heparin derivatives on stem-like cells in BCC lines

MDA-MB-231 and Hs578-T cells were cultured at a density of 2×10^5 in 10% FBS DMEM medium in 25 cm^2 culture flasks at 37 °C in a 5% CO_2 incubator for 24 hrs. After that, the medium was discarded and replaced with an equal volume (5 ml) of fresh medium containing various concentrations (0, 1, 10, 100, ng/ml, 1, 10, 100 µg/ml) of heparin, HS and modified heparins (Porcine Mucosal Heparin (PMH), Porcine Mucosal HS (PMHS), PerS H (1), NAc H (2), 2 deS-NS H (3), 6 deS- NS H (4), 2 deS-NAc H (5), 6 deS-NAc H (6), 2,6 deS-NS H (7) and 2,6 deS-NAc H (8)), then cells were incubated for an additional 48 hrs. Cells were washed twice with PBS and harvested with accutase for 7 min at 37°C. The resulting detached cells were centrifuged at 300 xg for 5 min then washed with PBS containing 5% FBS and incubated on ice for 20 min. Cells were labelled with a combination of 1:1000 of CD44 APC and 1:100 of CD24 FITC or their respective isotype controls and incubated at 4°C in the dark for 20 min. After incubation, cells were washed through two cycles of washing with PBS + 5% FBS and resuspended in 0.5 ml of PBS + 5% FBS. The cells were then analysed by flow cytometry (FACSCalibur cytometer from Becton Dickinson) and at least 30,000 events per sample were collected. Percentages of cells expressing $CD44^+/CD24^-$ were calculated from histograms and dot plots using Flowing Software (version 2.5.0).

2.2.2.3 Fluorescent-activated cell sorting (FACS)

Cell sorting was performed by Miss Carolyn Rainer and Sandra C. P. Cachinho, using flow cytometry (FACSAria III cell sorter, Becton Dickinson); at the cell sorting and flow cytometry core facility, Technology Directorate, University of Liverpool, UK). MDA-MB-231 and Hs578-T cells were prepared in a single-cell suspension form at a concentration of 5×10^6 cells/ml. In brief, cells were harvested using accutase for 7 min and transferred to 15 ml conical tube containing FBS and centrifuged at 300 xg for 5 min. The supernatant was then discarded and cells re-suspended in 1 ml of normal growth medium. Cells were counted by hemoytometer and seeded at 5×10^6 cell/ml, following centrifugation at 300 xg for 5 min and re-

suspension with PBS/10%FBS. Cell suspensions were filtered through a 0.22 µm MilliexGP filter unit to help disaggregate clumps prior to analysis and incubated on ice for 20 min. After the incubation period, each cell line was labeled with a combination of two different fluorescent dyes (APC-conjugated human CD44 and Monoclonal CD24 human conjugated to FITC antibodies) and their isotypes as a negative controls (FITC-conjugated mouse IgG1 and APC-conjugated mouse IgG1 isotype control) at the concentrations recommended by the manufacturer (Table 2.3). Labeled cells were incubated at 4°C, protected from light for 30 min. Unbound antibody was washed out through two cycles of washing with PBS + 5% FBS and re-suspended in 1.5 ml (per 5×10^6 cells) of PBS + 5% FBS. At the end of experiment, cells were labeled with DAPI staining at a concentration of 1:10000. A minimum of 10,000 events was recorded for all samples. Negative isotype controls were set in the first quadrant in the right bottom of the plot and gates were administrated. $CD44^-/CD24^-$ resides in the P7, $CD44^+/CD24^-$ in P4, $CD44^+/CD24^+$ in P6 and $CD44^-/CD24^+$ in P5. $CD44^-/CD24^-$, $CD44^+/CD24^-$, $CD44^+/CD24^+$ and $CD44^-/CD24^+$ cells were isolated in four separate tubes and cultured in $75cm^2$ culture flasks at 37 °C in a 5% CO_2 incubator. The culture medium was changed daily and the cell morphology was observed. When the cell number reached confluency, the cells were tested in different experiments to characterize the CSC properties and to evaluate the role of HS and modified heparin on CSC sub-populations.

Table 2.3 Antibody concentrations used in FACS

Antibodies	Dilution factor	Sample volume
APC-conjugated human CD44	1.1000	100 µl
FITC- conjugated human CD44	1.1000	100 µl
FITC- conjugated human CD24	1:100	100 µl
APC-conjugated human CD24	1:50	100 µl
PE-conjugated human CD24	1:50	100 µl
CD133/1 (AC133)-PE, human	1:11	100 µl
FITC-conjugated mouse IgG1 isotype control	1:100	100 µl
APC-conjugated mouse IgG1 isotype control	1:100	100 µl
PE- mouse IgG2b, isotype control	1:100	100 µl

2.2.2.4 Apoptosis by flow cytometry

The indices for MDA-MB-231 and Hs578-T BCC apoptosis and necrosis were quantified using flow cytometry as a percentage of Phosphatidylserine (PS) translocation. PS is expressed on the membrane and precedes the loss of membrane integrity resulting from either early apoptosis (detected by Annexin V, Alexa Fluor® 488 conjugate binding) or late apoptosis (DNA of necrotic processes that was quantified by propidium-iodide (PI) uptake due to leaky plasma membrane).

Cells were harvested and washed twice with PBS followed by trypsinisation with accutase for 7 min. Cells were centrifuged at 1000 rpm for 5 min. The media was removed and cells re-suspended at $1x10^6$ cells/ml in fresh medium in a $75cm^2$ culture flask. To measure apoptotic responses of cells, cells were treated with appropriate treatments (see section 2.2.1.5.2, 2.2.1.5.3). Cells were compared with a negative control that was incubated in the absence of inducing agents. Incubated was carried out for appropriate time points (see section 2.2.1.5.2). Cells were harvested again after the incubation period and washed twice with PBS, followed by trypsinization with accutase for 7 min and centrifugation at 1000 rpm for 5 min, then counting by

hemocytometer to seed at 1×10^6 cells/ml. Cells were then re-suspended in 1 ml fresh medium and transferred to 24 well-plate. 25 µl of cell suspension containing $1x10^6$ cells/ml were transfered to 96 well microtiter plate and incubated with 25 µl of HBSS and 0.5 µl of Annexin V, Alexa Fluor® 488 conjugate for 15 min, protected from light at RT. During this time, 1 mg/ml PI stock solution was prepared by adding 25 µl of PI to 200 µl of HBSS. Following this, 200 µl of PI with HBSS was added to 10^6 cells in each well in a 96-well microtiter plate just prior to the flow analysis. According to the manufacturer's instructions, 5000 gated cells were quantified using the Guava Viacount flow cytometer (Millipore). In the early stage of apoptosis, DNA content could be stained with Annexin V, Alexa Fluor® 488 conjugate, whereas cells in the late stage of apoptosis (necrotic stage) were stained by PI staining.

After each measurement of apoptosis by flow cytometry using annexinV/PI staining, the absolute numbers of cells were counted. Briefly, the measurement of % of cells that expressed apoptotic markers (e.g. Annexin V, Alexa Fluor® 488 conjugate binding) could underestimate the cell death level due to cell necrosis or lysis. Therefore, the measurement of apoptosis in all experiments, both the absolute number of cells and the % of apoptotic cells, were routinely measured. In all experiments, it was found that the cell number that recovered after incubation was always > 95% of the initial incubation ($1x10^6$ cells/ml). This indicates that there is no major effect on the values for % apoptosis with this small loss of cells. Therefore, (% apoptosis) values are presented in all experiment in this thesis.

2.2.3 Microscopy

2.2.3.1 Bright phase

$CD44^+/CD24^-$ sorted cells from MDA-MB-231 and Hs578-T human BCCs were cultured in 6 well tissue culture plates (Corning) at 20×10^3 cells/ well for 24 hrs. After that, cells were treated with either 10 mM sodium chloride (NaCl) or 10 mM sodium chlorate ($NaClO_3$) for a further 48 hrs. Cells were analysed using a bright phase light microscope (×20 magnification).

2.2.4 Cell viability assay (Dye exclusion method)

Briefly, FACS sorted cells from MDA-MB-231 or Hs578-T human BCCs were cultured in 24 well tissue culture plates (Corning) at density of 4×10^4 cells/ well for various time points (24, 48 and 72 hrs). After each time point, cells were washed twice with PBS and trypsinized using EDTA/PBS (2-5 nM) for 5 min. Detached cells were collected and centrifuged at 1000 rpm for 5 min. Cell suspensions were diluted in 0.4% sterile filtered Trypan blue solution at a ratio of 1:1. Cells were counting using a hemocytometer chamber under a microscope at low magnification. The number of total and blue staining cells were counted.

Viable cells = [1.00 – (Number of blue cells ÷ Number of total cells)]

2.2.5 Cell proliferation (MTT assay)

Briefly, MDA-MB-231 and Hs578-T sorted cell suspensions were harvested by centrifugation at 1000 rpm for 5 min after washing twice with PBS and trypsinizing with EDTA/PBS (2-5 nM). Media was removed and cells re-suspended in fresh medium. 100 µl of cell sub-populations were seeded in a 96-well microtiter cell culture plate at a density of 5×10^3 cells/well. Incubation time was carried out for appropriate time points. 10 µl (5 mg/ml) of 3-[4,5-dimethylthiazol-2-yl]-2,5-diphenyl-tetrazolium bromide (MTT reagent) was added to each well including controls and incubated for 4 hrs at 37°C. Cells were combined with 100 µl of detergent reagent (DMSO) to all wells to dissolve the formazan produced, then, incubated overnight at 37°C. Cell proliferation was determined according to the colorimetric comparison by reading optical density (OD) values from a microplate reader (Thermo, Multiskan EX, UK) at an absorption wavelength of 570 nm. The average values of triplicate culture readings was measured.

2.2.6 *In vitro* cell adhesion assay

For evaluating cellular adhesion, 24-well plates were coated with 15 µg/ml of fibronectin, evaporated under a hood for 20 min, using 3 ml of $5x10^4$ cells/well for either each sorted cell population ($CD44^-/CD24^-$, $CD44^+/CD24^-$, $CD44^+/CD24^+$ and $CD44^-/CD24^+$ from MDA-MB-231 and Hs578-T BCC lines) or for cells treated with

heparin derivatives. Cells were washed twice with PBS and trypsinized with 0.1% trypsin and 0.1% EDTA and incubated for 3-5 min. After trypsinization, cells re-suspended with equal volume of normal growth medium and centrifuged at 1000 rpm for 5 min. Substrates were removed and re-suspended with normal growth medium and seeded at the required number of cells. Cells were incubated for different time courses (0, 1, 3, 5 hrs) at 37°C in humidified incubator with 5% CO_2. After allowing cells to adhere for the fixed time, the plates were taken from the incubator and the media were rinsed away; non-adherent cells were removed and washed twice with PBS. After that, adherent cells were trypsinized with 250 µl/well of 0.1% trypsin and 0.1% EDTA and incubated at 37 °C for 3 min. Cells were re-suspended (1 ml/well) in normal growth medium with 10% FBS. For each replicate (n=3), the mean numbers of adherent cells in triplicate were counted using a hemocytometer by light microscope at 10x magnification, using four independent fields. Data are expressed as a mean number of adherent cells compared to untreated control cells.

2.2.7 *In vitro* matrigel invasion assay

The invasive potential of BCCs was assessed *in vitro* in a Matrigel invasion chambers with 8.0 µm PET membrane. Under sterile conditions, the Matrigel invasion chamber plate was removed from -20°C storage and warmed at RT for 20 min. 500 µl of warm normal growth medium was added to the interior of the inserts and incubated in a humidified tissue culture incubator for 1 hr at 37°C, 5% CO_2 atmosphere to rehydrate the basement membrane layer. After rehydration, the normal growth medium was removed thoroughly but gently without disturbing the Matrigel membrane layer. 600 µl of fresh DMEM medium supplemented with 1 µg/ml insulin, 500 ng/ml hydrocortisone, 1% pen/strep and 2mmol/l L-glutamine and 5 % heat inactivated FBS was added to a new clean 24 well-plate to serve as a chemoattractant to induce invasion. Chambers were transferred by using sterile forceps to the wells containing the chemoattractant. Immediately, 12×10^3 cells of four sub-populations of MDA-MB-231 and Hs578-T sorted cells ($CD44^-/CD24^-$, $CD44^+/CD24^-$, $CD44^+/CD24^+$ and $CD44^-/CD24^+$) either untreated or treated with heparin derivatives were seeded in 100 µl fresh medium containing 1% heat inactivated FBS and added into each upper chamber and incubated for 24 hrs in a humidified cell culture incubator at 37°C, 5% CO_2 atmosphere as outlined in Figure 2.1 After incubation,

the non-invading cells were removed gently from the upper surface of the membrane by swapping gently the interior of the inserts using cotton-tipped swabs. At the end of the experiment, the chambers were washed with PBS then transferred sequentially by sterile forceps to a clean well containing a 500 µl of Diff-Quik solution through each stain solution for 2 min in each stain solution. Each insert was transferred to the microscope slide and cover slip was placed on top of the membrane and gentle pressure applied to expel any air bubbles. A light microscope was used to count invading cells under 10 magnification objective with four individual fields/inserts. Data are expressed as the number of invaded cells per well. The *in vitro* invasion assay was conducted in triplicate, and repeated three times.

2.2.8 *In vitro* migration assay

An *in vitro* transwell migration assay was conducted using 24-well plates with 6.5mm Transwell inserts (8.0µm Pore Polycarbonate Membrane Coated with Cultrex Basement Membrane Extract). The principal technical setup of an *in vitro* transwell migration assay equals the transwell invasion assay that was described above, and outlined in Figure 2.1. The procedure was similarly measured by the placement of a coating of Cultrex Basement Membrane Extract on top of the membrane. In brief, the migration transwell plate was rehydrated with 500 µl warm medium and incubated for 1 hrs at 37°C, in 5% CO_2 atmosphere. After incubation, rehydration medium was carefully removed and chemoatractant media (5% FBS) as placed into the 24 well plate. 12×10^3 MDA-MB-231 and H578-T sorted cells ($CD44^-/CD24^-$, $CD44^+/CD24^-$, $CD44^+/CD24^+$ and $CD44^-/CD24^+$) untreated or treated with heparin derivatives were plated with conditioned medium (containing 1% FBS) on the top of the Transwell. Cells were incubated in humidified cell culture at 37°C, 5% CO_2 atmosphere. After 24 hrs incubation, non-migrated cells in the insert were carefully removed and migrated cells were stained with Diff-Quik solution. The number of migrated cells was observed with a light microscope under 10 magnifications. Mean numbers of migrated cells for triplicates were calculated. The *in vitro* migration assay was repeated three times.

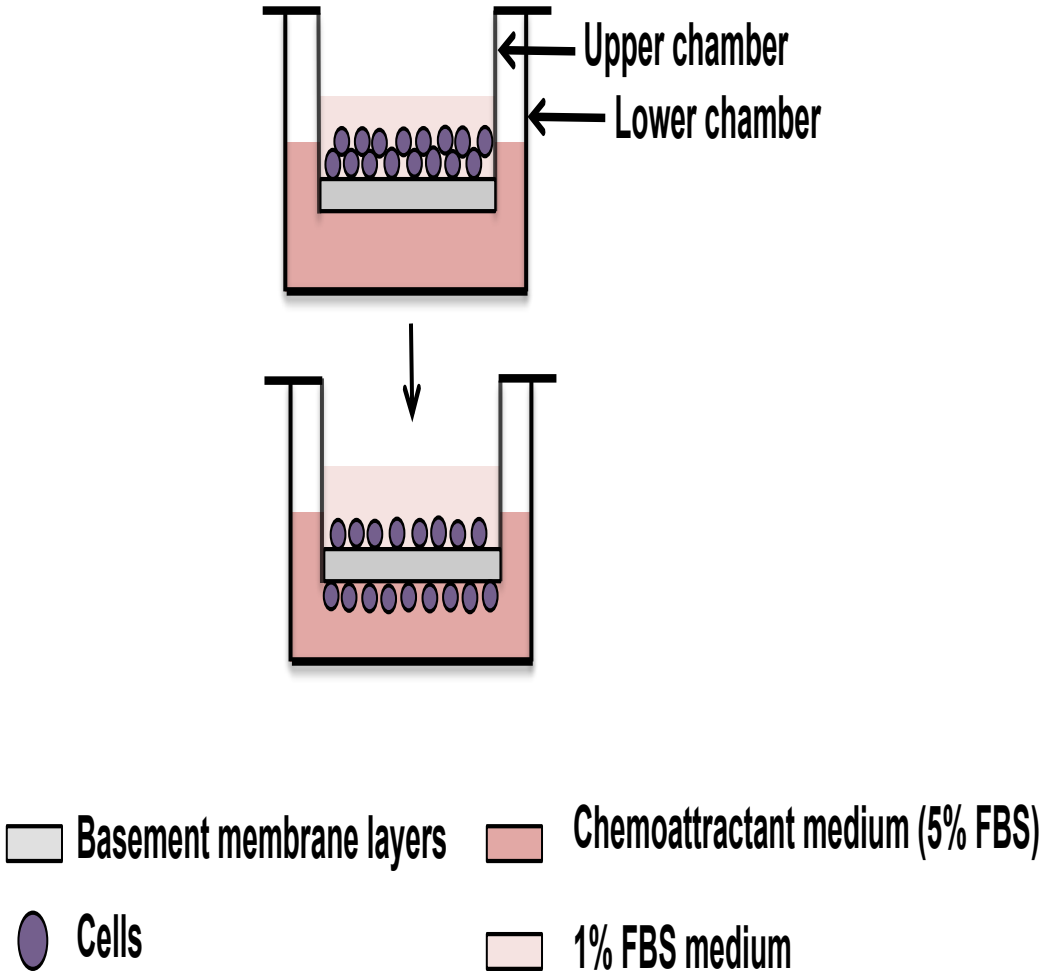

Figure 2.1 Schematic diagram of the invasion and migration assays. Invasion and migration assays were used to culture MDA-MB-231 and Hs578-T sub-population cells-based on either matrigel or polycarbonate membrane. Cells were seeded at 12×10^3/100 µl 1% FBS medium and added to upper chamber. 600 µl chemoattractant 5% FBS medium was added to the lower chamber in 24 well plate. Invaded or migrated cells were stained and counted.

2.2.9 Soft agar colon formation assay

In preparation for the assay, 2.5% semi-solid agar base layer (w/v) was made by dissolving 2.5 g of Ultrapure noble agar into 100 ml of distilled water (dH_2O). Agar mixture (Ultrapure noble agar /dH_2O) was autoclaved to sterilize and stored at 4 °C to insure solidification and heated at the time of the experiment until agar was completely dissolved. For plating of bottom layer of agar, 1.2x normal growth medium was prepared by supplementing DMEM medium with all supplements required to make 50 ml medium in 40 ml DMEM growth medium. 2.5% semi-solid

melted agar base layer (w/v), pre-warmed 1.2x normal growth medium and 50 ml conical tube in a tube holder were placed in an ice bucket containing 40°C water and transferred to tissue culture hood.

2.5% (w/v) autoclaved agar mixture/dH_2O was diluted 1:4 into 1.2 x concentrated normal growth medium and the tube was inverted several times to mix. 50µl of semi-solid agar base layer containing of 0.5% agar (w/v) in normal growth medium were plated into 96-well plates. As shown in Figure 2.2 plates were covered and the agar mixture allowed to solidify at 4°C, for 5 min. Once the lower layer of agar has solidified, preparation of the upper layer was began 1.5 % (w/v) low melting temperature agarose was prepared by microwaving in dH_2O and subsequently placed in a 40°C water bath until needed to keep it in liquid phase. $CD44^-/CD24^-$, $CD44^+/CD24^-$, $CD44^+/CD24^+$ and $CD44^-/CD24^+$ sorted populations from MDA-MB-231 and Hs578-T BCCs were grown to 70-80% confluence, harvested by trypsinization and diluted 1:3 in normal growth medium. Cells were counted using a hemocytometer and seeded at 2.5×10^4 cells/ml in 1.2x warm medium. For this cell number, cell suspension was diluted in a 1:4 ratio of warm 1.5% (w/v) agarose melted in a microwave and 50 µl (1×10^3 cells) were quickly and gently pipetted 2-3x to distribute cells and then placed onto agar base layer. The cell/agar mixtures were allowed to solidify at 4°C for 10 min, and then overlaid with 50 µl of normal growth medium (Figure 2.2). Plates were incubated at 37°C, 10% (v/v) CO_2 humidified cell culture incubator for four weeks. Normal growth medium were changed every week for four weeks by gently pipetting off the top medium layer and gently using a multi-channel pipette and adding new warm fresh medium. After four weeks, colonies were fixed and then stained with 0.4% crystal violet in 50% methanol crystal violet and quantified by EVOS FL microscope, Life technology, UK).

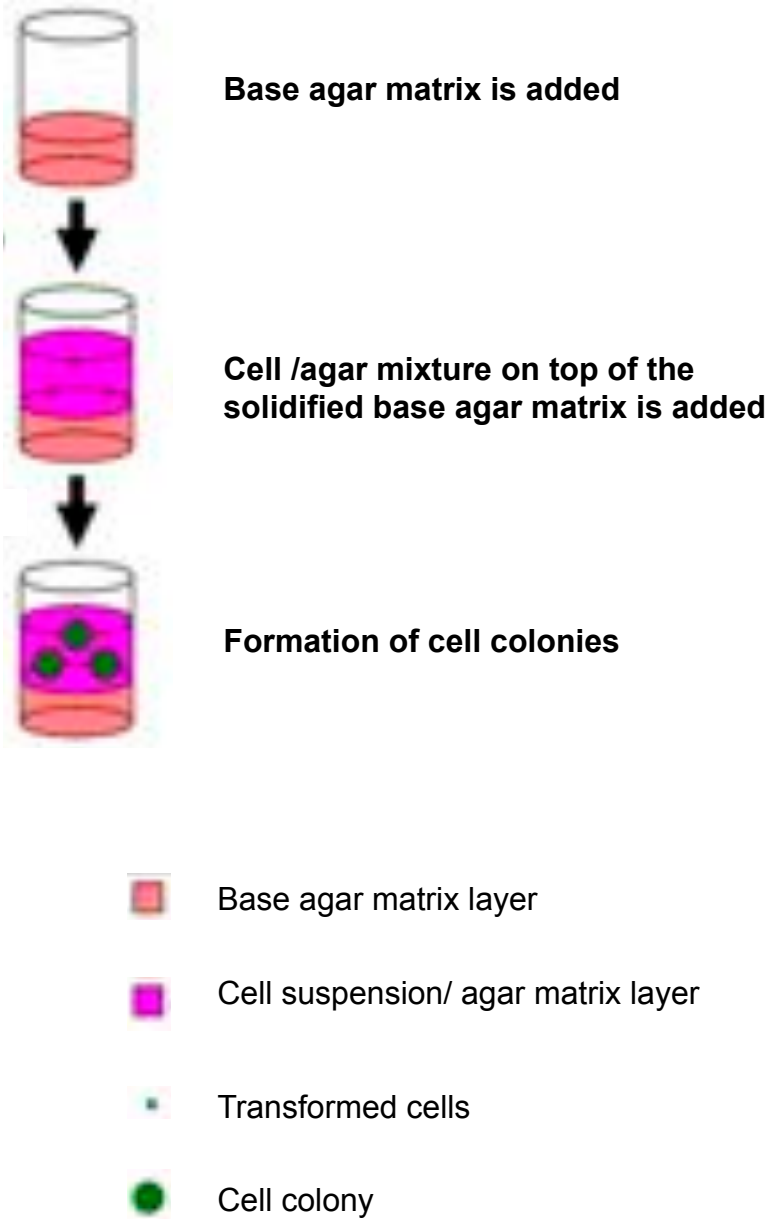

Figure 2.2 Schematic diagram assay principle for the soft agar colony formation assay. Cell colonies form after four weeks incubation in agar matrix.

2.2.10 Western blot analysis

2.2.10.1 Protein extraction from MDA-MB-231 and Hs578-T BCC lines for Western blotting

To prepare samples for running on a gel, cells need to be lysed to release proteins of interest. This solubilizes the proteins so they can migrate individually through a separating gel.

For protein extraction, cells were lysed to release proteins of interest. Briefly, cells were grown in 10 cm culture dishes and incubated for 48 hrs. After incubation time, cells were starved for 6 hrs with normal growth medium without FBS. Cells were stimulated with either 20 ng/ml FGF2 or 10 ng/ml IL-6 and treated with different HS and modified heparins at low concentration (10 ng/ml) at a appropriate time points. After each time point, plates were placed on ice and cells were washed twice with cold PBS. 250 µl cold RIPA buffer supplemented with 200x of 200 mM Sodium fluoride (NaF), 100X Sodium orthovanadate (Na_3OV_4) and 100x complete protease inhibitor cocktail were added to each plate and incubated for 5 min. Adherent cells were scraped off the dish using a plastic cell scraper and gently the cell suspension transferred into a microcentrifuge tube and incubated for 30 min on ice with agitation every 10 min. After incubation, the cells were centrifuged at 4°C at 12,000 rpm for 10 min. The supernatants were aspirated and placed in a clean fresh 1.5 ml tube and stored at - 20°C until use for Western blotting.

2.2.10.2 BCA Protein Assay

2.2.10.2.1 Preparation of Diluted Albumin (BSA) Standards

Table 2.4 was used as a guide to prepare a set of protein standards.

2.2.10.2.2 Preparation of the BCA working reagent (WR)

The following formula was used to determine the total volume of BCA working reagent (WR) required: (# standards + # unknowns) x (# replicates) x (volume of WR per sample) = total volume WR required.

10 µl of each standard and unknown sample were loaded in triplicate into each 96-well plate. 100 µl of 1:50 BCS working reagent (WR) were added to each well and

incubated on a plate shaker at 37°C for 30 min. After incubation, the absorbance of all triplicate standards and samples were measured using the spectrophotometer at 570 nm. A standard curve was plotted by plotting the average blank-corrected 570 nm measurement for each BSA standard vs. its concentration in µg/ml. The standard curve was used to determine the protein concentration of each unknown sample (Figure 2.3).

Table 2.4 Preparation of diluted BSA standards

Vial	Volume of diluent µl	Volume and source of BSA	Final BSA concentration µg/ml
A	0	300 µl of stock	2,000
B	125	375 µl of stock	1,500
C	325	325 µl of stock	1,000
D	175	175 µl of vial B dilution	750
E	325	325 µl of vial C dilution	500
F	325	325 µl of vial E dilution	250
G	325	325 µl of vial F dilution	125
H	400	325 µl of vial G dilution	25
I	400	0	0 = Blank

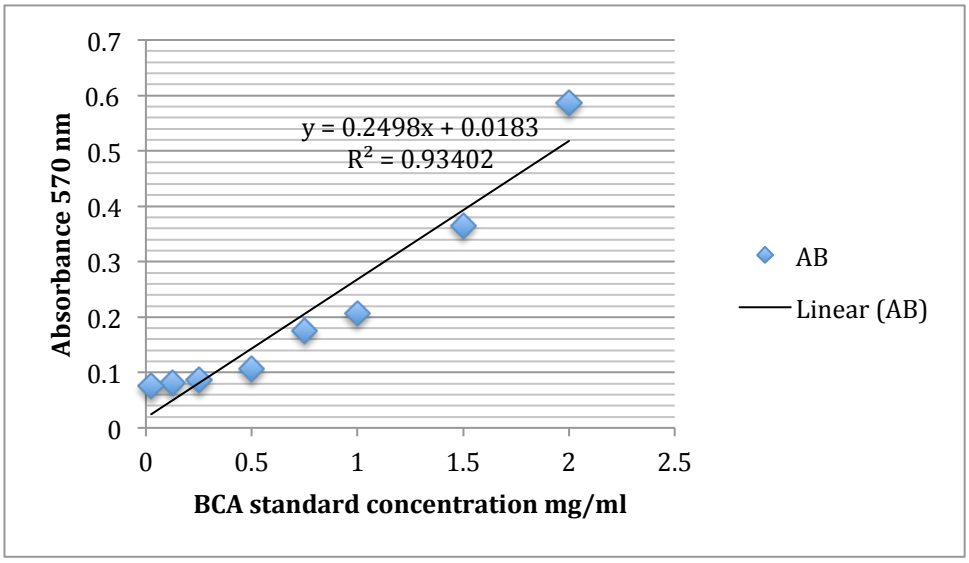

Figure 2.3 Colour response curves for BSA using the standard microplate protocol (37°C at 30 min incubation).

2.2.10.3 SDS-PAGE

Proteins were separated based on their molecular weight on SDS-polyacrylamide gels. Briefly, samples were pre-heated for 10 min at 95°C and immediately placed on ice. 40 µl of each sample was loaded using gel loading tips. Protein extracts were run on Tris-buffered SDS-polyacrylamide gels, made according to Table 2.5 or purchased from Bio-Rad (7.5%, 10% or 12% Mini-PROTEAN® TGX™ Precast Gels), in 1x SDS-PAGE running buffer, with the acrylamide concentration of the separating gel varying depending on the size of the proteins being separated. To determine protein size, 10 µl Precision Plus Protein™ WesternC™ prestained protein standards were used on each gel. Samples were run at approximately 140 volts until the proteins had clearly stacked, and then voltage was turned down to 100 volts with time varying depending on the level and size of separation required.

Table 2.5 Components for SDS-PAGE gels

Component	Separating Gel (10ml)					Stacking gel (5ml)
	6%	8%	10%	12%	15%	
DdH_2O	5.3 ml	4.6 ml	2.5 ml	3.0 ml	3.5 ml	3.4 ml
30% Acrylamide	2.0 ml	2.7 ml	2.5 ml	2.5 ml	2.5 ml	0.83 ml
1.5M Tris-HCl pH 8.8.	2.5 ml	2.5 ml	2.5 ml	2.5 ml	2.5 ml	-
1M Tris-HCl pH 6.8	-	-	-	-	-	0.1 ml
10% SDS	0.1 ml	0.1 ml	0.1 ml	0.1 ml	0.1 ml	0.05 ml
10% APS	0.1 ml	0.1 ml	0.1 ml	0.1 ml	0.1 ml	0.05 ml
TEMED	8 µl	6 µl	4 µl	4 µl	4 µl	5 µl

2.2.10.4 Transfer of proteins and staining

After separation by SDS-PAGE proteins were transferred onto a nitrocellulose membrane. Before setting up the transfer apparatus, four blotting paper per gel and membrane were pre-wetted with Tris-Glycine transfer buffer. The soaked sponge and two blotting papers were layered onto the black side of the transfer sandwich. Gel and membrane were layered onto the blotting paper. Two pieces of transfer-buffer wet blotting paper were layered on top of the membrane. Proteins were transferred with ice pack cooling at 250 mA constant for 1.5 hrs at 4°C. After blotting, membranes were stained for 30 sec with Ponceau S solution to check transfer was successful and to label the lanes with a pencil. Membranes then were transferred into RO water. After the de-staining, membranes were washed three times in 0.1% TBST to remove the Ponceau stain and incubated in blocking buffer (5% BSA) at room temperature for 1 hr to reduce non-specific binding of the antibody before incubation with a suitable primary antibody (Table 2.6) diluted in blocking buffer (BSA) overnight at 4°C on a roller. Membranes were then washed three times in 1% TBST for 10 minutes and incubated with an appropriate horseradish peroxidase (HRP) conjugated secondary antibody (Table 2.7) plus StrepTactin-HRP conjugate (1:10,000, Bio-Rad), detection in blocking buffer (BSA) for 1 hr at room temperature on a roller. Membranes were then washed three times in 1% TBST and twice in 10% TBS for 10 minutes.

2.2.10.5 Imaging and data analysis

ECL chemiluminescent substrate was used to detect the HRP-conjugated secondary antibodies on the membrane. The chemiluminescent signal was detected and imaged using the ImageQuant™ LAS 4000 Biomolecular Imager (GE Healthcare) and exposure for a length of time dependent on the signal intensity

The membranes were scanned and the intensities were compared using Image Studio Lite software V5.2 (Lil-COR Biotechnology, UK. Ltd). For relative quantification, equal sized rectangular boxes were drawn for each antibody around bands images and the mean value for each protein band was calculated. To correct for slight loading differences, the intensity of each band (eg. phosphorylated and total protein

levels) were divided by that of histone and α-tubulin house-keeping proteins as ontrols. Finally, the intensity of each normalized protein phosphorylation value was divided by its total protein values. The mean value of three separate experiments ± SEM were calculated.

Table 2.6 Primary antibodies used in Western blots

Primary Antibody	Supplier	Species	Concentration
pP42/44 MAPK (Erk1/2) (Thr202/Tyr204	Cell Signaling	Rabbit	1μg/ml
P42/44 MAPK (Erk1/2)	Cell Signaling	Rabbit	5μg/ml
Phospho-Stat3 (Tyr705)	Cell Signaling	Mouse	1μg/ml
Stat3 (D3Z2G)	Cell Signaling	Mouse	1:10
Histone H3 (3H1)	Cell Signaling	Rat	1:10
Tubulin (11H10)	Cell Signaling	Rat	1:20

Table 2.7 Secondary antibodies used in Western blots

Secondary Antibody	Supplier	Species	Concentration
Anti-mouse HRP	Santa Cruz	Donkey	1:10,000 (anti GFP); 1:5000 (anti-Histone)
Anti-rabbit HRP	Santa Cruz	Donkey	1:10,000
Anti-rat HRP	Santa Cruz	Goat	1:2000

2.2.10.6 Stripping WB membrane (harsher conditions)

After imaging, membranes were washed 3 times for 5 min in TBS-T and submerged in stripping buffer and incubated at 50°C for 30 min with occasional agitation. Membranes were then washed 2 times for 10 minutes in TBS-T at RT using large volumes of buffer. Membranes were probed with ECL to check antibody has been removed, before any re-probing.

2.2.11 Real Time Polymerase Chain Reaction

2.2.11.1 RNA extraction

MDA-MB-231 and Hs578-T sorted cells were cultured in T75 cell culture flasks and incubated for 24 hrs at 37°C, then medium were removed and replaced with fresh growth medium. Different HS mimetic heparin compounds, (PerS H, 2,6 deS-NS H, PMH and PMHS) at appropriate concentrations (10 ng/ml) were added and incubated for 48 hrs at 37°C. After the incubation period, cells were washed twice with PBS and harvested with 0.1% trypsin and 0.1% EDTA. 10^6 cultured cells were re-suspended in 200 µl PBS in a 1.5 ml clean microfuge tube. 400 µl Lysis/-Binding buffer were added and vortexed for 15 sec. Samples were transferred to a high pure filter tube and centrifuged at 8,000 xg for 15 sec. After centrifugation, the flowthrough liquids were discarded. A combination of 90 µl DNase incubation buffer and 10 µl DNase l, were added to the samples and incubated at RT for 15 min. 500 µl wash buffer l was added to the upper reservoir of the filter tube followed by centrifugation at 8,000 xg for 15 sec. The flowthrough liquids were discarded after centrifugation and filter tubes were combined with the used collection tube. The remaining pellet was washed with 500 µl wash buffer 11 and debris removed by centrifugation at 8,000 xg for 15 sec. A further 200 µl of wash buffer 11 was added and centrifuged for two min at maximum speed (approx. 13,000 xg) to remove any residual wash buffer. Collection tubes were discarded and the filter tubes were inserted into a sterile, clean 1.5 ml microfuge tube. RNA was eluted with 100 µl Elution buffer and centrifuged at 8,000 xg for 1 min. RNA concentration was measured using a NanoDrop™ (see section 2.2.9.2). If the eluted RNA was to be stored, rather than used directly for cDNA synthesis, the pellet was stored at -80°C for later analysis.

2.2.11.2 RNA quantification

RNA was measured using the Thermo Scientific NanoDrop™ 1000 Spectrophotometer according to the manufacturer's instructions. 1 µl of sample was quantified using the absorbance over a 220 nm-750 nm spectrum and gives an output of concentration and relative purity with 230/260 and 260/280 ratio measurements.

2.2.11.3 DNase treatment

To degrade DNA in applications that are sensitive to the presence of RNase, recombinant DNase 1, RNase-free, was used and the mixture was prepared in a final volume of 20 µl as shown in Table 2.8, and incubated at RT for 20 min. The reaction was stopped by adding 2 µl of 0.2 M EDTA (pH 8.0) and incubated at 75°C for 10 min. Samples were placed on ice in preparation for the reverse transcriptase reaction.

Table 2.8 Digestion of Genomic DNA in RNA samples

Component	Final concentration
Total RNA	10-50 µg
10X incubation buffer	5 µl
DNase 1 recombinant, RNase-free	25-10 units
Optionally: Protector RNase Inhibitor	10 units
Water, RNase-free	Up to 20 µl

2.2.11.4 cDNA synthesis

cDNA was synthesised with Transcriptor High Fidelity cDNA Synthesis Kit for RT-polymerase chain reaction (PCR) (Roche, UK) according to kit instructions. 9.4 µl RNA samples and water (PCR grade) were transferred to a 0.2 ml microfuge tube and 2 µl of 60 µM stock of random hexamer primers were added to make 11.4 µl total volume. The template-primer mixtures were denatured by heating at 65°C for 10 min in a block cycler with a heated lid (to minimize evaporation). The samples were chilled on ice for 1 min, and pulse centrifuged. 4 µl of 1x (8mM $MgCl_2$) Transcriptor High Fidelity Reserve Transcriptase Reaction Buffer, 5 µl of 20 U Protector RNase Inhibitor, 2 µl of 1 mM Deoxynucleotide mix, 1 µl of 5 mM DTT and 1.1 µl of 22 U Transcriptor High Fidelity Reserve Transcriptase were added to make a final volume 20 µl. The solution was mixed gently by pipetting and incubated

at 25°C for 5 min. A further incubation at 55°C for 10 min and inactivation of transcriptor high fidelity reverse transcriptase was achieved by heating to 85°C for 5 min. The reaction was stopped by placing samples on ice. At this point the reaction tube was stored at 4°C for 1 to 2 hrs or at -20°C if for a longer period. Summary of thermal cycling conditions was shown in table 2.9.

Table 2.9 Thermocycling conditions for reverse transcription

	Temperature	Incubation time
Step1	25 ºC	5 min
Step 2	55 °C	10 min
Step 3	85 °C	5 min
Step 3	4 °C	∞

2.2.11.5 Reverse transcriptase

cDNA was generated from RNA using a cDNA kit (Applied Biosystems, CS, USA) according to manufacturer instructions. Each reaction mixture consisted of: 10 µl RNA sample (200 ng – 1 µg total RNA), 2 µl 10x RT buffer, 2 µl 10x RT random primers, 0.8 µl 25x dNTP mix, 1 µl reverse transcriptase, 1 µl RNase inhibitor and 3.2 µl PCR grade water. The final reaction volume was 20 µl. Reaction mixtures were centrifuged briefly to eliminate air bubbles and spin down the contents. The reverse transcription was run in a DNA Engine DYAD peltier theromcycler (M Research Inc. UK), with the thermal cycling conditions detailed in Table 2.10.

Table 2.10 Thermocycling conditions for reverse transcription

	Temperature	**Incubation time**
Step1	37 ºC	60 min
Step 2	95 °C	5 min
Step 3	4 °C	∞

2.2.11.6 Oligonucleotides

Oligonucleotides were purchased from Bio Rad, UK, synthesised by MWG Biotech and diluted in water (PCR grade) according to the manufacturer's recommendations to give 100 µm stock solutions (stored at -80°C). A 10 µm stock was made with water (PCR grade) for use in PCR and sequencing (stored at -20°C). A list of primers is given in Table 2.11.

Table 2.11 Primer list

Gene		Primer Sequence
CD44	F	5′-GGCTTTCAATAGCACCTTGC-3′
	R	5′-ACACCCCTGTGTTGTTTGCT-3′
EpCAM	F	5′-CGCAGCTCAGGAAGAATGTG-3′
	R	5′-TGAAGTACACTGGCATTGACG-3′
ABCG2	F	5′-CACCTTATTGGCCTCAGGAA-3′
	R	5′-CCTGCTTGGAAGGCTCTATG-3′
VEGFA	F	5′-GGGCTGCTGCAATGATGAA-3′
	R	5′-GTGCTGGCTTTGGTGAGGTT-3′
VEGFB	F	5′-AAAAAAGGACAGTGCTGTGAAG-3′
	R	5′-GGAGTGGGATGGGTGATGT-3′
IL-8	F	5′-CCAACACAGAAATTATTGTAAAGC-3′
	R	5′-TGAATTCTCAGCCCTCTTCAA-3′
CXCR4	F	5′-GAGGAAATGGGCTCAGGG-3′
	R	5′-AGTCAGCAGGAGGGCAGGGA-3′
GAPDH	F	5′-GTGGACCTGACCTGCCGTCT-3′
	R	5′-GGAGGAGTGGGTGTCGCTGT-3′
18S rRNA	F	5′-GGCCCTGTAATTGGAATGAGTC-3′
	R	5′-CCAAGATCCAACTACGAGCTT-3′
IL-6	F	5′-GAGAAAGGAGAC ATGTAACAAGAGT-3′
	R	5′-GCGCAGAATGAGATGA GTTGT-3′

2.2.11.7 RT-qPCR

In a 1.5 ml reaction tube on ice, the PCR mix was prepared for one 20 µl reaction and were carried out in a total volume of 20 µl made up of 3 µl water PCR grade, 1 µl of 20x PCR primer and 10 µl of 2x master mix. The mixture was mixed gently by pipetting up and down. 15 µl PCR mix was added into each well of the LightCycler 480 Multiwell Plate. 5 µl of DNA template was added to each well. The LightCycler 480 Multiwell Plate were sealed with LightCycler 480 Multiwell Sealing Foil. The multiwell plate was centrifuged at 1,500 xg for 2 min. Reactions were carried out using the LightCycler 480 instrument (Roche, UK) using the conditions shown in Table 2.1. Reactions were done in duplicate per biological repeat and the quantity of immunoprecipitated DNA was calculated by % Input. Thermal cycling parameters for primers are shown in Table 2.12.

Table 2.12 Thermal cycling conditions used for qPCR

Programs	Temp °C	Acquisition	Time	Cycles	Ramp °C
Pre-incubation	95	None	5 min	1	4.4
Amplification				40	
Segment 1	95	None	20 sec		4.4
Segment 2	60	None	15 sec		2.2
Segment 3	72	Single	15 sec		4.4
Melting curve				1	
Segment 1	95	None	5 sec		4.4
Segment 2	70	None	1 min		2.2
Segment 3	95	Continuous	-		-

2.2.11.8 Taqman low density array microfluidic cards

Taqman low density array (TLDA) microfluidic cards were custom designed by the Troeberg lab group (Oxford University, ARUK Centre for Osteoarthritis Pathogenesis, Kennedy Institute of Rheumatology), to consist of pre-selected Taqman gene probes (Appendix 1.1). Each card could be run with total of 8 samples, testing for 48 genes, including the house keeping gene control 18s. Each reaction mixture well contained a final volume of 100 µl consisting of 50 µl cDNA template (200 ng starting RNA) in PCR grade water and 50 µl 2x universal PCR mix (Applied

Biosystems, USA). Prior to loading, reaction mixtures were vortexed and centrifuged, then added to the card. The card was centrifuged twice at 12,000 rpm for 1 min and sealed with the microfluidic card sealer. Finally, samples were run on the ViiA™ 7 Real-Time PCR System (Applied Biosystems, USA). The thermocycling conditions are shown in Table 2.13

Table 2.13 Thermal cycling parameters for primes

Programs	Temp °C	Incubation time	Cycles
Hold	50	2 min	40
Denature			
Segment 1	94.5	10 min	
Segment 2	97	30 sec	40
Anneal/Extend	60	1 min	40

2.2.11.9 Gene expression analysis

Since all primer pairs reported efficiency close to 100%, the data was calculated using the delta-delta ct method ($2^{-\Delta Ct}$ method), an adapted version of the $2^{-\Delta\Delta Ct}$ method (Livak and Schmittgen, 2001, Yuan et al., 2006) to calculate relative change in expression between different BCSCs, assuming primer efficiency.

Relative change in expression compared to control conditions = $2^{-\Delta\Delta Ct}$

$$\Delta\Delta CT=\Delta CT(\text{treated sample})-\Delta CT(\text{untreated sample})$$

,where

$$\Delta CT(\text{sample})= CT(\text{target})-CT(\text{ref})$$

,therefore

$$\Delta\Delta CT=(CT(\text{target, untreated})-CT(\text{ref, untreated}))-(CT(\text{target, treated})-CT(\text{ref, treated})).$$

The threshold cycle (C_t) refers to the cycle at which the fluorescence signal is

detectable above background due to the accumulation of amplified product. This value is proportional to the starting target sequence copy number. C_t was measured in the exponential phase and, therefore, it was not affected by possible limiting components in the reaction. For every run performed, the threshold was set at the same fluorescence value (100 relative fluorescence units [RFU]).

Taqman clustering results are achieved by using the Canberra distance metric ($d(p,q) = \sum_{i=1}^{n} \frac{|p_i - q_i|}{|p_i + q_i|}$), where p and q are vectors.

Control conditions were considered to be either $CD44^-/CD24^-$ sorted cells from MDA-MB-231 and Hs578-T or $CD44^+/CD24^-$ untreated cells. Treated samples were any conditions other than this.

2.2.12 PathScan® analysis

2.2.12.1 Cell Lysates assay for PathScan assay

Protein lysate from the $CD44^+/CD24^-$ sub-population of MDA-MB-231 and Hs578-T BCC cells were prepared. Briefly, cells were grown in 10 cm culture dishes and incubated for 24 hrs prior to treatment with compounds (10 ng/ml of PMH, PMHS, PerS H (1), NAc H (2), 2 deS-NS H (3), 6 deS- NS H (4), 2 deS-NAc H (5), 6 deS-NAc H (6), 2,6 deS-NS H (7) or 2,6 deS-NAc H (8)). Cells were then incubated for an additional 48 hrs. A further cell preparation was done by stimulating cells additionally with FGF2. Cells were grown in 10 cm culture dishes and incubated for 48 hrs. After incubation, cells were starved for 6 hrs with normal growth medium without FBS. Cells were stimulated with 1 µg/ml FGF2 and treated or not with different HS and modified heparin compounds at low concentration (10 ng/ml) for 60 min. After time incubation of cell culture, plates were placed on ice and cells were washed twice with cold PBS. 500 µl of cold lysis buffer were added to each plate and incubated on ice for 3 min. The plates were tilted and adherent cells were scraped using the scraper. Then, the cell lysates were collected and transferred to clean microcentrifuge tubes. Cell lysates were centrifuged at maximum speed for 3 minutes at 4°C. The supernatants were aspirated and placed in a clean fresh 1.5 ml tube to help remove any particles or large cell debris and stored at - 80°C until use for PathScan assay.

2.2.12.2 Assembled array preparation

The protective plastic film was removed and the multi-well gasket was placed on the bench top, with the silicone layer facing up. The glass slide was carefully placed on top of the multi-well gasket with the nitro-cellulose pads facing down. The metal clip was inserted into the groove in the gasket and the clip rotated into the locked position.

2.2.12.3 PathScan procedure

100 µl of array blocking buffer was added to each well, covered with sealing tape and incubated for 15 min at RT on an orbital shaker. Array blocking buffer was decanted by gently flicking out the Array Blocking Buffer into a sink. 75 µl of diluted lysate was added to each well and covered with sealing tape. Then, cell lysates in individual wells were incubated overnight at 4°C on an orbital shaker. Each well content was decanted again by gently flicking out the diluted lysate into a sink. 100 µl (1x) Array Wash Buffer was added to each well and incubated for 5 min at RT on an orbital shaker. The washing step was repeated three more times. Then, 75 µl of (1x) detection antibody cocktail was added to each well, covered with sealing tape and incubated for 1 hr at RT on an orbital shaker. Each well content was then decanted by gently flicking out the fluid into a sink and washed four times with 100 µl (1x) array wash buffer for 5 min. 75 µl of (1x) HRP-linked streptavidin was added to each well, covered with sealing tape and incubated for 30 min at RT on an orbital shaker. After the incubation period, the washing step was repeated four times for 5 min.

2.2.12.4 Imaging and data analysis

The slide was removed from the multi-well gasket and placed face up in a clean plastic plate, followed by washing with 10 ml (1x) array wash buffer. (1x) Array wash buffer was removed and LumiGLO®/Peroxide reagent was covered to the top of the slide and incubated for 2 min. Images of the slide were taken using the ImageQuant™ LAS 4000 Biomolecular Imager (GE Healthcare). The slide was scanned and the intensities were compared using Quantity One software. For relative quantification, the mean value for each phosphorylated signaling molecule's dot was

calculated. To correct for slight loading differences, the intensity of the negative background (b) was subtracted from each dot (eg. phosphorylated levels). Finally, the mean value of duplicate repeat of each normalized protein phosphorylation value was multiplyed by 100. The mean value of two separate experiments ± SD in duplicate was calculated.

2.2.12.5 Statistical analysis

All data are reported as the means ± SD, a part from Pathscan quantification data which are presented as means ± SEM. Significant differences were determined using the Student *t* test to compare between groups, with significance set to *P<0.05, **P<0.01, ***P<0.001. All statistical analysis and graphs were plotted using Excel 2007.

Prior to publication either a Bonferroni correction will need to be applied to all analyses or data will need to be reanalysed using an ANOVA test.

3 Expression of CSC markers in a sub-population of human BCCs: Correlation with enhanced metastatic and malignant properties

3.1 General introduction and aims

A large body of literature has identified CD44 as a putative CSC marker in breast tumours (Al-Hajj et al., 2003, Lee et al., 2015, Olsson et al., 2011). In addition to CD44, another putative CSC marker reported in human BCCs include low or no expression of CD24 (Al-Hajj et al., 2003, de Beça et al., 2013); however, the percentage of cells expressing these markers differed from one cell line to the other (Ricardo et al., 2011). Nevertheless, CD44 and CD24 have been used extensively in combination to isolate CSCs from BCCs and tumours based on their $CD44^{+}/CD24^{-/low}$ phenotype (Fillmore and Kuperwasser, 2007, Liu et al., 2014b). In addition to this $CD44^{+}/CD24^{-/low}$ phenotype, isolation strategies in human BCCs using combinations with ALDH and CD133 cell surface markers have also been successfully identified (Croker et al., 2009).

CSCs isolated via $CD44^{+}/CD24^{-/low}$ phenotype have been demonstrated to have enhanced capacity for invasion, migration, adhesion, and resistance to chemotherapeutic agents (Abdullah and Chow, 2013, Kim et al., 2009, Kim et al., Mukherjee et al., 2014, Sheridan et al., 2006). However, recently some studies demonstrated conflicting results regarding correlations between clinical value and prognostic significance of CD44 and CD24 markers in breast cancer. (Mylona et al., 2008) demonstrated that cells with $CD44^{+}/CD24^{-/low}$ phenotype exert no significant impact on a patients' prognosis. In addition, one paper found that patients with tumors expressing the $CD44^{-}/CD24^{+}$ phenotype had the worst prognosis, compared to tumors rich in $CD44^{+}/CD24^{-/low}$ cells. Furthermore, (Abraham et al., 2005) suggested that BCCs with $CD44^{+}/CD24^{-/low}$ phenotype may not be associated with the clinical outcome or the patients' survival, emphasizing the fact that putative tumorigenic ability may not be limited to cells displaying this phenotype. Thus other BCSC markers may remain to be identified. Nevertheless, it was considered that the significant number of studies demonstrating the $CD44^{+}/CD24^{-}$ sub-population as

having CSC properties prompted the screening of a number of BCC lines in order to establish a model system for exploring the possible role of HS in regulation of CSCs.

The aims of the work in this chapter were to:

- Establish a model system using human BCC lines to study whether it is possible to regulate the CSC phenotype by manipulating the stem cell niche via HS glycans.
- Measure multiple CSC markers (CD44, CD24 and CD133) to be able to define and separate CSC-like sub-populations in human BCC lines.
- Use a combination of anti-CD44 and anti-CD24 antibodies and FACS to identify and isolate CSCs and other sub-populations ($CD44^-/CD24^-$, $CD44^+/CD24^-$, $CD44^+/CD24^+$ and $CD44^-/CD24^+$) from 2 selected BCC lines (MDA-MB-231 and Hs578-T).
- To investigate whether $CD44^+/CD24^-$ sub-populations from MDA-MB-231 and Hs578-T cells have expected CSC properties by systemically analyzing their proliferation, invasion, migration capacity, adhesion, colony formation and chemosensitivity.

3.2 The differential expression of some human BCC lines to CSC markers

Previous results reported that CD44, CD24 and CD133 are markers for CSCs in breast tumours (Al-Hajj et al., 2003, Atkinson et al., 2013, Meyer et al., 2010). Flow cytometery was used to assess the expression of these 3 markers in 5 BCC lines, namely MCF-7-A, T-47D, ZR-75-1, MDA-MB-231 and Hs578-T; flow cytometry histograms of cells are shown in Figure 3.1. Two regions are shown (R1 and R2 regions); R2 demonstrates the cell expression of the CSC markers compared to the R1 antibody isotype control (Figure 3.1).

MCF-7-A, T-47D and ZR-75-1 cells did not show significant expression of CD44 (2.59 ± 2.03, 5.03 ± 1.87 and 8.5 ± 4.8% respectively), and conversely showed high positive expression of CD24 (47.8 ± 1.9, 81.65 ± 2.02 and 77.96 ± 2.93% respectively) (Figure 3.1A, B, C). In contrast, MDA-MB-231 and Hs578-T cells consistently displayed the highest expression of CD44 (67.8 ± 2.46 and 50.83 ± 2.29 % respectively, with very low expression of CD24 (8.32 ± 0.07 and 6.59 ± 1.3%

respectively (Figure 3.1D, E). The T-47D cell line was the only line to show expression of CD133 on their surfaces (Figure 3.1B); MCF-7-A, ZR-75-1, MDA-MB-231 and Hs578-T cells were all negative for CD133 expression (Figure 3.1A, C, D, E).

Quantitative analysis of expression in human BCC lines of the CSC markers conjugated to a number of alternative fluorochromes are shown in Figure 3.2. The expression levels of CD44 (FITC or APC), CD24 (FITC, PE or APC) and CD133 (PE alone) were analyzed by FACS. Consistent data was obtained irrespective of the fluorochrome used, and was in full support of the analysis described above. MCF-7-A and ZR-75-1 cells express low levels of CD44 conjugated to either (FITC or APC), negatively expressed CD133 conjugated to PE, with high positive expression of CD24 conjugated to either FITC, PE or APC. T-47D cells expressed very low levels of CD44 (with FITC or APC) and positively expressed CD24 (FITC, PE or APC) and CD133 PE. MDA-MB-231 and Hs578-T cells showed the highest expression of CD44 (with FITC or APC), with very low expression of CD24 (FITC, PE or APC) and negative expression of CD133 PE. Marker expression data are summarized in Table 3.1.

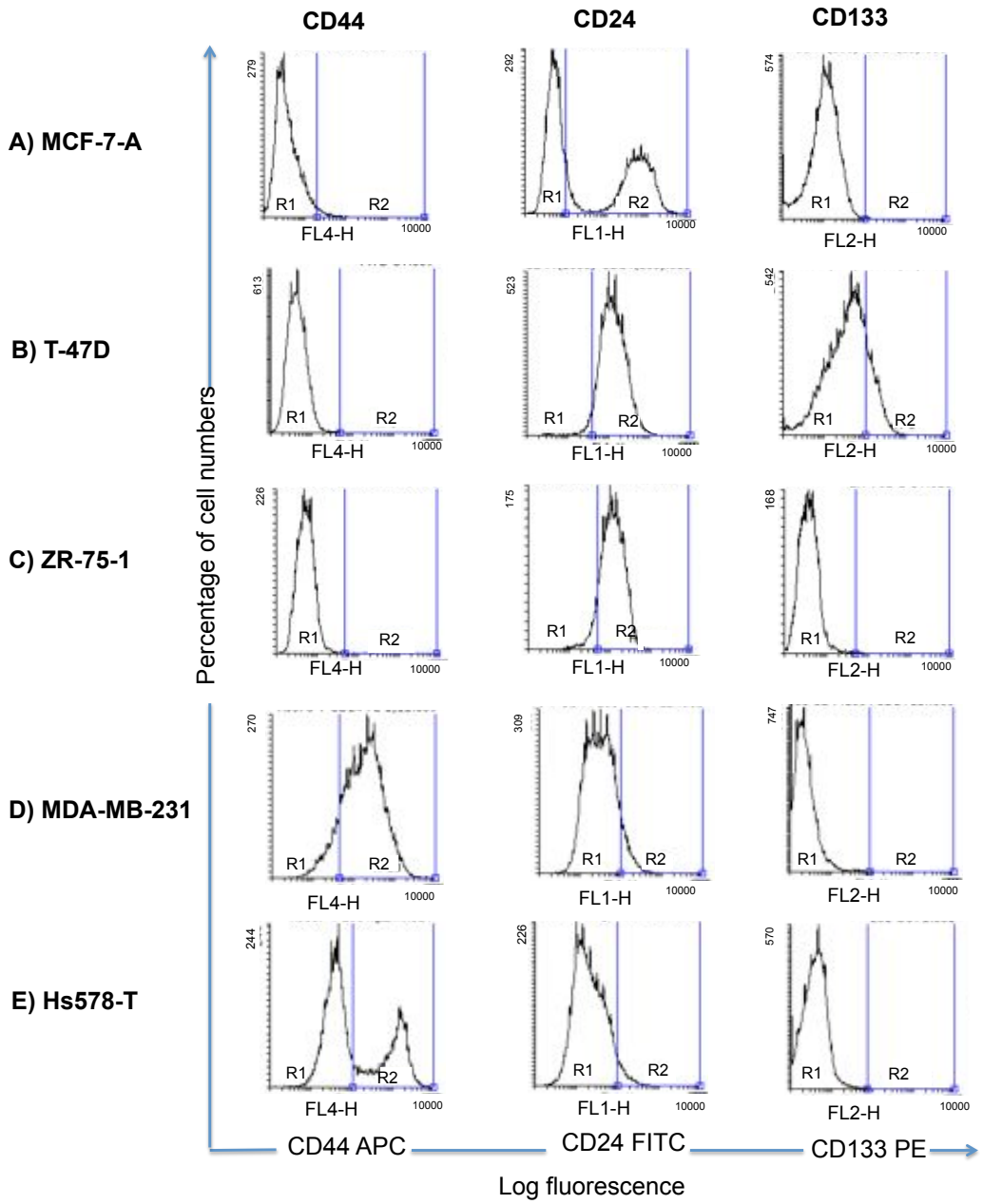

Figure 3.1 Percentage of cells expressing CSC markers CD44, CD24 and CD133 in human BCC lines. Single-cell suspensions of 10^6 cells from (A) MCF-7-A-1, (B) T47-D, (C) ZR-751-1, (D) MDA-MB-231 and (E) Hs578-T were stained with either anti-human CD44, CD24 and CD133 conjugated to APC, FITC and PE respectively, or appropriate APC, FITC and PE IgG1 isotype controls. Cells were analysed in a BD FACSCalibur flow cytometer. CD44, CD24 and CD133 fluorescence intensity histograms of R2 positive cell subpopulations with CD44, CD24 and CD133 (signal above threshold) versus R1 isotype controls (signal below threshold). Approximately 30,000 events were collected/sample. Data from one of four representative experiments are shown.

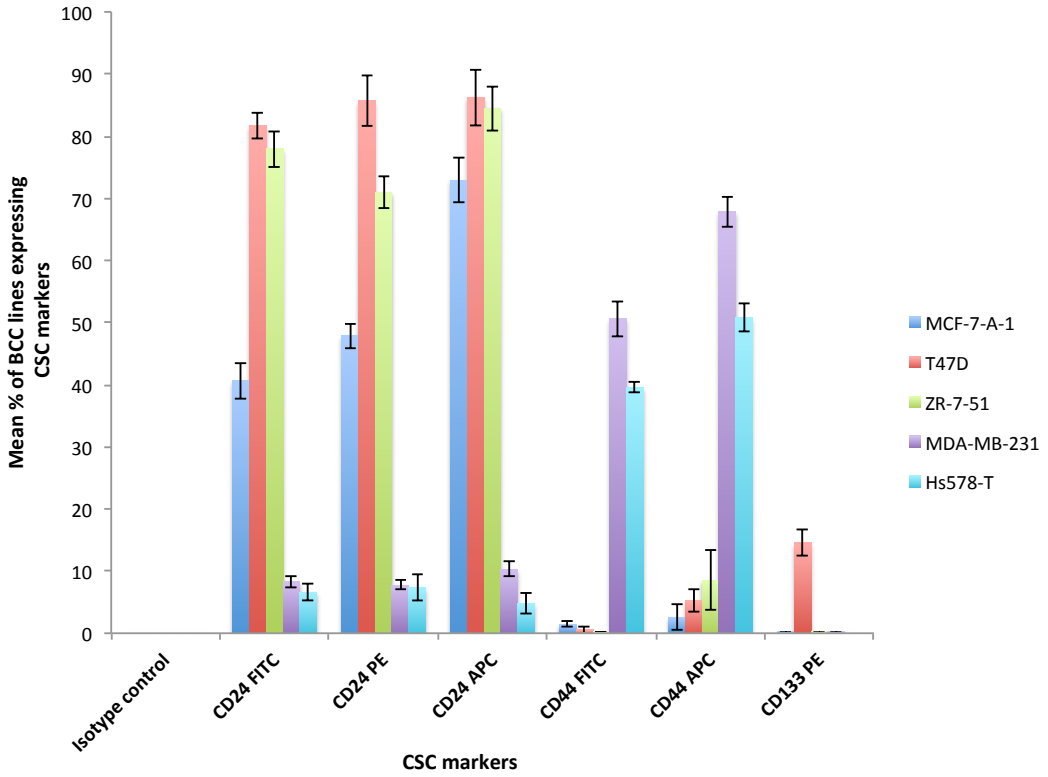

Figure 3.2 MCF-7-A, T-47D, ZR-75-1, MDA-MB-231 and Hs578-T cell lines were maintained as described in Methods. Upon reaching 80% confluence, total cells were incubated with either an anti-CD44 antibody conjugated to (FITC or APC), an anti-CD24 antibody conjugated to (FITC, PE or APC), or an anti-CD133 antibody conjugated to PE fluorochrome, or appropriate FITC, PE and APC-conjugated IgG isotype controls. The expression levels of CD44, CD24 and CD133 were analyzed by FACS (as in Figure 3.1). Data shown represent the mean ± SD, n=4 independent experiments (each with duplicate measurements).

Table 3.1 Summary of CSC marker expression in different human BCC lines

Cell line/Marker	CD44	CD24	CD133
MCF-7-A	+	+++	-
T-47D	+	+++	+
ZR-75-1	+	+++	-
MDA-MB-231	+++	++	-
Hs578-T	+++	++	-

Abbreviations -, not detectable; +, <5%; ++, 5-50% of the cells express the marker indicated; +++, >50% of the cells express the marker indicated.

3.3 Human BCC lines contain sub-populations of cells that differ quantitatively in their expression of CSC markers

In order to test the hypothesis that human BCC lines differ in the proportion of $CD44^{+}/CD24^{-}$ cells, the four BCC lines were characterized using FACS analysis for surface expression of CSC markers CD44 and CD24. Isotype controls were conducted for all cell lines investigated (Figure 3.3).

FACS analysis (n=4) of the least aggressive MCF-7-A and T-47D cell lines showed that these cells had the lowest proportion of $CD44^{+}/CD24^{-}$ cells (1.77 ± 0.66% and 0.03 ± 0.04% respectively) (Figure. 3.3A, B), whereas the most aggressive MDA-MB-231 cell line had the highest proportion of $CD44^{+}/CD24^{-}$ cells (47.52 ± 2.08%) (Figure 3.3C). The moderately metastatic Hs578-T cell line also contained a $CD44^{+}/CD24^{-}$ population (31.14 ± 2.46%; Figure 3.3D). This indicates a large amount of MDA-MB-231 and Hs578-T cells expressing these surface markers. The opposite was observed for the $CD44^{-}/CD24^{+}$ sub-population which was enriched in MCF-7-A and T-47D cell lines (34.77 ± 3.85% and 47.46 ± 4.67%), and was almost absent in the MDA-MB-231 and Hs578-T cell lines contained (7.05± 1.95 and 6.4 ± 1.3% respectively) (Figure 3.3).

A quantitative analysis is summarised in Figure 3.4 and Table 3.1, showing that the MDA-MB-231 cells contained significantly more cells with a $CD44^{+}/CD24^{-}$ phenotype than any of the other cell lines ($P<0.001$), and that the Hs578-T cell line had significantly more cells with a $CD44^{+}/CD24^{-}$ phenotype than either the MCF-7 or T-47D cell lines ($P<0.001$) (Figure 3.4). In addition, Table 3.2 shows the tumor type and classification based on gene expression profiling or expression of markers (Charafe-Jauffret et al., 2006, Thompson et al., 1992).

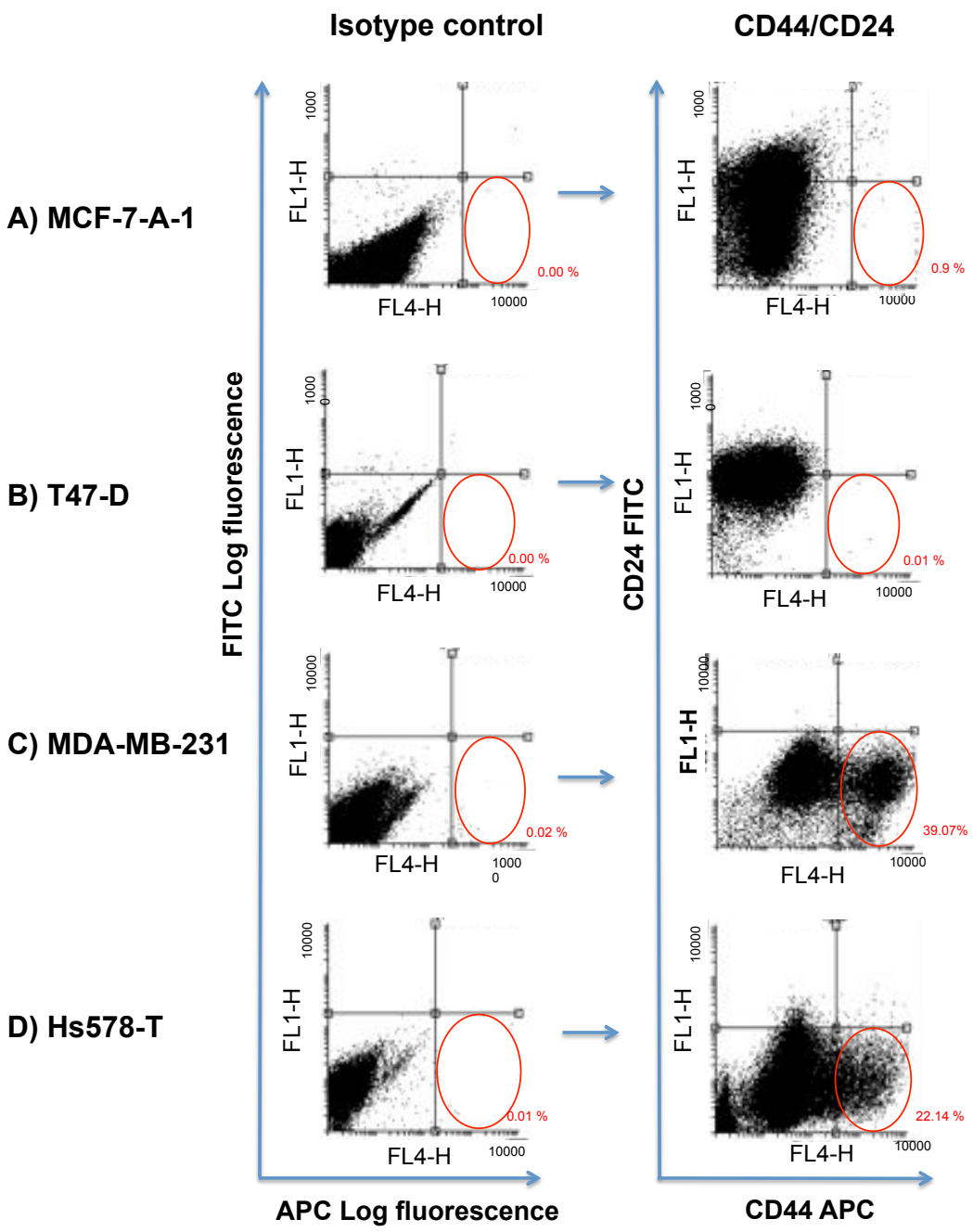

Figure 3.3 Human BCC lines contain sub-populations of cells that differ quantitatively in their expression of CSC markers. Flow cytometry analysis was carried out for CD44 and CD24 on (A) MCF7-A-1, (B) T-47D, (C) MDA-MB-231 and (D) Hs578-T cells. Cell were maintained as described in Methods. 105 single-cell suspensions of cells were subjected to double staining with anti-human CD44 and CD24. Left-hand panels show representative dot plots of APC versus FITC IgG-1 isotype control. Right-hand panels show dot plots of CD44 conjugated to APC versus CD24 conjugated to FITC expression. Cells in the red regions correspond to a designatedCD44+/CD24- Population. Approximately 30,000 events were collected/sample. Data from one of four representative experiments (each with duplicate measurements).

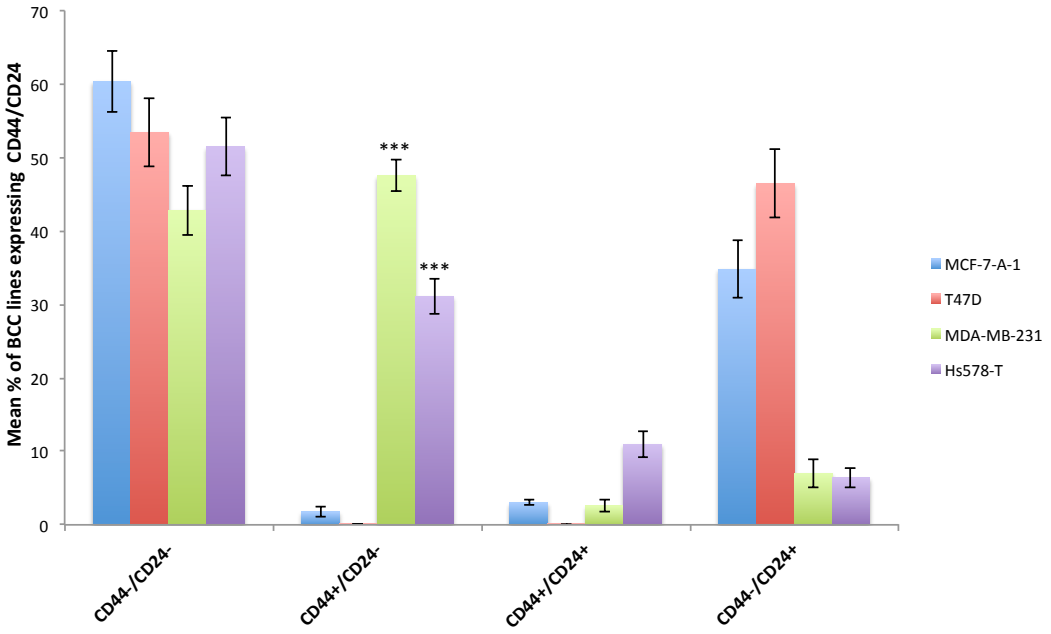

Figure 3.4 Quantitative analysis of expression of CD44/CD24 surface markers in human BCC lines. MCF-7-A-1, T-47D, MDA-MB-231 and Hs578-T cell lines were maintained as described in Methods. Upon reaching 80% confluence, total cells were incubated with an anti-CD44 antibody conjugated to APC and an anti-CD24 antibody conjugated to FITC, or appropriate APC and FITC-conjugated IgG isotype controls. The percentage of $CD44^{+}/CD24^{-}$ expressing cells were analyzed by FACS as in Figure 3.3 (in duplicate). Data are presented as the mean ± SD from 4 independent experiments (n=4) (each with duplicate measurements). *** MDA-MB-231 and Hs578-T have significantly larger $CD44^{+}/CD24^{-}$ populations relative to the MCF-7-A-1 and T-47D cell lines ($P<0.001$).

Table 3.2 Summary of CSC marker CD44/CD24 sub-populations of various human BCC lines

Cell line	$CD44^{+}/CD24^{-}$	$CD44^{+}/CD24^{+}$	$CD44^{-}/CD24^{+}$	$CD44^{-}/CD24^{-}$	Tumour type	Cell type classification
MCF-7-A	1.77 ± 0.66	3.05 ± 0.4	34.77 ± 3.85	60.39 ± 4.17	Adenocarcinoma	Luminal
T-47D	0.03 ± 0.4	0.03 ± 0.08	47.46 ± 4.67	53.46 ± 4.66	Ductal carcinoma	Luminal
ZR-75-1	0.01 ± 0.3	0.03 ± 0.02	43.7 ± 2.4	56.29 ± 1.8	Breast, ductal carcinoma	Luminal
MDA-MB-231	47.52 ± 2.08	2.56 ± 0.76	7.05 ± 1.95	42.85 ± 3.39	Adenocarcinoma	Claudin-low
Hs578-T	31.14 ± 2.46	10.99 ± 1.78	6.4 ± 1.3	51.45 ± 3.39	Carcinoma	Claudin-low

3.4 Strategy for isolation of $CD44^+/CD24^-$ cells from human BCC lines

Since the MDA-MB-231 and Hs578-T human BCC lines demonstrated that they had the most distinct sub-sets of cells with stem-like characteristics (CSC markers) these cell lines were chosen for further studies as models to establish the effect of HS and chemically modified heparin on cell morphology, growth rates and molecular mechanisms. Flow cytometery was used to assess the isolation of suitable CSC sub-populations based on the marker expression pattern $CD44^+/CD24^-$; the cell sorting strategies developed are represented in Figure 3.5 (MDA-MB-231) and Figure 3.6 (Hs578-T).

CD44 and CD24 antibody staining resulted in four distinct sub-populations designated here for simplicity as P4, P5, P6 and P7 (P7=$CD44^-/CD24^-$, P4=$CD44^+/CD24^-$, P6=$CD44^+/CD24^+$ and P5=$CD44^-/CD24^+$). These four phenotypic subpopulations were separated by FACSAria (as described in Methods). The percentages of $CD44^+/CD24^-$, $CD44^+/CD24^+$, $CD44^-/CD24^+$, and $CD44^-/CD24^-$ cells for MDA-MB-231 cell line were 52.7%, 9.3%, 1.7%, and 19.2%, respectively (Figure 3.5). The percentages of $CD44^+/CD24^-$, $CD44^+/CD24^+$, $CD44^-/CD24^+$, and $CD44^-/CD24^-$ cells for Hs578-T cell line were 36.3%, 3.8%, 8.0%, and 49.5%, respectively (Figure 3.6). The phenotype of the putative CSC sub-population was characterized as described in the following sections. This was undertaken in order to confirm that they displayed the expected behaviour of CSCs linked with tumor malignancy or aggressiveness, as described previously in the literature.

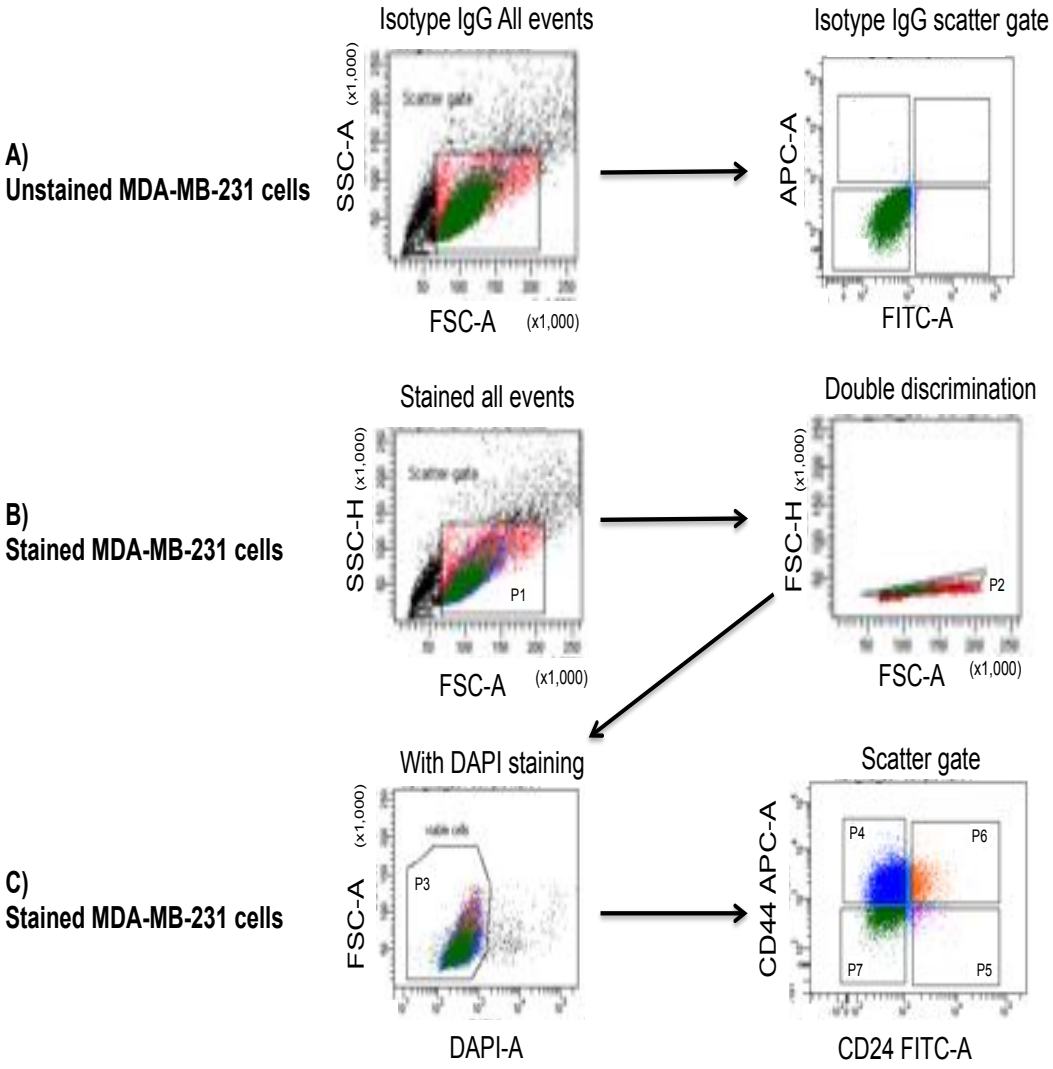

Figure 3.5 Strategy for isolation of CD44$^+$/CD24$^-$ cells from MDA-MB-231 human BCC line. FACS was used to isolate CD44$^+$ and CD24$^-$ sub-population from MDA-MB-231 cells for functional assays (see Figure 3.3). Cells were concurrently labelled with DAPI, and the fluorescent antibodies anti-CD44 APC and anti-CD24 FITC. Cell sub-populations were isolated using a four colour protocol on a FACSAria cell sorter (CD44$^+$/CD24$^-$, CD44$^+$/CD24$^+$, CD44$^-$/CD24$^+$ and CD44$^-$/CD24$^-$ sub-populations were collected). (A–C): Representative schematic of a sequentially gated MDA-MB-231 cell line sort. (A) Unstained cells (Isotype IgG) were set as a control based on light scatter (left panel) and on expression of APC/FITC flurochrome (right panel). (B) Cells were first selected for viability based on light scatter (P1, left panel) and for double discrimination (P2, right panel). (C) Cells were then selected based on DAPI negativity (P3, left panel) and finally, divided into four sub-populations based on expression of CD44 and CD24 expression phenotype (gated on P4 (CD44$^+$/CD24$^-$) ≈ 52.7% + P5 (CD44$^-$/CD24$^+$) ≈ 1.7% + P6 (CD44$^+$/CD24$^+$) ≈ 9.3% + P7 (CD44$^-$/CD24$^-$) ≈ 19.2% of parent population) (right panel). The resulting cell sub-populations were designated as CD44$^+$/CD24$^-$ (P4), 'stem-like', and were collected and compared with the other three sub-populations in further functional analyses for differences in malignant and metastatic behavior *in vitro*. Representative example from multiple cell sorting experiments during the project.

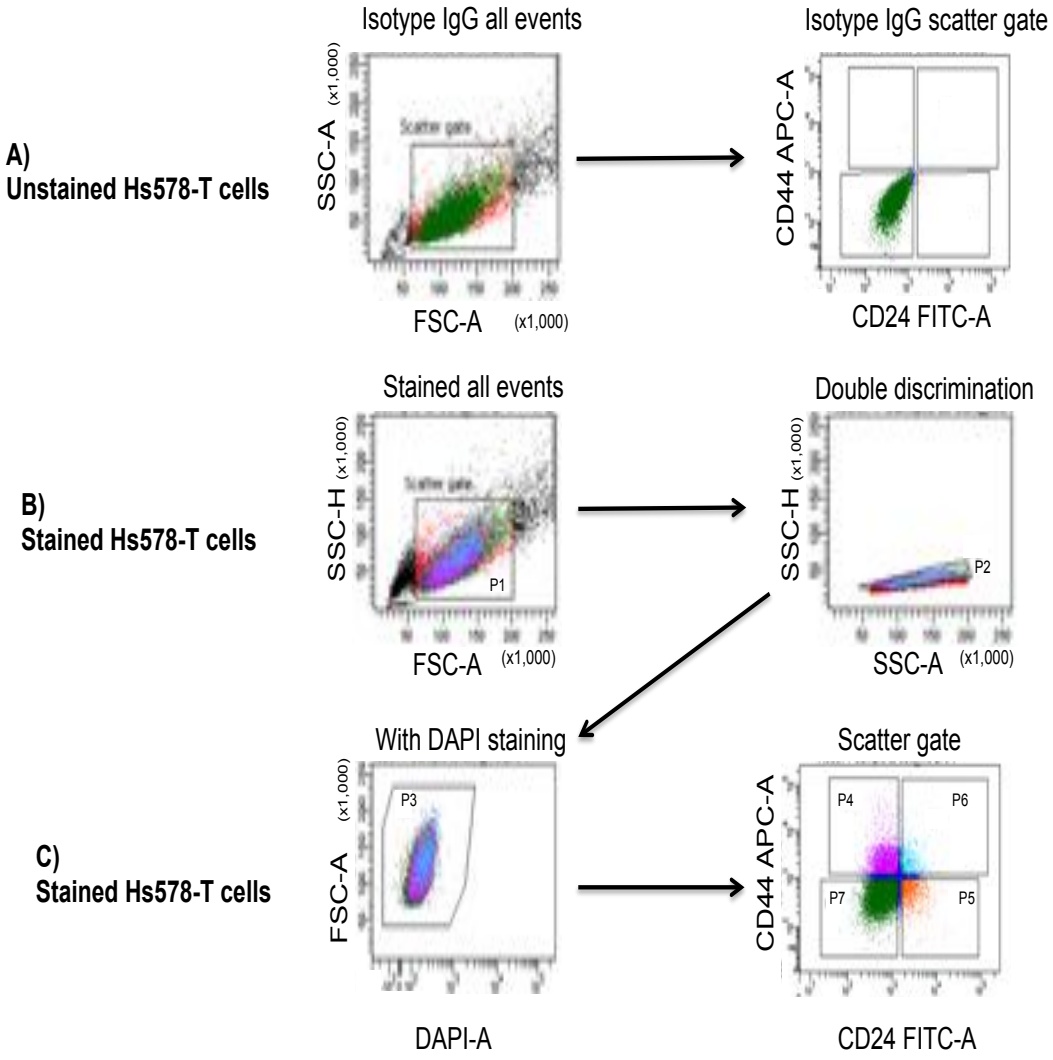

Figure 3.6 Strategy for isolation of CD44$^+$/CD24$^-$ cells from Hs578-T human BCC line. FACS was used to isolate CD44$^+$ and CD24$^-$ sub-population from Hs578-T cells for functional assays (see Figure 3.3). Cells were concurrently labelled with DAPI, and the fluorescent antibodies anti-CD44 APC and anti-CD24 FITC. Cell sub-populations were isolated using a four colour protocol on a FACSAria cell sorter (CD44$^+$/CD24$^-$, CD44$^+$/CD24$^+$, CD44$^-$/CD24$^+$ and CD44$^-$/CD24$^-$ sub-populations were collected). (A–C): Representative schematic of a sequentially gated Hs578-T cell line sort. (A) Unstained cells (Isotype IgG) were set as a control based on light scatter (left panel) and on expression of APC/FITC flurochrome (right panel). (B) Cells were first selected for viability based on light scatter (P1, left panel) and for double discrimination (P2, right panel). (C) Cells were then selected based on DAPI negativity (P3, left panel) and finally, divided into four sub-populations based on expression of CD44 and CD24 expression phenotype (gated on P4 (CD44$^+$/CD24$^-$) ≈ 36.3% + P5 (CD44$^-$/CD24$^+$) ≈ 8.0% + P6 (CD44$^+$/CD24$^+$) ≈ 3.8% + P7 (CD44$^-$/CD24$^-$) ≈ 49.5% of parent population) (right panel). The resulting cell sub-populations were designated as CD44$^+$/CD24$^-$ (P4), 'stem-like', and were collected and compared with the other three sub-populations in further functional analyses for differences in malignant and metastatic behavior *in vitro*. Representative example from multiple cell sorting experiments during the project.

3.5 Human BCSC $CD44^+/CD24^-$ sub-populations demonstrate enhanced viability and cell growth in vitro

In order to undertake phenotypic characterization of the four sub-populations of BCC lines (MDA-MB-231 and Hs578-T) linked with tumor malignancy or aggressiveness, they were initially assessed by evaluating their cell viability in vitro. FACS-sorted cells were cultured in 24 well plates at a density of $4x10^4$ cells/well and counted after trypan blue staining at various time points (24, 48 and 72 hrs). As shown in Figure 3.7A, B, the viability of all the cell sub-populations was demonstrated, with increasing cell proliferation observed over the time points investigated. No significant differences in viability were noted at 24 hrs, but after 48 and 72 hrs incubation the $CD44^+/CD24^-$ cells had shown the greatest increase in both MDA-MB-231 and Hs578-T lines. In some cases these differences were statistically significant, in particular the $CD44^+/CD24^-$ cells compared to $CD44^-/CD24^-$, $CD44^-/CD24^+$ and $CD44^+/CD24^+$ cell sub-sets ($P<0.05$, $P<0.01$, $P<0.001$) (Figure 3.7A, B).

To corroborate the results obtained using trypan blue, proliferation assays were also was measured in an MTT assay (Figure 3.8). Results obtained after various time points 6, 24, 48 and 72 hrs of incubation were consistent with those using trypan blue (Figure 3.7), indicating proliferation MDA-MB-231 and Hs578-T BCCs. In addition, these results clearly indicate the enhanced proliferation of $CD44^+/CD24^-$ cells compared to other sub-populations for both MDA-MB-231 and Hs578-T cells, at 24, 48 and 72 hours (Figure 3.8A, B).

In MDA-MB-231 and Hs578-T cells, the proliferation rates of cell sub-populations were not significantly different after only 6 hrs of incubation, as might be expected at this early time point when cells have just become adherent. A significant increase of growth rates of these cell sub-populations was detected after 24, 48 and 72 hrs ($P<0.05$, $P<0.01$, $P<0.001$) (Figure 3.8). The $CD44^+/CD24^-$ cell numbers were significantly increased compared to $CD44^-/CD24^-$ ($P<0.001$) and $CD44^+/CD24^+$ and $CD44^-/CD24^+$ ($P<0.05$, $P<0.01$, $P<0.01$) at all time points except at 6 hrs, for MDA-MB-231 (Figure 3.8A). Similarly the $CD44^+/CD24^-$ sub-population from Hs578-T showed significantly increased compared to $CD44^-/CD24^-$ ($P<0.001$), and $CD44^+/CD24^+$ and $CD44^-/CD24^+$ ($P<0.01$) at 24 hrs, and significantly increased

compared to all other sub-populations (P<0.001) at 48 and 72 hrs (Figure 3.8B).

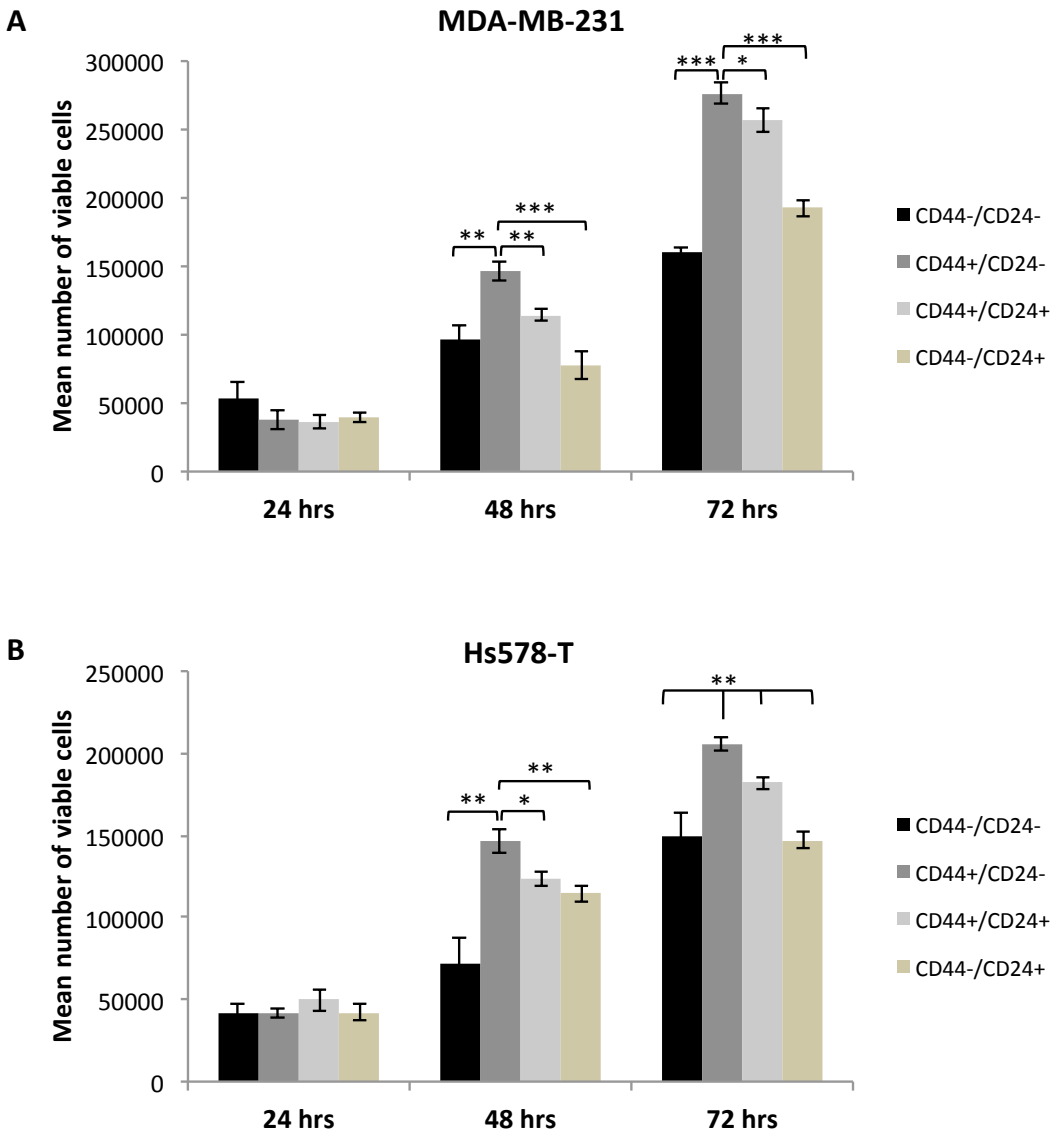

Figure 3.7 Relative cell viability potential of BCSCs *in vitro*. The cell viability of the four CD44/CD24 expression sub-populations of (A) MDA-MB-231 and (B) Hs578-T cell lines was evaluated by trypan blue staining assay at various time points (24, 48 and 72 hrs). Results are expressed as mean value ± S.D from 3 independent experiments (each with duplicate measurements). *P<0.05, **P<0.01, ***P<0.001 vs. $CD44^{+}/CD24^{-}$ sub-population.

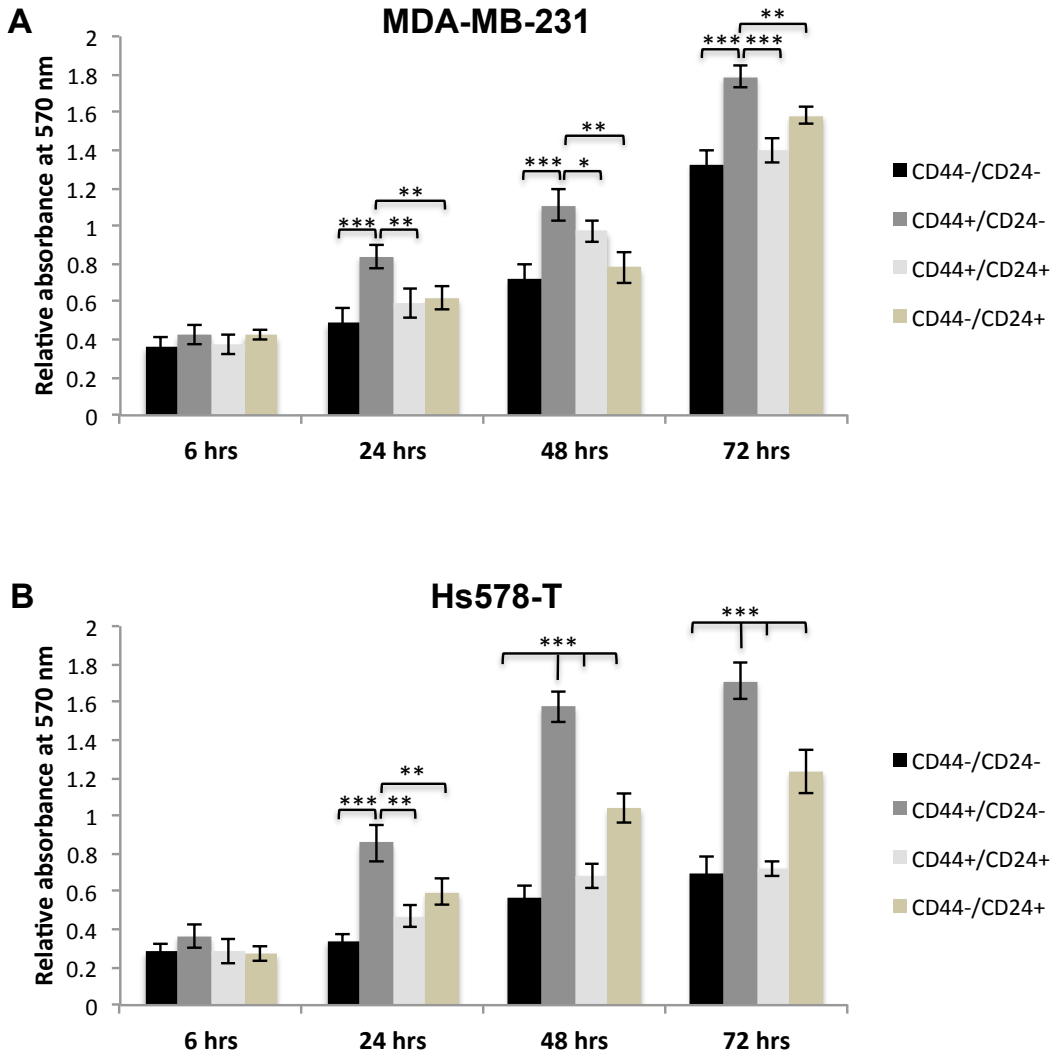

Figure 3.8 Cell growth differs between four CD44/CD24 expression sub-populations from MDA-MB-231 and Hs578-T human BCCs. Four sub-populations ($CD44^-/CD24^-$, $CD44^+/CD24^-$, $CD44^+/CD24^+$ and $CD44^-/CD24^+$) isolated from the (A) MDA-MB-231 and (B) Hs578-T BCC lines were cultured at a density of $4x10^4$ for various time points 6, 24, 48 and 72 hrs and cell number was determined by MTT assay. Data shown are the means ± SD, from 2 independent experiments, each with triplicate measurements. *=P<0.05, **=P<0.01, ***=P<0.001 corresponding to $CD44^+/CD24^-$ cells.

3.6 Human BCSC $CD44^+/CD24^-$ sub-populations demonstrate enhanced adhesion abilities in vitro

Cell adhesion assays were performed to further investigate the adhesion properties of the two cell types MDA-MB-231 and Hs578-T with the objective of identifying any preferential properties of the BCSCs. To assess the total number of adhered cells, cells were seeded on 96 well plates coated with fibronectin; after the experimental time points (0, 1, 3 and 5 hrs), cells were detached enzymatically using trypsin/EDTA and counted using a hemocytometer.

The number of sorted attached cells at the time points of 0, 1, 3 and 5 hrs is presented in Figure 3.9. The results from the four sub-population of MDA-MB-231 cells are represented in the Figure 3.9A. At each time point the $CD44^+/CD24^-$ cells displayed more attached cells compared to the other three sub-populations ($CD44^-/CD24^-$, $CD44^+/CD24^+$ and $CD44^-/CD24^+$). After 1 and 3 hrs incubation, the adhesion of $CD44^+/CD24^-$ cells were only slightly higher than for $CD44^+/CD24^+$ cells but this difference was not statistically significant. On the other hand, statistically significant differences were evident for the higher mean number of attached $CD44^+/CD24^-$ cells at 1 and 3 hrs compared to $CD44^-/CD24^-$ and $CD44^-/CD24^+$ cells ($P<0.001$) (Figure 3.9A). However, comparing the sub-populations after 5 hrs incubation it was evident that $CD44^+/CD24^-$ cells showed a significantly higher number of attached MDA-MB-231 cells compared to all three sub-populations ($CD44^-/CD24^-$ and $CD44^-/CD24^+$, $P<0.001$ and $CD44^+/CD24^+$, $P<0.01$) (Figure 3.9A). Overall these data indicated that $CD44^+/CD24^-$ cells show significantly greater adhesive capacity compared to other MDA-MB-231 BCC sub-populations.

The cell adhesion data from Hs578-T cells (mean ± SD, n = 3) is shown in Figure 3.9B. In general the data were similar to that for the MDA-MB-231 cells. Firstly, the $CD44^+/CD24^-$ cells displayed higher adhesive capacity than $CD44^-/CD24^-$ cells at all time points, and these differences were statistically significant ($P<0.001$) (Figure 3.9B). For the $CD44^-/CD24^+$ cells adhesion was lower at all time points but was only statistically significant at 3 and 5 hrs ($P<0.05$ and $P<0.001$ respectively). Although there was a consistent trend for $CD44^+/CD24^+$ cells to exhibit lower adhesion than $CD44^+/CD24^-$ cells at all time points, this difference did not reach statistical

significance except only statistically significant at 5 hrs ($P<0.01$). (Figure 3.9B). Overall these data indicated that $CD44^+/CD24^-$ cells show significantly greater adhesive capacity compared to other Hs578T BCC sub-populations, with the possible exception of the $CD44^+/CD24^+$ cells.

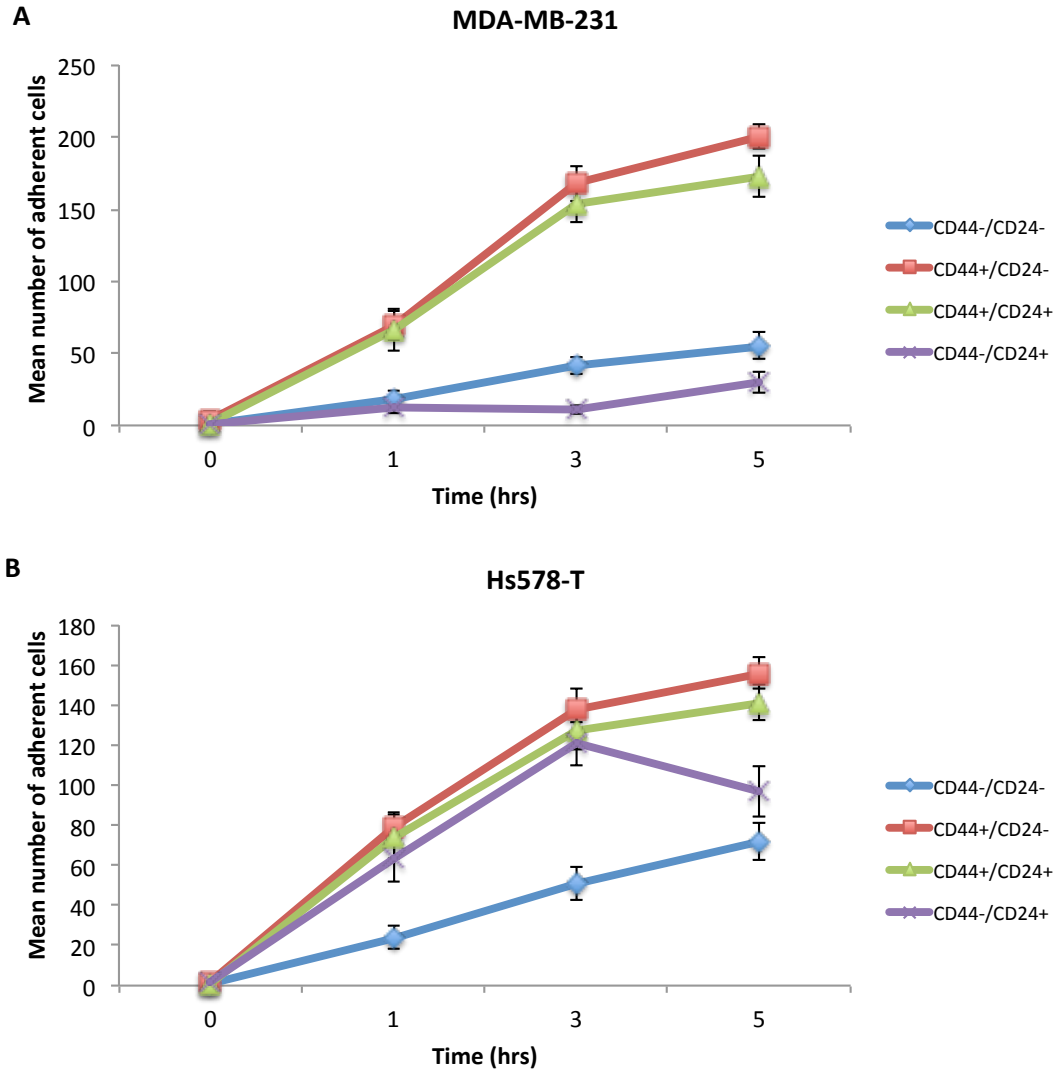

Figure 3.9 $CD44^+/CD24^-$ CSCs from MDA-MB-231 and Hs578-T human BCCs display elevated cell adhesion capacity. $CD44^-/CD24^-$, $CD44^+/CD24^-$, $CD44^+/CD24^+$ and $CD44^-/CD24^+$ cells (2×10^4) isolated from the (A) MDA-MB-231 and (B) Hs578-T BCC lines by FACS-sorting were plated in triplicate for various time points (0, 1, 3, 5 hrs) onto fibronectin-coated sterile 96-well non-tissue culture plates. Non-nadherent cells were removed and adherent cells were quantified by manual counting using a hemocytometer at a magnification of ×10. Data are presented as the mean adhesion from three independent experiments (mean ± SD; 3 replicates in each experiments).

3.7 Human BCSC $CD44^+/CD24^-$ sub-populations demonstrate enhanced migratory abilities *in vitro*

To further determine whether human BCSCs display traits linked with tumor malignancy or aggressiveness, the migration ability of the sorted sub-populations from MDA-MB-231 and Hs578-T human BCC lines was investigated. The $CD44^-/CD24^-$, $CD44^+/CD24^-$, $CD44^+/CD24^+$ and $CD44^-/CD24^+$ sorted sub-populations were assessed in a Transwell migration assay with FBS as chemoattractant (Figure 3.10A).

The numbers of $CD44^-/CD24^-$, $CD44^+/CD24^-$, $CD44^+/CD24^+$, and $CD44^-/CD24^+$ MDA-MB-231 cells that migrated through the basement membrane were 116 ± 15.5, 214 ± 15.6, 170 ± 10.1, and 99 ± 7.1 / field) respectively. The numbers of $CD44^-/CD24^-$, $CD44^+/CD24^-$, $CD44^+/CD24^+$, and $CD44^-/CD24^+$ Hs578-T cells that migrated through the basement membrane were 66 ± 7.62, 156 ± 7.55, 81 ± 8.6, and 118 ± 12.3 / field) respectively (Figure 3.10B).

We observed that the number of migrating cells in $CD44^+/CD24^-$ in both cell lines (MDA-MB-231 and Hs578-T cells) towards serum was significantly higher than respective $CD44^-/CD24^-$, $CD44^+/CD24^+$ and $CD44^-/CD24^+$ sub-populations ($P<0.001$). The migration of $CD44^-/CD24^+$ sub-population cells from MDA-MB-231 was lower than $CD44^+/CD24^+$ sub-population ($P<0.001$) and also $CD44^-/CD24^-$ cells ($P<0.05$). Similar results were seen for Hs578-T cells, [except that $CD44^-/CD24^+$ cell migration only showed a strong trend towards higher migration capacity than $CD44^+/CD24^+$ and $CD44^-/CD24^-$ cells, ($P<0.001$) (Figure 3.10B)]. These results revealed that $CD44^+/CD24^-$ cells exhibited elevated migrative capacity compared to the other three sub-population of both MDA-MB-231 and Hs578-T cells.

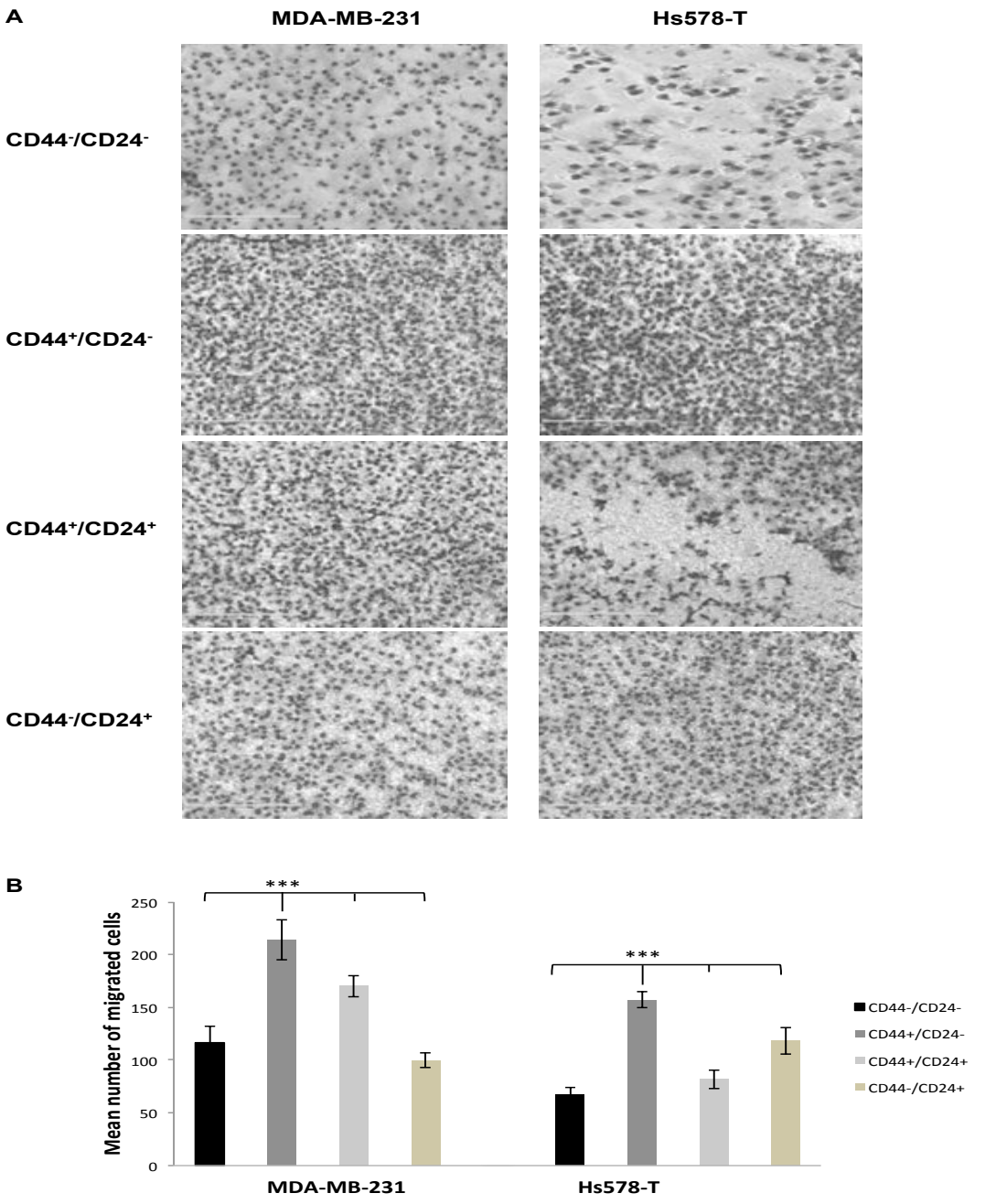

Figure 3.10 $CD44^+/CD24^-$ CSCs from MDA-MB-231 and Hs578-T human BCCs display elevated migratory capacity. The migration of four sorted sub-population cells $CD44^-/CD24^-$, $CD44^+/CD24^-$, $CD44^+/CD24^+$ and $CD44^-/CD24^+$ were assessed in Transwell cell culture chambers for 24 hours in response to a chemoattractant media (5% FBS) as described in Methods. (A) Representative photos of migration assay in human BCSCs (MDA-MB-231 and Hs578-T) cells. MDA-MB-231 and Hs578-T $CD44^+/CD24^-$ sub-population cells show higher more migration capability than $CD44^-/CD24^-$, $CD44^+/CD24^+$ and $CD44^-/CD24^+$ cells. Scale bar=400 μm (B) The mean number of FACS-sorted cells (12×1^3 cells/well), n=3 for each cell population migrating through the chamber towards chemoattractant was assessed. Migrated cells were quantified by manual counting four fields/well. Data from one of three representative experiments shown; mean ± SD, n=2 replicates in each assay. ***=significantly different than respective population of $CD44^+/CD24^-$ cells migrating through transwell towards FBS ($P<0.001$).

3.8 Human BCSC $CD44^+/CD24^-$ sub-populations demonstrate enhanced invasive potential *in vitro*

In order to establish the cell invasive phenotype of the two human BCC lines (MDA-MB-231 and Hs578-T) Matrigel invasion assays were performed. Sorted cells were seeded onto Matrigel-coated transwell membranes and after 24 hrs cells that invaded to the lower side of the filter were counted and shown (Figure 3.11A). Following incubation period, the numbers of $CD44^-/CD24^-$, $CD44^+/CD24^-$, $CD44^+/CD24^+$, and $CD44^-/CD24^+$ of MDA-MB-231 cells that invaded through the basement membrane were 105 ± 8.8, 241 ± 16.4, 189 ± 12.1, and 176 ± 12 / field; magnification, ×10) respectively. The equivalent data for Hs578-T cells were 71 ± 10.5, 211 ± 11.1, 194 ± 10.4, and 128 ± 9 / field; magnification, ×10) respectively (Figure 3.11B).

$CD44^+/CD24^-$, $CD44^+/CD24^+$ and $CD44^-/CD24^+$ subpopulations of MDA-MB-231 and Hs578-T were observed to be significantly more invasive towards serum through Matrigel than the $CD44^-/CD24^-$ sub-population ($P<0.001$). The number of invading cells from the $CD44^+/CD24^-$ subset was significantly higher compared to the two sub-populations $CD44^+/CD24^+$ and $CD44^-/CD24^+$ cells in MDA-MB-231 cell line ($P<0.001$). $CD44^+/CD24^-$ and $CD44^+/CD24^+$ cells from Hs578-T cells displayed approximately similar levels of invasion, while the level for $CD44^+/CD24^-$ cells was significantly higher than the $CD44^-/CD24^-$ and $CD44^-/CD24^+$ cells ($P<0.001$) (Figure 3.11B). These results revealed that $CD44^+/CD24^-$ cells have a higher metastatic capacity, consistent with the hypothesis that CSCs contribute to migration and invasion of tumours.

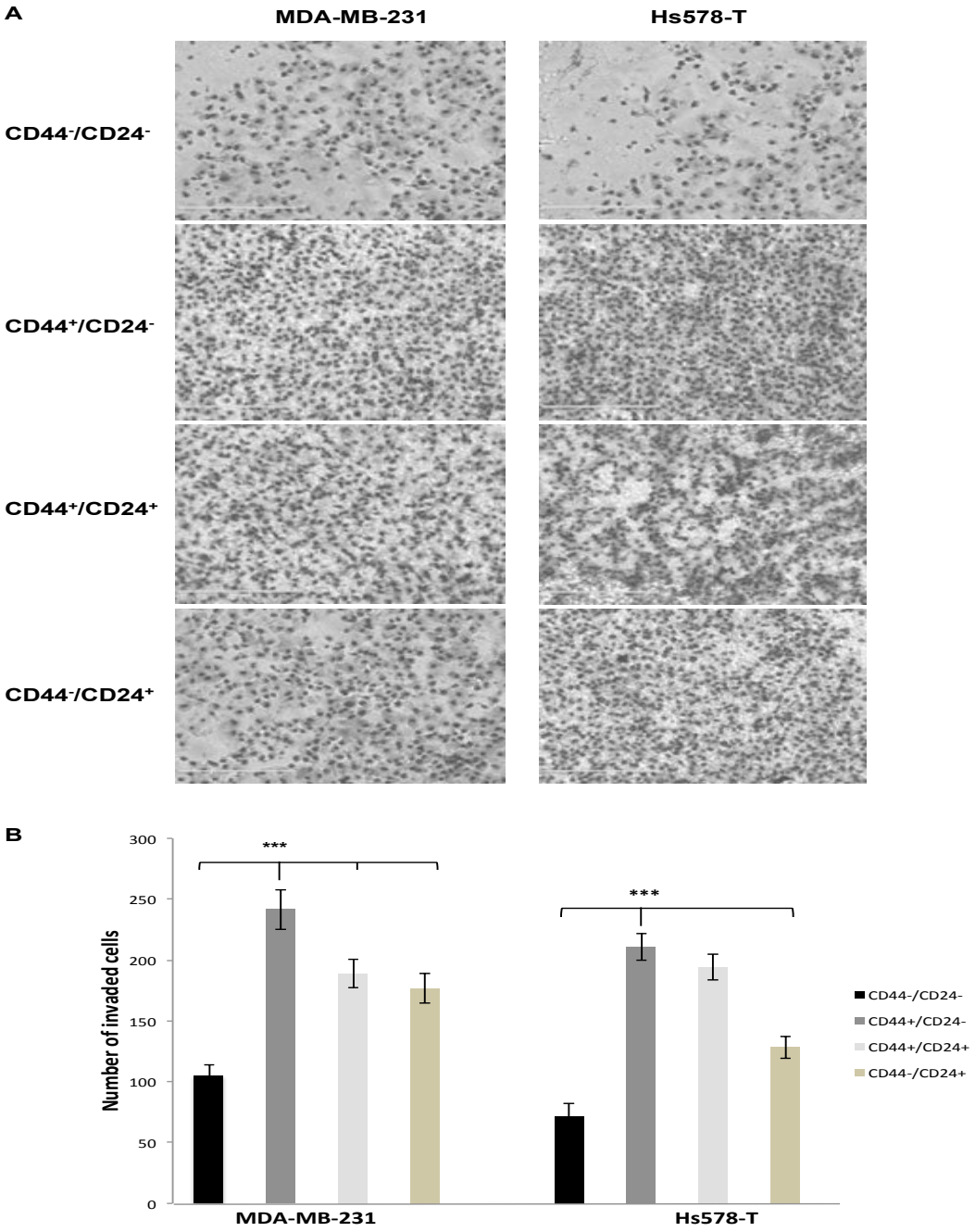

Figure 3.11 $CD44^+/CD24^-$ CSCs from MDA-MB-231 and Hs578-T human BCCs display high invasive potential. Four sub-populations ($CD44^-/CD24^-$, $CD44^+/CD24^-$, $CD44^+/CD24^+$ and $CD44^-/CD24^+$) were isolated from the MDA-MB-231 and Hs578-T BCC lines. Transwells (8µm) were pre-coated with 10 µg/well Matrigel and FACS-sorted cells (12×10^3 cells/well), (n=2) for each cell population). Cells were allowed to invade through the Matrigel for 24 hrs towards chemoattractant media (5% FBS). (A) Representative photos of invasion assay data from each set of cell line sub-populations from human BCSCs (MDA-MB-231 and Hs578-T). Invasion of the four sorted sub-population cells $CD44^-/CD24^-$, $CD44^+/CD24$, $CD44^+/CD24^+$ and $CD44^-/CD24^+$ were measured in Transwell cell culture chambers following 24 hrs incubation. $CD44^+/CD24^-$ cells sorted from MDA-MB-231 and Hs578-T show more invasion capability than the other three sub-populations. The mean number of cells invaded to the lower surface was counted. Scale bar=400 µm. (B) The number of invading cells was quantified by manual counting of four fields/well. Data from one of three representative experiments shown; mean ± SD, n=2 replicates in each assay. ***=$CD44^+/CD24^-$ cells were significantly different than other sub-populations of MDA-MB-231 and Hs578-T cells invading through Matrigel towards FBS ($P<0.001$).

3.9 Human BCSC $CD44^+/CD24^-$ sub-populations exhibit higher colony forming efficiency compared with other sub-populations

To further investigate possible functional differences between $CD44^+/CD24^-$ CSCs and other sub-populations from MDA-MB-231 and Hs578-T BCC lines, these cells were also FACS-sorted and tested in a colony-formation efficiency assay. After four weeks of incubation, colonies were seen in the soft agar and cells were counted. The colony-formation capacity of $CD44^+/CD24^-$ and other respective sub-populations indicated that putative CSC $CD44^+/CD24^-$ cells from the MDA-MB-231 and Hs578-T cell lines have a significantly higher potential to form colonies compared to the other respective sub-populations ($P<0.01$, $P<0.001$) (Figure 3.12).

On average, $CD44^+/CD24^-$ and $CD44^+/CD24^+$ cells from MDA-MB-231 cell line gave rise to 28 colonies per 1×10^3 input cells and $CD44^-/CD24^-$, $CD44^-/CD24^+$ cells gave rise to 20 and 17 colonies per 1×10^3 input cells, respectively. The number of colonies of $CD44^+/CD24^-$ cells was significantly higher compared to $CD44^-/CD24^-$, and $CD44^-/CD24^+$ cells ($P<0.01$, $P<0.001$), whereas $CD44^+/CD24^-$ and $CD44^+/CD24^+$ cells from MDA-MB-231 cells displayed approximately similar levels of colony formation efficiency (Figure 13.12).

Broadly similar results were obtained in experiments performed with sub-populations from Hs578-T cells (Figure 13.12). On average, $CD44^+/CD24^-$ cells gave rise to 25 colonies per 1×10^3 input cells, $CD44^+/CD24^+$ cells gave rise to 17 colonies per 1×10^3 input cells, and $CD44^-/CD24^-$, $CD44^-/CD24^+$ cells gave rise to 16 and 11 colonies per 1×10^3 input cells, respectively. $CD44^+/CD24^-$ cells were observed to be significantly higher in number of colonies than other Hs578-T sub-populations ($P<0.01$, $P<0.001$) (Figure 13.12). Overall the data from both cells lines support the view that $CD44^+/CD24^-$ cells have a more aggressive colony-forming ability which is characteristic of putative CSCs.

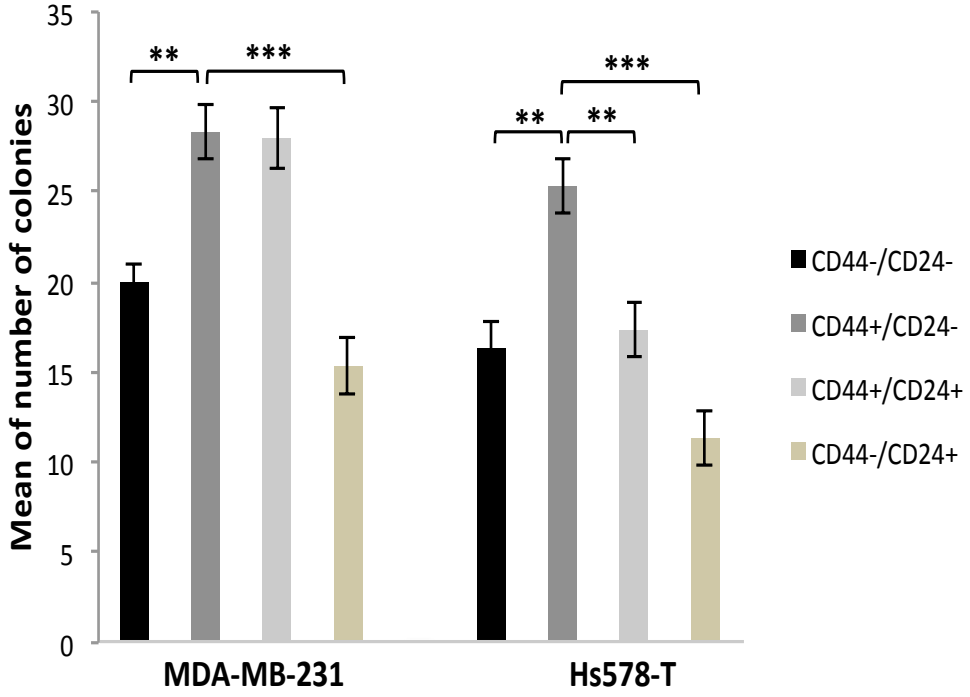

Figure 3.12 $CD44^+/CD24^-$ CSCs from MDA-MB-231 and Hs578-T human BCCs display elevated colony forming ability. FACS-sorted cells were grown in soft agar (0.6%) for 4 weeks ($1x10^3$ cells/96 well plate, n=3 wells/cell population). Colonies were quantified and the results represent combined data (mean ± SD) from two independent experiments (each with triplicate measurements). Statistical analysis was performed using a Student's t-test. **P < 0.01, ***P < 0.001 for $CD44^+/CD24^-$ vs. other respective populations.

3.10 Human BCSC $CD44^+/CD24^-$ sub-populations display higher chemoresistance to chemotherapeutic agents

Since CSCs have been reported to display higher resistance to chemotherapeutic agents, the effect of such agents on apoptosis of cell sub-populations from MDA-MB-231 and Hs578-T BCC lines was studied, by staining for Annexin V and PI. Cell subsets were stained with Annexin V and PI, which can be detected in the early and late stage of apoptosis respectively. The use of annexin V along with PI staining made it possible to distinguish apoptotic cells from cells with a damaged cell membrane. Cells were grown and treated separately with three different agents tamoxofin (Tam), doxorubicin (Dox) or cisplatin (Cis) and incubated for 24, 48 and 72 hrs. After incubation, sorted cells were subjected to Annexin V/PI staining and analyzed using flow cytometry. Figure 3.13 and 3.14 show representative data analysis of apoptotic cells in $CD44^+/CD24^-$ and $CD44^-/CD24^-$ sorted cells from MDA-MB-231 and Hs578-T human BCCs respectively, treated with doxorubicin,

and tamoxifen for 48 hrs and cisplatin for 72 hrs. For comparison data are also provided for unsorted cells, since insufficient cells were available for the other 2 minor cell sub-populations to permit these experiments. Complete FACS datasets are provided in Appendix 2.1, 2.2 and 2.3.

Individual experiments showed that treatment of the $CD44^-/CD24^-$, $CD44^+/CD24^-$ sorted and unsorted MDA-MB-231 cells with different doses of doxorubicin after 48 hrs were affected and the number of apoptotic cells were increased steadily in approximately 5% with the increase of doxorubicin concentrations, as compared to untreated cells (Figure 3.13 A). 5 μg/ml doxorubicin resulted in the highest percentages of apoptotic cells compared to untreated cells ($P<0.001$). It was shown that, no significant differences between $CD44^-/C24^-$ and $CD44^+/C24^-$ untreated cells, and apoptotic percentage of $CD44^+/C24^-$ cells were significantly lower compared to untreated unsorted cells ($P<0.05$). $CD44^-/C24^-$ cells were significantly the highest percentage of apoptotic cells compared to unsorted cells and $CD44^+/C24^-$ cells in cell cultures treated with various concentration of doxorubicin ($P<0.05$, $P<0.01$, $P<0.001$) (Figure 3.13A). As a proof of principle chemoresistance of cancer initiating-like cells, $CD44^+/C24^-$ sorted cells from MDA-MB-231 were more resistant to doxorubicin at various concentrations than other sub-populations cells ($P<0.05$, $P<0.001$) (Figure 3.13A).

To determine whether the increase of cell apoptosis observed after treatment with different concentrations of other chemotherapeutic agent (cisplatin), MDA-MB-231 cells were also tested with flow cytometry (Figure 3.13B). After incubation of MDA-MB-231 cells with various concentrations of cisplatin for 72 hrs, cisplatin treatment significantly induced apoptosis compared to untreated cells ($P<0.01$, $P<0.001$). $CD44^+/CD24^-$ cells treated with 0.001, 0.01 or 0.1 μM cisplatin for 72 hrs did not show increased levels of apoptosis compared with untreated cell groups, but showed significantly levels of apoptosis at 1 and 10 μM ($P<0.01$). The apoptotic percentages of $CD44^+/CD24^-$ cells treated with 0.001, 0.01 or 0.1 μM for 72 hrs were significantly lower compared to the other cell populations ($P<0.01$, $P<0.001$). In contrast, $CD44^+/CD24^-$ cells treated with 10 μM of cisplatin were significantly higher than respective populations ($P<0.05$, $P<0.01$). No significant differences were observed between $CD44^+/CD24^-$ and $CD44^-/CD24^-$ after treatment with 1 μM of

cisplatin, while a significant decrease was observed compared to unsorted cells ($P<0.001$) (Figure 3.13B).

Tamoxifen treatments were also tested on MDA-MB-231 cell populations. Figure 3.13C shows mean ± SD values of the percentages of apoptotic unsorted and sorted cells ($CD44^-/CD24^-$ and $CD44^+/CD24^-$) after 48 hrs incubation with various concentrations. Percentages of apoptosis in isolated MDA-MB-231 cells treated with low concentrations of tamoxifen for 48 hrs were not detected at all time points. Higher concentrations of tamoxifen (1000, 10000 and 100000 nM) were significantly higher than in those of untreated cells ($P<0.01$, $P<0.001$). Moreover, significant differences were not observed between sorted and unsorted cells in most treated cells. $CD44^+/CD24^-$ cells were significantly lower than unsorted cells at 10000 and 100000 nM tamoxifen ($P<0.05$, $P<0.001$). In addition, $CD44^+/CD24^-$ cells were significantly lower than $CD44^-/CD24^-$ cells at 100000 ($P<0.05$) and no significant effect was observed at 10000 nM tamoxifen Figure 3.13C.

To further investigate the effect of chemotherapeutic agents on induction of apoptosis on $CD44^+/CD24^-$ of other human BCC (Hs578-T) cells, sorted and unsorted cells of Hs578-T cells were also tested with flow cytometry (Figure 3.14A).

Hs578-T cells treated with various concentrations of doxorubicin at 48 hrs showed a significant effect on cell apoptosis compared to untreated cells ($P<0.01$, $P<0.001$) (Figure 3.14A). Percentages of apoptosis in unsorted Hs578-T cells treated with doxorubicin after 48 hrs of incubation was significantly higher than other isolated cells ($P<0.05$, $P<0.01$, $P<0.001$). Similar results to MDA-MB-231 cells were observed in Hs578-T with $CD44^+/CD24^-$ sub-population, cells were significantly less sensitive to chemoagent doxorubicin in comparison to the other respective unsorted and sorted cell subpopulation ($P<0.01$, $P<0.001$), but no significant differences were observed between them in untreated cells. (Figure 3.14A). $CD44^+/CD24^-$ isolated cells treated with 5 and 10 µg/ml of doxorubicin for 48 hrs showed a significant decrease of apoptotic percentage compared to untreated cells ($P<0.05$).

Various concentrations of cisplatin clearly induced significant apoptosis after 72 hrs in unsorted and sorted cells from Hs578-T cells compared to untreated cells ($P<0.01$, $P<0.001$), while no statistical significant was observed at 0.01 μM compared to untreated cells (Figure 3.14B). Moreover, significant differences were not detected between $CD44^-/CD24^-$ and $CD44^+/CD24^-$ sub-population cells at 0.01 and 1 μM, but a significant decrease was observed at 0.001, 0.1 and 10 μM ($P<0.01$, $P<0.001$). $CD44^+/CD24^-$ cells were observed significantly lower in apoptotic percentages compared to unsorted cells at all various concentrations cells ($P<0.05$, $P<0.01$, $P<0.001$) except at 0.001 μM. (Figure 3.14B).

Broadly similar results to MDA-MB-231 cells were obtained in tamoxifen treatments performed with sub-populations from Hs578-T cells (Figure 3.14C). Low concentrations of tamoxifen at 1 and 10 nM did not induce apoptosis in Hs578-T sub-populations compared to untreated cells. Modulatory concentration of 100 nM tamoxifen significantly decreased cell apoptosis ($P<0.05$) compared to untreated cells. In contrast, higher concentrations of tamoxifen (10000, 100000 μM) were significantly induced apoptosis than in those of untreated cells ($P<0.01$, $P<0.001$). Cell apoptosis of $CD44^+/CD24^-$ cells treated with those high concentrations of tamoxifen were significantly lower than unsorted or $CD44^-/CD24^-$cells ($P<0.05$, $P<0.01$, $P<0.001$) at most of he time points. In addition, untreated cells and cells treated with 10 nM tamoxifen showed a significant decrease in $CD44^+/CD24^-$ compared to unsorted cells ($P<0.05$, $P<0.01$).

These results show a significant increase in apoptosis and decrease in survival in both unsorted and sorted MDA-MB-231 and Hs578-T cells that were treated with various concentrations of three different chemotherapeutic agents compared with the untreated groups. These results suggest that the anti-proliferative effect of treatment is caused by apoptosis. In addition, $CD44^+/CD24^-$ human BCCs showed less sensitivity to chemotherapeutic agents compared to unsorted and $CD44^-/CD24^-$ sorted cells.

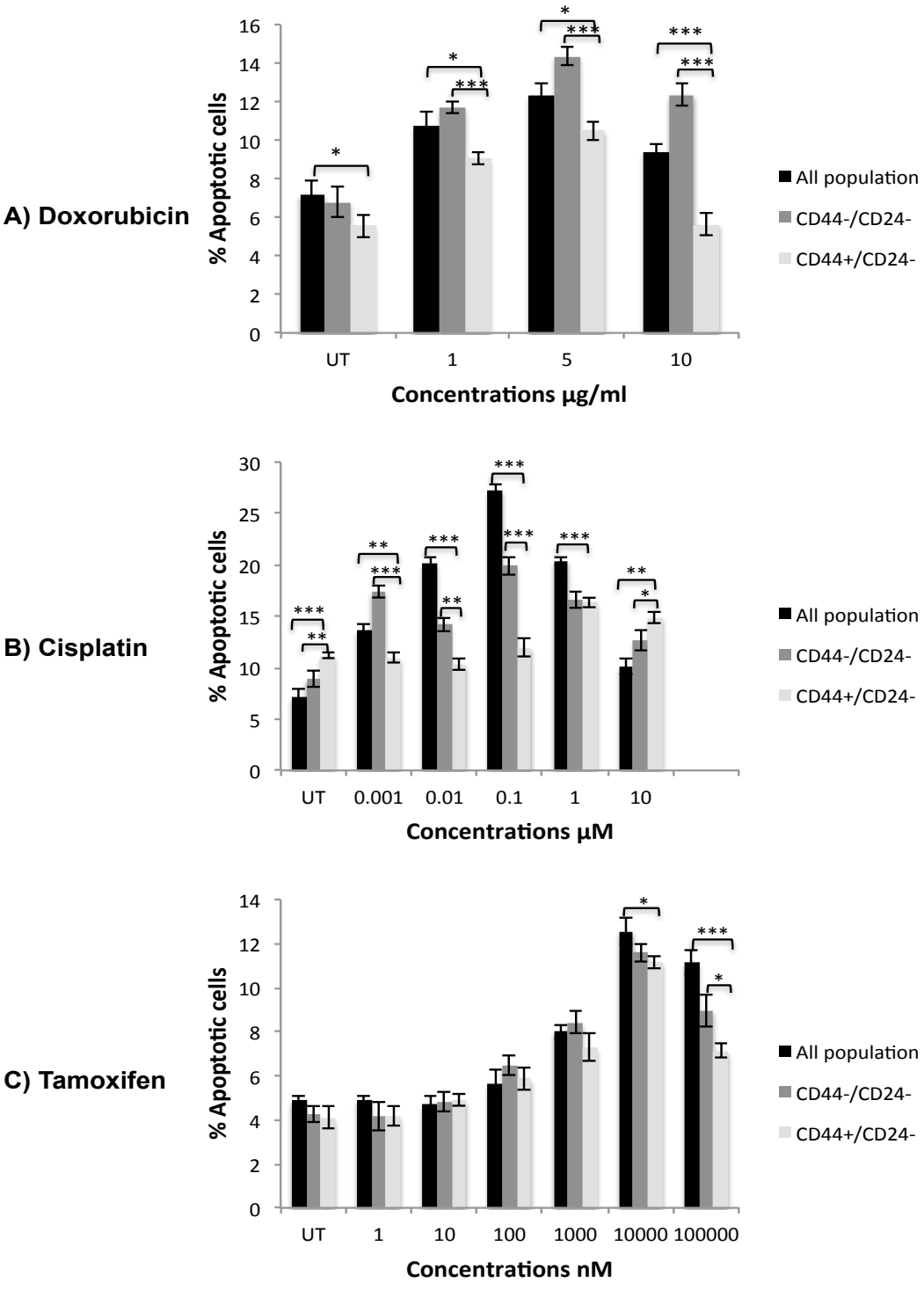

Figure 3.13 Comparison of chemosensitivity of MDA-MB-231 unsorted and sorted cells to various concentrations of (A) Doxorubicin at 48 hrs, (B) Cisplatin at 72 hrs and (C) Tamoxifen at 48 hrs. MDA-MB-231 unsorted and FACS sorted cells were exposed to chemotherapeutic agents at increasing concentrations for 48 hrs or 72 hrs. Untreated cells (UT) were used as a control. Apoptotis was measured by Annexin V/PI staining and FACS sorting as described in Methods, and the percentage of early and late apoptotic cells were calculated. Data from one of two representative experiments is shown (mean ± SD, n=3). Data in inset show statistical significance at *= P< 0.05; **= P< 0.01 and ***= P< 0.001 for $CD44^{+}/CD24^{-}$ vs. other respective populations.

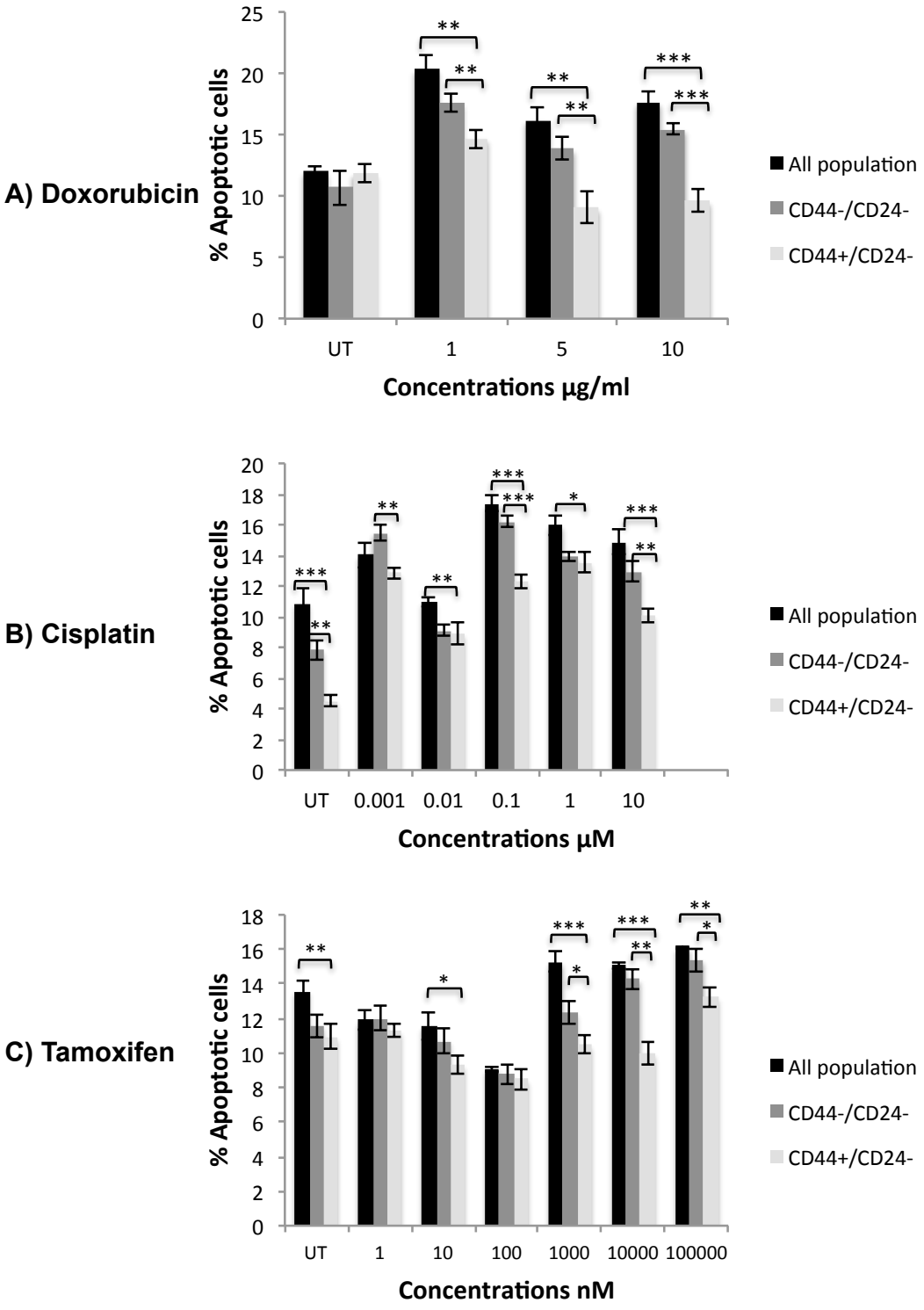

Figure 3.14 Comparison of chemosensitivity of Hs578-T unsorted and sorted cells to various concentrations of (A) Doxorubicin at 48 hrs, (B) Cisplatin at 72 hrs and (C) Tamoxifen at 48 hrs. Hs578-T unsorted and FACS sorted cells were exposed to chemotherapeutic agents at increasing concentrations for 48 hrs or 72 hrs. Untreated cells (UT) were used as a control. Apoptotis was measured by Annexin V/PI staining and FACS sorting as described in Methods, and the percentage of early and late apoptotic cells were calculated. Data from one of two representative experiments is shown (mean ± SD, n=3). Data in inset show statistical significance at *= $P< 0.05$; **= $P< 0.01$ and ***= $P< 0.001$ for $CD44^{+}/CD24^{-}$ vs. other respective populations.

3.11 Discussion

The existence of small sub-populations of CSCs in solid human cancers is widely reported, and cancer-derived cell lines have also been described as containing putative CSCs with similar characteristics, including a number of BCC lines. Results described here confirmed that a number of established BCC lines contain sub-fractions of CSCs, defined by marker expresson patterns; these cells have been reported to be tumor-initiating cells with the capacity to differentiate into phenotypically diverse progeny and are thus of significant interest for cancer treatment. The findings in this chapter indicated that the MDA-MB-231 and Hs578-T BCC lines contain significant $CD44^{+}/CD24^{-}$ cell populations with phenoptypic characteristics typical of CSCs, indicating that they would be good models for studying effects of HS on CSCs.

As the various markers identified in previous studies are not sufficient to identify a single CSC population, the existence of various lineages of BCSCs, likely leading to different types of BC and also coexisting within the same tumour, have been suggested (Hwang-Verslues et al., 2009). BCSC characteristics generally associate with differential expression of CD44 and CD24, since $CD44^{+}/CD24^{-}$ cells have been reported as having higher tumourigenic properties in immunodeficient mice and also express EMT markers (Al-Hajj et al., 2003, Mani et al., 2008). When we analysed CD44, CD24 and CD133 in human BCC lines (MCF-7-A, T-47D, ZR-75-1, MDA-MB-231 and Hs578-T), the pattern of CD44 and CD24 expression in different cell lines generally corresponded to their previously observed pattern of CSC marker expression. For example, in the case of the moderately metastatic MDA-MB-231 and Hs578-T cell lines, two distinct subpopulations were also observed with respect to CD44 and CD24 expression. Similarly, non-metastatic MCF-7-A, T-47D and ZR-75-1 cells did not contain a detectable $CD44^{+}/CD24^{-}$ or $CD133^{+}$ subpopulation. CD133 marker was found negative labeling for all cell lines, except for T-47D, and was not considered to be useful for cell selection in our further studies. In contrast, CD44 and CD24 markers displayed staining that was heterogeneous between cell lines but also within each cell line (Table 3.1) and is thus useful for selection purposes; furthermore, the $CD44^{+}/CD24^{-}$ percentage has been reported to be correlated with

histological subtype and parallels the classification of MDA-MB-231 and Hs578-T cells as a function of tumourigenicity (Table 3.2).

Here we confirmed that commonly studied human BCC lines contain sub-sets of tumour initiating-like cells based on the expression of putative CSC markers CD44 and CD24. Moreover, cell lines that contain these stem-like cell $CD44^{+}/CD24^{-}$ populations at significant levels show a correlation with their previously established aggressiveness at tumour formation *in vivo* in animal models. Our findings demonstrated that $CD44^{+}/CD24^{-}$ isolated from the human BCC lines MDA-MB-231 and Hs578-T display significantly greater characteristics associated with malignant/metastatic properties compared to other corresponding sub-populations ($CD44^{-}/CD24^{-}$, $CD44^{-}/CD24^{+}$, and $CD44^{+}/CD24^{+}$). These characteristics included increased *in vitro* proliferation (Figure 3.8), adhesion (Figure 3.9), migration (Figure 3.10), invasion (Figure 3.11) and colony forming ability (Figure 3.12).

When the *in vitro* proliferative capacity and viability of $CD44^{+}/CD24^{-}$ cells isolated from MDA-MB-231 and Hs578-T cells versus the other corresponding $CD44^{-}/CD24^{-}$, $CD44^{-}/CD24^{+}$, and $CD44^{+}/CD24^{+}$ sub-populations was compared in this study, it was shown that the $CD44^{+}/CD24^{-}$ cells showed enhanced growth. Compared to the classic view of stem cell phenotypes, the present proliferation results were initially a bit surprising, due to the fact that stem cells typically have a lower proliferation rate than that of committed cells (Beckmann et al., 2007). However, in context of the CSC concept (Introduction, Figure 1.8), these sub-sets of cells may divide and proliferate at very low rate when located in restrictive niche environments. Indeed, previous studies showed that ALDH-expressing stem cells in human bone marrow and umbilical cord blood has been observed to divide rapidly, and represent a progenitor cell population (Nagano et al., 2007); this may also be true in the context of some BCCs. The proliferation studies described here are consistent with previous studies showing increased proliferative capacity of $CD44^{+}/CD24^{-}$ cells sorted from other tumor cells (from MDA-MB-231 and Hs578-T human BCC lines) (Croker et al., 2009); it might be that when separated from their niche environments (stromal cells, neighboring cells, ECM etc) and without immune interaction, they gain the ability to proliferate faster, in contrast to $CD44^{-}/CD24^{-}$ cells (Ghaffari et al., 2015, Pietilä et al., 2016, Qian et al., 2015, Wu and Dai, 2016). Consequently, it has been

considered that $CD44^+/CD24^-$ cells were similar to stem cells, being capable of self-renewal, including extensive proliferative capacity, as well as invasion, migration, colony formation and adhesion at potentially greater levels than $CD44^-/CD24^-$ cells. In line with an earlier report (Sheridan et al., 2006, Yan et al., 2013), these results indicate that $CD44^+/CD24^-$ cells have the highest invasion capacity compared to the other three sub-populations of MDA-MB-231 and Hs578-T cells and indicated that the increase of CSC markers expression selects for BCSCs with enhanced malignant and metastatic ability indicating the potential for metastatic activity.

In the context of the CSC concept, chemotherapeutic agents target most cells in a tumor; however, a small sub-set of cells that proliferate slowly become resistant to chemotherapeutic agents, potentially providing a pivotal mechanism in the development of chemoresistance (Introduction, Figure 1.9). Indeed, CSCs *in vitro* have been shown to be significantly resistant to various types of chemotherapeutic agents (Hong et al., 2015, Liu et al., 2015). In agreement with this, findings here showed that $CD44^+/CD24^-$ cells were significantly more resistant to chemotherapeutic agents (doxorubicin and cisplatin) than for example $CD44^-/CD24^-$ cells. However, after longer time periods of treatment, the level of apoptotic cells increases in all cell populations but remains significantly lower in $CD44^+/ CD24^-$ cells compared to $CD44^-/CD24^-$ and other sub-populations; this may be observed if resistant cells are emerging from the few clones displaying a lower proliferation rate or having less susceptibility to the chemotherapy agent. So, $CD44^+/CD24^-$ cells may expand as the progeny of chemoresistant-treated cells.

In conclusion, we were able to demonstrate and isolate $CD44^+/CD24^-$ cells and other sub-populations from human BCCs by FACS, allowing them to be cultured and studied separately in conditioned medium. The $CD44^+/CD24^-$ cells were demonstrated to have expected CSC properties of self-renewal and proliferation, as well as high adhesion, migration, invasion and colony formation capacity; they also displayed resistance to chemotherapy agents relative to other cell sub-populations. This characterization indicated that these BCSCs provide useful models from which to gain new insights into how HSs might regulate these important cells, and potentially provide novel therapeutic targets for breast cancer treatment.

4 Modulatory effects of HS/heparins on the phenotype of BCSCs

4.1 General introduction and aims

As outlined in detail previously, HSPGs are key components of the ECM, which have a crucial role in mediating cell proliferation, migration, invasion and cellular signaling (Ibrahim et al., 2013, Okolicsanyi et al., 2014). These studies found that the siRNA-mediated syndecan-1 silencing resulted in a reduced a side population (SP) of MDA-MB-231 and MCF-7 BCC lines, and a reduced ALDH1-positive cell pool (Ibrahim et al., 2013). In addition, the knockdown of syndecan-1 in MDA-MB-231 cells decreased the $CD44^+/CD24^-$ CSC sub-population and increased the $CD44^+/CD24^+$ population (Ibrahim et al., 2013).

The invasive phenotype of the $CD44^+/CD24^-$ sub-population of MDA-MB-231 BCCs has been observed to be higher than the $CD44^+/CD24^+$ sub-population (Sheridan et al., 2006). Another study found that, syndecan-1-depleted MDA-MB-231 cells displayed increased invasiveness (Ibrahim et al., 2012).

A well established model of BCSCs is the triple negative, highly invasive and metastatic MDA-MB-231 and Hs578-T cell lines. They have been employed in this project to investigate a potential role of HS/heparin and chemically modified heparins on CSC phenotype, in terms of proliferation, adhesion, migration and invasion. After growth in suspension culture, MDA-MB-231 and Hs578-T cells were sorted by flow cytometry to isolate $CD44^-/CD24^-$ and $CD44^+/CD24^-$ sub-populations, and then tested in various cell culture conditions for the above characteristics. Sorted cells were then treated with various concentrations of a small library of HS, heparin and chemically modified heparins.

The aims of the work in this chapter were to:

- Study the role of HS/heparin and chemically modified heparins on BCSC phenotype in terms of growth, adhesion, migration and invasion.
- Investigate a possible effect of HS/heparin treatment on chemo-resistance of BCSCs.

These studies will allow us to determine whether the phenotype of CSCs can be modulated to reduce or prevent their tumorigenicity, to regulate the level of the renewing CSC population, and possibly to render them more sensitive to chemotherapeutic agents.

4.2 Effect of chlorate treatment on $CD44^+/CD24^-$ BCSCs

Since our main objective was to identify whether HS modulates CSC behaviour, bright phase microscopy analysis was first used to ask whether CSC-like cells from MDA-MB-231 and Hs578-T cell cultures were affected by chlorate treatment to prevent HS sulphation. Sodium chlorate inhibits the generation of 3'-phosphoadenosine-5'-phosphosulfate (PAPS), the sulphate donor used by most of the cell sulfotransferase enzymes, including those that mediate transfer of sulphate groups onto nascent HS chains (Guimond et al., 1993). Thus, treatment of cell cultures with sodium chlorate leads to a general inhibition of sulphation and is a method for studying HS function, since distinct HS functions are associated with different degrees and patterns of sulphation (Powell et al., 2004, Rudd et al., 2010). In order to examine the effects of chlorate on CS-like cells from MDA-MB-231 and Hs578-T cells, morphology were examined using bright field light microscopy.

Briefly, $CD44^+/CD24^-$ sorted cells were seeded at 20×10^3 and cultured in 6 well tissue culture plates for 24 hrs prior to treatment. Cells were treated with either 10 mM of sodium chloride (NaCl) as a control or with 10 mM of sodium chlorate ($NaClO_3$) and cultured for further 48 hrs. Cell morphology was observed for the $CD44^+/CD24^-$ sub-set of MDA-MB-231 and Hs578-T cell lines cultured in serum-supplemented medium as control (Figure 4.1). In the presence of chlorate (10 mM) (Figure 4.1A), it was evident that cell growth was significantly diminished ($P<0.01$) (Figure 4.1B). This effect was related to the reduced sulphation and not simply ionic strength of the added chlorate, since treatment with an equal concentration of sodium chloride yielded no major effects (Figure 4.1). This experiment gave an initial indication that endogenous HS is important for cell growth in CSCs.

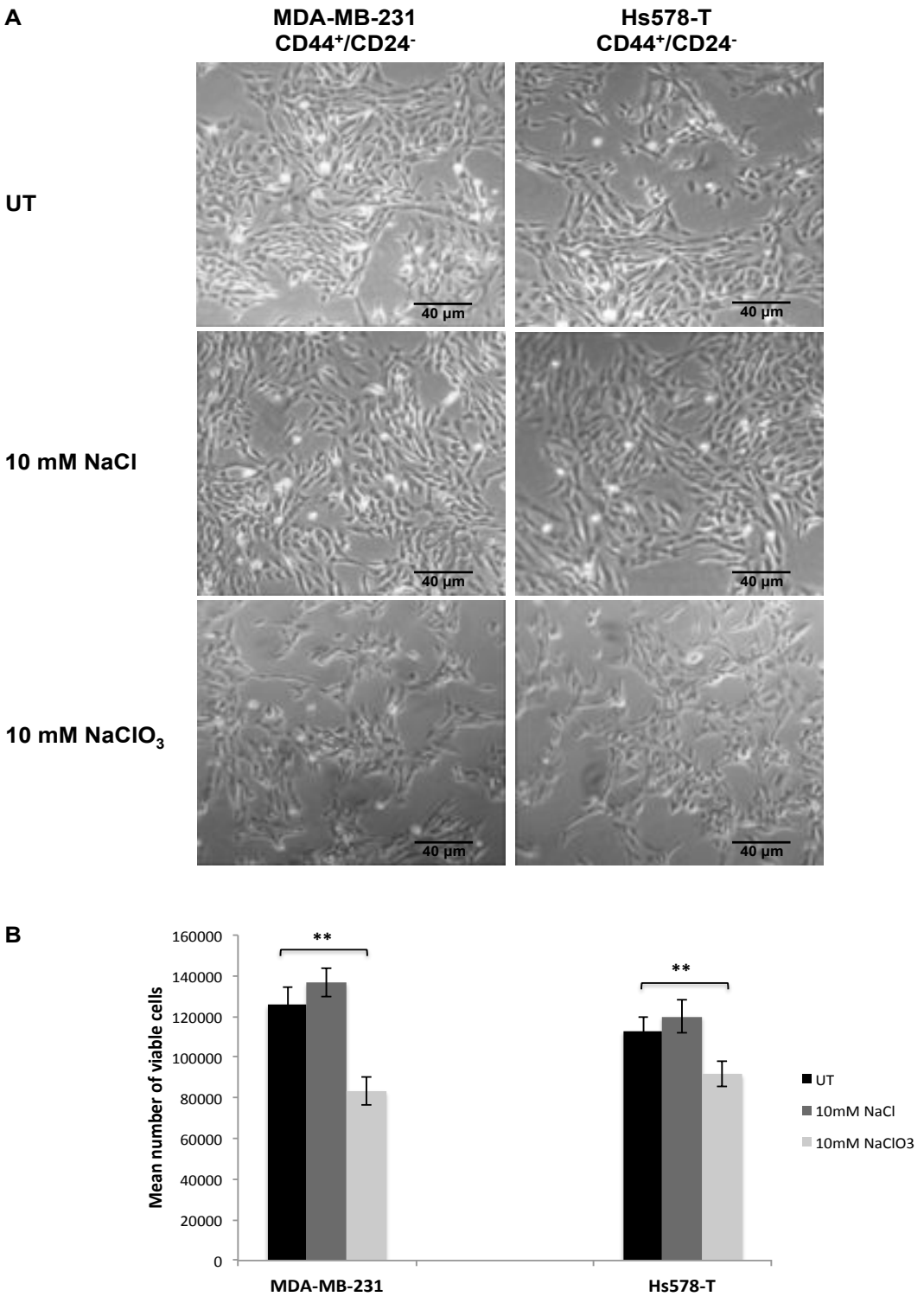

Figure 4.1 CSCs from MDA-MB-231 and Hs578-T BCCs are affected by chlorate treatment. (A) Bright Phase images of $CD44^{+}/CD24^{-}$ sub-population of MDA-MB-231 and Hs578-T cells cultured for [48 hrs] either untreated, or in the presence of 10 mM sodium chlorate or sodium chloride (×20 magnification). Scale bar, 40 µm. (B) The cell viability of both cell lines was evaluated by trypan blue staining assay at 48 hrs. Results are expressed as mean value ± S.D. **P<0.01 vs. untreated cells. The experiment was performed three independent experiment, each in duplicate n=2. UT, untreated control cells; NaCl, sodium chloride; $NaClO_3$, Sodium chlorate.

4.3 Effects of HS/heparins on CSC sub-population levels in BCC lines

Since our main objective was to identify modulation of CSC proliferation and cell fate, flow cytometry was used to assess whether CSC-like cells from MDA-MB-231 and Hs578-T cell cultures are differentially affected by treatment with various concentrations of HS/heparins. As mentioned before, various work showed that BCC lines express putative CSC markers, such as CD44 in combination with low/- CD24 (de Beça et al., 2013, Gong et al., 2010, Velasco-Velázquez et al., 2011). We have been able to confirm $CD44^+/CD24^-$ expression in MDA-MB-231 and Hs578-T cells, and focused on this sub-population of cells. When we analyzed HS/heparin-treated MDA-MB-231 and Hs578-T cells by flow cytometry to identify the $CD44^+/CD24^-$ sub-population, we observed that some of these treatments, even at very low concentrations (sub to low ng/ml), reduced the proportion of $CD44^+/CD24^-$ cells in culture (Figure 4.2; 4.3, and Appendix 3.1- 3.8 for the FACS analyses; quantitative data is summarised in Figures 4.4 and 4.5).

As a first example, porcine mucosal heparin (PMH) caused a significant decrease (~25%) in the CSC-like subpopulation of MDA-MB-231 cells treated with a low concentration of PMH (1, 10, 100 ng/ml) ($P<0.01$, $P<0.001$) for 48 hrs prior to sorting, although an exception was an increase of the proportion of $CD44^+/CD24^-$ observed at the lowest concentration (0.001 ng/ml). The biggest decreases were observed at 1-100 ng/ml, whereas higher concentrations of PMH (1 μg/ml and above) caused a less significant reduction in the CSC population (Figures 4.2 and 4.4). PMH treatment gave similar effects on the CSC-like subpopulation of Hs578-T cells, causing a reduction of ~ 40 to 50% in the $CD44^+/CD24^-$ proportion at all various concentrations (Figures 4.2 and 4.5).

PMHS also induced significant reduction in the CSC sub-population from MDA-MB-231 cells, with the statistically significant and strongest reductions noted in the concentration range 0.001, 0.01, 1, 10, 100 ng/ml ($P<0.05$, $P<0.01$), and also at high concentrations at 1 μg/ml ($P<0.05$) (with the exception of an increase observed at 10 and 100 μg/ml ($P<0.01$) (Figure 4.3 and 4.4). Similar reductions in the $CD44^+/CD24^-$ sub-population were also observed after PMHS treatment of Hs587-T cells at all various concentrations ($P<0.05$, $P<0.01$, $P<0.001$) (Figure 4.3 and 4.5).

The various modified heparins were also tested at a wide range of concentrations for their effects on the levels of $CD44^+/CD24^-$ cells in MDA-MB-231 and Hs578-T cells. The results are summarised as follows:

Compound 1 – Persulfated heparin (PerS H): MDA-MB-231 cells showed a significant decrease in the proportion of $CD44^+/CD24^-$ cells when treated with PerS H (Figure 4.4; Appendix 3.1). The maximal effect was at 10 ng/ml (reduction to ~2.5% of total cells, compared to ~15% in untreated cells). Effects at some concentrations were not significant due to experimental variation, and the data suggested decreased loss of $CD44^+/CD24^-$ cells at the higher concentration (100 ng/ml and 100 µg/ml; Figure 4.4; Appendix 3.1). Similar results were seen in Hs578-T cells subjected to PerS H treatment, with maximal effect at ~1-10 ng/ml, and loss of this effect at the highest concentrations (100 µg/ml) (Figure 4.5; Appendix 3.1).

Compound 2 – N-acetylated heparin (NAc H): Treatment with this modified heparin resulted in a significant reduction of the proportion of $CD44^+/CD24^-$ cells from MDA-MB-231 compared to untreated control cells at concentrations in the range 1-100 ng/ml and 1-10 µg/ml ($P<0.05$, $P<0.01$); low doses (0.001, 0.01 and 0.1 ng/ml) and the highest dose (100 µg/ml) were apparently inneffective due to large experimental variation) (Figure 4.4; Appendix 3.2). In contrast, more pronounced reductions in the $CD44^+/CD24^-$ sub-population were observed in Hs587-T cells treated with NAc H, with this effect occurring with all doses range ($P<0.01$) (Figure 4.5; Appendix 3.2).

Compound 3 – 2-deS, N-sulphated heparin (2 deS-NS H): at low concentrations in the range 0.001 to 100 ng/ml this compound produced a significant decrease in the $CD44^+/CD24^-$ population of MDA-MB-231 cells ($P<0.01$, $P<0.001$), but not at higher doses except 10 µg/ml ($P<0.05$). (Figure 4.4; Appendix 3.3). Similar results were seen in Hs578-T cells, this compound did produce a significant reduction (25 to 50%) in the $CD44^+/CD24^-$ population at doses in the range 0.001 to 100 ng/ml ($P<0.05$, $P<0.01$). This effect was lost at 1 and 10 µg/ml treatments except 100 µg/ml ($P<0.01$) (Figure 4.5; Appendix 3.3).

Compound 4 – 6-deS, N-sulphated heparin (6 deS-NS H): produced a significant reduction (~30-50%) in the $CD44^+/CD24^-$ population of MDA-MB-231 cells ($P<0.01$, $P<0.001$), but with a very flat dose response, and the effects at 0.01 ng/ml and 1 µg/ml were not statistically significant (Figure 4.4 and Appendix 3.4). Effects on reduction of the $CD44^+/CD24^-$ population in Hs578-T cells were less clear, and only observed at 0.001, 0.01, 100 ng/ml and 1 µg/ml ($P<0.01$) (Figure 4.5; Appendix 3.4)

Compound 5 – 2-deS, N-acetylated heparin (2 deS-NAc H): This compound produced more divergent effects. No significant effect on the level of the $CD44^+/CD24^-$ population in MD-MBA-231 at most doses, except that doses of 0.001, 10 ng/ml and 1 µg/ml showed a significant increase in the proportion of these cells compared to untreated cells ($P<0.001$) (Figure 4.4; Appendix 3.5). The $CD44^+/CD24^-$ sub-population of Hs578-T cells was not significantly decreased by treatment with 2 deS-NAc H, most prominently at 0.001, 0.01 ng/ml and 1 µg/ml, but with significant effect at most other concentrations ($P<0.05$, $P<0.01$, $P<0.001$) (Figure 4.5; Appendix 3.5).

Compound 6 – 6-deS, N-acetylated heparin (6 deS-NAc H): Similar results were seen with this compound caused a large decrease in the proportion of $CD44^+/CD24^-$ cells from MDA-MB-231 at 0.1 ng/ml to 1 µg/ml ($P<0.05$, $P<0.01$). No significant effect was observed at low dose 0.001 ng/ml and high doses 10 and 100 µg/ml (Figure 4.4; Appendix 3.6). In marked contrast to the MDA-MB-231 cells, this compound did not produce a significant effect on $CD44^+/CD24^-$ cell numbers from Hs578-T cells at most doses range, except at 10 and 100 ng/ml ($P<0.05$, $P<0.01$) (Figure 4.5; Appendix 3.6). This compound at lower dose 0.01 ng/ml caused a large increase in the proportion of $CD44^+/CD24^-$ cells from both MDA-MB-231 (Figure 4.4; Appendix 3.6) and Hs578-T cell line (Figure 4.5; Appendix 3.6) cell lines.

Compound 7 – 2,6-deS, N-sulphated heparin (2,6 deS-NS H): Low concentration of compound 7 (0.001 ng/ml) did not show any significant effect on the $CD44^+/CD24^-$ cell population of the MDA-MB-231 cell line, but significant reductions were observed at 0.01 ng/ml and higher, with maximal effects (~75% reduction) at 10 µg/ml ($P<0.05$, $P<0.01$, $P<0.001$) (Figure 4.4; 3.7). Compound 7 also had similar

effects on the CSC-like subpopulation of Hs578-T cells, but with a more U-shape dose response with maximal effect at 10 ng/ml ($P<0.05$, $P<0.01$), and no effect at 100 µg/ml (Figure 4.5; Appendix 3.7).

Compound 8 – 2,6-deS, N-acetylated heparin (2,6 deS-NAc H): This compound produced a significant reduction in the $CD44^{+}/CD24^{-}$ population of MDA-MB-231 cells at all doses in the range 0.001 ng/ml to 100 µg/ml ($P<0.05$, $P<0.01$, $P<0.001$) (Figure 4.4; Appendix 3.8). However, 2,6 deS-NAc H did not produce a significant effect on $CD44^{+}/CD24^{-}$ cell numbers from Hs578-T cells except at 10 ng/ml and 1µg/ml ($P<0.05$, $P<0.01$) (Figure 4.5; Appendix 3.8).

It can be concluded that addition of exogenous HS, heparin and modified heparins have significant effects on the level of the CSC sub-population in BCC lines. These effects were dose responsive, with some occurring at remarkably low concentrations (in the low ng/ml range), and in some cases the effects are lost at high concentrations. Some of the compounds exert effects which vary with the cell-type. Further investigation is warranted to examine the effects of heparin and other modified heparin compounds on MDA-MB-231 and Hs578-T BCCs and the phenotype of their CSC sub-populations. For these studies PMH, and PMHS, along with the modified heparins PerS H, 2,6 deS-NS H and NAc H were selected since they were the most potent at inducing reductions in the $CD44^{+}/CD24^{-}$ population, in some cases at very low concentrations, and were consistently effective in both BC cell lines.

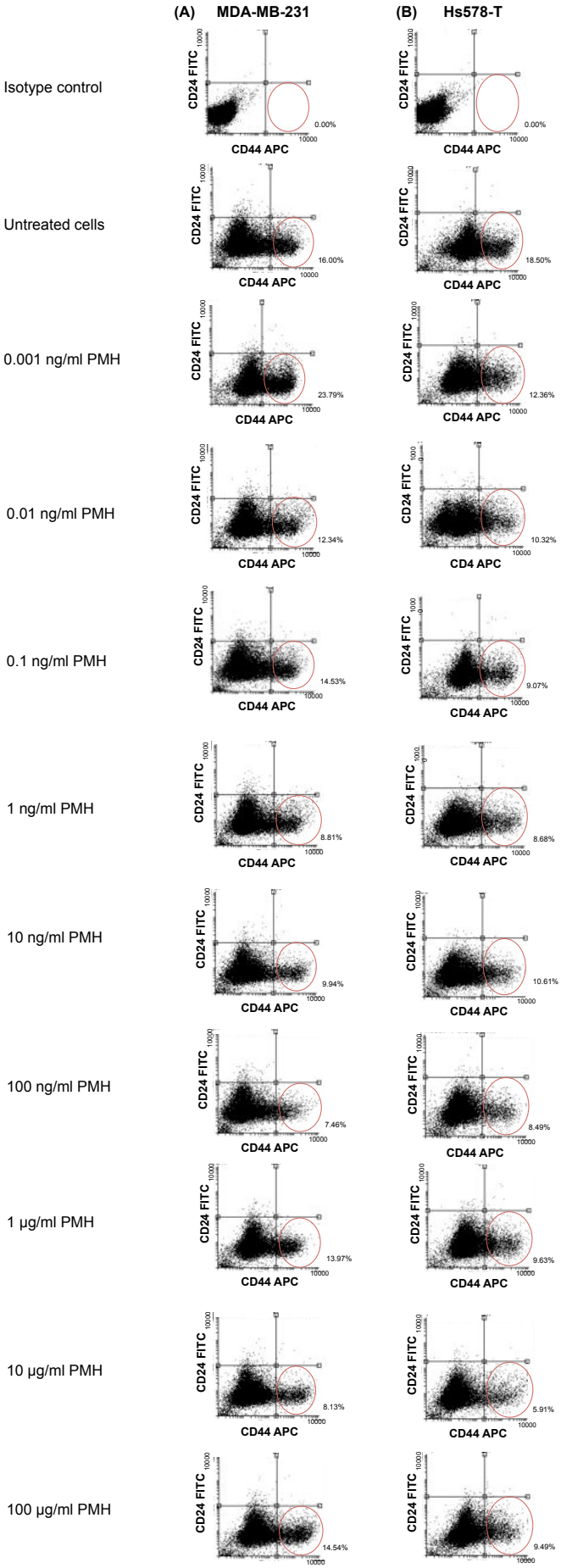

Figure 4.2 Treatment with porcine mucosal heparin (PMH) reduces the $CD44^+/CD24^-$ subpopulation in BCC lines. Following 48 hrs treatment with PMH at various concentrations flow cytometry was used to measure the $CD44^+/CD24^-$ subpopulation. MDA-MB-231 (A) and Hs578-T (B) cell lines were maintained in DMEM supplemented with 10% FBS, 10µg/ml insulin, 0.5 µg/ml hydrocortisone and 2 mmol/l L-glutamine, in a humidified atmosphere containing 5% CO_2 at 37°C. Cells were treated with 1, 10, 100 ng/ml, 1,10, 100 µg/ml of PMH for 48 hrs. 10^5 single-cell suspensions of MDA-MB-231 and Hs578-T were double stained with anti-human CD44 and CD24. Cells in red region corresponding to $CD44^+/CD24^-$ Isotype controls corresponding to MD-MB-231 and Hs578-T cells are shown. Representative data from one of four experiments are shown.

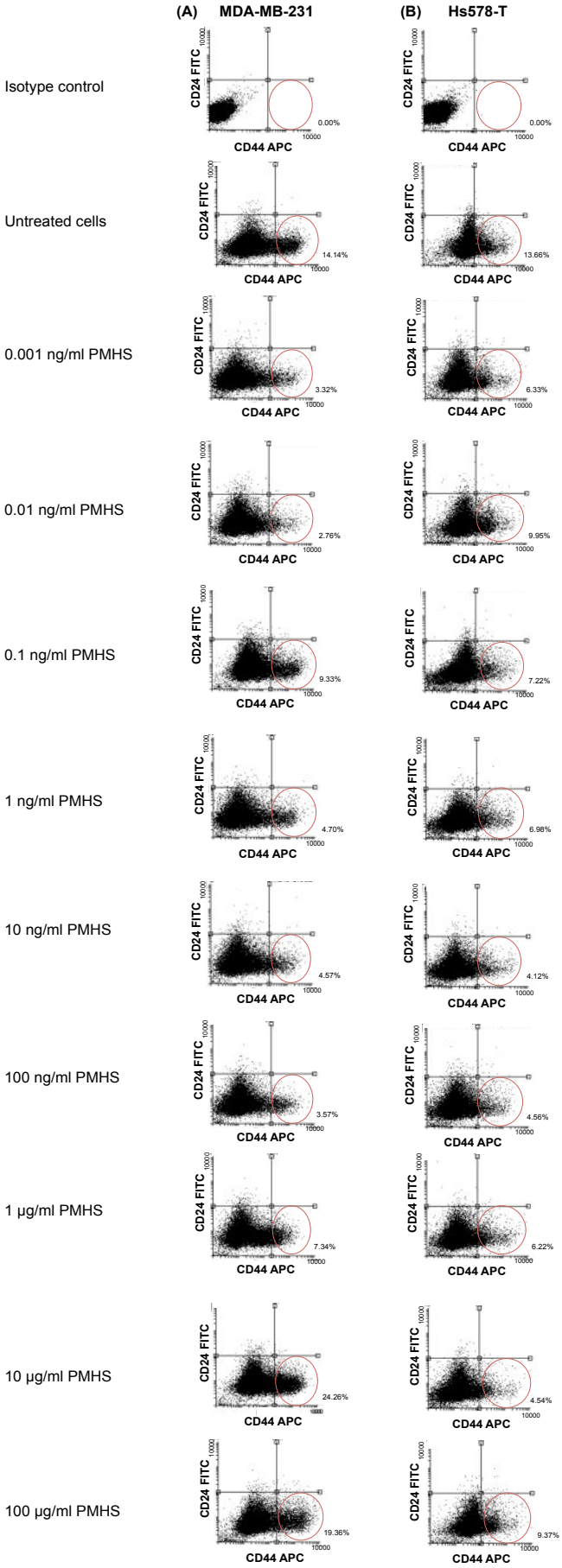

Figure 4.3 Treatment with porcine mucosal heparin sulphate (PMHS) reduces the $CD44^+/CD24^-$ subpopulation in BCC lines. Following 48 hrs treatment with PMHS at various concentrations, flow cytometry was used to measure the $CD44^+/CD24^-$ subpopulation. MDA-MB-231 (A) and Hs578-T (B) cell lines were maintained in DMEM supplemented with 10% FBS, 10µg/ml insulin, 0.5 µg/ml hydrocortisone and 2 mmol/l L-glutamine, in a humidified atmosphere containing 5% CO_2 at 37°C. Cells were treated with 1, 10, 100 ng/ml, 1,10, 100 µg/ml of PMHS for 48 hrs. 10^5 single-cell suspensions of MDA-MB-231 and Hs578-T were double stained with anti-human CD44 and CD24. Cells in red region corresponding to $CD44^+/CD24^-$ Isotype controls corresponding to MD-MB-231 and Hs578-T cells are shown. Representative data from one of four experiments are shown.

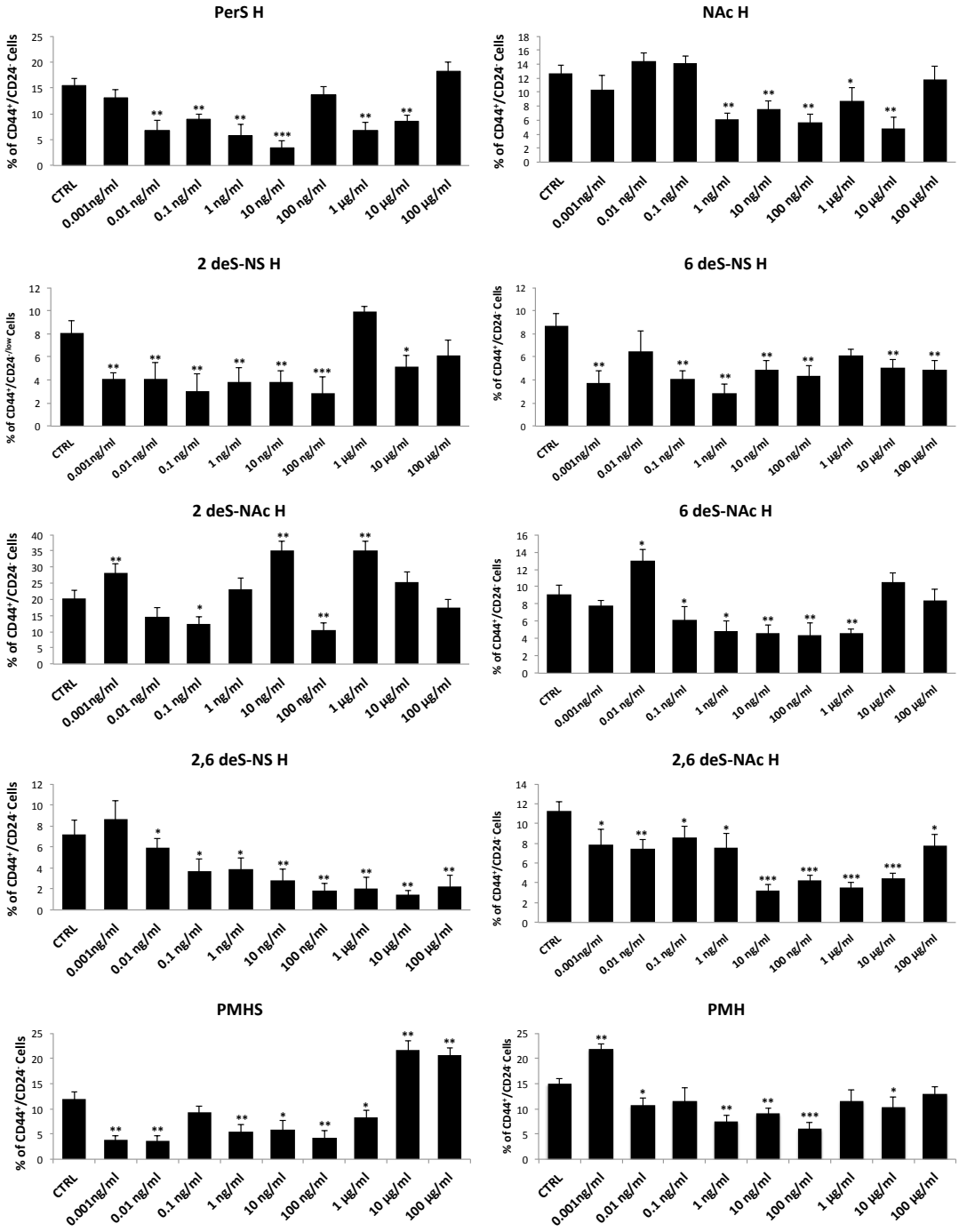

Figure 4.4 Quantification of the inhibitory effects of HS/heparin and chemically modified heparins on the CSC sub-population from MDA-MB-231 BCCs. Flow cytometric analysis of $CD44^{+}/CD24^{-}$ expression in MDA-MB-231 cells following 48 hours treatment with compounds 1-8, PMHS or PMH (at 0.001, 0.01 0.1, 1, 10, 100 ng/ml, and 1, 10 100 µg/ml) for 48 hrs. Values expressed as isotype control APC/FITC. Error bars correspond to SD from the total of four independent experiments. *P<0.05, **P<0.01, ***P<0.001=significantly different than respective population of untreated cells.

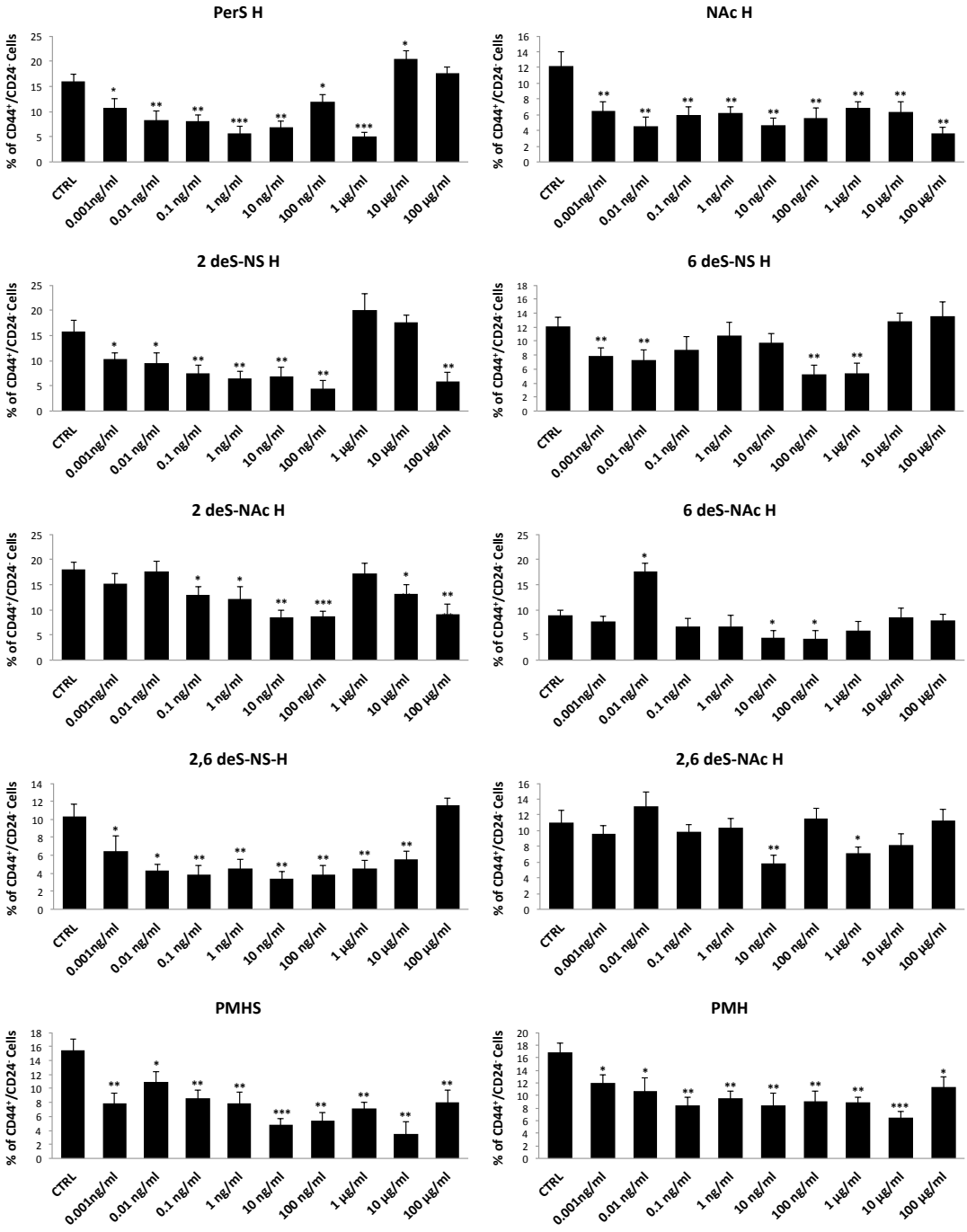

Figure 4.5 Quantification of the inhibitory effects of HS/heparin and chemically modified heparin on the CSC sub-population from Hs578-T BCCs. Flow cytometric analysis of $CD44^{+}/CD24^{-}$ expression in Hs578-T cells following 48 hrs treatment with compounds 1-8, PMHS or PMH (at 0.001, 0.01 0.1, 1, 10, 100 ng/ml, and 1, 10 100 µg/ml) for 48h. Values expressed as isotype control APC/FITC. Error bars correspond to SD from the total of four independent experiments. *P<0.05, **P<0.01, ***P<0.001=significantly different than respective population of untreated cells.

4.4 Effects of selected HS/heparins on proliferation of CSCs from BCC lines

HSPGs are well known to have a role in cell growth, so the effects of the heparins on proliferation was examined in $CD44^+/CD24^-$ cells sorted from human MDA-MB-231 and Hs578-T BCC lines. Proliferation was measured using the MTT assay over 3 days and compared with the corresponding untreated cells (Figure 4.6). A dose of 10 ng/ml was chosen since this was a typical effective dose for the previously observed effects on the $CD44^+/CD24^-$ sub-population levels.

Untreated $CD44^+/CD24^-$ cells sorted from MDA-MB-231 cells proliferated over a period of 3 days, with a steady increase observed between days 1-3 (Figure 4.6A). Treatment with NAc H resulted in a significantly higher apparent rate of growth ($P<0.001$), However, all the other compounds tested (PMH, PMHS and 2,6 deS-NS H) had no significant effect on cell growth over day, but thereafter resulted in a marked slowing of cell growth, such that cell growth was greatly diminished by day 3 ($P<0.05$, $P<0.01$, $P<0.001$). Treatment with PerS H resulted in a significantly higher apparent rate of growth at day 1 ($P<0.001$), but thereafter, significant changes were not detected at day 2 and 3 (Figure 4.6A).

In the case of $CD44^+/CD24^-$ cells sorted from Hs578-T cells, NAc H again appeared to significantly increase the proliferation rate, though day 1-3 time points ($P<0.001$) (Figure 4.6B). For the other compounds there was no difference from the control untreated cells at days 1, but they all appeared to decrease proliferation at days 2 and 3, particularly in the case of PMHS, PMH and 2,6 deS-NS H for MDA-MB-231, PMHS, PMH and PerS H for Hs578-T cells. Treatment with 2,6 deS-NS H resulted in a significantly lower apparent rate of growth at day 2 and 3. Thus overall the selected heparins have broadly similar effects on the proliferation of CSCs from these two BCC lines. NAc H tends to promote growth, whereas PMH, PMHS, PerSH and 2,6 deS-NS H tend to inhibit growth.

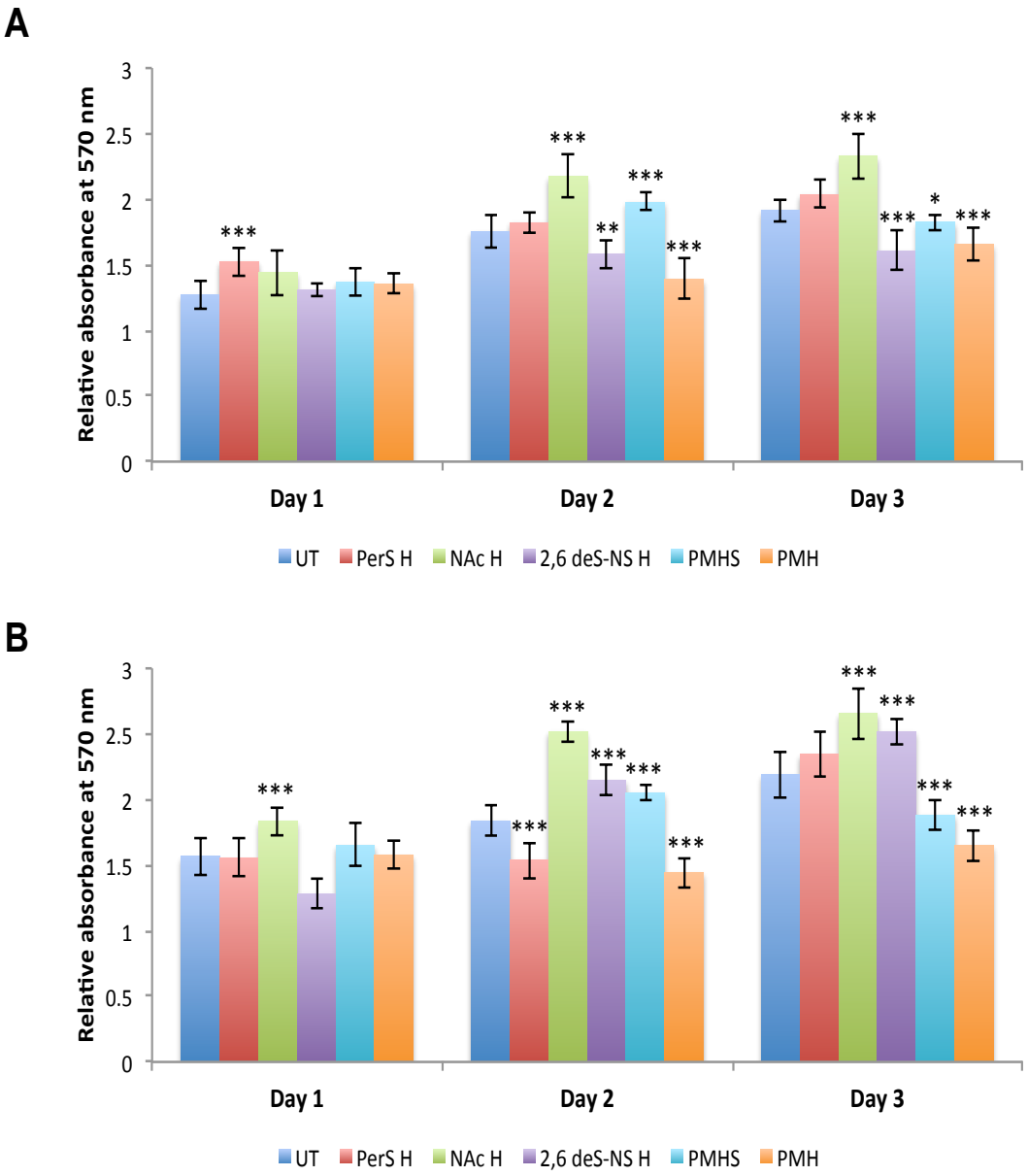

Figure 4.6 Effect of HS, heparin and selected chemically modified heparins on proliferation of the CD44^{+}/CD24^{-} sub-population from MDA-MB-231 and Hs578-T cells. An MTT assay was used to test cell proliferation: CD44^{+}/CD24^{-} of (A) MDA-MB-231 and (B) Hs578-T cells were treated or not with10 ng/ml of PerS H, 2, 6 deS-NS H, NAc H, PMHS and PMH and maintained over a period of 3 days. Cells were harvested each day for MTT reduction colorimetric assay. Data are shown as absorbance at optical density (OD) 570 nm (means ± SD from three separate experiments in triplicate.

4.5 Effects of HS/heparins on adhesion of CSCs from BCC lines

Since HSPGs have a crucial role in tumour cell adhesion, the activity of soluble HS, heparin and modified heparin were evaluated here on adhesion of BCSCs. Briefly, unsorted and sorted cells ($CD44^-/CD24^-$ and $CD44^+/CD24^-$) from MDA-MB-231 and Hs587-T BCC lines were treated with 10 ng/ml HS/heparin and modified heparins (PerS H, 2,6 deS-NS H, PMH and PMHS) for 48 hrs before the assay was performed. The cells were seeded into pre-coated 24-well plate with 15 µg/ml of fibronectin (FN) at a density of approximately $2x10^4$ cells/well and allowed to adhere 3 hrs. After incubation period, non-adherent cells were removed and washed twice with PBS and adherent cells were counted. For each replicate (n=3), the mean numbers of adherent cells in triplicate were counted using a hemocytometer by light microscope at a magnification of ten high-powered fields (10x) by using four independent fields.

Cell adhesion to substrata coated with 15 µg/ml of FN was significantly inhibited in the presence of 10 ng/ml levels of soluble 2,6 deS-NS H, PMHS and PMH in $CD44^+/CD24^-$ sub-population isolated from both MDA-MB-231 and Hs578-T cells ($P<0.001$), while PerS H induced no change in cell adhesion in all sub-populations in both cell lines compared to untreated cells (Figure 4.7). In addition, cell adhesion to FN of $CD44^-/CD24^-$ of MDA-MB-231 and Hs578-T cells was not induce to the effects of 2,6 deS-NS H and heparin treatments compared to untreated cells (Figure 4.7). Unsorted cells from MDA-MB-231 cell line treated with 2,6 deS-NS H, PMH and PMHS showed a significant decrease in cell adhesion ($P<0.001$) (Figure 4.7A). PMHS/heparin and selected chemically modified heparins did not show any significant change on cell adhesion in parental Hs578-T cells compared to untreated control cells. Only PMHS treatment significantly increased cell adhesion in all sub-population in Hs578-T cells ($P<0.01$, $P<0.001$) (Figure 4.7B). PMHS treatment was significantly increased negative cell population to CD44 and CD24 markers in MDA-MB-231. In contrast, PMHS treatments were significantly decreased cell adhesion in $CD44^-/CD24^-$ isolated cells from Hs578-T cells (Figure 4.7).

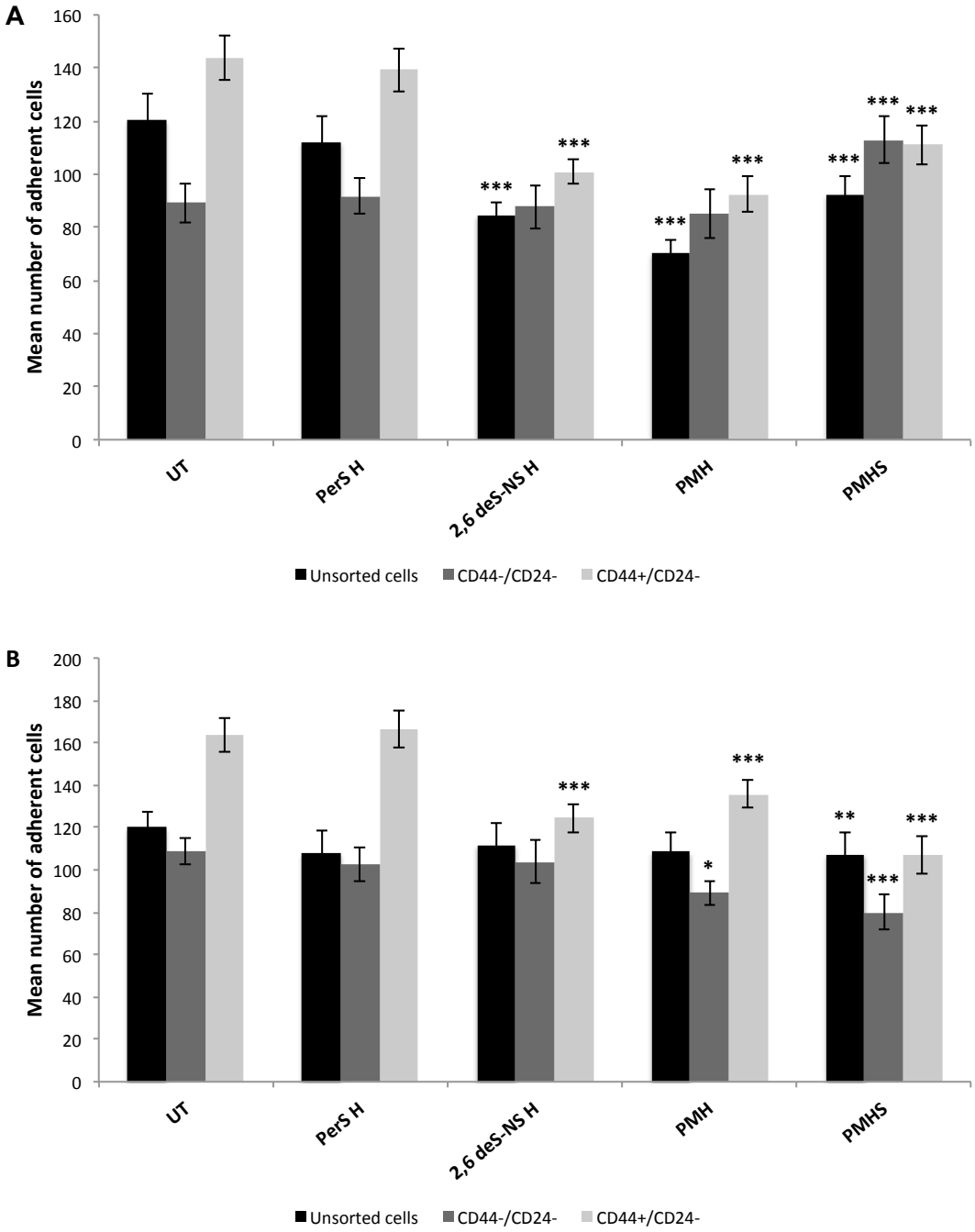

Figure 4.7 Effect of HS, heparin and selected chemically modified heparins on cell adhesion of the CD44^{+}/CD24^{-} sub-population from MDA-MB-231 and Hs578-T cells. (A) MDA-MB-231 and (B) Hs578-T treated with 10 ng/ml of PerS H, 2,6 deS-NS H, PMH and PMH for 48 hrs. Cell adhesion after 3 hrs on plastic coated with fibronectin were washed and adhered cells were counted with light microscope (magnification, ×10). Black bars denote unsorted cells, dark grey bars denote CD44^{-}/CD24^{-} and light grey bars denote CD44^{+}/CD24^{-}. Graphs represent mean ± SD. Data are expressed as mean ± SD/microscopic field. Data from one of three representative experiments shown; n=3 replicates in each assay, *P<0.05, **P<0.01, ***P<0.001 compared with untreated control.

4.6 Effects of selected HS/heparins on migration of CSCs from BCC lines

In order to evaluate whether HS/heparin and selected chemically modified heparins inhibited cancer cell migration, a classical migration assay in Boyden chambers was performed with sorted and unsorted MDA-MB-231 and Hs578-T BCCs (Fig 4.17). Cells were initially plated and incubated for 24 hrs, followed by exposure to a 48 hr treatment with 10 ng/ml of HS/heparin and selected modified heparins (PerS H, 2,6 deS-NS H, PMH and PMHS). Upon expansion, cells were plated on collagen IV-coated upper wells for 24 hrs and migrated cells were then counted. The untreated $CD44^+/CD24^-$ cells displayed higher migration than $CD44^-/CD24^-$ cells (MDA-MB-231, Figure 4.8A; Hs578-T, Figure 4.8B) as observed previously (Chapter 3, Figure 3.10). For MDA-MB-231 the results in Figure 4.8A show that 10 ng/ml pre-treatment with PMHS or PerS H caused a significant reduction in migration of the $CD44^+/CD24^-$ cells to levels comparable to untreated unsorted cells Figure 4.8A. Treatment with PMH or 2,6 deS-NS H caused an even greater reduction in migration of $CD44^+/CD24^-$ cells (Figure 4.8A). Treatments with the compounds also caused small but significant reductions in migration of unsorted and $CD44^-/CD24^-$ cells compared to their untreated counterparts, especially with PMH and 2,6 deS-NS H (Figure 4.8A).

Figure 4.8B shows that PerS H and 2,6 deS-NS H (but not PMHS or PMH) caused a reduction on migration of $CD44^+/CD24^-$ cells from Hs578-T cells. In addition, all the compounds caused significant reductions in migration of unsorted and $CD44^-/CD24^-$ cells (Figure 4.8B). Thus there are some cell type dependent effects of the compounds on migration, but for both cells lines at least some of the compounds can reduce the higher migration of the $CD44^+/CD24^-$ cell sub-populations.

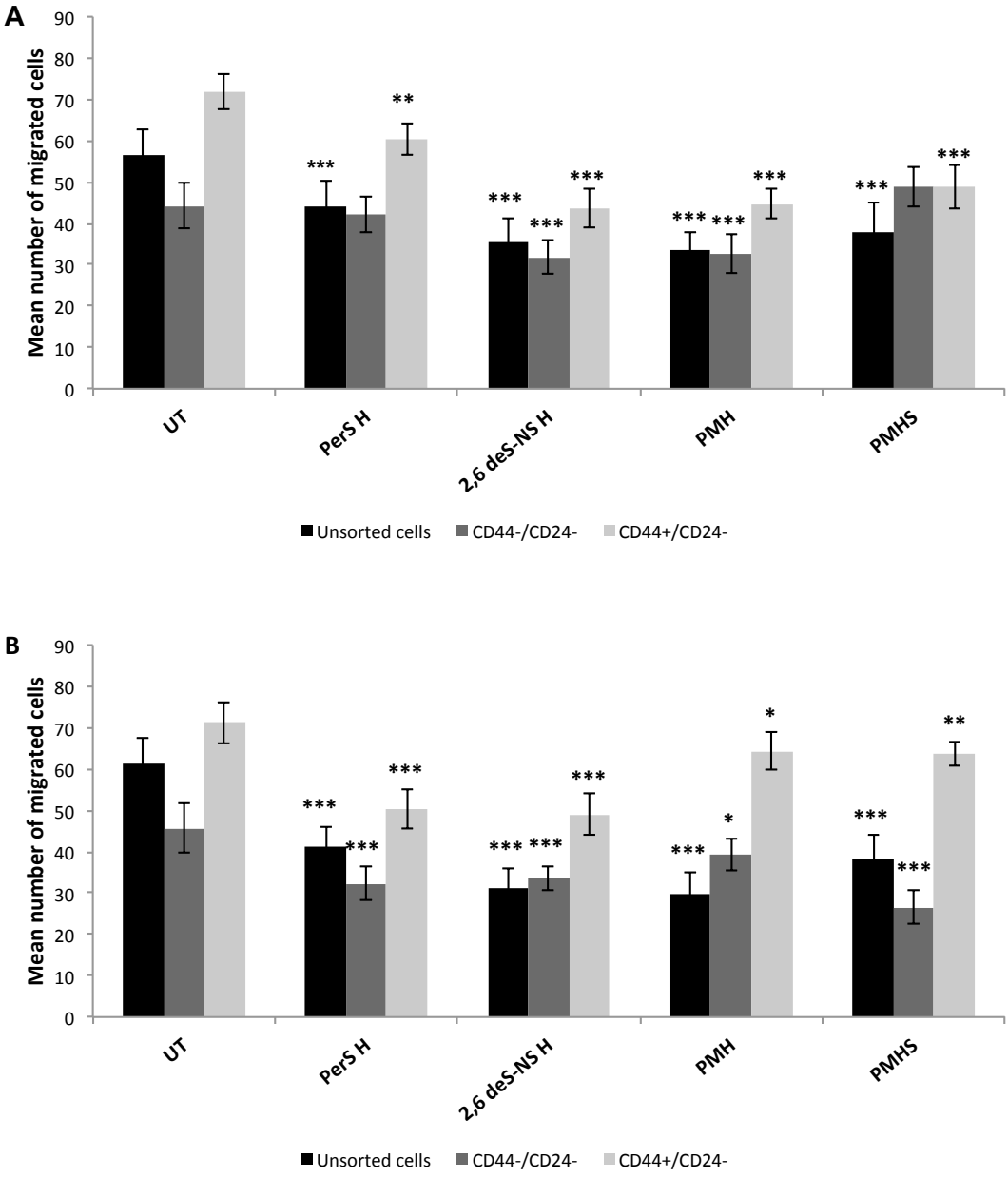

Figure 4.8 Effect of HS, heparin and selected chemically modified heparins on migration of the CD44^{+}/CD24^{-} sub-population from MDA-MB-231 and Hs578-T cells. Boyden chamber assays were used to compare the migration of unsorted and sorted (A) MDA-MB-231 and (B) Hs578-T cells pre-treated or not with 10 ng/ml of PerS H, 2,6 deS-NS H, PMH and PMHS for 48 hrs. Equal numbers of treated MDA-MB-231 and Hs578-T cells were subjected to cell migration and incubated for 24 hrs. Then, migrated cells were detected on the membrane after stating with Diff-Quik solution. Data are expressed as mean ± SD/microscopic field. Data from one of three representative experiments shown; n=2 replicates in each assay, with (*P<0.05, **P<0.01, ***P<0.001 vs control). Control cells did not receive treatment.

4.7 Effects of selected HS/heparins on invasiveness of CSCs from BCC lines

HS play an important role in regulating metastatic behaviors in tumor cells. Since HSPGs is known to inhibit and promote cell invasion, with their function being determined by their location (cell surface or ECM) (Sanderson, 2001), it was important to establish whether the effects of HS/heparin and selected chemically modified heparins on BCSC invasion. The malignant breast carcinoma cell lines MDA-MB-231 and Hs578-T were sorted to $CD44^-/CD24^-$ and $CD44^+/CD24^-$ sub-populations as described in methods (see section 2.2.2.3). Unsorted and sorted cells were treated with various HS/heparin and chemically modified heparins at low does 10 ng/ml of (PerS H, 2,6 deS-NS H, PMH and PMHS). Cells then were plated in Matrigel invasion chambers for 24 hrs and invaded cell number was counted. (Figure 4.9) represents the quantification of cell invasion. The untreated $CD44^+/CD24^-$ cells displayed higher matrix invasion than $CD44^-/CD24^-$ cells (MDA-MB-231, Figure 4.9A) as observed previously (Chapter 3, Figure 3.10). For MDA-MB-231 the results in Figure 4.9A show that pre-treatment with 10 ng/ml of PMHS, PM heparin and also two chemically modified heparins (PerS H and 2,6 deS-NS H) caused a marked reduction in invasion of the $CD44^+/CD24^-$ cells to levels comparable to untreated unsorted cells ($P<0.001$). 2,6 deS-NS H also caused a small decrease in invasion of the unsorted cells, and possibly minor decreases for the $CD44^-/CD24^-$ cells (Fig 4.9A). For Hs578-T cells the effects on invasiveness were less pronounced. The untreated $CD44^+/CD24^-$ cells displayed higher matrix invasion than $CD44^-/CD24^-$ cells (Figure 4.9B) as observed previously (Chapter 3, Figure 3.10). For the $CD44^+/CD24^-$ cells decreases were noted upon treatment with PMH, PerS H and 2,6 deS-NS ($P<0.05$), but not PMHS. Similarly, small decreases were also noted for unsorted and $CD44^-/CD24^-$ cells from Hs578-T BCSC treated with PMH, PerS H and 2,6 deS-NS H ($P<0.05$, $P<0.01$), but not PMHS (Figure 4.9B).

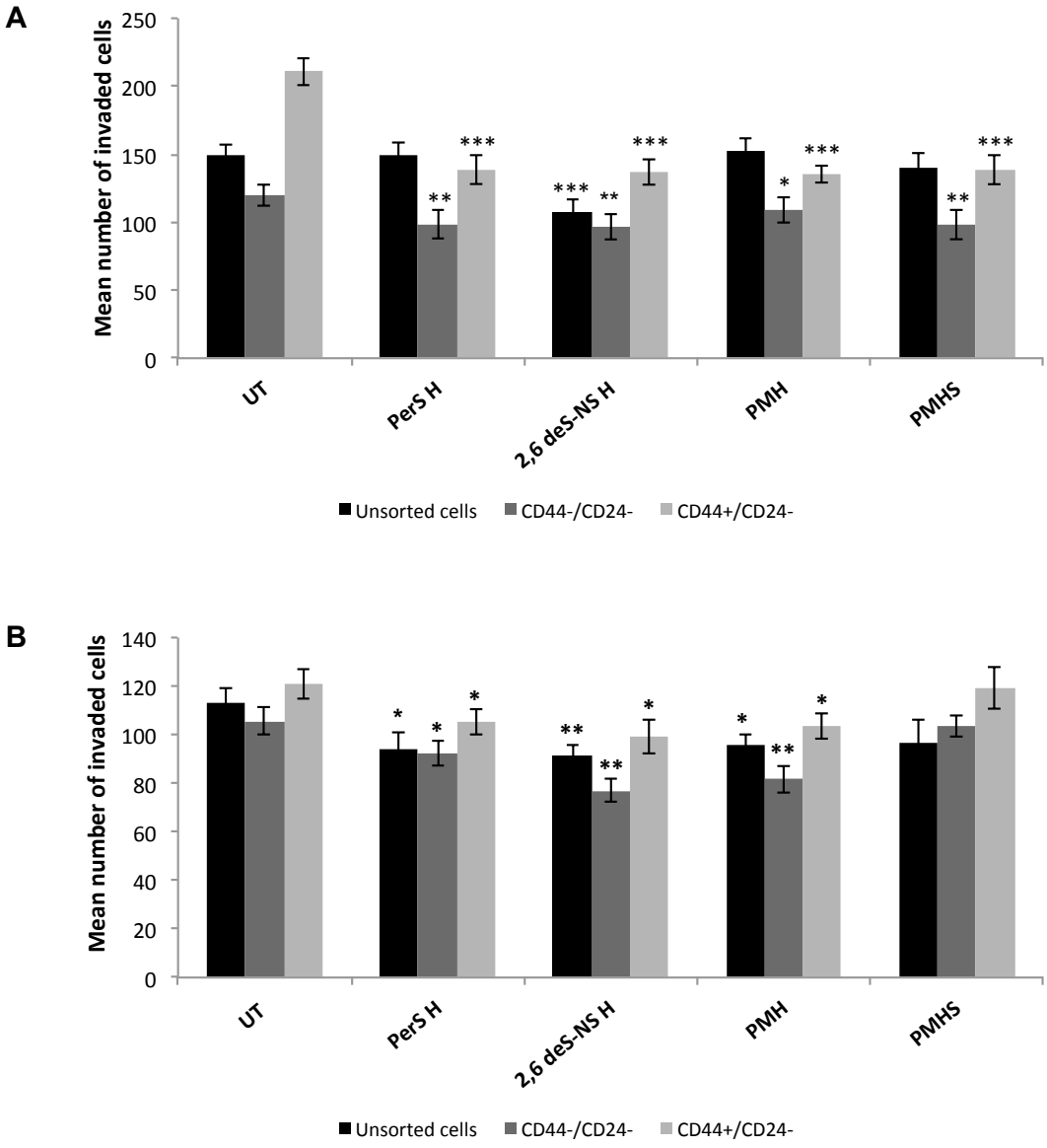

Figure 4.9 Effect of HS, heparin and selected chemically modified heparins on invasion by the CD44^{+}/CD24^{-} sub-population from MDA-MB-231 and Hs578-T cells. Unsorted and sorted (A) MDA-MB-231 and (B) Hs578-T cells were treated (or not) with 10 ng/ml of PerS H, 2,6 deS-NS H, PMH or PMHS for 48 hrs and plated on Matrigel-coated champers, and the number of cells that invaded through the membrane after 24 hrs was counted for statistical analysis and expressed as the mean ± SD/microscopic field. Data from one of three representative experiments shown; n=2 replicates in each assay. Significantly lower invasion was observed for cells treated with HS, heparin and selected chemically modified heparins versus untreated cells, *P<0.05, **P<0.01; ***P<0.001.

4.8 Effects of selected HS/heparins on chemoresistance of $CD44^+/CD24^-$ CSCs from BCC lines

To investigate whether the treatments with HS and other compounds impact apoptosis $CD44^+/CD24^-$ cells, unsorted and FACS sorted MDA-MB-231 and Hs578-T cells (based on CD44 and CD24 expression) were grown and treated with optimum doses of either 5 μg/ml doxorubicin, 0.1 μM cisplatin or 1000 nM tamoxifen, in combination with 10 ng/ml of PMHS, PMH and selected chemical modified heparins (PerS H, NAc H and 2,6 deS-NS H) for 48 hrs; cell apoptosis was then assessed by flow cytometry.

Figures 4.10 and 4.11 show dot plots of fluorescence intensities of cells labeled with annexin V/PI, showing the effects of HS/heparin and selected chemically modified heparins on BCSCs treated with the different chemotherapy agents. This allows comparison with the early and late apoptosis rates in non-treated and agent treated cells ($CD44^-/CD24^-$ and $CD44^+/CD24^-$ sorted cells). Quantitation of the data is shown in Figures 4.12 and 4.13.

For MDA-MB-231 cells it was evident that doxorubicin induced early and late apoptosis in $CD44^-/CD24^-$, but not in $CD44^+/CD24^-$ cells compared to untreated controls ($CD44^-/CD24^-$, 12.4 ± 1.25 vs 7.48% UT ($P<0.001$); and $CD44^+/CD24^-$, 8.43 ± 1.07 vs 8.14% UT) (Figure 4.12A). In contrast, simultaneous treatment with selected chemically modified heparins PerS H, NAc H, 2,6 deS-NS H, PMH or PMHS induced marked increases in early and late apoptosis in $CD44^+/CD24^-$ cells (to 10.56 ± 1.1, 11.76 ± 1.12, 14.34 ± 1.08, 14.78 ± 1.19, 8.87 ± 0.95 respectively, $P<0.05$, $P<0.01$, $P<0.001$) (Figure 4.12A). For $CD44^-/CD24^-$ cells treatment with the combination of doxorubicin with PerS H and NAc H did not alter the sensitivity to doxorubicin treatment (11.95 ± 1.27, 13.76 ± 0.71 respectively vs 12.4% for doxorubicin alone), while 2,6 deS-NS H, PMH and PMHS treatment all caused significant increases in $CD44^-/CD24^-$ cell apoptosis compared to doxorubicin treatment alone (18.98 ± 0.90, 20.75.20 ± 0.95, 16.17 ± 1.29 vs 12.4% Dox alone, $P<0.001$) (Figure 4.12A).

Figure 4.12B shows comparison data between $CD44^-/CD24^-$ and $CD44^+/CD24^-$ sorted cells from MDA-MB-231 treated with the chemotherapeutic agent cisplatin. Compared with the untreated control groups, cisplatin alone induced increased apoptosis in $CD44^-/CD24^-$ (10.47 ± 1.29 vs 7.07% in UT; $P<0.001$) and also a smaller increase for $CD44^+/CD24^-$ cells (7.84 ± 1.34 vs 6.29% in UT; $P<0.05$) (Figure 4.12B). Notable increases in apoptosis were induced when cells were treated with the modified heparins PerS H, NAc H and 2,6 deS-NS H in the presence of cisplatin: $CD44^-/CD24^-$ (19.87 ± 1.38, 20 ± 1.20, 14.48 ± 1.20 respectively vs 7.07% Cis alone), and $CD44^+/CD24^-$ (17.12 ± 1.18, 18.45 ± 1.39, 10.35 ± 1.07 respectively vs 6.29% Cis alone) (all $P<0.001$). In addition PMH with cisplatin were significantly decreased cell apoptosis in $CD44^+/CD2^-$ cells (6.01 ± 1.11 vs 7.84% Cis alone; $P<0.05$) but not in $CD44^-/CD24^-$ cells (10.28 ± 1.52 vs. 10.42% Cis alone). In addition a combination of PMHS with cisplatin had no significant effect on both types of sorted cells $CD44^-/CD24^-$ and $CD44^+/CD24^-$ compared to cisplatin alone (11.04 ± 1.52 vs 10.47% Cis alone and 9.04 ± 1.11 vs 8.25% Cis alone, respectively) (Figure 4.12B).

The effects of HS/heparin and chemically modified heparins on sensitivity of BCCs to tamoxifen was also tested (Figure 4.12C). Both $CD44^-/CD24^-$ and $CD44^+/CD24^-$ sorted cells from the MDA-MB-231 cell line were significantly sensitive to tamoxifen treatment alone, with increased apoptosis compared to untreated cell group (17.20 ± 1.4 vs 10% UT alone, and 12.05 ± 1.72 vs 7.54% UT alone, respectively; $P<0.001$). For $CD44^-/CD24^-$ cells only 2,6 deS-NS H, PMH and PMHS significantly increased cell apoptosis compared to similar sub-population treated with tamoxifen alone (20.23 ± 1.68, 28.24 ± 1.88, 21.76 ± 1.91 respectively vs 17.2% for Tam alone; $P<0.001$). For $CD44^+/CD24^-$ cells all of the compounds induced significant increases in apoptosis compared to tamoxifen alone ($P<0.01$, $P<0.001$). (Figure 4.12C); Overall, it is thus clear that CSCs from MDA-MB-231 cells can be sensitized to induction of apoptosis via a number of chemotherapeutic agents if treated with heparin-based compounds.

To determine whether Hs578-T BCC lines share similar enhanced chemosensitivity in response to treatment with the compounds, sorted cells were cultured with optimum doses of either 5 μg/ml doxorubicin, 0.1 μM cisplatin or 1000 nM

tamoxifen, alone or in combination with 10 ng/ml of HS/heparin and selected modified heparin (PerS H and 2,6 deS-NS H) for 48 hrs, with cell apoptosis was assessed by flow cytometry (Figure 4.13). As shown in Figure 4.13A,C, combinations of any of the compounds with the anticancer agents doxorubicin or tamoxifen induced increased apoptosis for both $CD44^-/CD24^-$ and $CD44^+/CD24^-$ Hs578-T cells compared to untreated control cells ($P<0.01$, $P<0.001$), the only exception being 2,6 deS-NS H treatment in combination with doxorubicin for $CD44^+/CD24^-$ cells (13.12 ± 1.22 vs 10.58% UT alone), (Figure 4.13A). The largest increases were noted with the combination of PerS H with doxorubicin (28.1 ± 1.53 vs 14.42% Dox alone, $P<0.001$) or (tamoxifen with PMH or PMHS) (27.79 ± 1.77, 30.72 ± 1 respectively vs 13.02% Tam alone, $P<0.001$) compared to single agent groups alone. In marked contrast, although a significant increase in apoptosis was observed in $CD44^+/CD24^-$ cells treated with cisplatin (14.73 ± 1.02 vs 11.5% UT, $P<0.001$), addition of the various compounds did induce significant decreases in apoptosis compared cisplatin alone ($P<0.05$, $P<0.001$); (Figure 4.13B). Cisplatin alone did not induce increased apoptosis in the $CD44^-/CD44^-$ sub-population, but each of the compounds (PerS H, 2,6 deS-NS H, PMH or PMHS) induced significant decreases in the apoptotic percentage in these cells compared to cisplatin alone (7.05 ± 1.28, 11.32 ± 2.15, 7.86 ± 1.11, 7.06 ± 1.12 respectively vs 15.09% Cis alone, $P<0.001$) (Figure 4.13C). Thus Hs578-T cells also displayed enhanced chemosensitivity in response to treatment with exogenous HS/heparins, though there were some differences compared to MDA-MB-231 cells in terms of responses to different chemotherapeutic agents.

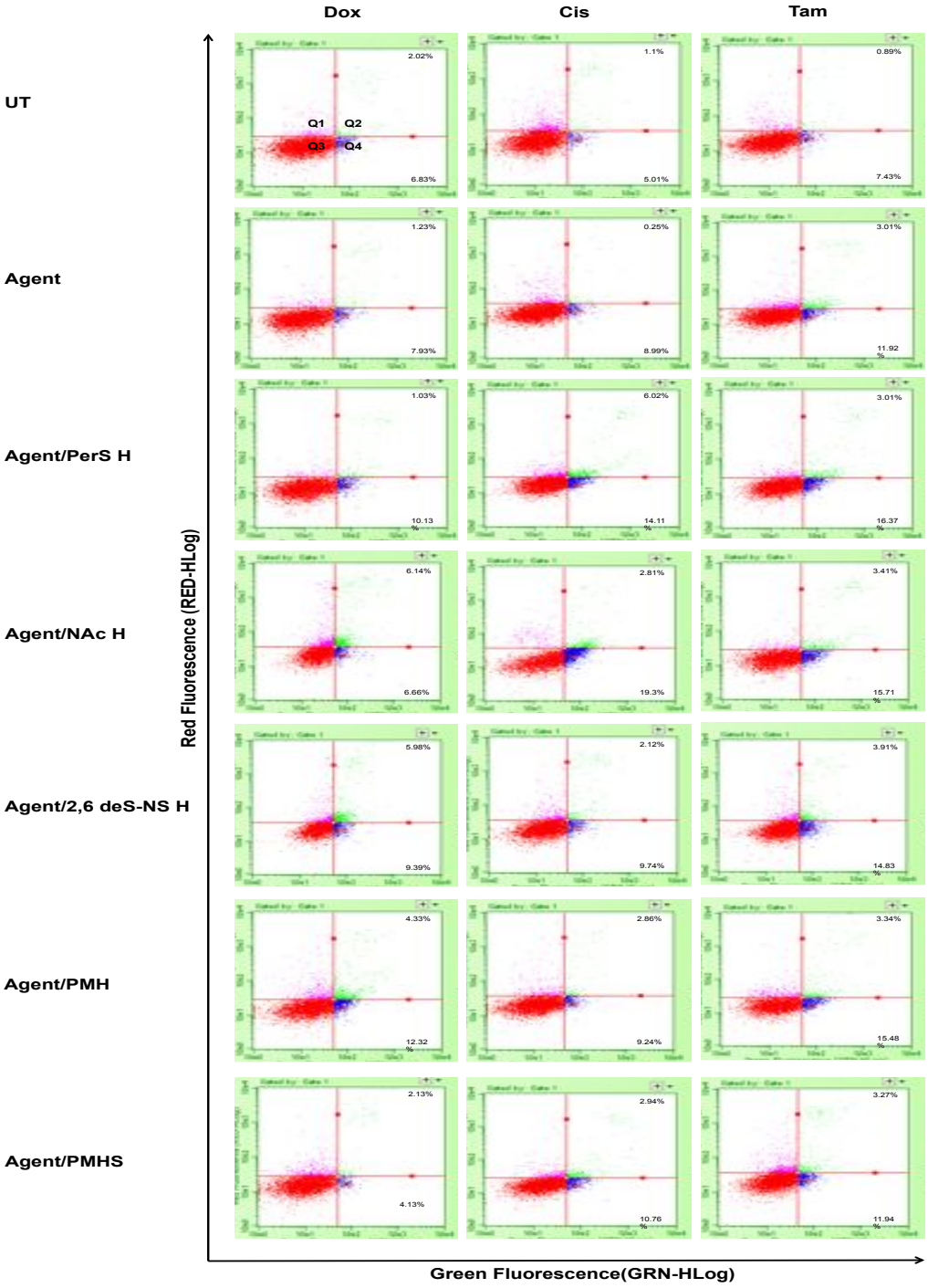

Figure 4.10 Apoptosis analysis in CSCs from MDA-MB-231 cells by flow cytometry. $CD44^{+}/CD24^{-}$ sub-population of MDA-MB-231 human BCC line were treated with optimum concentrations of chemotherapeutic drugs (1 µg/ml Dox, 0.1 µM Cis, 1 µM Tam) alone or combination with of PMHS, PMH or modified heparin (perS H, NAc H and 2,6 deS-NS H) for 48 hrs. Cells then stained with Annexin V-Alexa Fluor® 488 and PI staining. Representative cytograms of apoptosis in $CD44^{+}/CD24^{-}$ sub-population in the absence or presence of agents and HSPGs and the positive stained cells were counted using the Guava Viacount flow cytometer. Within a cytogram, Q1 represents necrotic cells; Q2 and Q4 represent late and early apoptotic cells, respectively and Q3 represents viable cells. Both early and late apoptotic cells were calculated. Data shows a representative example from two independent experiment.

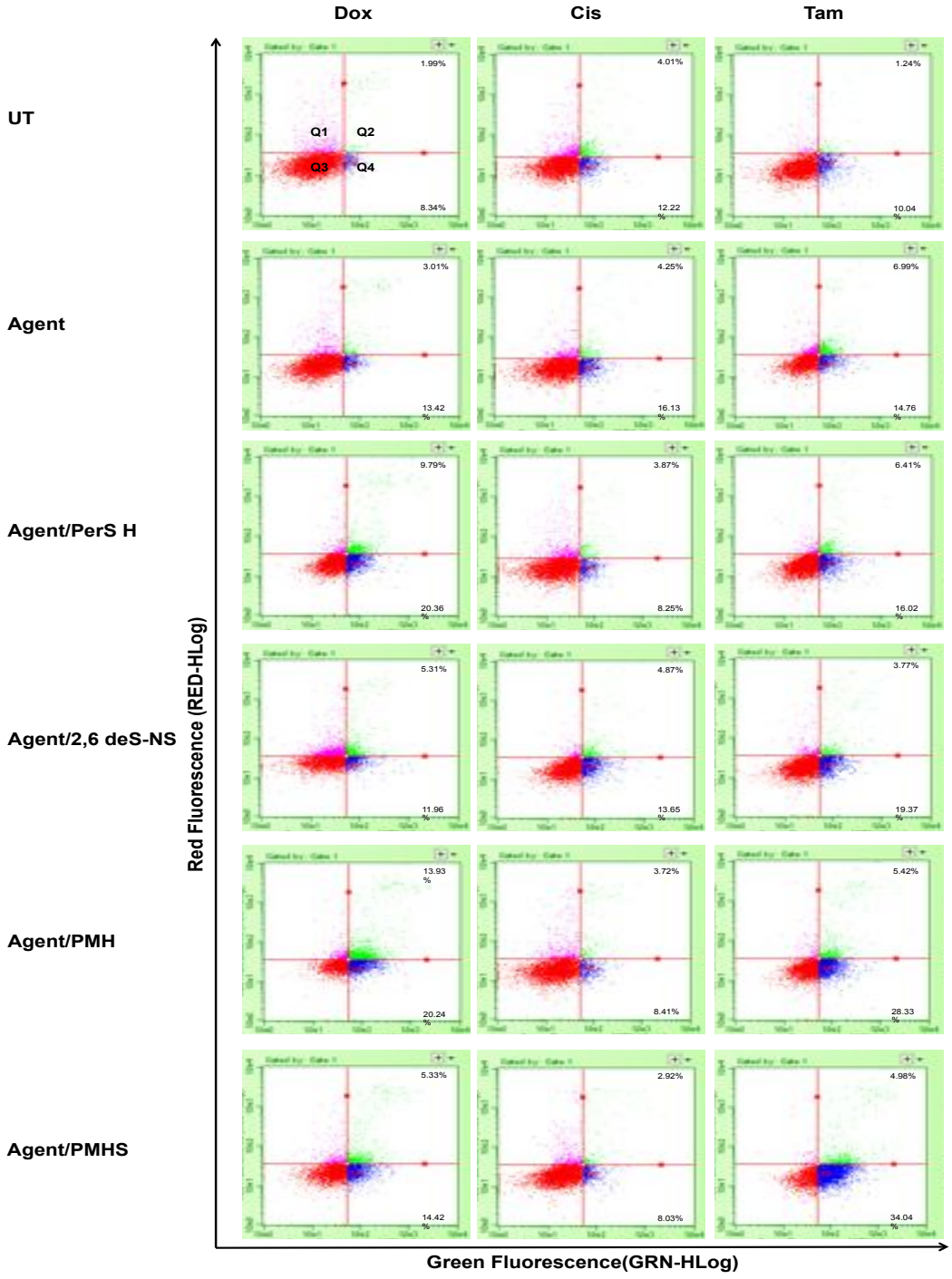

Figure 4.11 Apoptosis analysis in CSCs from Hs578-T cells by flow cytometry. $CD44^+/CD24^-$ sub-population of Hs578-T human BCC line were treated with optimum concentrations of chemotherapeutic drugs (1 µg/ml Dox, 0.1 µM Cis, 1 µM Tam) alone or combination with of PMHS, PMH or modified heparin (perS H, NAc H and 2,6 deS-NS H) for 48 hrs. Cells then stained with Annexin V-Alexa Fluor® 488 and PI staining. Representative cytograms of apoptosis in $CD44^+/CD24^-$ sub-population in the absence or presence of agents and HSPGs and the positive stained cells were counted using the Guava Viacount flow cytometer. Within a cytogram, Q1 represents necrotic cells; Q2 and Q4 represent late and early apoptotic cells, respectively and Q3 represents viable cells. Both early and late apoptotic cells were calculated. Data shows a representative example from two independent experiments.

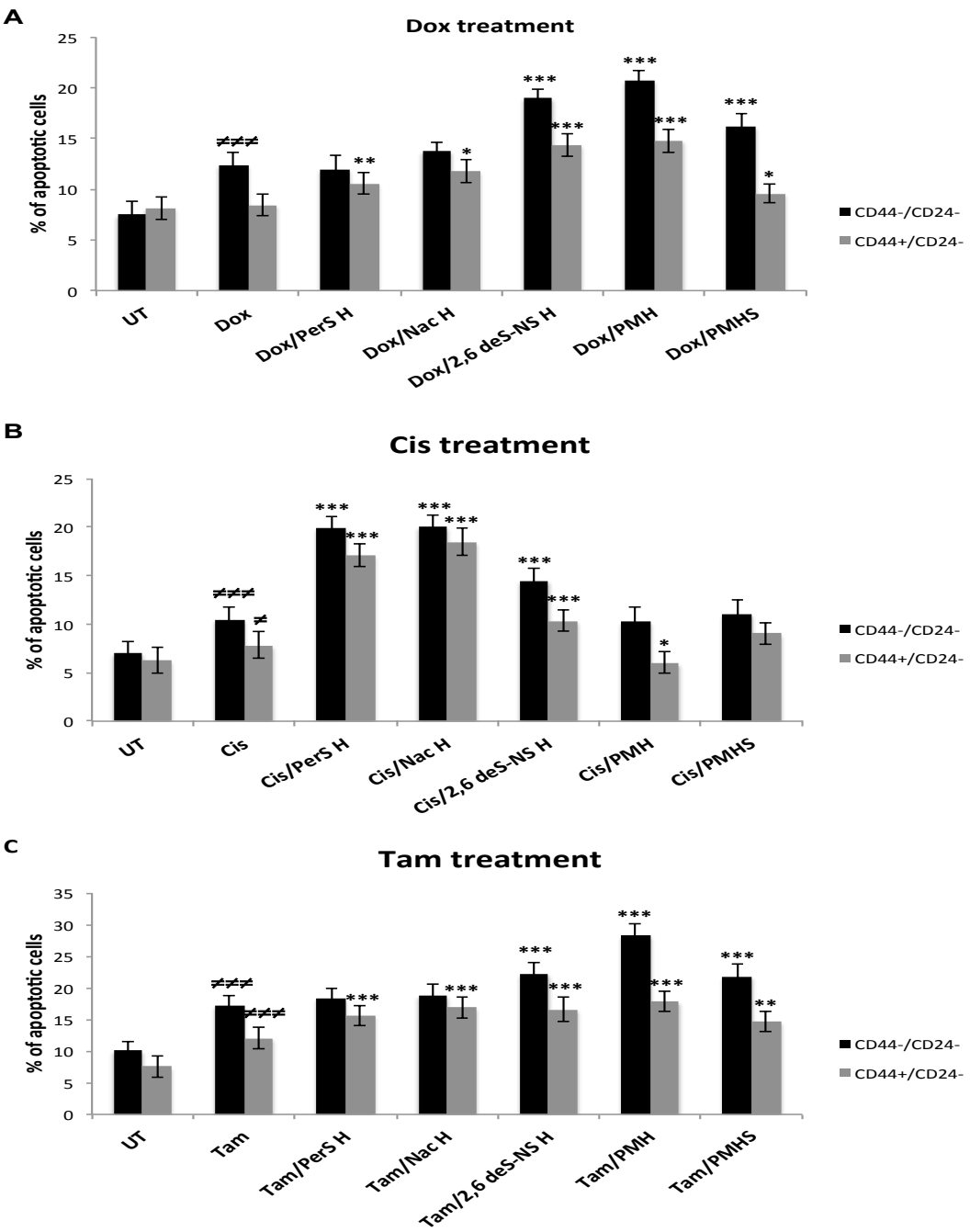

Figure 4.12 Effect selected HS, heparin and modified heparins on the induction of early and late apoptosis by chemotherapeutic agents in CSCs from MDA-MB-231 cells. After exposure to the different treatments for 48 hrs, the proportion of early and late apoptotic cells was analysed by flow cytometry using annexin V-FITC and PI. MDA-MB-231 treated cells with optimum concentrations of chemotherapeutic drugs alone or combination with 10 ng/ml of PMHS, PMH or modified heparin (perS H, NAc H and 2,6 deS-NS H) for 48 hrs. (A) 5 µg/ml Dox, (B) 0.1 µM Cis, (C) 1 µM Tam. Differences in drug resistance between $CD44^-/CD24^-$ and $CD24^+/CD44^-$ cells were calculated. Data represent the average of the early and apoptotic cells and shown as mean ± SD. Data in inset show statistical significance at ≠P<0.05, ≠≠≠P<0.001 vs. untreated cell group. *P<0.05, **P<0.01; ***P<0.001 for all treatment compared with single chemotherapy agent group. Data from one of two representative experiments shown; n=3 replicates in each assay.

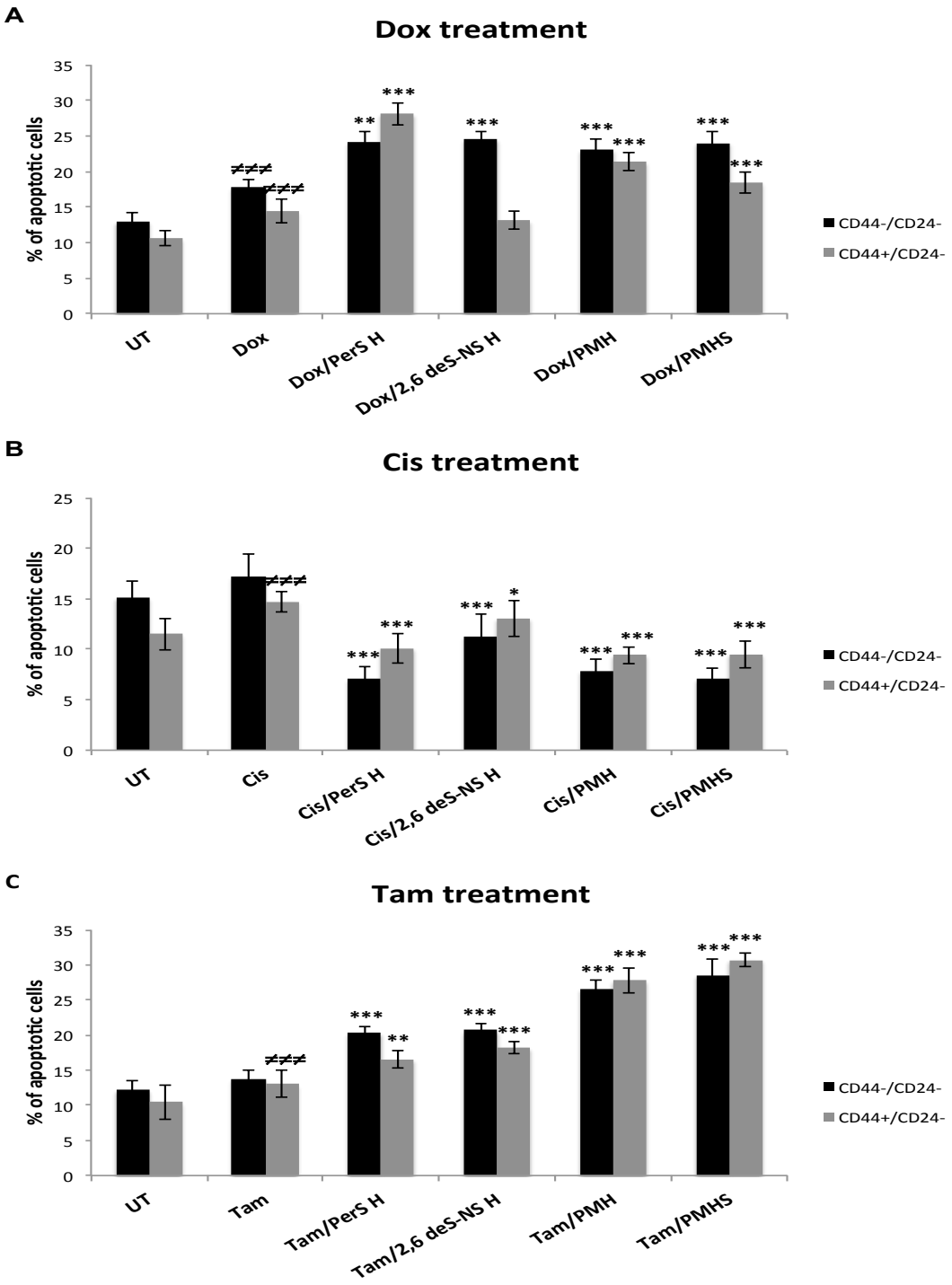

Figure 4.13 Effect selected HS, heparin and modified heparins on the induction of early and late apoptosis by chemotherapeutic agents in CSCs from Hs578-T cells. After exposure to the different treatments for 48 hrs, the proportion of early and late apoptotic cells was analysed by flow cytometry using annexin V-FITC and PI. Hs578-T treated cells with optimum concentrations of chemotherapeutic drugs alone or combination with 10 ng/ml of PMHS, PMH or modified heparin (perS H, NAc H and 2,6 deS-NS H) for 48 hrs. (A) 5 µg/ml Dox, (B) 0.1 µM Cis, (C) 1 µM Tam. Differences in drug resistance between $CD44^-/CD24^-$ and $CD24^+/CD44^-$ cells were calculated. Data represent the average of the early and apoptotic cells and shown as mean ± SD. Data in inset show statistical significance at ≠P<0.05, ###P<0.001 vs. untreated cell group. *P<0.05, **P<0.01; ***P<0.001 for all treatment compared with single chemotherapy agent group. Data from one of two representative experiments shown; n=3 replicates in each assay.

4.9 Discussion

HS is a multifunctional regulator of different biological processes (Turnbull et al., 2001), including aspects important to cancer cell behaviour such as proliferation and differentiation. HS plays important roles in cell growth and development, tissue homeostasis and cell migration, through interactions with a wide variety of proteins such as chemokines, enzymes and growth factors (Powell et al., 2010). These activities represent novel targets for therapeutic or diagnostic approaches. For that reason, a targeted modulation of HS expression or function in CSCs may be a promising approach, leading to either reduced proliferation or apoptosis, or loss of malignant properties of the cells. To study HS involvement in CSCs, the present studies aimed to use model BCSCs in culture.

A wide range of commonly available BCC lines were investigated (see Chapter 3); some lines such as MDA-MB-231 and Hs578-T were found to express appropriate markers ($CD44^+/CD24^-$) indicating the expected sub-populations, based on previous studies (Hwang-Verslues et al., 2009, Sheridan et al., 2006). The potential differential effects of differently modified heparins was undertaken, along with dose-response experiments to determine the minimal concentrations required for the observed effects. Low concentrations of chemically modified heparin (as low as 1-100 ng/ml) were found to induce a reduction of 40-50% in the $CD44^+/CD24^-$ CSC sub-population in both cell lines, indicating the potential to interfere with this aspect of BC tumour phenotype. Further studies are now needed to investigate whether this effect might be due to specific effects of the heparin on the CSC sub-population (eg. reduced proliferation or increased apoptosis), and the mechanisms involved (see Chapter 5).

Removal of overall HS sulphation through cell treatment with a low concentration of chlorate ($NaClO_3$) did appear to exert a specific effect on $CD44^+/CD24^-$ sub-population of MDA-MB-231 and Hs578-T BCC in terms of reduced cell proliferation.

Another possible mechanism by which cell surface HSPGs may be involved in BCSC regulation is through regulation of cell growth/proliferation. MTT assays of

the MDA-MB-231 and Hs578-T cell lines showed a significant reduction of cell proliferation after treatment by HS and selected chemically modified heparins and a significant increase of cell multiplication, if NAc H treatment was applied on both cell lines, suggesting an important contribution of HS and chemically modified heparin in the proliferative response of BCSCs.

HSPGs play an important role in regulating tumour cell metastasis. Previous work has demonstrated that HSPGs mediate the activities of growth and motility factors, control cell adhesion (Laterra et al., 1983), migration (Moon et al., 2005, Yenigun et al., 2013) and invasion (Sanderson, 2001). HSPGs inhibit or promote cell invasion, migration and adhesion with their function being determined by the HSPGs location (ECM or cell surface), the heparin-binding molecules they can interact with, modifying enzymes such as heparanases, and the precise structural characteristics of the HSPGs (Sanderson, 2001).

Previous experiments examined the role of cell surface levels of syndecan-2 using knockdown of syndecan-2 by siRNA. FACS analysis confirmed that syndecan-2 level was reduced to near background; a crucial role in focal adhesion was observed due to loss of the PG, whereas focal adhesion was enhanced by HS treatment (Lim et al., 2015). These data demonstrate a considerable impact of depletion of the HSPGs syndecan-1 and syndecan-2 on the CSC SP and invasiveness. Consistent with this, the present study shows that HS/heparin and chemically modified heparin (PerS H, 2,6 deS-NS H) are all regulators of $CD44^{+}/CD24^{-}$ stem-like cells in terms of their invasiveness and ability to migrate. In terms of adhesion, some HS/heparins were found to regulate the invasiveness and migration in non-cancer stem-like cell sub-population of MDA-MB-231. Matrigel cell invasion and collagen migration were remarkably inhibited [after HSPGs for CSCs and normal cancer cells of MDA-MB-231 cell line].

Hs578-T cells showed a significant reduction of migrating cells when treated with HSPGs, while a small affect in invasive BCSCs treated with HSPGs. Small significant effect of HSPGs on invaded unsorted and $CD44^{+}/CD24^{-}$ sorted cells of Hs578-T cells was reported in this study. Heparin and chemically modified heparin PerS H, 2,6 deS-NS H induced a reduction of cell migrated of noncancer stem-like

cells in Hs578-T breast carcinoma.

HS chains associate with various heparin binding growth factors and ligands such as fibronectin (Bernfield et al., 1999). Syndecans are the most well-characterized HSPGs in terms of regulating ECM adhesion via interactions with fibronectin (Tumova et al., 2000). The current study showed that HS, heparin and chemically modified heparin 2,6 deS-NS H significantly reduced the $CD44^{+}/CD24^{-}$ sub-population of MDA-MB-231 and Hs578-T BCCs. In contrast, PerS H has no impact on adhesion of BCSCs and normal BCCs in both cell line.

Cisplatin, tamoxifen and doxorubicin are used for treatment of a wide range of tumours, including breast tumours (Prabhakaran et al., 2013, Smith et al., 2006, Yenigun et al., 2013). Although these kinds of drugs have been used for chemotherapeutic treatment of patients with breast tumours, many patients are intrinsically resistant to them, resulting in poor responses and/or recurrence of tumours after therapy (McDermott and Wicha, 2010). Moreover, previous studies demonstrated that cells which overexpress heparanase were found to be more resistant to chemotherapeutic agents; these studies identified a role for heparanase in modulating autophagy in cancer and normal cells, conferring growth advantages under stress as well as chemoresistance (Shteingauz et al., 2015).

Of particular interest is that CSCs have been reported to be resistant to chemotherapy agents compared to the bulk tumour population (Olsson et al., 2011). Here I hypothesised that heparin may alter the chemosensitivity of CSCs, and in agreement with this idea it has recently been reported that cancer cells are sensitised to chemotherapeutic agents by treatment with low molecular weight heparin (Phillips et al., 2011). Thus it was of interest to explore the structure-activity relationships which might underlay this activity by using a library of differently modified heparins (Yates et al., 2004) in combination with chemotherapeutic agents. Here I found that HS/ heparin and chemically modified heparin in combination with chemotherapeutic (cisplatin, or doxorubicin) and anti-oestrogen agents (tamoxifen) have significant effects on normal BCCs and BCSCs through inducing apoptosis in two cell line models (MDA-MB-231 and Hs578-T cells). However, cisplatin with these modified heparins reduced cell apoptosis in both $CD44^{-}/CD24^{-}$ and $CD44^{+}/CD24^{-}$ of Hs578-T

cells. Low molecular weight heparin (LMWH) has recently been shown to cause reversal of cisplatin resistance, likely by interfering with function of endogenous GAGs/cell surface HSPGs (Pfankuchen et al., 2015). In addition, syndecan-1 is correlated with higher resistance to radiation of BCCs (Pfankuchen et al., 2015). The data presented here and summarized in Tables 4.1 and 4.2 are consistent with these observations, and support the idea that HSPGs have roles in regulating breast tumor progression. These insights could be used to develop strategies employing modified heparins to reduce chemoresistance, which could be used in combination with chemotherapy regimes.

Table 4.1 Summary table of effects of HS/heparin and modified heparins in MDA-MB-231 BCSC phenotype

	Proliferation	**Adhesion**	**Migration**	**Invasion**	**Chemosinsitivity**		
					Dox	**Cis**	**Tam**
PerS H	No effect	No effect	Sig -	Sig -	Sig +	Sig +	Sig +
NAc H	Sig +	-	-	-	Sig +	Sig +	Sig +
2,6 deS-NS H	Sig -	Sig -	Sig -	Sig -	Sig +	Sig +	Sig +
PMHS	Sig +	Sig -	Sig -	Sig -	Sig +	Sig +	Sig +
PMH	Sig -	Sig -	Sig -	Sig -	Sig +	Sig +	Sig +

*Sig, statistically significant.

Table 4.2 Summary table of effects of HS/heparin and modified heparins in Hs578-T BCSC phenotype

	Proliferation	**Adhesion**	**Migration**	**Invasion**	**Chemosinsitivity**		
					Dox	**Cis**	**Tam**
PerS H	No effect	No effect	Sig -	Sig -	Sig +	Sig -	Sig +
NAc H		-	-	-	-	-	-
2,6 deS-NS H	Sig +	Sig -	Sig -	Sig -	No effect	Sig -	Sig +
PMHS	Sig -	Sig -	Sig -	Sig -	Sig +	Sig -	Sig +
PMH	Sig -	Sig -	Sign -	No effect	Sig +	Sig -	Sig +

*Sig, statistically significant.

5 HS/Heparin and modified heparins mediate angiogenesis and molecular signaling in BCSCs

5.1 General introduction

BCSCs are being intensely investigated largely owing to their contributions towards heterogeneity and chemotherapy resistance in breast tumorigenesis. In this regard, CSCs are considered as a target to treat or cure breast tumorigenesis; however, understanding of BCSC biology, including their critical regulatory pathways, remains incompletely understood.

CD44 and ABCG2: The expression of CD44 glycoprotein is found in multiple isoforms on different types of cells where it functions as a receptor for hyaluronan-mediated motility. Recently, interest has centered on the expression of CD44 in human malignancies due to CD44 acting as a metastasis-related molecule with multiple functions including promoting cell migration, invasion, adhesion and presentation of growth factors and cytokines (Kuniyasu et al., 2001). Multiple studies demonstrated that tumorigenic $CD44^{+}/CD24^{-}$ BCC populations have tumour-initiating abilities (Al-Hajj et al., 2003, Ponti et al., 2005). This tumorigenic property has been associated with display of stem cell–like properties (Ponti et al., 2005), enhanced metastasis (Ratajczak et al., 2010), invasive properties (Zhang et al., 2012), and chemo/radio resistance (Arima et al., 2012).

High expression of the ATP binding cassets (ABC) transporter protein ABCG2 has also been identified in various cancer samples from patients such as breast cancer (Mao and Unadkat, 2015). In addition, it has been shown that there is a correlation between the expression of ABCG2 and the response to many types of chemotherapeutic agents as well as a reduction in survival rate, and ABCG2 expression levels may be used as a reliable indicator of prognosis in cancer patients (Natarajan et al., 2012). The ABC transporter family is primarily responsible for the phenotype of CSC-like populations identified in some stem cell derived organs and tumours. Recently, the upregulation of ABCG2 has been shown in human cancer cell

lines side-populations; and significantly this is an efflux transporter implicated in broad-spectrum chemoresistance (Sicchieri et al., 2015).

Angiogenic molecules: Angiogenesis is also a master event in tumour growth. This event is mediated by pro- and anti-angiogenic factors balanced secreted by multiple cell types in the tumour niche. Different cell types can enhance angiogenesis by secreting vascular endothelial growth factor (VEGF) family that form new blood vessels. However, direct evidence that BCSCs can contribute to angiogenesis properties is still lacking (Byrne et al., 2005).

Several lines of evidence implicate the importance of VEGFA and VEGFB in breast cancer (Gasparini, 2000). VEGF was found to be overexpressed in BC tissue when compared to normal breast tissue and VEGF levels in these tissues have been associated with disease-free and overall survival (Byrne et al., 2007, Dent, 2009).

HS polysaccharide chains bind to wide range of protein ligands, such as, serine proteases, growth factors and their receptors. These chains can mediate angiogenesis driven by a number of growth factors including all but one splice variant of VEGF (Chen et al., 2004, Ruhrberg et al., 2002). A number of *in vivo* and *in vitro* studies have examined the roles of HSPGs in VEGF activity: most importantly, HS seems to be essential to spatially restrict VEGF to create the appropriate gradient to allow blood vessel branching to occur (Ruhrberg et al., 2002). HS proteoglycans can also re-activate oxidation-damaged forms of VEGF, a function that may be essential in hypoxic sites where new vessels are required (Gengrinovitch et al., 1999). They potentiate VEGF binding to its two specific signal-transducing receptors (Gitay-Goren et al., 1992) and may interact directly with the receptors (Chiang and Flanagan, 1995, Cohen et al., 1995, Dougher et al., 1997) analogous to the widely studied HS–FGF-2–FGF receptor signaling complex (Delehedde et al., 2000, Lundin et al., 2000).

Angiopoietins are ligands for the receptor tyrosine kinase (Tie2), which is expressed by endothelial cells and their precursors, and these molecules are also important for regulation of angiogenesis. Three angiopoietins have been identified, including Ang-1, Ang-2 and Ang-3 (Xu et al., 2004). Studies have shown that, Ang-2 and Ang-3 are antagonists of the Tie-2 receptor (Maisonpierre et al., 1997, Valenzuela et al., 1999).

It is believed that both Angiopoietins 2 and 3 compete with Ang-1 for binding to Tie-2, and block Tie-2 phosphorylation induced by Ang-1 (Holash et al., 1999, Maisonpierre et al., 1997, Valenzuela et al., 1999).

Other signaling pathway molecules: Chemokines are important molecules in regulating cancer cell phenotype. The C-X-C chemokine receptor type 4 (CXCR4) is one of the most common studied cell surface chemokine receptors expressed on many different types of tumour cells. It was reported that, CXCR4 signalling correlates with aggressiveness and metastasis promotion. Previous studies reported that CXCR4/CXCL12 signalling regulates BC metastases *in vivo* and *in vitro* respectively (Kucia et al., 2005). The expression of CXCR4 has been detected in the stem cell population of brain tumours and breast cancer (Dontu et al., 2003, Reya et al., 2001, Singh et al., 2004).

It is thought that the metastasis of BCSCs is stimulated by the interaction between CXCL12 and CXCR4 presented by HS on the ECM and vascular endothelium. This induces. The activation and expressing of CXCR4 causes cell migration followed by angiogenesis resulting the metastasis in secondary tumours (Harvey et al., 2007, Luker and Luker, 2006, Mellor et al., 2007, Müller et al., 2001, Würth et al., 2015).

Previous studies have also emphasized the upregulated role of the proinflammatory cytokine IL-8 in a wide variety of solid tumors, including, bladder, gastric prostate, lung, ovarian and melanoma. It has been reported that IL-8 contributes to multiple hallmarks of cancer, including, increased angiogenesis, proliferation, invasion, and metastases (Singh et al., 2013).

Several other signaling pathways including ERK1/2 MAPK (Wang et al., 2010), STAT3 (Fouse and Costello, 2013), Wnt/β-catenin and Notch signaling pathways help in maintaining the normal and cancer stem cell program (Karamboulas and Ailles, 2013). In addition, these pathways support EMT of cancer cells as well as multiple drug transporter expression. Cells that have undergone EMT are known as progenitor cells and have chemoresistance properties. Thus, stem cell properties, drug resistance and induction of EMT programs appear to be interlinked (Kotiyal and Bhattacharya, 2014, McDermott and Wicha, 2010).

The signaling pathway through ERK is considered as one of the main determinants in the control of diverse cellular process including maintenance of CSCs, due to its an important role in EGFR signaling. ERK signaling is significantly upregulated in CSCs (Wang et al., 2010). Recent reports have revealed a requirement for Notch signaling for the maintenance of BCSCs (Mittal et al., 2014, Sharma et al., 2012). Furthermore, the inhibition of Notch and Ras/MAPK signaling may be beneficial for BC treatment and results in a significant decrease in the BCSC population (Jung et al., 2016, Mittal et al., 2014, Sharma et al., 2012). ERK1/2 are widely expressed and involved in regulation of cell functions, via protein phosphorylation, such as, regulation of apoptosis, downstream kinases and several transcription factors. Different stimulation such as cytokines, growth factors, virus infection and other stimuli also activate the ERK1 and ERK2 pathways (Chua et al., 2004, Johnson and Lapadat, 2002).

Fibroblast growth factor-2 (FGF2) is one of the prototypic members of the fibroblast growth factor family. It plays an important role in the regulation of cell survival, angiogenesis, differentiation and migration. (Chua et al., 2004). It has been demonstrated that FGF2 binds to its cell-surface tyrosine kinase FGF receptor (FGFRs), triggering receptor dimerization and autophosphorylation of tyrosine residues, resulting in modulaiton of intracellular docking sites for downstream proteins leading to cell responses (Chua et al., 2004). HS has been demonstrated to be an important requirement for the binding of FGF-2 to its receptor (Chan et al., 2015). In addition, it has been reported that both the 2-*O*-sulfate groups of IdoUA and the 6-*O*-sulfate groups of *N*-sulfated GlcN are required for this FGF-2 mitogenic activity (Guimond et al., 1993). HSPGs modulate the activity of FGF2 via functioning as coreceptors to enhance the binding of FGF2 to its receptors. However, FGF2 might also signal directly through HSPG via inducing aggregation of syndecan-4 and activation of protein kinase Cα. Previous studies demonstrated that the syndecan-4 cytoplasmic tail is phosphorylated on Ser^{138}. Indeed, FGF2 can reduce the phosphorylation 2 to 3 fold, inducing multimerization and activation of protein kinase Cα (Horowitz and Simons, 1998). FGF2-mediated signaling via syndecan-4 proceeds to downstream signal transduction, such as ERK1/2, to regulate cell activity independent of FGFRs. The biological response mediated by ERK1/2 is dependent on the kinetics, extent, and context of activation. Hence, ERK1/2 could be

a site of convergence for FGF2-mediated signaling through HSPG and FGFR (Chua et al., 2004, Horowitz and Simons, 1998).

STAT3 also plays an important role in maintenance of BCSCs (Xiong et al., 2014). Accumulating evidence indicates that, Wnt and IL-6/JAK2/STAT3 pathways were found to be active in $CD44^{+}/CD24^{-}$ sub-populations isolated from BCCs, and xenograft tumours growth can be supressed due to blocking this pathway via specific inhibitors. In addition, normal cancer cell populations can be converted to CSC populations through activation of the IL-6/JAK2/STAT3 signalling pathway via upregulation of OCT-4 (Kim et al., 2013). Many different inhibitors of STAT3, such as niclosamide, have been found to prevent the production of OCT-4, thus, these studies support that STAT3 plays a plays a prominent role in regulating BCSC self-renewal(Kim et al., 2013). Recent studies have shown that Syndecan-1 (CD138), a heparan sulfate proteoglycan, was found to modulate all of these pathways in BC. High Syndecan-1 expression in breast carcinomas is related to an aggressive phenotype (Barbareschi et al., 2003), and reduced BC-specific overall survival (Leivonen et al., 2004). Both Wnt signaling and Syndecan-1 modulate the mammary progenitor population growth and differentiation in BCSCs, (Ibrahim et al., 2013), demonstrating a pivotal role for Syndecan-1 in CSC function.

Aims of this chapter: To explore mechanisms by which exogenous HS/heparins may influence the phenotype of BC CSCs, more specifically:

- To evaluate the effect of exogenous HS/heparins on stem cell and drug resistance genes in BCSCs. The relative mRNA expression of CSC markers, including CD44 and EpCAM and drug resistance genes ABCG2 has been tested in $CD44^{-}/CD24^{-}$ and $CD44^{+}/CD24^{-}$ sub-populations from MDA-MB-231 and Hs578-T untreated and treated cells.
- To identify whether a $CD44^{+}/CD24^{-}$ phenotype might induce angiogenesis via HSPGs; $CD44^{+}/CD24^{-}$ BCCs from cultures of MDA-MB-231 and Hs578-T cells were examined to determine the effect of HS/heparins as enhancers or supressors of expression of VEGFA, VEGFB, Ang-1, Ang-2, CXCR4 and IL-8 by qRT-PCR.
- To study the potential role of HS in FGF2-mediated ERK1/2 activation in CSCs. The effect ofHS and highly sulphated modified heparin in ERK1/2 signaling *in vitro on*

the CD44$^+$/CD24$^-$ CSC-like sub-population was assessed using MDA-MB-231 and Hs578-T human BCC lines as a model.

- To investigate the regulatory role of HSPGs on inflammatory signaling pathways in BCSCs. qRT-PCR and western blot technologies were employed in MDA-MB-231 and Hs578-T BCSCs to assess the effects of HS/heparins. The functional impact of HS and highly sulphated chemically modified heparin on the expression of effectors of the stemness-related IL-6/STAT3 and signaling pathways, was also analyzed.
- To elucidate the regulatory role of HS/heparin and chemically modified heparin on signalling molecules mediated by FGF2 in in MDA-MB-231 and Hs578-T BCSCs. The phosphorylation of 18 well-characterized signalling molecules was examined by PathScan analysis.
- To study the possibility that HS/heparins might affect on HSPG's biological function in BCSCs. Study was undertaken by analyzing effect of HS/heparins on the expression patterns of the genes involved in HSPG biosynthesis and comparing them with untreated cell group.

5.2 CSC and drug resistance genes are highly expressed in CD44$^+$/CD24$^-$ BCC lines

In order to investigate the relative mRNA expression of CSC and drug resistance genes between CD44$^+$/CD24$^-$ and CD44$^-$/CD24$^-$ BCC lines, quantitative RT-PCR assay was performed. Briefly, CD44$^+$/CD24$^-$ and CD44$^-$/CD24$^-$ sorted cells from MDA-MB-231 and Hs578-T cells were cultured for three days. Cells were harvested and total RNA was extracted followed by cDNA synthesis. qRT-PCR analysis was performed and measurements were normalized against GAPDH using $2^{-\Delta C}{}_{\mathrm{T}}$.

The BCSC marker (CD44) has been shown to regulate invasion and metastasis of BCCs either positively or negatively. The results showed that CD44, commonly used to isolate a sub-set with CSC-like characteristics, was as expected highly expressed in CD44$^+$/CD24$^-$ cells from MDA-MB-231 and Hs578-T (Figure 5.1A, B; CD44$^+$/CD24$^-$ vs. CD44$^-$/CD24$^-$: 7.22 ± 0.74 and 6.17 ± 0.24 fold respectively [mean ± SD] ($P<0.001$)) relative to CD44$^-$/CD24$^-$. Another marker of CSCs, epithelial cell adhesion molecule (EpCAM), was not detectable after 40 cycles in the CD44$^+$/CD24$^-$ cells isolated from the MDA-MB-231 and Hs587-T cultures (Figure. 5.1A, B;

$CD44^+/CD24^-$ vs. $CD44^-/CD24^-$: 1.12 ± 0.14 and 1.23 ± 0.15 fold respectively [mean ± SD]). Over-expression of BCRP/ABCG2 is an essential mechanism of drug resistance. Results showed that $CD44^+/CD24^-$ cells isolated from MDA-MB-231 and Hs587-T cells expressed significantly increased levels of ABCG2 (Figure 5.1A, B; $CD44^+/CD24^-$ vs. $CD44^-/CD24^-$: 5.08 ± 0.27 and 5.01 ± 0.64 fold respectively [mean ± SD] ($P<0.001$)), compared with 1% in $CD44^-/CD24^-$ cells. These data demonstrated that some CSC and drug resistance genes are increased in $CD44^+/CD24^-$ sub-population of some BCC lines compared with $CD44^-/CD24^-$ cells.

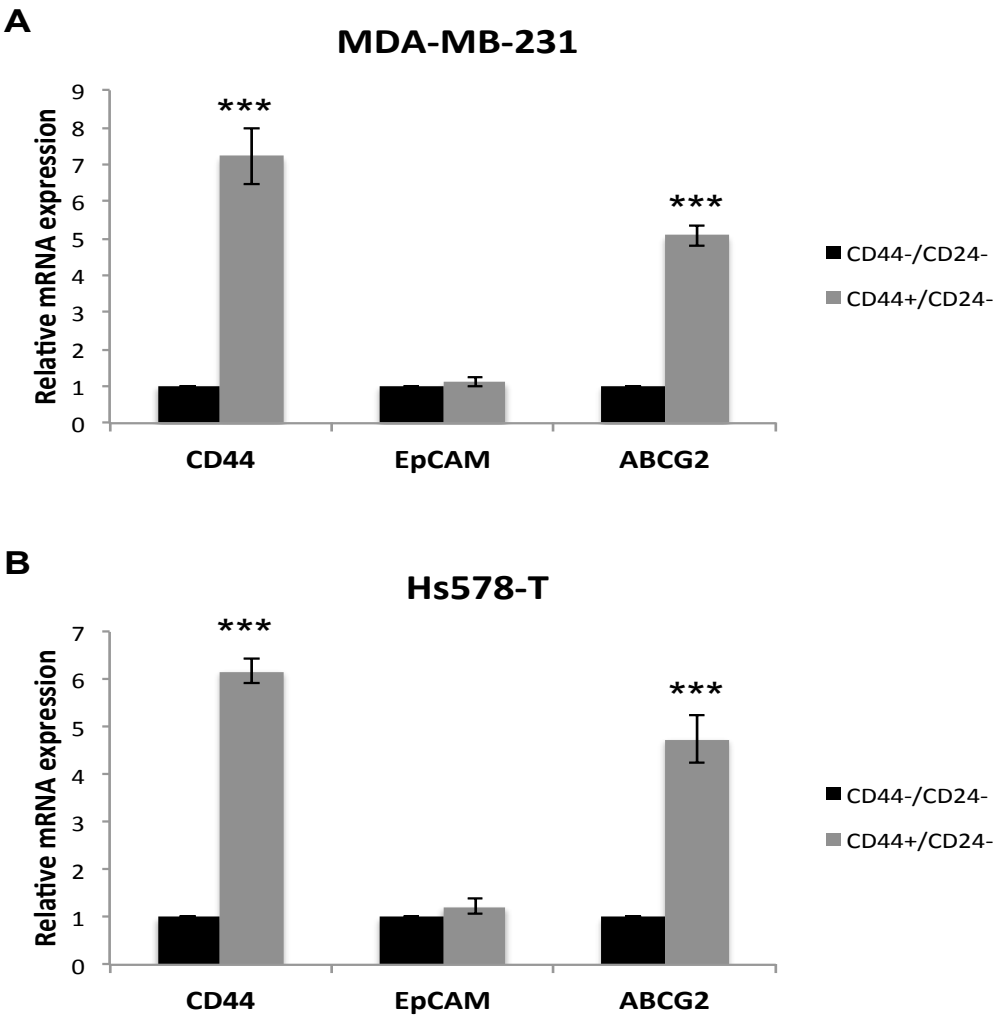

Figure 5.1 The relative mRNA expression of CSC and drug resistance markers in $CD44^-/CD24^-$ and $CD44^+/CD24^-$ BCCs. (A) MDA-MB-231 and (B) Hs578-T BCC lines were maintained as described in the Methods section. CD44, ABCG2 and EpCAM mRNA levels (measured by qRT-PCR) were found to be significantly higher in $CD44^+/CD24^-$ cells than in $CD44^-/CD24^-$ sub-populations (***$P<0.001$). GAPDH mRNA served as a control. All the results are presented as the mean ± SD of data (n=3) and obtained in three independent experiments.

5.3 Angiogenic markers are highly expressed in $CD44^+/CD24^-$ BCC lines

Angiogenesis plays an important role in the growth and metastasis of BC (Sun et al., 2013). Hence the expression of angiogenic genes was tested by qRT-PCR. As shown in Figure 5.2A, B, the expression of various proangiogenesis genes were analyzed in $CD44^-/CD24^-$ and $CD44^+/CD24^-$ BCCs, including VEGFA, VEGFB, Ang-1, Ang-2, the chemokine CXCL8 (IL-8) and the chemokine receptor CXCR4. The results showed that $CD44^+/CD24^-$ sub-population isolated from MDA-MB-231 and Hs578-T cells expressed high levels of the panel of proangiogenic genes mentioned above compared to $CD44^-/CD24^-$ cells. In detail, as shown in Figure 5.2A, proangiogenic factors VEGFA, VEGFB, IL-8, CXCR4, Ang-1 and Ang-2 were highly expressed in the $CD44^+/CD24^-$ MDA-MB-231 cells (fold expression $CD44^+/CD24^-$ vs. $CD44^-/CD24^-$: 3.48 ± 0.54, 3.33 ± 0.21, 5.06 ± 0.39, 5.62 ± 0.39, 5.58, ± 0.25 and 2.77 ± 0.38 respectively [mean ± SD] $P<0.001$, $P<0.01$). Figure 5.2B shows that proangiogenic factors VEGFB, IL-8, CXCR4 and Ang-1 were highly expressed in the highly invasive and metastatic $CD44^+/CD24^-$ Hs578-T cells (fold expression $CD44^+/CD24^-$ vs. $CD44^-/CD24^-$: 3.17 ± 0.25, 2.88 ± 0.21, 3.57 ± 0.15 and 2.72 ± 0.23 respectively [mean ± SD] $P<0.001$). VEGFA and Ang-2 mRNA expression were not significantly different between the $CD44^+/CD24^-$ and $CD44^-/CD24^-$ cells isolated from Hs578-T cells.

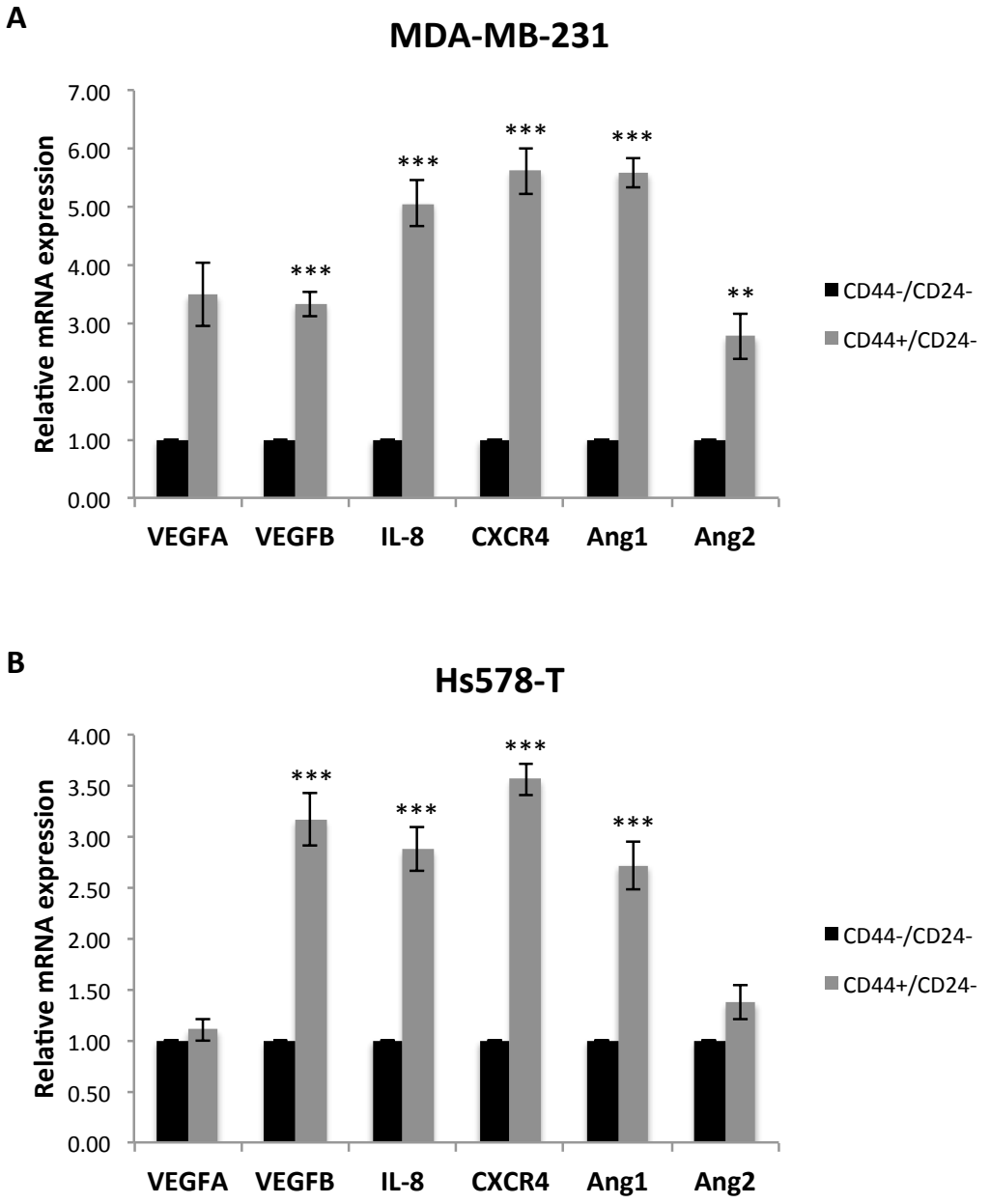

Figure 5.2 Analysis of angiogenic genes in $CD44^{+}/CD24^{-}$ vs $CD44^{-}/CD24^{-}$ BCCs by qRT-PCR. Proangiogenic mRNA levels after 48 hrs cell culture incubation of (A) MDA-MB-231 cell line, and (B) Hs578-T cell lines. 'Control' represents $CD44^{-}/CD24^{-}$ cells. Proangiogenic mRNA levels were determined using qRT-PCR and the relative expression was calculated by normalizing the amplification of DNA samples to GAPDH and compared with the $CD44^{-}/CD24^{-}$ expression levels. Error bars indicate SD of data (n=2) and obtained in three independent experiments. **P<0.01, ***P<0.001 proangiogenic mRNA levels relative to control for the corresponding gene.

5.4 Determination of the effects of HS/heparin and chemically modified heparins on CSC markers in BCCs

To characterize the potential mechanisms involved in the effect of HS/heparin/modified heparins on human BCSCs from the $CD44^+/CD24^-$ side population isolated from MDA-MB-231 and Hs578-T cells, the expression of CSC markers was analysed by qRT-PCR in response to treatment conditions. In this study, HS, heparin and two highly sulphated modified heparin derivatives, PerS H and 2,6 deS-NS H, were added to the $CD44^+/CD24^-$ sub-population isolated from both MDA-MB-231 and Hs578-T cells, following by culturing for 48 hrs. An untreated group was defined as the control calibrator for the $2^{-\Delta C_T}$ analysis after performing qRT-PCR for selected marker genes.

As shown in Figure 5.3, results showed that both CD44 and ABCG2 genes in both cell lines (MDA-MB-231 and Hs578-T) showed changes in levels of mRNA expression in all analysed treatments in $CD44^+/CD24^-$ compared to calibrator untreated cells (Figure 5.3A). The $CD44^+/CD24^-$ sub-population in both MDA-MB-231 and Hs578-T cells that were treated with PerS H, 2,6 deS-NS H and PMHS showed down-regulation of expression of CD44 ($P<0.001$) (Figure 5.3A; (MDA-MB-231 fold changes: -0.75 ± 0.13, -1.34 ± 0.13 and -1.10 ± 0.16 respectively [mean ± SD]; Hs578-T fold changes: -0.65 ± 0.16, -0.84 ± 0.13 and -1.29 ± 0.09 respectively [mean ± SD]). No change in CD44 expression was detectable in both cell lines (MDA-MB-231 and Hs578-T) treated with PMH (expression 1.23 ± 0.19 and 1.13 ± 0.47 respectively [mean ± SD]) compared to untreated cells, as a calibrator.

As shown in Figure 5.3B, ABCG2 mRNA expression was found to be increased compared to the untreated control in MDA-MB-231 and Hs578-T cultures. MDA-MB-231 treated cells with PMH and PMHS showed significant increases in ABCG2 expression (2.20 ± 0.17 and 1.53 ± 0.2 respectively [mean ± SD] $P<0.05$, $P<0.001$). MDA-MB-231 and Hs578-T cells treated with PerS H also showed an increase in expression of ABCG2 by approximately 50% compared to untreated cells (mean 1.50 ± 0.11, 1.60 ± 0.11 respectively [mean ± SD], $P<0.01$). Hs578-T treated cells with 2,6 deS-NS H and PMHS showed significant increases in ABCG2 expression

(expression 2.75 ± 0.30 and 2.16 ± 0.09 respectively [mean ± SD], P<0.01, P<0.001). In contrast, no significant change in expression of ABCG-2 could be detected in MDA-MB-231 cells treated with 2,6 deS-NS H and Hs578-T cells treated with PMH compared to untreated cells (expression 1.26 ± 0.22 and 1.36 ± 0.16 respectively [mean ± SD]) (Figure 5.3B).

The expression of EpCAM mRNA was found to be largely unchanged with most treatments of the CSC sub-population in both MDA-MB-231 and Hs578-T cells (Figure 5.3C). Changes in expression of EpCAM genes in MDA-MB-231 cells were not detected in cells treated with all compounds, except PMHS which induced a small increase by approximately 45% (1.45 ± 0.2, P<0.05) compared to untreated control cells. Similarity, significant changes in EpCAM expression were not observed in Hs578-T cells treated with PerS H or 2,6 deS-NS H, whereas PMH treatment showed a significant increase in EpCAM (2.17 ± 0.32, -0.78 ± 0.16 [mean ± SD] (P<0.01). Interestingly, the expression of EpCAM mRNA was found to be strongly down-regulated in the CSC sub-population from Hs578-T cells treated with PMHS (fold change -0.78 ± 0.16 [mean ± SD] (P<0.001)) (Figure 5.3C).

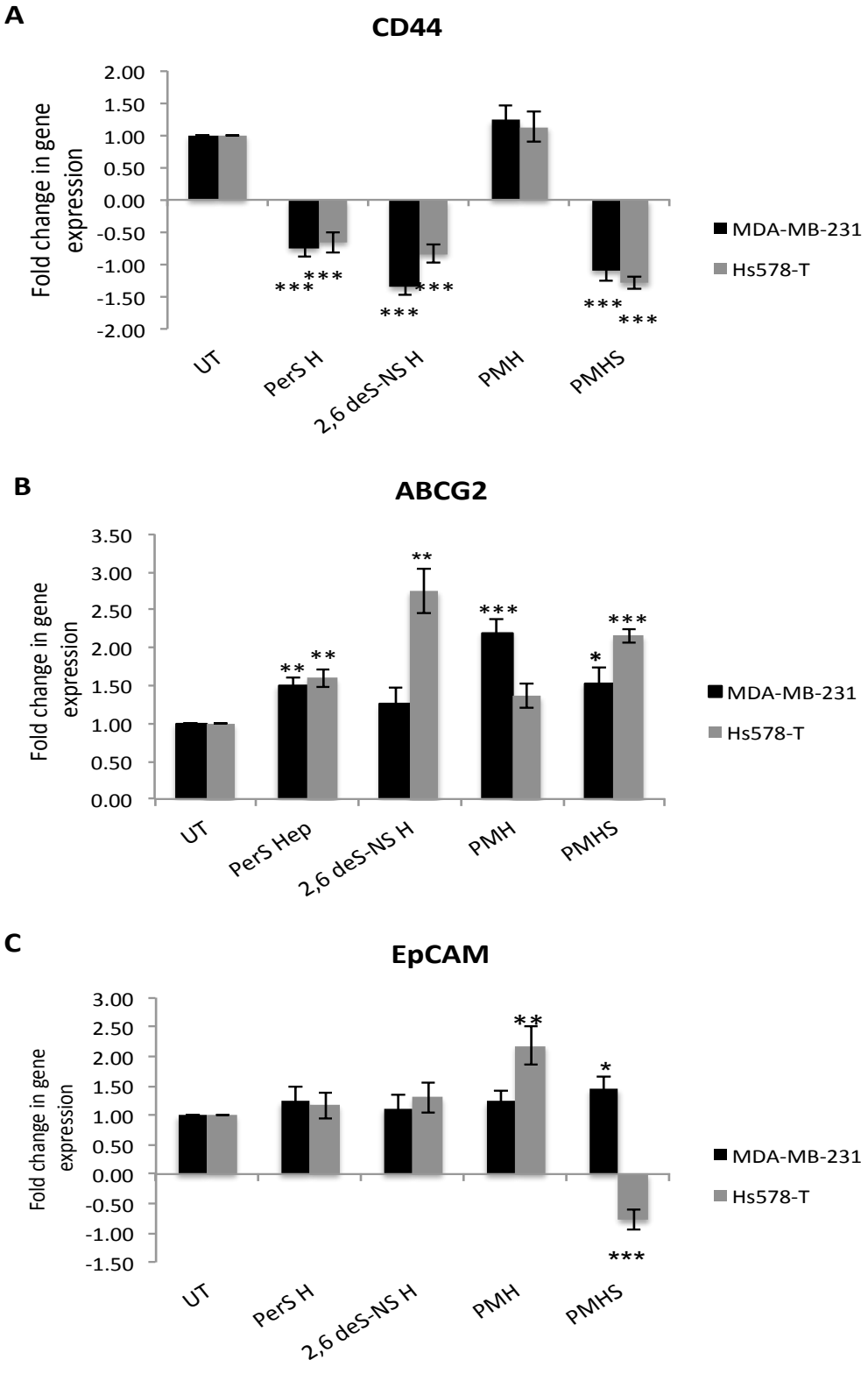

Figure 5.3 CD44, ABCG2 and EpCAM expression in BCCs treated with HS and modified heparins. (A) CD44, (B) ABCG-2 and (C) EpCAM expression in $CD44^{+}/CD24^{-}$ sub-population isolated from MDA-MB-231 and Hs578-T BCCs, relative to untreated group (UT), treated with 10 ng/ml of PerS H, 2,6 deS-NS H, PMH or PMHS for 48 hrs. Expression was assessed using qRT-PCR normalized to human GAPDH. Data are representative of two measurements per sample of two individual experiments; bars are expressed as mean ± SD. *P<0.05, **P<0.01, ***P<0.001 compared to UT.

5.5 Determination of the effects of HS/heparin and modified heparin on angiogenesis cell markers in BCCs

As described above, angiogenesis leads to the formation of blood vessels from pre-existing ones, allowing tumour growth. VEGFA, VEGFB and Angiopoietins (Ang-1, Ang-2) have important roles in tumour angiogenesis (Samples et al., 2013), but few data regarding their role in BCSCs phenotype are available. The expression of these markers of the angiogenic phenotype (VEGFA, VEGFB and Angiopoietins (Ang-1, Ang-2) was noted in BCSCs in section 5.3 above. We next examined whether treatment of these cells with HS, heparin or modified heparins might alter their expression. In addition, both the expression of CXCR4 and IL-8 were examined using qRT-PCR to assess similar questions regarding effects of heparins on chemokines. In this study, HS, heparin and two highly sulphated modified heparin derivatives (PerS H and 2,6 deS-NS H) were added to the $CD44^{+}/CD24^{-}$ sub-population isolated from both MDA-MB-231 and Hs587-T cells following by culturing for 48 hrs. Quantitative PCR analysis was performed as described in Methods.

The effect of HS, heparin and modified heparins on the expression of VEGFA (Figure 5.4A), VEGFB (Figure 5.4B), Ang-1 (Figure 5.4C), Ang-2 (Figure 5.4D), CXCR4 (Figure 5.4E) and IL-8 (Figure 5.4F), on the $CD44^{+}/CD24^{-}$ sub-population of MDA-MB-231 and Hs578-T cells is shown in Figure 5.4.

The expression of VEGFA increased in MDA-MB-231 $CD44^{+}/CD24^{-}$ cells treated with HS, heparin, 2,6 deS-NS H and PerS H (fold change, 1.14 ± 0.12, 1.57 ± 0.10, 2.01 ± 0.16 and 2.25 ± 0.14 respectively [mean ± SD], ($P<0.05$, $p<0.001$) (Figure 5.4A). Significant up-regulation of VEGFA expression in the $CD44^{+}/CD24^{-}$ sub-population in Hs578-T cells was observed with PerS H and PMH ($P<0.01$, $P<0.001$) compared to untreated cells (fold change 2.22 ± 0.21 and 1.56 ± 0.10 respectively, [mean ± SD]). No changes in expression level of VEGFA was found to be detectable in $CD44^{+}/CD24^{-}$ sub-set of Hs578-T treated cells with 2,6 deS-NS H or PMHS (expression 1.09 ± 0.14 and 1.28 ± 0.2 respectively, [mean ± SD]) (Figure 5.4A).

Changes in VEGFB expression were undetectable in both MDA-MB-231 and Hs78-T CSC sub-population cells treated with PerS H or PMH, while increases were detected with PMHS treatment (fold expression 1.48 ± 0.08, 1.19 ± 0.09 respectively, [mean ± SD] ($P<0.05$, $P<0.01$)). MDA-MB-231 cells treated with 2,6 deS-NS H showed a significant increase in VEGFB expression compared to untreated cells (1.28 ± 0.12, [mean ± SD] ($P<0.05$)). In contrast Hs578-T cells did not show a significant change in expression to VEGFB in response to 2,6 deS-NS H (Figure 5.4B).

Ang-1 expression (Figure 5.4C) was strongly down-regulated in the $CD44^{+}/CD24^{-}$ Hs578-T cells exposed to PerS H, 2,6 deS-NS H or PMH (fold change, -1.66 ± 0.21, -1.52 ± 0.12, -1.06 ± 0.07 respectively, [mean ± SD] ($P<0.001$), and was found to be up-regulated in cells treated with PMHS (fold 1.57 ± 0.19 [mean ± SD]) ($P<0.01$). In contrast, the $CD44^{+}/CD24^{-}$ cells sorted from the MDA-MB-231 line showed significant up-regulation in cells treated with 2,6 deS-NS H or PMHS compared to control (fold 1.98 ± 0.15 and 2.51 ± 0.33 respectively, [mean ± SD], $P<0.01$, $P<0.001$). Cells treated with PerS H and PMHS did not significantly change in expression of Ang-1 (1.22 ± 0.16, 1.24 ± 0.31 respectively) (Figure 5.4C).

Ang-2 expression was found to be downregulated in the $CD44^{+}/CD24^{-}$ sub-population isolated from MDA-MB-231 and Hs578-T treated with PerS H, or 2,6 deS-NS H (MDA-MB-231 fold changes: -1.01 ± 0.13, -1.09 ± 0.07 respectively, [mean ± SD], $P<0.001$; and Hs578-T fold changes: 1.45 ± 0.22 and 1.09 ± 0.15 respectively [mean ± SD], $P<0.001$). In contrast both cell lines treated with PMH or PMHS expressed higher levels of Ang-2 compared to untreated controls (MDA-MB-231 expression, 1.82 ± 0.07 and 3.31 ± 0.28, respectively, [mean ± SD], $P<0.001$; and Hs578-T expression, 2.31 ± 0.37 and 3.22 ± 0.17 respectively, [mean ± SD], $P<0.001$) (Figure 5.4D).

The expression of CXCR4 mRNA was found to be strongly down-regulated in response to all analysed treatments, for both MDA-MB-231 and Hs578-T cells with approximately 1-1.5 fold decreases compared to untreated cells (Figure 5.4E; MDA-MB-231 treated with PerS H, 2,6 deS-NS H, PMH or PMHS, fold changes: -0.97 ± 0.17, -1.41 ± 0.21, -0.88 ± 0.21, -0.95 ± 0.22 respectively, [mean ± SD], $P<0.001$;

Hs578-T with same treatments, fold expression: -1.18 ± 0.19, -1.09 ± 0.19, -0.85 ± 0.17, -1.14 ± 0.14 respectively, [mean ± SD], P<0.001).

As for the Ang-1 and Ang-2 expression results (Figure 5.4C, D), the expression levels of IL-8 (Figure 5.4F) displayed significant differences amongst the different treatments evaluated. As shown in Figure 5.4F, the modified heparins PerS H and 2,6 deS-NS H significantly reduced the expression of IL-8 in $CD44^+/CD24^-$ cells isolated from MDA-MB-231 cells (fold change -0.35 ± 0.13 and 0.98 ± 0.16 respectively, mean ± SD) and Hs578-T cells (fold change: -1.1 ± 0.14 and -1.01 ± 0.18 respectively, mean ± SD; P<0.001)). PMH reduced the expression of IL-8 in $CD44^+/CD24^-$ cells from Hs578-T (fold change -0.66 ± 0.22 [mean ± SD]; P<0.001) while MDA-MB-231 cells showed no significant change in expression of IL-8 (expression 1.17 ± 0.12 [mean ± SD]) compared to controls. PMHS significantly increased the expression of IL-8 in both cell lines compared to untreated controls (expression 1.27 ± 0.01 and 1.32 ± 0.15 respectively, [mean ± SD]) (P<0.05).

5.6 HS, heparin and modified heparins differentially effect FGF2 activation of ERK1/2 in MDA-MB-231 and Hs578-T BCSCs

Given that ERK/MAPK is an important pathway that can be activated by FGF2 in some cell types, the effects of HS/heparin/modified heparins on FGF2 mediated ERK1/2 expression in $CD44^+/CD24^-$ MDA-MB-231 or Hs578-T cells was analyzed by Western blot. Cells were starved for 6 hrs, then treated with or without 20 ng/ml FGF2 combined with either 10 ng/ml PerS H, 2,6 deS-NS H, PMH or PMHS for 15 and 60 min. Figure 5.5A shows representative results from stimulated $CD44^+/CD24^-$ sub-population from MDA-MB-231 cells, and Figures 5.5B and C represent the quantitated levels of FGF2-activated p-ERK1/2 and t-ERK1/2 to α-tubulin ratios under the various HS and chemically modified heparin treatments. Figure 5.5D represents the quantitated level of p-ERK1/2 to t-ERK1/2 ratio.

When cells were stimulated with FGF2, a shift in the activation pattern was observed. After FGF2 stimulation, levels of phosphorylated ERK1/2 were significantly increased in FGF2 stimulated $CD44^+/CD24^-$ cells compared to unstimulated cells (P<0.001) (Figure 5.5A). HS/heparin and chemically modified heparin induced a significant decrease in ERK1/2 phosphorylation compared to

control (FGF2 alone) cells ($P<0.01$, $P<0.001$) at all time points, in some cases back to the control (no FGF2) level. Some variations in the ratio of t-ERK1/2 to α-tubulin in $CD44^+/CD24^-$ cells was noted; for example 2,6 deS-NS H significantly lower levels than cells stimulated with FGF2 alone at 15 and 60 min ($P<0.05$, $P<0.001$) (Figure 5.5C). A small increase of t-ERK1/2 was noted in cells treated with PerS H, PMHS and PMH at 15 min ($P<0.05$), whereas, no significant changes were detected in cells treated with the same compounds at 60 min compared to untreated stimulated cells with FGF2 (Figure 5.5C). Figure 5.15D shows the ratios of p-ERK1/2 to t-ERK1/2 expression levels; although the ratios vary due to altered t-ERK1/2 levels, in most cases the compounds caused a reduction in this ratio compared to FGF2 alone, with the notable exception of 2,6 deS-NS H.

Similar experiments were carried out in $CD44^+/CD24^-$ cells isolated from the Hs578-T line. Figure 5.6A,B shows that p-ERK1/2 levels are elevated in response to stimulation with FGF2 ($P<0.01$). Once again, p-ERK levels were generally lowered significantly by treatment with the compounds ($P<0.05$, $P<0.01$, $P<0.001$) (Figure 5.6B). When cells were stimulated with FGF2, no significant change in the t-ERK activation pattern was observed. After FGF2 stimulation, a significant reduction of t-ERK1/2 was noted in cells treated with 2,6 deS-NS H, PMHS and PMH at 15 min ($P<0.05$, $P<0.01$, $P<0.001$), whereas, no significant changes were detected in cells treated with the same compounds at 60 min compared to untreated stimulated cells with FGF2 (Figure 5.6C) After FGF2 stimulation, the compounds induced significant reductions in p-ERK/t-ERK ratios compared to FGF2 alone at both time points, except PerS H, which only caused a reduction at 60 min. However, there was an anomaly since FGF2 treatment unexpectedly induced a reduction in the p-ERK/t-ERK ratio. In general there may be a problem with measurement of t-ERK in these experiments, and measurement of p-ERK alone may be the best guide to effects of the compounds on ERK phosphorylation. Nevertheless, overall the data supported the view that the compounds can act to attenuate FGF2 signals transduced via the MAPK pathway in BCCs, and this signaling pathway is thus implicated at least in part as one of the mechanisms by which they influence BCSC phenotype.

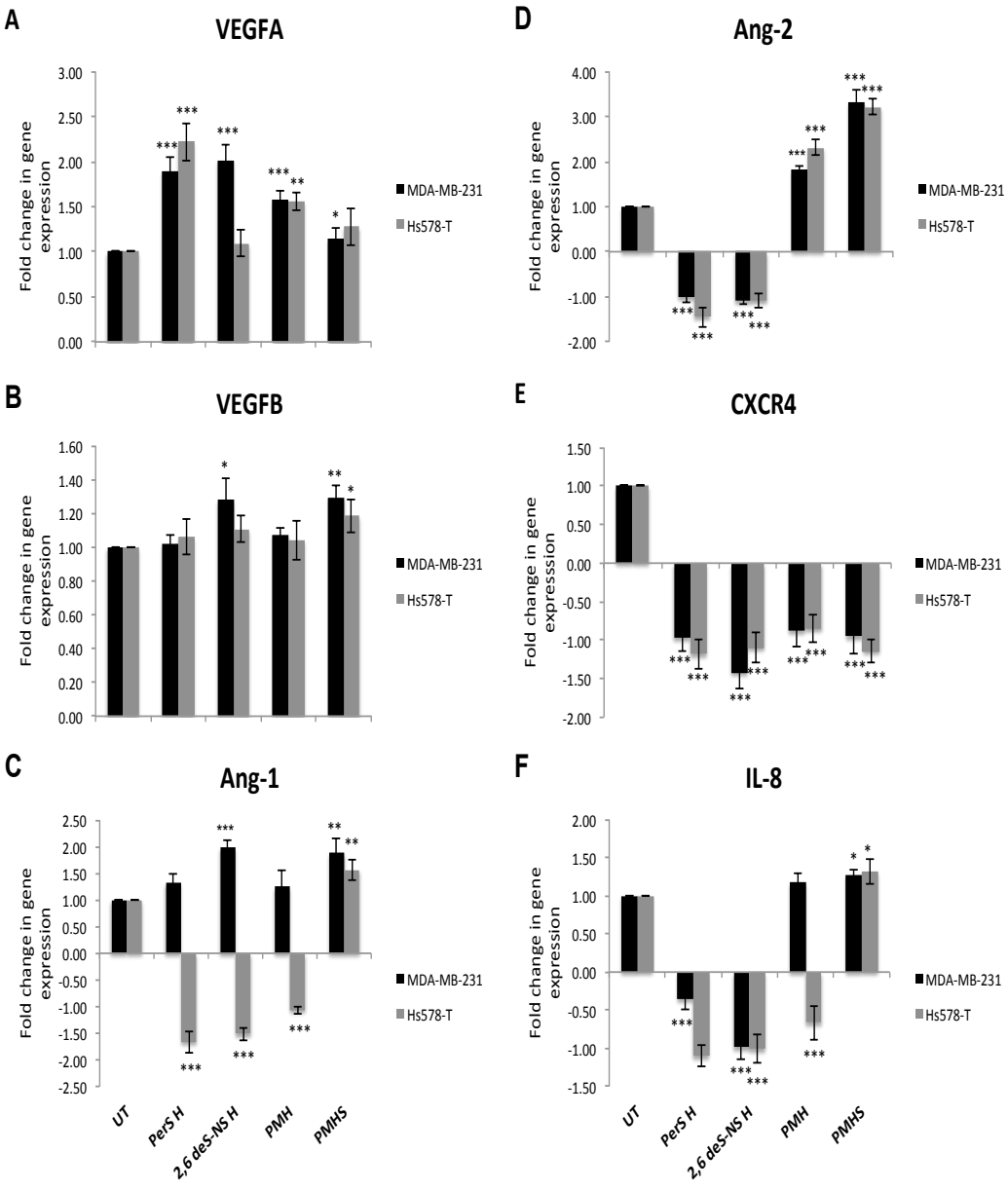

Figure 5.4 Effects of HS/heparin and modified heparins on the expression of angiogenic markers in BCCs. $CD44^{+}/CD24^{-}$ sub-population cells isolated from BCC line MDA-MB-231 and Hs578-T were treated with 10 ng/ml of PerS H, 2,6 deS-NS H, PMH or PMHS for 48 hrs. mRNA was extracted and subjected to qRT-PCR analysis to ascertain levels of (A) VEGFA, (B) VEGFB, (C) Ang-1, (D) Ang-2, (E) CXCR4 and (F) IL-8 mRNA expression levels. Expression values were normalised to GAPDH. Error bars=SD (n=2) from two independent experiments. *P<0.05, **P<0.01, ***P<0.001.

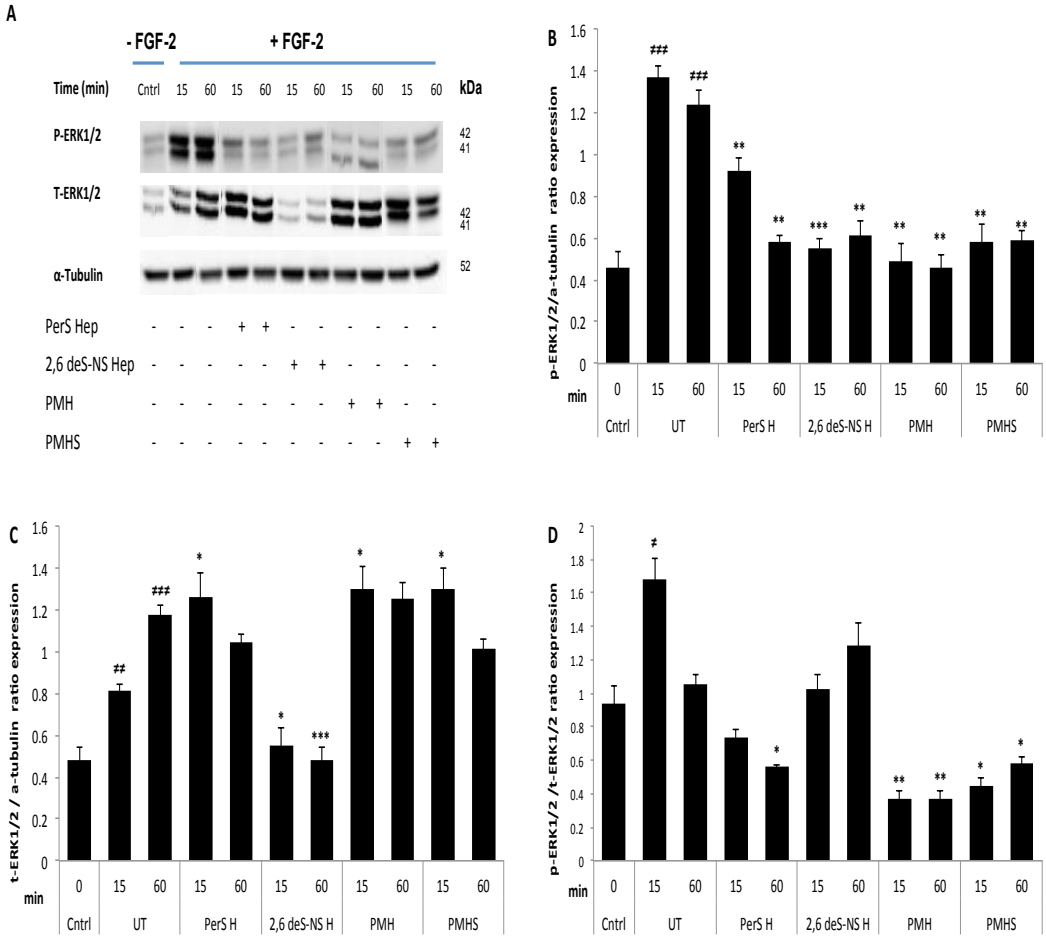

Figure 5.5 Effects of heparins on FGF2-stimulated ERK1/2 activation in BCSCs from MDA-MB-231. The $CD44^{+}/CD24^{-}$ sub-populations isolated from MDA-MB-231 BCCs were treated with or without FGF2 (20 ng/ml) in the presence or absence of 10 ng/ml PerS H, 2,6 deS-NS H, PMH or PMHS for 15 or 60 min. Western blots from cell protein extracts were probed with anti-phospho and anti-total ERK1/2 antibodies. The blots were scanned using and quantified using ImageStudioLite software. ERK1/2 activation is represented by the amount of ERK1/2 phosphorylation normalized to the total amount of ERK1/2. (A) Representative western blot analysis showing effects of various compounds on FGF2-activation of ERK1/2. (B) Densitometric measurements converted to ratios of p-ERK1/2 to α-tubulin. (C) Densitometric measurements converted to ratios of t-ERK1/2 to α-tubulin. (D) Densitometric measurements converted to ratios of p-ERK1/2 to t-ERK1/2. Values are presented as the means ± SD of two independent experiments in duplicate expressed as ratio of the values measured in MDA-MB-231 cells (##P<0.01, versus to untreated unstimulated cells), (*P<0.05, **P<0.01, ***P<0.001 versus to untreated stimulated cells).

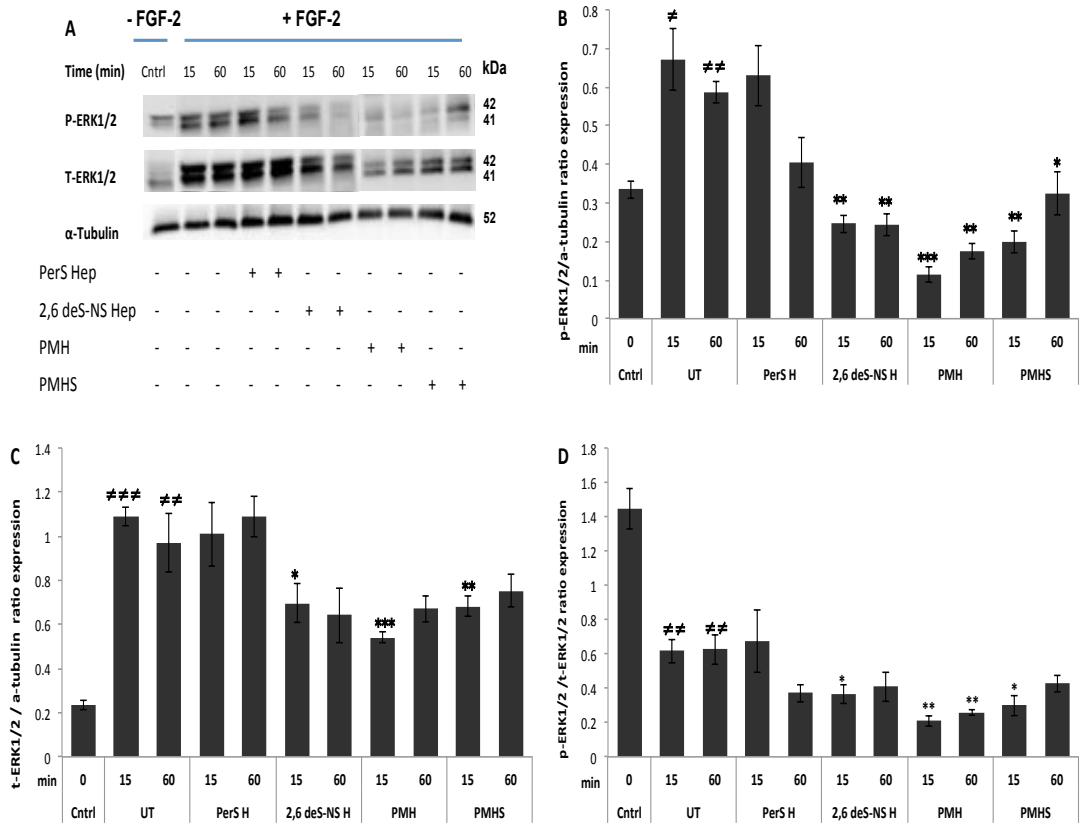

Figure 5.6 Effects of heparins on FGF2-stimulated ERK1/2 activation in BCSCs from Hs578-T cells. The $CD44^{+}/CD24^{-}$ sub-populations isolated from Hs578-T BCCs were treated with or without FGF2 (20 ng/ml) in the presence or absence of 10 ng/ml PerS H, 2,6 deS-NS H, PMH or PMHS for 15 or 60 min. Western blots from cell protein extracts were probed with anti-phospho and anti-total ERK1/2 antibodies. The blots were scanned using and quantified using ImageStudioLite software. ERK1/2 activation is represented by the amount of ERK1/2 phosphorylation normalized to the total amount of ERK1/2. (A) Representative western blot analysis showing effects of various compounds on FGF2-activation of ERK1/2. (B) Densitometric measurements converted to ratios of p-ERK1/2 to α-tubulin. (C) Densitometric measurements converted to ratios of t-ERK1/2 to α-tubulin. (D) Densitometric measurements converted to ratios of p-ERK1/2 to total ERK1/2. Values are presented as the means ± SD of two independent experiments in duplicate expressed as ratio of the values measured in MDA-MB-231 cells (##P<0.01, versus to untreated unstimulated cells), (*P<0.05, **P<0.01, ***P<0.001 versus to untreated stimulated cells).

5.7 HS and modified heparins induce downregulation of components of the IL-6 signaling pathway in BCSs

To investigate whether HS and modified heparins might affect expression of IL-6 and the STAT3 signaling pathway in MDA-MB-231 and Hs578-T BCCs qRT-PCR (Figure 5.7) and western blotting (Figure 5.8;9) were used respectively. The $CD44^{+}/CD24^{-}$ sub-population isolated from MDA-MB-231 and Hs578-T human BCCs was pre-treated with 10 ng/ml PerS H, 2,6 deS-NS H, PMH or PMHS for 48 hrs and mRNA extracted. Compared to untreated controls the expression level of IL-6 mRNA was significantly suppressed by treatment with 2,6 deS-NS H or PMHS in both cell lines. PMH treatment differentially affected on IL-6 expression levels in MDA-MB-231 and Hs578-T cells. $CD44^{+}/CD24^{-}$ of MDA-MB-231 significantly reduced the expression of IL-6 whereas significant increased was detected in Hs578-T cells treated with PMH compared to untreated control cells (Figure 5.7).

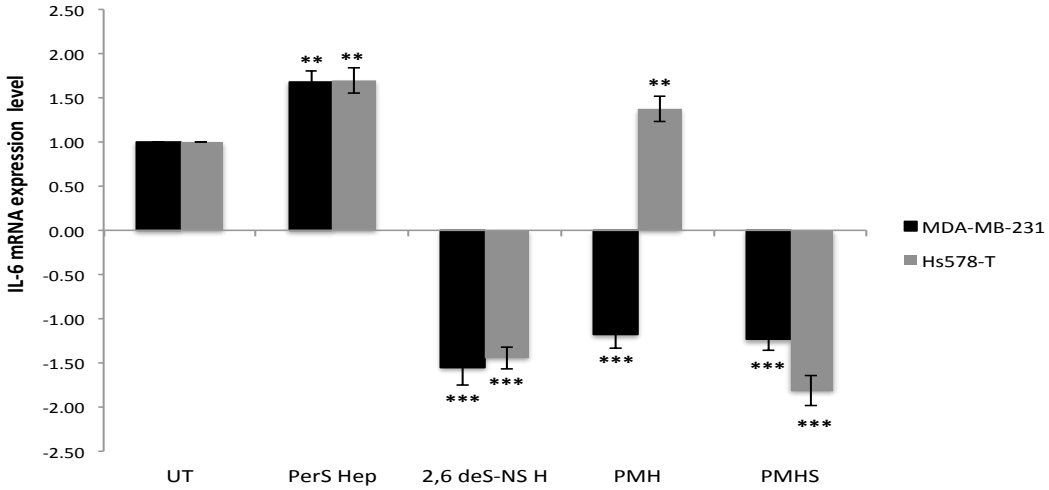

Figure 5.7 qRT–PCR analysis of IL-6 expression in BCSCs subjected to treatment with HS or chemically modified heparins. Total RNA was extracted from CD44+/CD24- cells from MDA-MB-231 and Hs578-T BCSCs after treatment with 10 ng/ml PerS H, 2,6 deS-NS H, PMH or PMHS for 48 hrs. Expression levels of IL-6 mRNA were measured using RT–PCR (relative to untreated control). Comparisons between groups were analyzed using t-test analysis. **P<0.01 and ***P<0.001 denote significant differences compared with the untreated control. Error bars represent mean ± SD; n= 2 independent preparations, each assay performed in duplicate. The relative expression levels of IL-6 mRNA were normalized to the internal reference 18S rRNA and untreated control cells.

5.8 HS, heparin and modified heparins differentially affect IL-6 activation of STAT3 in MDA-MB-231 and Hs578-T BCSCs

IL-6 is known to signal via activation of transcription factor including STAT3. The functional impact of HS and modified heparins on STAT3 activation status was thus investigated by western blotting using phosphorylation-specific antibodies (Figure 5.8A). $CD44^+/CD24^-$ MDA-MB-231 and Hs578-T BCCs were starved for 6 hrs, and then treated with 10 ng/ml IL-6 in the absence or presence of 10 ng/ml PerS H, 2,6 deS-NS H, PMH or PMHS for different time intervals (15, 30 and 60 min). Levels of phosphorylated and total STAT3 were assessed by quantitating the densities of the respective immunoreactive bands. Results showed that Tyr705 in STAT3 is phosphorylated after cell stimulation with IL-6 at all time points compared to unstimulated cells ($P<0.001$) (Figure 5.8A). 2,6 deS-NS H, PMH or PMHS treatments significantly decreased STAT3 phosphorylation after stimulation with IL-6 at all time points ($P<0.001$). No significant effect on STAT3 phosphorylation was observed in cells treated with PerS H at 15 and 30 min, though a significant decrease was observed at 60 min for this compound ($P<0.01$) (Figure 5.8A). The expression of t-STAT3 level was not significantly affected by IL-6 treatment or additional treatment with HS or chemically modified heparins, except for a minor decrease with 2,6 deS-NH or PMHS treatment at 15 and 60 min respectively ($P<0.01$) (Figure 5.8B).

Representative data from Hs578-T cells is shown in Figure 5.9. IL-6 triggers a rapid increase in phosphorylation of Tyr705 on STAT3 compared to unstimulated cells ($P<0.001$). $CD44^+/CD24^-$ Hs578-T stimulated cells treated with HS/heparin and chemically modified heparins displayed significantly decreased STAT3 phosphorylation levels and this response was observed at all time points (with the exception of PerS H at 15 and 30 min) ($P<0.01$, $P<0.001$), compared to untreated stimulated cells (Figure 5.9B). The expression of t-STAT3 was not altered in cells treated with HS/heparin and chemically modified heparins at all time points.

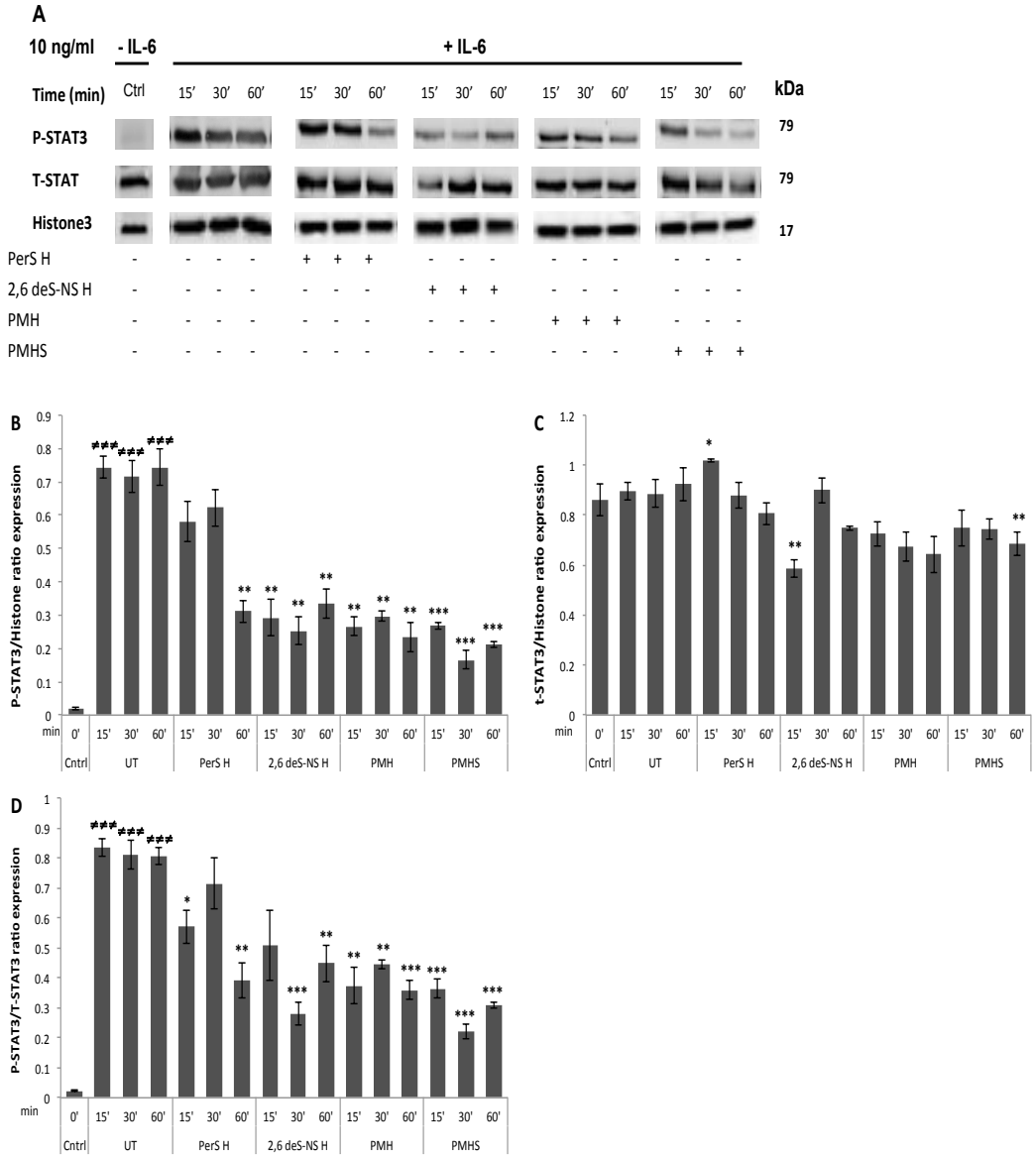

Figure 5.8 Effects of HS/heparins on IL-6-stimulated STAT3 activation in BCSCs from MDA-MB-231 cells. The $CD44^{+}/CD24^{-}$ sub-populations isolated from MDA-MB-231 BCCs were treated with or without IL-6 (10 ng/ml) in the presence or absence of 10 ng/ml PerS H, 2,6 deS-NS H, PMH or PMHS for 15, 30 or 60 min. Western blots from cell protein extracts were probed with anti-phospho and anti-total STAT3 antibodies. The blots were scanned using and quantified using ImageStudioLite software. STAT3 activation is represented by the amount of STAT3 phosphorylation normalized to the total amount of STAT3. (A) Representative western blot analysis showing effects of various compounds on IL-6-activation of STAT3. (B) Densitometric measurements converted to ratios of p-STAT3 to histone 3. (C) Densitometric measurements converted to ratios of t-STAT3 to histone 3. (D) Densitometric measurements converted to ratios of p-STAT3 to t-STAT3. Values are presented as the means ± SD of two independent experiments in duplicate expressed as ratio of the values measured in MDA-MB-231 cells (###P<0.001, versus to untreated unstimulated cells), (*P<0.05, **P<0.01, ***P<0.001 versus to untreated stimulated cells).

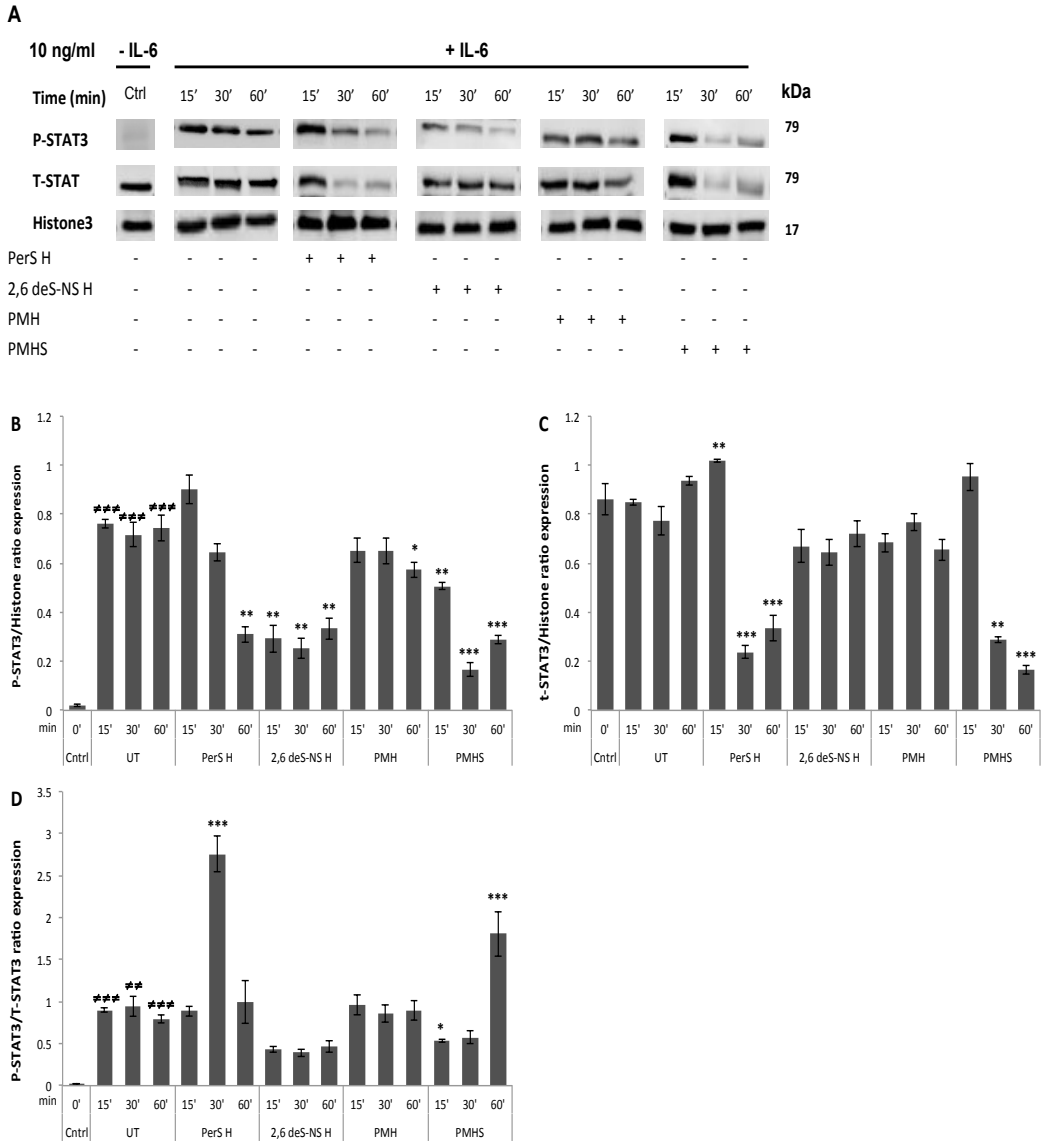

Figure 5.9 Effects of HS/heparins on IL-6-stimulated STAT3 activation in BCSCs from Hs578-T cells. The $CD44^{+}/CD24^{-}$ sub-populations isolated from Hs578-T BCCs were treated with or without IL-6 (10 ng/ml) in the presence or absence of 10 ng/ml PerS H, 2,6 deS-NS H, PMH or PMHS for 15, 30 or 60 min. Western blots from cell protein extracts were probed with anti-phospho and anti-total STAT3 antibodies. The blots were scanned using and quantified using ImageStudioLite software. STAT3 activation is represented by the amount of STAT3 phosphorylation normalized to the total amount of STAT3. (A) Representative western blot analysis showing effects of various compounds on IL-6-activation of STAT3. (B) Densitometric measurements converted to ratios of p-STAT3 to histone 3. (C) Densitometric measurements converted to ratios of t-STAT3 to histone 3. (D) Densitometric measurements converted to ratios of p-STAT3 to t-STAT3. Values are presented as the means ± SD of two independent experiments in duplicate expressed as ratio of the values measured in MDA-MB-231 cells (##P<0.01, ###P<0.001, versus to untreated unstimulated cells), (*P<0.05, **P<0.01, ***P<0.001 versus to untreated stimulated cells).

5.9 Effects of HS and chemically modified heparin mechanism on cell signaling in $CD44^+/CD24^-$ sub-populations from MDA-MB-231 and Hs578-T BCC lines.

One hypothesis for the mechanisms underlying the effects of treatment BCSCs with HS/heparin and chemically modified heparins is that they cause activation and/or inactivation of signalling pathways. To investigate this hypothesis, protein extracts were examined using a PathScan® Intracellular Signaling Array (a slide-based antibody array that uses sandwich immunoassay to detect phosphorylation status of 18 well-characterized signaling molecules). Attention was focused on the activation and inhibition of multiple signaling pathways in the $CD44^+/CD24^-$ sub-populations from MDA-MB-231 and Hs578-T cell lines. $CD44^+/CD24^-$ sub-population sorted from MDA-MB-231 and Hs578-Tcells were treated with 10 ng/ml of various compounds (PerS H, NAc H, 2 deS-NS H, 6 deS-NS H, 2,6 deS-NS H, PMHS and PMH) and incubated for 48 hrs (Figure 5.10). Complete PathScan intracellular signalling datasets are provided in Appendix 4.1 and 4.2.

As shown in a quantitative graphical summary (Figure 5.11), significant decreases in phosphorylation of multiple signaling molecules, including S6 Ribosomal, mTOR and PRAS40 in MDA-MB-231 and Hs578-T cells, were detected in response to HS and chemically modified heparins compared to untreated control cells ($P<0.001$). Interestingly, although 10 ng/ml of compounds, including PerS H, NAc H, 2 deS-NS H, 6 deS-NS H and 2,6 deS-NS H, did not affect the phosphorylation level of ERK1/2, there was an 86% increase in ERK1/2 phosphorylation with 10 ng/ml PMHS or PM heparin treatment, for both MDA-MB-231 and Hs578-Tcells ($P<0.001$), while NAc H, 2,6 deS-NS H, PMHS and PMH induced a significant expression compared to untreated cells; this suggests the possibility that the growth-inhibitory and apoptotic mechanisms of PMHS and PMH may be mediated at least in part through the activation of ERK1/2. In addition, for MDA-MB-231 cells, some of the modified heparins (PerS H, NAc H, 2 deS-NS H and 6 deS-NS H) broadly induced AMPKα activation, while all except 2 deS-NS H caused a significant decrease in PRAS40 phosphorylation ($P<0.001$) (Figure 5.11).

In contrast, for Hs578-T cells no effects on AMPKα or PRAS40 were noted, whilst NAc H, PMHS and PMH induced activation of STAT3 (which was unaffected in MDA-MB-231 cells) (Figure 5.11). ERK1/2 activation also was noted in $CD44^{+}/CD24^{-}$ cells, treated with NAc H, 2,6 deS-NS H, PMHS and PMH ($P<0.001$) (Figure 5.11).

Strong inhibition of phosphorylation of two tested signaling molecules, S6 ribosomal protein and mTOR, were also noted for Hs578-T cells treated with PerS H, NAc H or 2 deS-NS H (Figure 5.11).

Overall, the compounds induced changes in multiple signaling pathways, with both activation and inhibition noted; furthermore, interesting cell type differences were noted in the cell responses to the different compounds.

5.10 Effects of treatments with HS/modified heparins on FGF2 stimulation of the $CD44^{+}/CD24^{-}$ sub-populations from MDA-MB-231 and Hs578-T BCCs

Since changes in ERK1/2 phosphorylation were noted in response to some of the compounds (section 5.6), and FGF2 is a HS-dependent growth factor known to activate this pathway, FGF2 stimulation alone or in combination with HS/chemically modified heparins in BCSCs was measured using the PathScan intracellular signaling array kit (Figure 5.12). The corresponding complete PathScan intracellular signaling datasets are provided in Appendix 4.3 and 4.4.

As shown quantitatively in Figure 5.13, there were significant increases in phosphorylation of ERK1/2 (as expected) and also STAT3 ($P<0.001$) in both cell types; in contrast, mTOR activation was inhibited by FGF2. Many of the pathways were not significantly affected by FGF2 treatment or additional treatment with HS or chemically modified heparins ($P<0.001$) (Figure 5.13 and Appendix 4.3 and 4.4). Although PMHS and PMH did not affect the phosphorylation of ERK1/2 after stimulation with FGF2, there was a 25 to 50% decrease in ERK1/2 phosphorylation with 10 ng/ml of PerS H, NAc H, 2, deS-NS H and 2,6 deS-NS H compared to FGF2-stimulated MDA-MB-231 CSCs untreated cells. This was not observed for Hs578-T CSCs, but these demonstrated inhibition of p-ERK1/2 upon treatment with 2, deS-NS H, PMHS or PMH (Figure 5.13). STAT3 signaling showed a significant

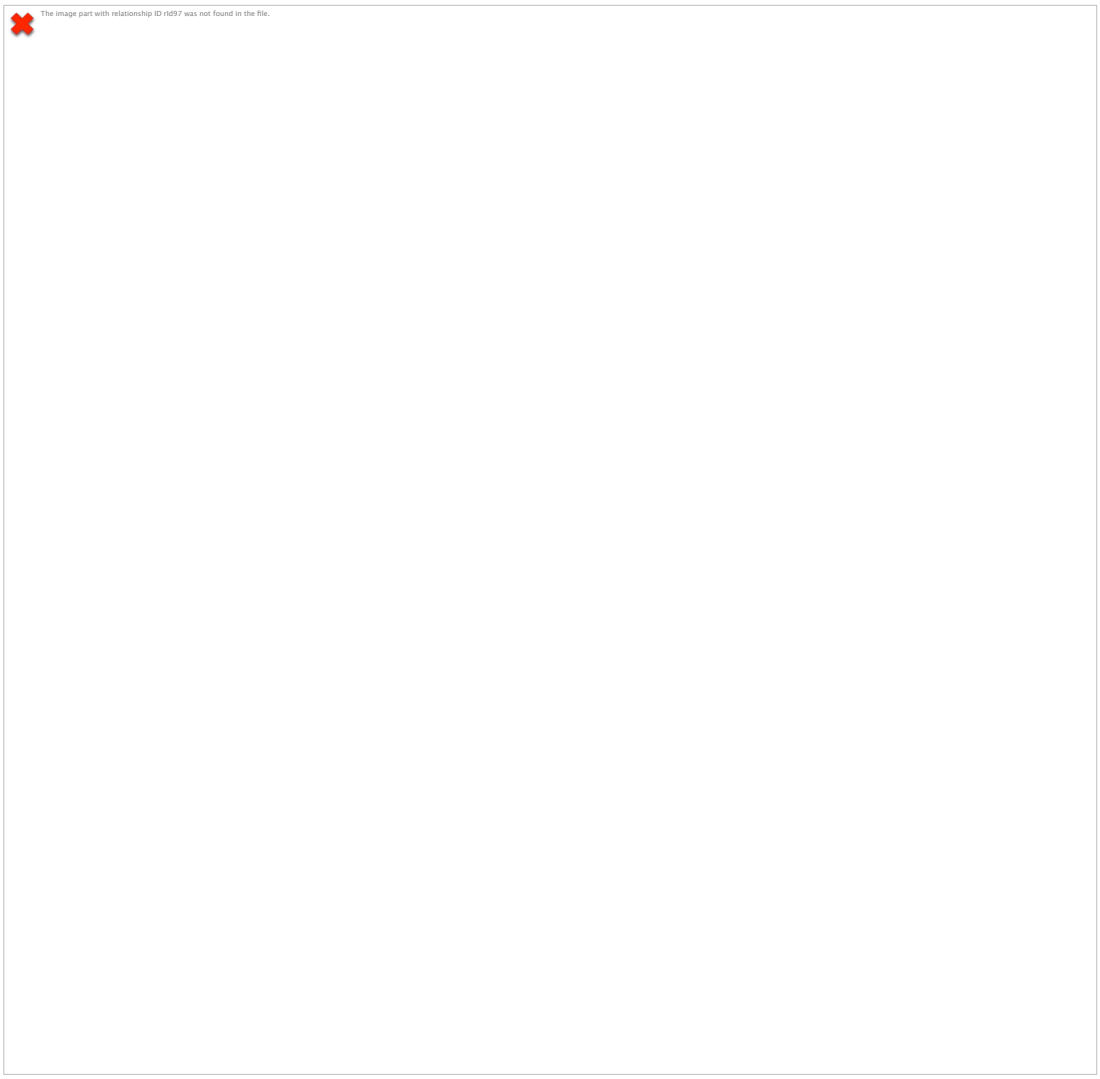

Figure 5.10 PathScan intracellular signalling array analysis. The $CD44^{+}/CD24^{-}$ sub-population sorted from MDA-MB-231 and Hs578-T BCCs were treated (or not) with 10 ng/ml of HS compounds (PerS H, NAc H, 2 deS-NS H, 6 deS-NS H, 2,6 deS-NS H, PMHS and PMH) for 48 hrs. Following treatments, cell extracts were prepared and analyzed using the PathScan® intracellular signalling array kit, according to the manufacturer's protocol. The slide was incubated with Lumi-GLO/peroxide reagent and exposed in an ImageQuant™ LAS 4000 Biomolecular Imager (with exposure for a length of time dependent on the signal intensity). The result is representative of two experiments, each run in duplicate.

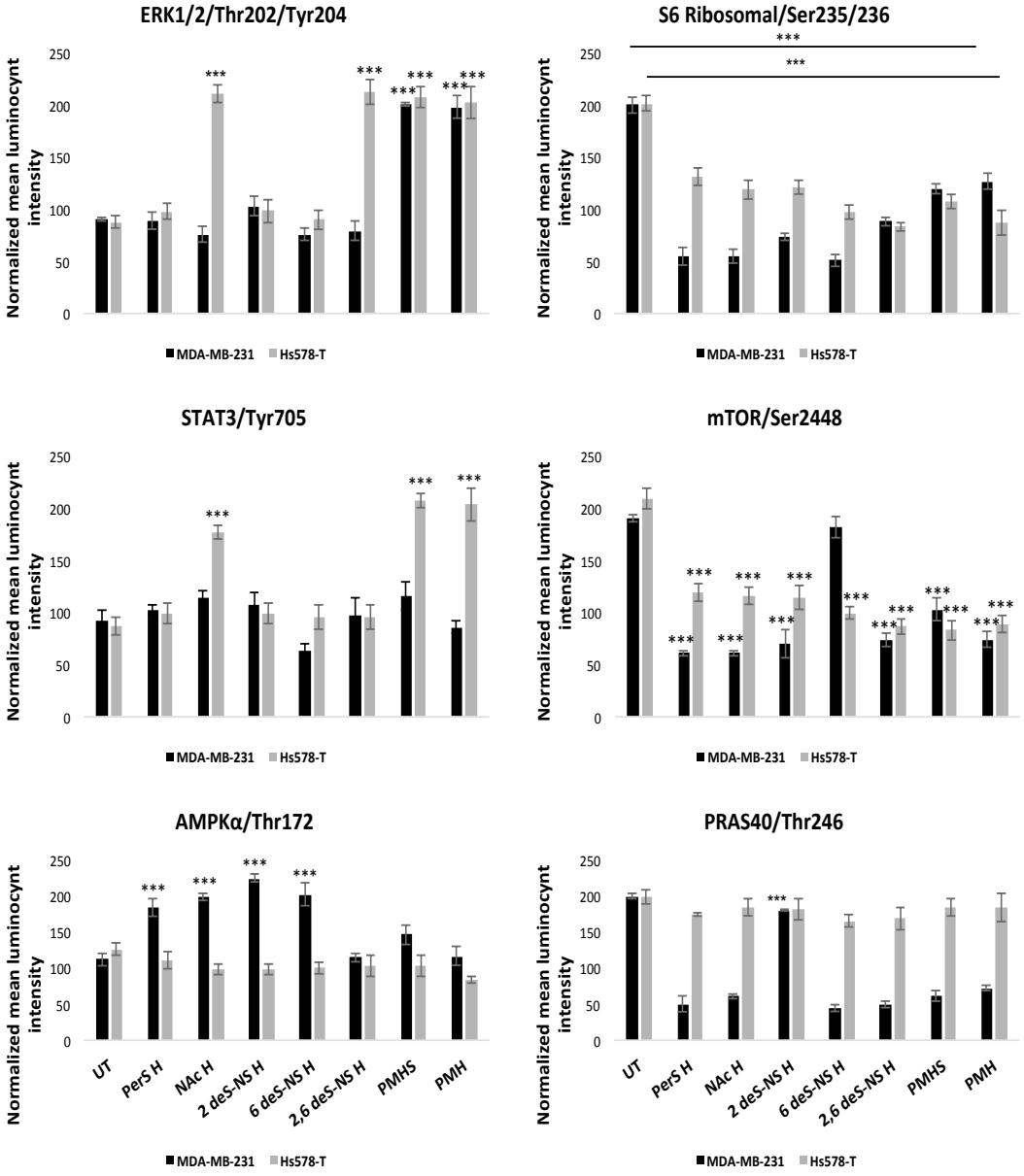

Figure 5.11 Quantitative analysis of intracellular signalling array data from HS and chemically modified heparin treatment of CD44^{+}/CD24^{-} sorted cells from MDA-MB-231 and Hs578-T BCCs. Cells were treated, and cell extracts prepared and analyzed using the PathScan® intracellular signalling array kit as described in Figure 5.10. The results are representative of two experiments, each run in duplicate. Normalized mean luminescence intensity ± SD, n=2. ***P<0.001 relative to untreated cells.

decrease of phosphorylation level when MDA-MB-231 CSCs were treated with NAc H, 2 deS-NS H, 2,6 deS-NS H or PMHS compared to untreated FGF2-stimulated

cells (P<0.001). 2 deS-NS H, PMHS and PMH induced a reduction in activation of STAT3 in Hs578T CSCs. Stimulation of MDA-MB-231 CSCs with FGF2 resulted in strongly decreased Bad and p38 signaling (P<0.001), but no significant effects were observed in these pathways with additional treatment with HS or chemically modified heparins. Stimulation of Hs578-T CSCs with FGF2 was not detected compared to untreated cells, but significant reductions were observed in Bad pathway with additional treatment with HS or chemically modified heparins (P<0.001).

AMPKα phosphorylation in MDA-MB-231 CSCs was not increased by FGF2 stimulation, but was decreased by treatments with 2,6 deS-NS H, PMHS or PMH (P<0.05, P<0.001), whereas Hs578T CSCs were largely unaffected.

Akt/Thr473, S6 ribosomal protein, mTOR and p53 were all significantly activated in untreated Hs578-T CSCs, whereas significant reductions in all their phosphorylation levels were noted in FGF2 stimulated cells (p<0.001); however, the additional treatment with compounds did not significantly alter the levels of these pathways. Although no marked difference of Bad activation was evident in Hs578T CSCs stimulated with FGF2 relative to the unstimulated cells, a significant decreased of Bad phosphorylation levels were noted with additional treatment with the compounds (p<0.001). Analysis of the PathScan results indicated that there was no alteration in the phosphorylation of the other 12 signalling molecules in Hs578-T CSCs under the experimental conditions tested (Figure 5.13).

Overall the results suggest selectivity in the action of the various compounds for targets in CSCs, with effects on a number of signaling pathways (both upregulation and downregulation). The most notable effects were on ERK1/2, STAT3 and mTOR pathways, making them prime candidates for mediating the growth-inhibitory and apoptotic mechanisms observed in CSCs upon treatment with the heparin compounds.

Figure 5.12 PathScan® Intracellular Array analysis. $CD44^{+}/CD24^{-}$ sub-population sorted from MDA-MB-231 and Hs578-T BCCs were stimulated with 20 ng/ml FGF2 and treated (or not) with 10 ng/ml of HS compounds (PerS H, NAc H, 2 deS-NS H, 6 deS-NS H, 2,6 deS-NS H, PMHS and PMH) for 60 min. Following treatments, cell extracts were prepared and analyzed using the PathScan® intracellular signalling array kit, according to the manufacturer's protocol. The slide was incubated with Lumi-GLO/peroxide reagent and exposed in an ImageQuant™ LAS 4000 Biomolecular Imager (with exposure for a length of time dependent on the signal intensity). The result is representative of two experiments, each run in duplicate.

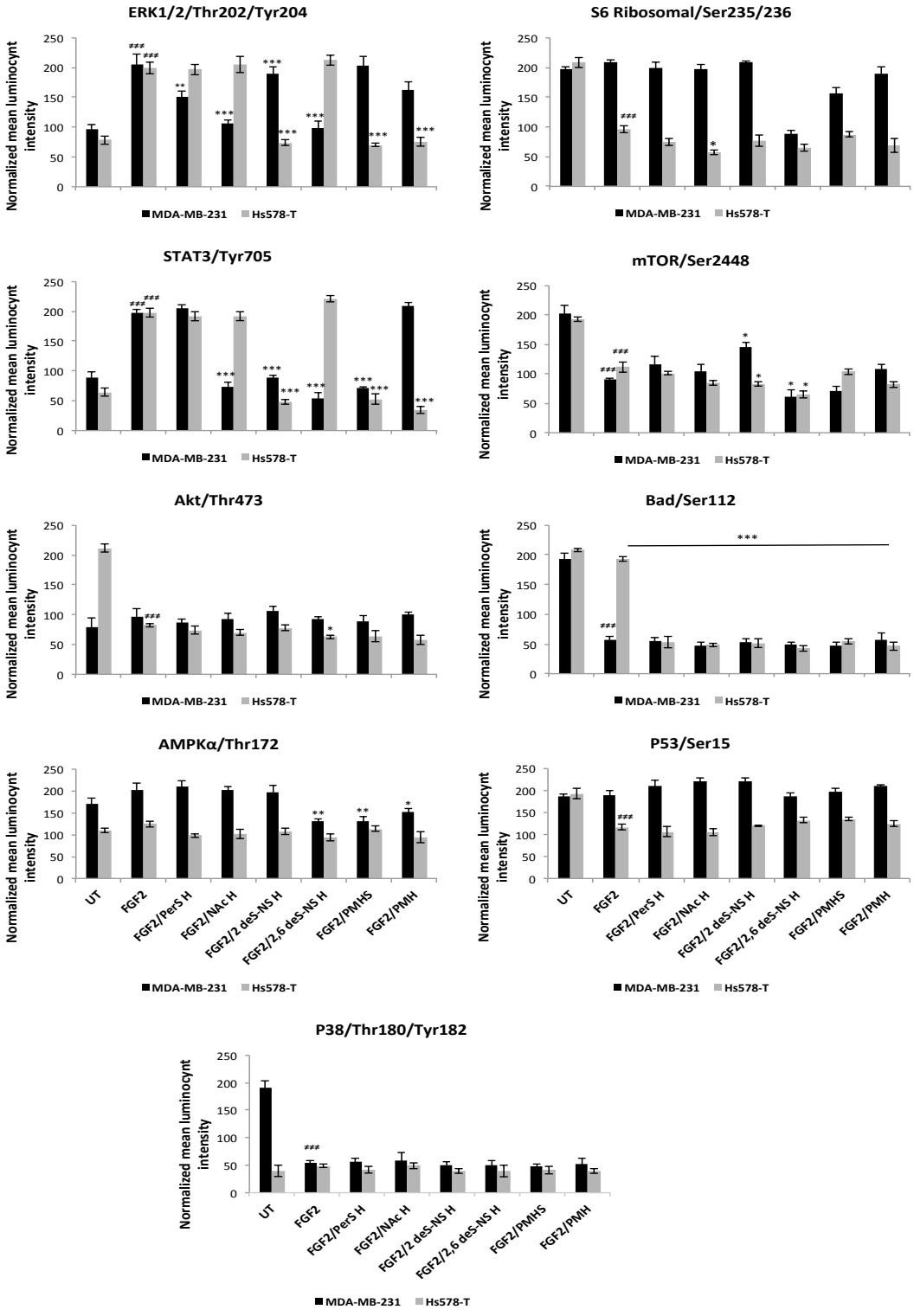

Figure 5.13 Pathscan quantitative analysis of CD44^{+}/CD24^{-} sorted cells from MDA-MB-231 and Hs578-T BCCs with FGF2 stimulation of signaling molecules. Cells were stimulated with 20 ng/ml FGF2 and treated (or not) with 10 ng/ml of HS compounds (PerS H, NAc H, 2 deS-NS H, 6 deS-NS H, 2,6 deS-NS H, PMHS and PMH) for 60 min. cell extracts were prepared and analyzed using the PathScan® intracellular signalling array kit as described in Figure 5.12. The results are representative of two experiments, each run in duplicate. Normalized mean luminescence intensity ± SD, n=2. ###P<0.001 relative to untrteated cells. (*P<0.05, **P<0.01, ***P<0.001 versus to untreated stimulated cells).

5.11 Effects of HS/heparin and chemically modified heparins on specific genes involved in synthesis and editing of HSPGs in BCSCs

5.11.1 Effects of HS/heparin derivatives on the expression of genes encoding core proteins carrying HS chains

About 11 HSPG core proteins encoded genes were demonstrated in present study The most cell surface HSPGs gene families including syndecans and glypicans. These families comprise 4 syndecans (*SDC1-4*) and 6 glypicans (*GPC1-6*) respectively. The other remaining gene is an ECM HSPG, (*AGRN*) (Iozzo, 2001, Park et al., 2000).

MDA-MB-231 CSCs: For the agrin protein, PMHS and 2,6 deS-NS H significantly decreased agrin levels ($P<0.05$, $P<0.001$), while heparin significantly increased agrin levels in $CD44^{+}/CD24^{-}$ sorted cells from the MDA-MB-231 line (Figure 5.14; Table 5.1). Within the syndecan and glypican groups, a down regulation was observed in the transcript levels of $CD44^{+}/CD24^{-}$ cells treated with PMHS, however, SDC-2 and GPC-3 and 4 displayed up-regulation. 2,6 deS-NS H and heparin significantly increases the expression of SDC1-4 ($P<0.05$), wherase, 2,6 deS-NS H and heparin significantly decreased the expression of the GPC group; however, GPC-1 displayed up-regulation with both treatments (Figure 5.14; Table 5.1).

Hs578-T CSCs: No significant differences in the transcript levels of $CD44^{+}/CD24^{-}$ cells from Hs578-T treated with heparin and 2,6 deS-NS H were noted for agrin; however, a significant increase and decrease was shown in cells treated with PMHS and PMH, respectively ($P<0.05$) (Figure 5.15; Table 5.2). PMHS significantly increased the GPC group in $CD44^{+}/CD24^{-}$ cells; however only GPC-3 displayed a decrease in these cells. Within the SDC group, SDC-1 was not detected in cells treated with PMHS, whereas, SDC-2 and 4 showed a significant down-regulation and SDC-3 showed a significant up-regulation in cells treated with PMHS ($P<0.01$). For SDC-1 no significant differences in the transcript levels of $CD44^{+}/CD24^{-}$ cells could be detected. For heparin treatment, no significant changes were noted for SDC-2 and 4 compared to untreated cells and increases were noted for SDC-1 and 3 respectively. GPC-2 and 5 displayed a significant decrease, while GPC-1 and 6 displayed a significant increase in cells treated with heparin ($P<0.01$). GPC-6

showed no significant differences compared to untreated cells and GPC-3 and 4 were not detected at all in cells treated with heparin (Figure 5.15; Table 5.2).

HS chains are synthesized by biosynthetic enzymes in the Golgi apparatus (Presto et al., 2008). The present study examined the glycosyltransferases (GTs) encoding genes which are involved in HS chain polymerization, including EXTL1-3 (responsible for HS initiating and possessing the first GlcNAc residue), and EXT1 and 2 polymerase complex (responsible for chain extension). The transcript level of EXTs and EXTLs groups were significantly higher in $CD44^{+}/CD24^{-}$ sup-population of MDA-MB-231 treated with heparin and Hs578-T cells treated with PMHS (Figure 5.14; Table 5.1) and (Figure 5.15; Table 5.2). These gene groups did not show clear alteration patterns in $CD44^{+}/CD24^{-}$ sorted from MDA-MB-231 cells treated with PMHS and 2,6 deS-NS H; however, EXTL1 and 2 showed increased with 2,6 deS-NS H treatment, although its high expression did not allow for definitive conclusions to be drawn (Figure 5.14; Table 5.1). EXTL2 and 3 showed a decrease with PMHS ($P<0.05$, $P<0.001$). 2,6 deS-NS H and heparin showed an increased in EXTs and EXTLs groups, whereas heparin different effects of EXTs and EXTLs group in $CD44^{+}/CD24^{-}$ sup-population of Hs578-T cells (Figure 5.15; Table 5.2).

The above GT activities are involved in HS chain synthesis resulting in an unmodified HS chain (GlcA-GlcNAc repeating units). NDSTs clearly have a crucial role in the modification of HS chains by removing acetyl groups from GlcNAc residues and creating sulphation of the amino group. This is catalyzed by four different isoforms of N-deacetylase/N-sulfotransferases, (NDST1-4) (Esko and Lindahl, 2001, Lindahl et al., 1998). Transcripts of all these isoforms, NDST1-4 showed up regulation and down regulation in the $CD44^{+}/CD24^{-}$ sup-population of MDA-MB-231 treated with PMHS. The NDST group showed an increase in the transcript level in $CD44^{+}/CD24^{-}$ cells treated with 2,6 deS-NS H; however, NDST2 showed a decrease in the transcript levels, while a significant increase in NDST3 and 4 was noted (Figure 5.14; Table 5.1). When the analysis was conducted in the $CD44^{+}/CD24^{-}$ sub-population of Hs578-T cells, transcripts of all these isoforms, NDST1-4, were significantly increased in cells treated with PMHS ($P<0.01$, $P<0.001$); however, only NDST3 showed a decrease in cells treated with PMH. None of the NDSTs genes showed a significant change in their transcript levels in cells

treated with heparin or 2,6 deS-NS-H (Figure 5.15; Table 5.2).

In biosynthesis epimerization of GlcA is the next step, mediated by glucuronosyl C5-epimerase. The C5-GlcA epimerase enzyme (GLCE) catalyzes the conversion of GlcA into IdoA. The addition of 2-O-sulphation is at C2 to IdoA or GlcA residues by HS 2-O- sulphotransferase (HS2ST1), and the addition of 6-O-sulphation at the C6 position of GlcNAc and GlcNS residues is catalyzed by HS 6-O-sulphotransferase isoforms 1–3 (HS6ST1, HS6ST2 and HS6ST3) (Esko and Lindahl, 2001, Lindahl et al., 1998, Turnbull et al., 2001, Whitelock and Iozzo, 2005) After that, the modification step of HS chain involves the final addition of rare 3-*O*-sulphates at the C3 position of GlcNS residues. This step is catalyzed by HS 3-O-sulphotransferase isoforms 1–6 (HS3ST1, HS3ST2, HS3ST3A1, HS3ST3B1, HS3ST4, HS3ST5 and HS3ST6) (Turnbull et al., 2001, Whitelock and Iozzo, 2005). None of these enzymes showed statistically significant alterations in transcriptional level in $CD44^{+}/CD24^{-}$ sorted cells from MDA-MB-231 cells treated with 2,6 deS-NS H compared to untreated cells; however, adding 2,6 deS-NS H to the cells significantly increased the HS3ST3A1 expression level and significantly decreased the expression level of HS3ST3B1 ($P<0.01$, $P<0.001$). In addition, these enzymes showed a significant decrease with PMHS treatment and a significant increase with heparin treatment (Figure 5.14; Table 5.1). When the analysis was conducted in $CD44^{+}/CD24^{-}$ sorted cells from Hs578-T cells treated with heparin, no significant differences of transcript levels of these enzymes were detected. Adding PMHS to the cells significantly increased the expression of these enzymes; however only HS3ST2, HS3ST3A1, HS3ST4, HS3ST5 and HS6ST2 showed a significant decrease in cells treated with HS. Adding 2,6 deS-NS H to the cells significantly increased the expression of (HS2ST2, HS3ST2, HS2ST3A1, HS2ST3B1 and HS2ST4) enzymes; however only HS3ST2, HS3ST3A1, HS3ST4, HS3ST5 and HS6ST2 showed a significant decrease in cells treated with HS (Figure 5.15; Table 5.2).

The last step of HS chain modification during biosynthesis is carried out at the cell surface by two sulphatase enzymes (Sulf1 and Sulf2). Theses enzymes remove GlcN-6S from specific regions of HS chain (Taylor and Gallo, 2006). Interestingly, the transcript of Sulf1 in $CD44^{+}/CD24^{-}$ sorted cells from MDA-MB-231 cells was not significantly detected in cells treated with PMHS, PMH and 2,6 deS-NS H. In

addition the Sulf2 enzyme did not show clear alteration patterns in HS/heparin and 2,6 deS-NS H treated cells (Figure 5.14; Table 5.1). Sulf1 enzyme was not detected in $CD44^{+}/CD24^{-}$ sorted cells from the Hs578-T line treated with heparin or 2,6 deS-NS H. PMHS increased the transcript level of Sulf2 enzyme in $CD44^{+}/CD24^{-}$ sorted cells from the Hs578-T line. Adding heparin or 2,6 deS-NS H to the cells resulted in a decreased transcript level of the Sulf2 enzyme (Figure 5.15; Table 5.2).

5.11.2 Effects of HS/heparin and chemically modified heparins on the expression of heparanases

Heparanase (HPSE) is an endo-β-D-glucuronidase enzyme that degrades polymeric HS into shorter length HS oligosaccharides, generating biologically active molecules. This enzyme, along with Sulf1 and Sulf2 were analyzed in relation to addition of HS/ heparin and chemically modified heparins to BCSCs. Heparanase 2 (HPSE2) is another related molecule which lacks HS-degrading activity, but it is still able to interact with HS with high affinity (Arvatz et al., 2011). Performing Taqman assays we failed to detect significant changes in *HPSE2* transcript levels either in $CD44^{+}/CD24^{-}$ of MDA-MB-231 cells with PMHS, heparin or 2,6 deS-NS H. The transcript level of HPSE1 in MDA-MB-231 cell line showed a significant increase with PMHS and a significant decrease with heparin. No significant changes were detected with 2,6 deS-NS H (Figure 5.14; Table 5.1). When the analysis was conducted in the $CD44^{+}/CD24^{-}$ sub-population of Hs578-T cells, the transcript levels of both enzymes were increased upon treatment with HS/heparin and the selected modified heparin 2,6 deS-NS H (Figure 5.15; Table 5.2).

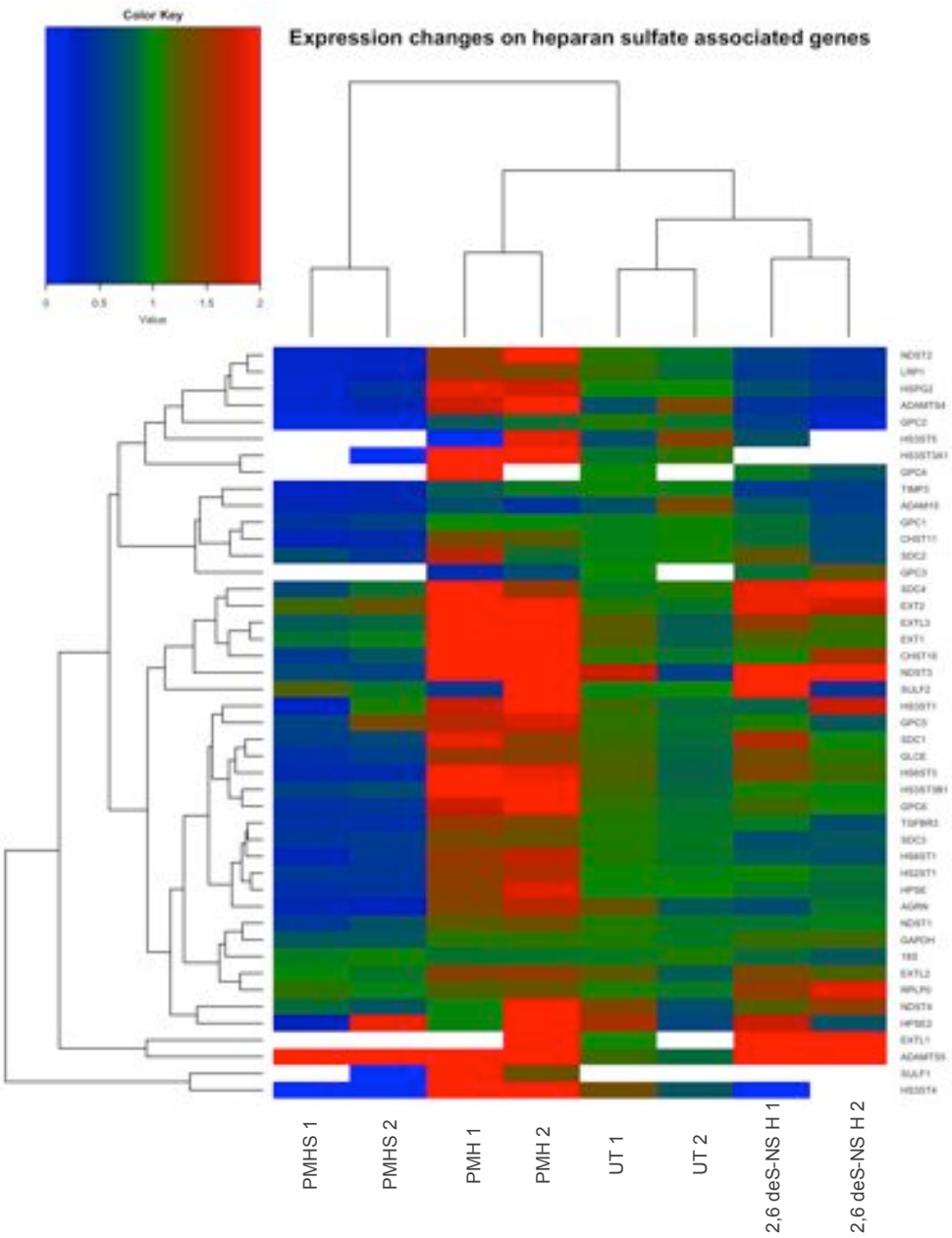

Figure 5.14 Heat map depicting changes in expression of HS associated genes induced by HS/heparin and selected chemically modified heparins in CD44^{+}/CD24^{-} cells sorted from the MDA-MB-231 line. RNA isolated from the CD44^{+}/CD24^{-} cells was analysed after treatment for 48 hrs with either HS/heparin or selective modified heparins (2,6 deS-NS H) at 10 ng/ml. The mRNA expression of MDA-MB-231 cells was analyzed by Taqman real time PCR relative to the house keeping genes 18S and GAPDH using the 2−ΔΔCt method. Expression changes were compared relative to untreated cells. Red: significantly increased expression; blue; significantly decreased expression; green: non-significant change; white; not detected. UT 1 and UT 2 represent biological replicates in untreated cells, while PMHS 1 and PMHS 2 represent biological replicates in cells treated with PMHS; PMH 1 and PMH 2 indicate biological replicates in cells treated with PMH; 2,6 deS-NS H 1 and 2,6 deS-NS H 2 represent biological replicates in cells treated with 2,6 deS-NS H.

Table 5.1 Summary of quantitative analysis of changes in expression of genes involved in synthesis and editing of HS induced by HS/heparin and selected chemically modified heparins in $CD44^{+}/CD24^{-}$ cells sorted from the MDA-MB-231

Gene Name	Gene ID	Mean log (fold change) in PMHS ± S.E.M (n=3)	Up/Down reg. in PMHS vs. UT	t-test p-value P<0.05*	Mean log (fold change) in PMH ± S.E.M (n=3)	Up/Down reg. in PMH vs. Ctrl	t-test p-value P<0.05*	Mean log (fold change) in 2,6 deS-NS H ± S.E.M (n=3)	Up/Down reg. in AD vs. 2,6 deS-NS	t-test p-value P<0.05*
18S	Hs99999901_s1	-0.100 ± 0.131	DOWN	0.485	-0.213 ± 0.079	DOWN	0.054	-0.314 ± 0.025	DOWN	**0.000** ***
GAPDH	Hs99999905_m1	0.032 ± 0.262	UP	0.910	0.548 ± 0.261	UP	0.104	0.607 ± 0.246	UP	0.069
AGRN	Hs00394748_m1	-2.445 ± 0.155	DOWN	**0.000** ***	-0.295 ± 0.219	DOWN	0.249	-1.306 ± 0.396	DOWN	**0.030** *
EXT1	Hs00609162_m1	-0.060 ± 0.133	DOWN	0.674	1.370 ± 0.212	UP	**0.003** **	0.282 ± 0.199	UP	0.229
EXT2	Hs00181158_m1	-0.355 ± 0.301	DOWN	0.303	0.779 ± 0.318	UP	0.071	0.286 ± 0.211	UP	0.247
EXTL1	Hs00184929_m1	28.708 ± 1.395	UP	**0.000** ***	20.304 ± 9.432	UP	0.098	1.430 ± 1.202	UP	0.300
EXTL2	Hs01018237_m1	-0.168 ± 0.126	DOWN	0.255	0.417 ± 0.095	UP	**0.012** *	0.280 ± 0.166	UP	0.167
EXTL3	Hs00918601_m1	-0.869 ± 0.175	DOWN	**0.008** **	0.745 ± 0.152	UP	**0.008** **	-0.119 ± 0.020	DOWN	**0.004** **
GPC1	Hs00892476_m1	-0.534 ± 0.112	DOWN	**0.009** **	0.498 ± 0.205	UP	0.072	0.155 ± 0.368	UP	0.695
GPC2	Hs00415099_m1	-4.269 ± 0.569	DOWN	**0.002** **	-1.618 ± 0.583	DOWN	0.050	-2.674 ± 0.106	DOWN	**0.000** ***
GPC3	Hs01018936_m1	8.224 ± 8.834	UP	0.405	-18.508 ± 8.609	DOWN	0.098	-17.451 ± 8.893	DOWN	0.121
GPC4	Hs00155059_m1	11.141 ± 11.752	UP	0.397	-9.848 ± 11.237	DOWN	0.430	-23.482 ± 11.542	DOWN	0.112
GPC5	Hs00270114_m1	-1.288 ± 0.788	DOWN	0.177	-0.166 ± 0.365	DOWN	0.672	-1.001 ± 0.232	DOWN	**0.013** *
GPC6	Hs00170677_m1	-1.286 ± 0.066	DOWN	**0.000** ***	0.830 ± 0.174	UP	**0.009** **	-0.003 ± 0.050	DOWN	0.962
HPSE	Hs00935036_m1	-1.311 ± 0.115	DOWN	**0.000** ***	0.550 ± 0.107	UP	**0.007** **	-0.265 ± 0.039	DOWN	**0.003** **
HPSE2	Hs00222435_m1	-1.257 ± 0.763	DOWN	0.175	0.710 ± 1.258	UP	0.603	-0.076 ± 0.522	DOWN	0.891
HS2ST1	Hs00202138_m1	-0.292 ± 0.395	DOWN	0.501	1.319 ± 0.399	UP	**0.030** *	0.678 ± 0.441	UP	0.199
HS3ST1	Hs00245421_s1	-1.394 ± 0.643	DOWN	0.096	0.772 ± 0.145	UP	**0.006** **	-0.059 ± 0.330	DOWN	0.868
HS3ST2	Hs00428644_m1	21.055 ± 10.574	UP	0.117	-2.835 ± 10.294	DOWN	0.797	-3.756 ± 11.903	DOWN	0.768
HS3ST3A1	Hs00925624_s1	18.403 ± 11.768	UP	0.193	3.350 ± 0.470	UP	**0.002** **	30.389 ± 0.601	UP	**0.000** ***
HS3ST3B1	Hs00797512_s1	-1.140 ± 0.158	DOWN	**0.002** **	0.975 ± 0.081	UP	**0.000** ***	-0.351 ± 0.050	DOWN	**0.002** **
HS3ST4	Hs00901124_s1	-3.640 ± 0.505	DOWN	**0.002** **	3.650 ± 1.016	UP	**0.023** *	6.088 ± 11.553	UP	0.626
HS3ST5	Hs00999394_m1	10.829 ± 11.440	UP	0.397	-24.541 ± 10.601	DOWN	0.082	-11.282 ± 22.641	DOWN	0.644
HS3ST6	Hs03007244_m1	9.404 ± 17.811	UP	0.625	-0.671 ± 16.357	DOWN	0.969	-7.675 ± 9.667	DOWN	0.472
HS6ST1	Hs00757137_m1	-0.661 ± 0.216	DOWN	**0.038** *	1.361 ± 0.445	UP	**0.038** *	0.319 ± 0.459	UP	0.525
HS6ST2	Hs02925656_m1	1.598 ± 0.845	UP	0.132	-7.216 ± 10.169	DOWN	0.517	-4.473 ± 9.820	DOWN	0.672
HS6ST3	Hs00542178_m1	-1.530 ± 0.037	DOWN	**0.000** ***	0.843 ± 0.043	UP	**0.000** ***	0.249 ± 0.141	UP	0.153
NDST1	Hs00925442_m1	0.315 ± 0.440	UP	0.514	1.457 ± 0.638	UP	0.084	1.010 ± 0.596	UP	0.165
NDST2	Hs00234335_m1	-1.963 ± 0.011	DOWN	**0.000** ***	0.725 ± 0.244	UP	**0.041** *	-0.978 ± 0.169	DOWN	**0.004** **
NDST3	Hs01128584_m1	-0.716 ± 0.437	DOWN	0.177	1.504 ± 0.345	UP	**0.012** *	1.983 ± 0.605	UP	**0.031** *
NDST4	Hs00224024_m1	0.845 ± 0.890	UP	0.396	2.685 ± 2.114	UP	0.273	1.490 ± 0.718	UP	0.107
SDC1	Hs00896423_m1	-0.264 ± 0.286	DOWN	0.409	1.314 ± 0.304	UP	**0.012** *	0.973 ± 0.587	UP	0.173
SDC2	Hs00299807_m1	0.239 ± 0.592	UP	0.707	1.397 ± 0.399	UP	**0.025** *	0.994 ± 0.740	UP	0.251
SDC3	Hs01568665_m1	-0.427 ± 0.310	DOWN	0.241	1.018 ± 0.339	UP	**0.040** *	0.121 ± 0.296	UP	0.702
SDC4	Hs00161617_m1	-1.221 ± 0.586	DOWN	0.105	0.236 ± 0.543	UP	0.686	0.267 ± 0.492	UP	0.616
SULF1	Hs00290918_m1	18.872 ± 11.506	UP	0.176	0.094 ± 0.959	UP	0.927	20.459 ± 10.739	UP	0.129
SULF2	Hs01016476_m1	-0.774 ± 0.345	DOWN	0.088	-0.738 ± 0.933	DOWN	0.473	0.296 ± 0.642	UP	0.669

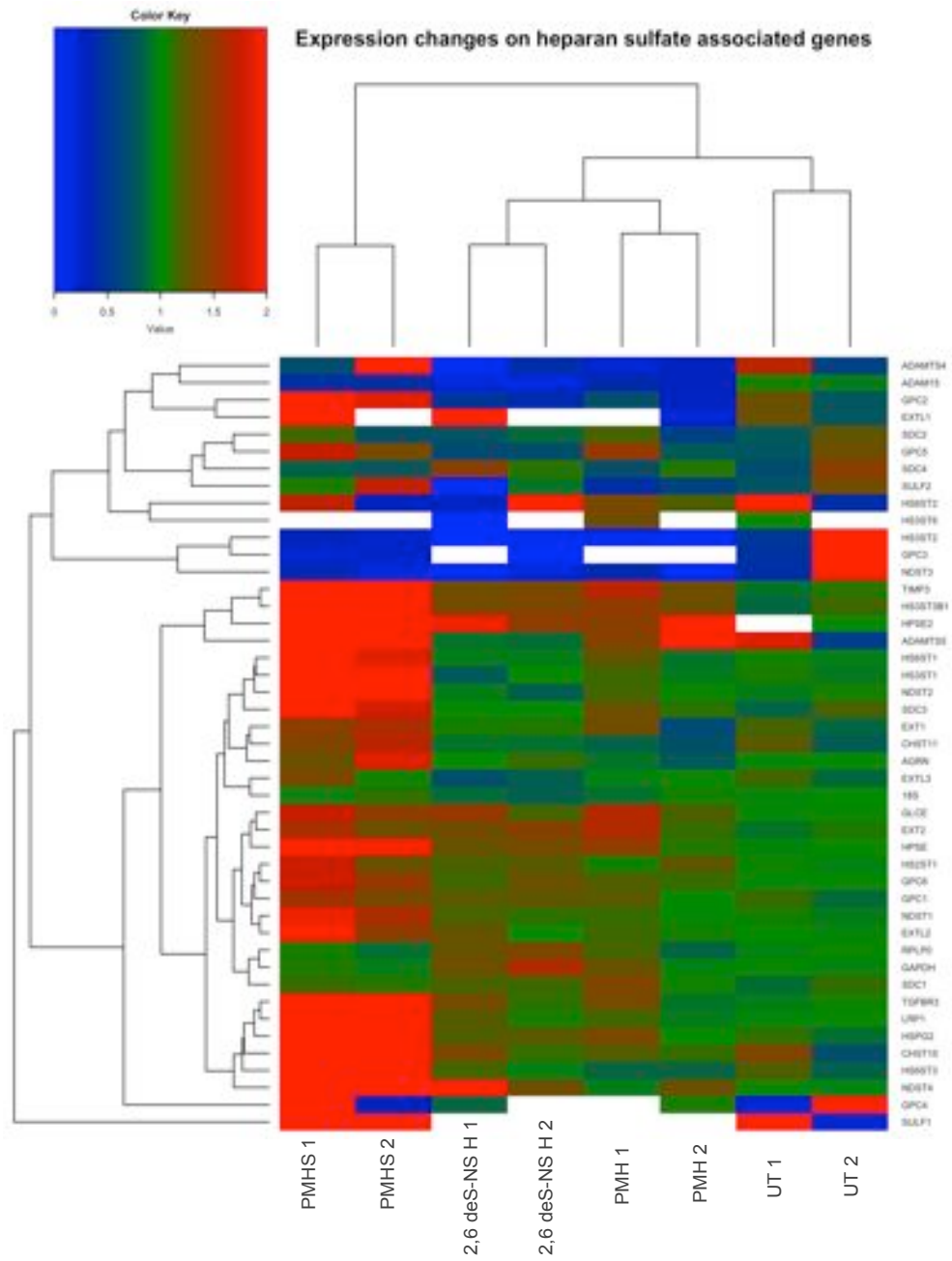

Figure 5.15 Heat map depicting changes in expression of HS associated genes induced by HS/heparin and selected chemically modified heparins in $CD44^{+}/CD24^{-}$ cells sorted from the Hs578-T line. RNA isolated from the $CD44^{+}/CD24^{-}$ cells was analysed after treatment for 48 hrs with either HS/heparin or selective modified heparins (2,6 deS-NS H) at 10 ng/ml. The mRNA expression of MDA-MB-231 cells was analyzed by Taqman real time PCR relative to the house keeping genes 18S and GAPDH using the $2^{-\Delta\Delta Ct}$ method. Expression changes were compared relative to untreated cells. Red: significantly increased expression; blue; significantly decreased expression; green: non-significant change; white; not detected. UT 1 and UT 2 represent biological replicates in untreated cells, while PMHS 1 and PMHS 2 represent biological replicates in cells treated with PMHS; PMH 1 and PMH 2 indicate biological replicates in cells treated with PMH; 2,6 deS-NS H 1 and 2,6 deS-NS H 2 represent biological replicates in cells treated with 2,6 deS-NS H.

Table 5.2 Summary of quantitative analysis of changes in expression of genes involved in synthesis and editing of HS induced by HS/heparin and selected chemically modified heparins in CD44^{+}/CD24^{-} cells sorted from the Hs578-T

Gene Name	Gene ID	Mean log (fold change) in PMHS ± S.E.M (n=3)	Up/Down reg. in PMHS vs. UT	t-test p-value P<0.05*	Mean log (fold change) in PMH ± S.E.M (n=3)	Up/Down reg. in PMH vs. UT	t-test p-value P<0.05*	Mean log (fold change) in 2,6 deS-NS H ± S.E.M (n=3)	Up/Down reg. in 2,6 deS-NS H vs. UT	t-test p-value P<0.05*
18S	Hs99999901_s1	0.032 ± 0.069	UP	0.671	-0.011 ± 0.066	DOWN	0.875	-0.215 ± 0.025	DOWN	**0.001** ***
GAPDH	Hs99999905_m1	0.042 ± 0.065	UP	0.555	0.103 ± 0.117	UP	0.429	0.488 ± 0.091	UP	**0.006** **
AGRN	Hs00394748_m1	0.553 ± 0.177	UP	**0.035** *	-0.266 ± 0.073	DOWN	**0.022** *	0.075 ± 0.058	UP	0.269
EXT1	Hs00609162_m1	0.525 ± 0.138	UP	**0.019** *	-0.182 ± 0.183	DOWN	0.375	0.025 ± 0.151	UP	0.875
EXT2	Hs00181158_m1	0.622 ± 0.086	UP	**0.002** **	0.325 ± 0.254	UP	0.270	0.490 ± 0.104	UP	**0.009** **
EXTL1	Hs00184929_m1	10.792 ± 9.005	UP	0.297	8.270 ± 10.131	UP	0.460	10.353 ± 9.231	UP	0.325
EXTL2	Hs01018237_m1	0.884 ± 0.167	UP	**0.006** **	0.128 ± 0.032	UP	**0.017** *	0.234 ± 0.120	UP	0.123
EXTL3	Hs00918601_m1	0.262 ± 0.242	UP	0.340	0.053 ± 0.161	UP	0.760	-0.494 ± 0.126	DOWN	**0.017** *
GPC1	Hs00892476_m1	0.506 ± 0.172	UP	**0.042** *	0.173 ± 0.037	UP	**0.010** **	0.250 ± 0.128	UP	0.123
GPC2	Hs00415099_m1	1.114 ± 0.380	UP	**0.043** *	-1.227 ± 0.165	DOWN	**0.002** **	-1.294 ± 0.323	DOWN	**0.016** *
GPC3	Hs01018936_m1	-1.710 ± 0.797	DOWN	0.098	26.954 ± 0.790	UP	**0.000** ***	17.055 ± 10.475	UP	0.179
GPC4	Hs00155059_m1	1.252 ± 1.414	UP	0.426	10.879 ± 13.191	UP	0.456	12.364 ± 12.664	UP	0.384
GPC5	Hs00270114_m1	0.814 ± 0.233	UP	**0.025** *	-0.150 ± 0.571	DOWN	0.805	-0.431 ± 0.280	DOWN	0.198
GPC6	Hs00170677_m1	0.750 ± 0.075	UP	**0.001** ***	0.214 ± 0.027	UP	**0.001** **	0.265 ± 0.055	UP	**0.008** **
HPSE	Hs00935036_m1	1.023 ± 0.016	UP	**0.000** ***	0.258 ± 0.160	UP	0.183	0.402 ± 0.030	UP	**0.000** ***
HPSE2	Hs00222435_m1	-20.619 ± 11.325	DOWN	0.143	-10.367 ± 11.658	DOWN	0.424	-21.982 ± 11.473	DOWN	0.128
HS2ST1	Hs00202138_m1	0.653 ± 0.158	UP	**0.014** *	0.258 ± 0.105	UP	0.071	0.248 ± 0.024	UP	**0.000** ***
HS3ST1	Hs00245421_s1	1.251 ± 0.114	UP	**0.000** ***	0.048 ± 0.035	UP	0.243	-0.251 ± 0.106	DOWN	0.076
HS3ST2	Hs00428644_m1	-1.400 ± 0.612	DOWN	0.084	-4.361 ± 0.875	DOWN	**0.008** **	-4.596 ± 1.040	DOWN	**0.012** *
HS3ST3A1	Hs00925624_s1	-27.008 ± 0.056	DOWN	**0.000** ***	-0.026 ± 0.082	DOWN	0.771	0.256 ± 0.090	UP	**0.047** *
HS3ST3B1	Hs00797512_s1	2.140 ± 0.135	UP	**0.000** ***	0.390 ± 0.206	UP	0.131	0.536 ± 0.154	UP	**0.025** *
HS3ST4	Hs00901124_s1	-28.245 ± 0.127	DOWN	**0.000** ***	-0.026 ± 0.082	DOWN	0.771	0.256 ± 0.090	UP	**0.047** *
HS3ST5	Hs00999394_m1	-33.885 ± 0.041	DOWN	**0.000** ***	-0.026 ± 0.082	DOWN	0.771	0.256 ± 0.090	UP	**0.047** *
HS3ST6	Hs03007244_m1	17.581 ± 8.784	UP	0.116	0.064 ± 0.172	UP	0.729	-3.353 ± 16.738	DOWN	0.851
HS6ST1	Hs00757137_m1	1.035 ± 0.110	UP	**0.001** ***	0.045 ± 0.121	UP	0.730	-0.095 ± 0.040	DOWN	0.076
HS6ST2	Hs02925656_m1	-0.498 ± 1.451	DOWN	0.749	0.746 ± 0.774	UP	0.390	-0.295 ± 1.680	DOWN	0.869
HS6ST3	Hs00542178_m1	1.361 ± 0.197	UP	**0.002** **	-0.150 ± 0.177	DOWN	0.444	0.036 ± 0.234	UP	0.886
NDST1	Hs00925442_m1	0.824 ± 0.122	UP	**0.003** **	0.091 ± 0.007	UP	**0.000** ***	0.188 ± 0.072	UP	0.059
NDST2	Hs00234335_m1	1.255 ± 0.044	UP	**0.000** ***	0.073 ± 0.110	UP	0.544	-0.121 ± 0.062	DOWN	0.125
NDST3	Hs01128584_m1	-1.402 ± 0.740	DOWN	0.131	-6.375 ± 3.114	DOWN	0.110	-3.692 ± 1.364	DOWN	0.054
NDST4	Hs00224024_m1	1.318 ± 0.024	UP	**0.000** ***	0.242 ± 0.177	UP	0.244	0.956 ± 0.298	UP	**0.033** *
SDC1	Hs00896423_m1	0.233 ± 0.113	UP	0.110	0.143 ± 0.269	UP	0.624	0.292 ± 0.117	UP	0.067
SDC2	Hs00299807_m1	0.099 ± 0.223	UP	0.681	-0.563 ± 0.573	DOWN	0.381	-0.230 ± 0.273	DOWN	0.447
SDC3	Hs01568665_m1	1.051 ± 0.141	UP	**0.002** **	0.151 ± 0.242	UP	0.567	0.085 ± 0.163	UP	0.629
SDC4	Hs00161617_m1	-0.120 ± 0.343	DOWN	0.744	-0.253 ± 0.156	DOWN	0.179	0.586 ± 0.315	UP	0.136
SULF1	Hs00290918_m1	2.555 ± 1.607	UP	0.187	35.389 ± 1.431	UP	**0.000** ***	34.157 ± 1.439	UP	**0.000** ***
SULF2	Hs01016476_m1	0.477 ± 0.448	UP	0.347	-1.047 ± 0.111	DOWN	**0.001** ***	-2.911 ± 1.630	DOWN	0.149

5.12 Discussion

Expression of a number of markers associated with BCSCs, including CD44, EpCAM and ABCG2, and the effect of HS/heparin and chemically modified heparin on theses markers were studied in the $CD44^{+}/CD24^{-}$ population from MDA-MB-231 and Hs578-T cell lines and summarized in Tables 5.3 and 5.4. Multiple previous studies have demonstrated that the $CD44^{+}/CD24^{-}$ population from BCC have tumor-initiating abilities (Al-Hajj et al., 2003, Ponti et al., 2005). These tumorigenic properties have been identified as stem cell–like properties (Al-Hajj et al., 2003), enhanced metastasis, invasive properties (Sheridan et al., 2006), and chemo/radio resistance (Kim et al., 2009). As expected from the FACS selection, CD44 was highly expressed in our studies. Interestingly, treatment with a number of HS/heparin compounds resulted in down-regulation of CD44, and thus would produce $CD44^{low}$ and/or $CD44^{-}$ cells which have reduced tumorigenicity. This mechanism may be in part responsible for the altered phenotype of the cells in terms of reduced adhesion, invasion and migration. In contrast, previous experiments examined the role of CD44 variant exon 3 (CD44v3), a HS-binding isoform of CD44, in invasion and metastasis associated with HS in colon cancer cell lines (Kuniyasu et al., 2001). It was found that CD44v3 expression correlated with increased cell invasion after human colon cancer cells are treated with HS. However HS treatment did not show any effect on cell growth. In addition, these cells that express CD44v3 were found to be stimulated by free HS to invade, which also correlated with poor prognosis (Kuniyasu et al., 2001). The $CD44^{+}$ phenotype is also positively corresponded with breast, prostate, colon, and pancreatic cancer initiator cells (Yan et al., 2015). Variants of CD44 isoforms are differentially expressed during pregnancy and involution, indicating a role in normal breast epithelial homeostasis (Fillmore and Kuperwasser, 2007). In future studies is may be of interest to examine the exact CD44 variants expressed in the MDA-MB-231 and Hs578-T cell lines, and to see whether these vary upon treatment with HS/heparins, since these effects may be dynamic.

(Al-Hajj et al., 2003) demonstrated that the frequency of CSCs was >10-fold higher in the $EpCAM^{+}$ fraction of BCSCs than in the $EpCAM^{-}$ fraction; therefore, EpCAM

is considered as one of the cell surface markers of several types of CSCs. However, some available immortalized human BCC lines lack EpCAM expression. Here we found that MDA-MB-231 and Hs578-T BCCs expressed none or only very little EpCAM mRNA and protein compared to the other established and well characterized BCC lines such as SK-BR-3 or MCF-7 (Prang et al., 2005). Our findings are in line with the previous studies by (Prang et al., 2005) regarding MDA-MB-231 and Hs578-T human BCCs, so it appears that this marker is not involved in the aggressive phenotype of these two BCC lines, and is not related to the responses we observed to HS/heparin treatments.

In further experiments, the expression of ABCG2 was characterised. Previous studies showed that MDA-MB-231 cells treated with heparin at relatively low concentrations (0.25–32 IU/ml) exhibited inhibition of the ATPase activity of ABCG2 (Chen et al., 2014). Thus, HS/heparin compounds may inhibit the efflux activity of ABCG2 transporter which otherwise confers higher drug resistance to CSCs which express higher levels of this transporter. In contrast, our results showed that MDA-MB-231 treated cells with PerS H, PMH and PMHS at low concentration (10 ng/ml) exhibit higher levels of expression of ABCG2, while no significant affect was observed in cells treated with 2,6 deS-NS H. The $CD44^{+}/CD24^{-}$ sub-population of Hs578-T treated with PerS H, 2,6 deS-NS H and PMHS also showed a significant increase in ABCG2 expression, though no significant increase was detected in cells treated with heparin. Thus, a number of the compounds can induce increased expression of ABCG2 which is counter to the observation here that they induce increased chemoresistance in CSCs, presumably via increased cytotoxicity of ABC transporter substrates such as doxorubicin and cisplatin; chapter 4.8). It can be concluded that the HS/heparin compounds do not enhance chemoresistance of the $CD44^{+}/CD24^{-}$ sub-population of MDA-MB-231 and Hs578-T cells via reducing expression of the ABCG2 transporter proteins. Rather, since the ATPase activity of ABC transporters is essential to their efflux transport activity, and heparin has previously been reported to inhibit this activity (Chen et al., 2014), it is reasonable to hypothesise that the compounds may be acting via inhibition of ABCG2 and possibly other drug transporters. This would result in increased chemosensitivity of BCCs, via reducing drug efflux and enhacing drug retention and thus cytotoxicity. Indeed, this inhibition may result in a feedback mechanism that promotes enhanced expression of

ABCG2 as the cells attempt to increae drug efflux. Future experiments should thus focus on testing the effects of the compounds on the activity of the ABCG2 transporter to test this hypothesis.

Previous studies have shown that CSCs consistently secrete markedly elevated levels of a panel of angiogenic factors that increase endothelial cell migration and tube formation (Bao et al., 2006). Angiogenesis is an essential process for tumour formation and maintenance, while anti-angiogenic therapies may effectively target and reduce CSCs self-renewal (Bao et al., 2006). However, the roles of angiogenic molecules in BCSCs and their contribution to tumor angiogenesis remained largely unknown. In the current study, $CD44^{+}/CD24^{-}$ sub-population cells isolated from MDA-MB-231 and Hs578-T were used as a model of CSCs to study links between CSCs, drug resistance genes and angiogenesis. The expression levels of pro-angiogenic genes and chemokines that we detected in the $CD44^{+}/CD24^{-}$ cells were similar to those described in recent reports in other BC cell lines such as MCF-7A (Sun et al., 2013). The data presented here showed that the expression of pro-angiogenic genes, such as VEGFA, VEGFB, IL-8, Ang-1, and Ang-2 were higher in $CD44^{+}/CD24^{-}$ sub-population compared with $CD44^{-}/CD24^{-}$ sub-population isolated from MDA-MB-231 and Hs578-T human BCCs. Previous studies reported that, chemokines and their receptors are involved in the CSC-mediated production of angiogenic factors (Cojoc et al., 2013). Chemokine receptor CXCR4 is known to play an important role in tumor angiogenesis and has been shown to be preferentially expressed by glioblastoma stem cells (Ehtesham et al., 2009). Previous studies found that CXCR4 was highly expressed in the $CD44^{+}/CD24^{-}$ sub-set compared with the $CD44^{-}/CD24^{+}$ sub-set isolated from MCF-7 human BCCs (Sun et al., 2013). Here we confirmed similar findings in 2 other human BCC lines (MDA-MB-231 and Hs578-T); the results showed that the expression of CXCR4 was also higher in $CD44^{+}/CD24^{-}$ cells compared with $CD44^{-}/CD24^{+}$ cells. Multiple studies have demonstrated evidence of angiogenesis related to a $CD44^{-}$ phenotype in BCCs (Jeyapalan et al., 2011). Reduced expression of CD44 was noted with some compound treatments here, suggesting the possibility that this may result in reduction of the $CD44^{+}/CD24^{-}$ angiogenic properties with a switch towards a $CD44^{-}/CD24^{-}$ phenotype. On the other hand, CD24 has been shown to either inhibit (Schabath et al., 2006) or promote (Bretz et al., 2012) BCC invasion and metastasis. Here the

$CD44^+/CD24^-$ sub-population of MDA-MB-231 and Hs578-T cells appeared to correlate more with expression of increased levels of angiogenic factors than the $CD44^-/CD24^-$ sub-population of the same cell line. The relationship between the $CD44^+/CD24^-$ phenotype and enhanced expression of angiogenic molecules demonstrated in this study may not be directly linked to the function of these individual genes. Nevertheless, increased angiogenic properties seem to be intrinsic to cells with a $CD44^+/CD24^-$ phenotype and can apparently be differentially modulated by treatment with HS/heparins.

Previous studies have shown that soluble heparin or HS can inhibit the interaction between CXCL12 chemokine and its receptor CXCR4, preventing the adhesion, invasion and migration of CXCR4-expressing T-cells (Dowsland et al., 2003, Hecht et al., 2004, Kuschert et al., 1999). The work presented here has shown that HS and highly sulphated modified heparins are capable of inhibiting CXCR4 expression in $CD44^+/CD24^-$ cells sorted from both MDA-MB-231 and Hs578-T cell lines. Thus, reducing CXCR4 expression may represent a plausible mechanism for reducing the angiogenic properties of BCSCs, though direct effects on inhibiting chemokine-receptor functions cannot be ruled out as an additional mechanism. The present study demonstrated that CSC-like cells contribute to a greater pro-angiogenic potential of BCCs, and may present targets for effective anti-angiogenic therapies which could include heparins. However, the usefulness of heparin itself, having high anticoagulant activity, might limited its applicability for treating BC patients. On the other hand, PMHS or modified heparins, with intrinsically much lower anticoagulant activities, might be candidates for such applications.

Previous evidence demonstrated that IL-8 binds to GAGs, especially heparin/HS and it has been reported that HSPGs on endothelial cell surfaces localize and present chemokines to selectin-bound leukocytes (Dowsland et al., 2003). Other studies suggest that chemokines bind to cell-surface HS *in vitro,* and that HS may promote IL-8-dependent transmigration of neutrophils and enhance IL-8 activity (Dowsland et al., 2003). In addition, IL-8 was found to be highly expressed in breast cancer compared to normal breast tissue. IL-8 may also promote breast cancer initiation and progression via the IL-8 signaling pathway, and there is evidence indicates that IL-8 is a key regulator of CSC activity (Singh et al., 2013). IL-8 was thus considered a

potential candidate molecule for mediating the effects of exogenous HS/heparins on BCSCs. The findings here indicated that some modified heparin (PerS H and 2,6 deS-NS H), but not heparin, did significantly inhibit IL-8 expression in $CD44^{+}/CD24^{-}$ cells from the MDA-MB-231 cell line. On the other hand PMHS treatment enhanced IL8 expression in these cells. Hs578-T cells showed a significant downregulation of IL-8 expression when treated with heparin and modified heparins (PerS H and 2,6 deS-NS H), and PMHS treatment again showed a significant upregulation of IL-8 expression. Thus modulation of IL-8 expression could be an additional mechanism of action of at least some of the compounds in reducing CSC tumorigenic properties.

Binding of HS/heparin to growth factors is modulated by differential sulphation of the polysaccharide backbone, creating a multitude of protein binding domains (Kreuger et al., 2005) . One of the aims of the present study was to define whether exogenous HS/heparin might influence VEGF functions. Data presented here showed that VEGFA expression was increased 1.5- 2 fold in MDA-MB-231 and Hs578-T cells treated with HS and modified heparin compared to untreated cells. In contrast, VEGFB expression was not detected in either MDA-MB-231 or Hs578-T cells treated with heparin and modified heparins compared to untreated control cells. However, PMHS treatment induced a significant increase in VEGFB expression. The lack of response of $CD44^{+}/CD24^{-}$ cells treated with HS and modified heparin in terms of VEGFB expression may relate to the fact that VEGF-A165 is a heparin binding growth factor (Ruhrberg et al., 2002).

Angiopoietin activities are differentially regulated by the ECM and HSPGs. This might provide the basis for modulating activities of angiopoietins *in vivo* and thereby angiogenesis regulation in physiologic and pathologic situations (Xu et al., 2004). In the present study it was found that Ang-1 is downregulated in CSC-like cells in MDA-MB-231 cell culture treated with PerS H, 2,6 deS-NS H and PMH, but upregulated in cells treated with PMHS. On the contrary, Ang-1 was found to be upregulated in CSC-like cells from Hs578-T cells treated with HS, heparin, and modified heparin, whereas PerS H and 2,6 deS-NS H treatment downregulated Ang-2 expression. PMH and PMHS upregulated Ang2 expression in both cells. Role of HS/heparin and chemically modified heparins in angiogenesis are summarized in

Tables 5.3 and 5.4.

Table 5.3 Summary table of effect of HS/heparin and modified heparins effects on CSC, drug resistance and angiogenic markers in MDA-MB-231 BCSCs

	CSC markers			Angiogenesis					
	CD44	**ABCG2**	**EpCAM**	**VEGF A**	**VEGF B**	**Ang-1**	**Ang-2**	**CXCR 4**	**IL-8**
PerS H	Sig -	Sig +	No	Sig +	No	No	Sig -	Sig -	Sig -
2,6 deS-NS H	Sig -	No	No	Sig +	Sig +	Sig +	Sig -	Sig -	Sig -
PMHS	No	Sig +	No	Sig +	No	No	Sig +	Sig -	No
PMH	Sig -	Sig +	Sig +	Sig +	Sig +	Sig +	Sig +	Sig -	Sig +

*Sig, statistically significant.

Table 5.4 Summary table of effect of HS/heparin and modified heparins effects on CSC, drug resistance and angiogenic markers in Hs578-T BCSCs

	CSC markers			Angiogenesis					
	CD44	**ABCG2**	**EpCAM**	**VEGF A**	**VEGF B**	**Ang-1**	**Ang-2**	**CXCR 4**	**IL-8**
PerS H	Sig -	Sig +	No	Sig +	No	Sig -	Sig -	Sig -	Sig -
2,6 deS-NS H	Sig -	Sig +	No	No	No	Sig -	Sig -	Sig -	Sig -
PMHS	No	No	Sig +	No	No	Sig -	Sig +	Sig -	No
PMH	Sig -	Sig +	Sig -	Sig +	Sig +	Sig +	Sig +	Sig -	Sig +

*Sig, statistically significant.

HSPGs are known to be involved in several biological functions of heparin-binding growth factors (GFs) (Chua et al., 2004), including the prototypical FGF family members. FGF-2 signaling mediated by HSPGs activates the ERK1/2 signaling pathway to regulate cell activity. Several studies have revealed that HSPGs regulate the activity of growth factors due to either HSPGs playing an important roles as co-receptors in binding FGF ligands to their FGFRs (Ornitz, 2000), or indirectly as FGF2 receptors (Mundhenke et al., 2002). Several indirect ERK-specific inhibitors have been revealed by targeting the upstream kinases, including Raf and MEKs (Jung et al., 2016, Lee et al., 2013). However, studies with these inhibitors of ERK on CSCs have not been reported. The present results suggest that HS and some modified heparins induced a significant reduction of FGF-2 mediated ERK1/2

activation, suggesting that FGF mediate ERK1/2 activation through HSPGs in CSCs. These investigations suggest the possibility that HS or specific chemically modified heparins could potentially be used to target CSCs functions including signaling that supports their growth.

BCCs stimulated with or without FGF2 and treated with different compounds of HSPGs. As expected FGF2 was able to stimulate ERK1/2 phosphorylation, presumably dependent on endogenous cell surface HSPGs. The kinetics of FGFR-mediated ERK1/2 activation the $CD44^{+}/CD24^{-}$ sub-population isolated from MDA-MB-231 and Hs578-T human BCCs was altered significantly by FGF stimulation, HS and chemically modified heparin treatments were observed to prevent FGF2 from stimulating and activating ERK1/2 signaling, seen as a significant decrease in FGF2-induced ERK1/2 phosphorylation. $CD44^{+}/CD24^{-}$ of MDA-MB-231 cells expressed significantly less total ERK1/2 and showed a greater response to 2,6 deS-NS H and HS treatments. In contrast with the other modified heparin compounds (PerS H and HS) there was no effect on decreasing the expression levels of ERK1/2. These results indicated that 2,6 deS-NS H and HS treatments showed a greater overall effect on the FGF2 mediated ERK1/2 signaling pathway. $CD44^{+}/CD24^{-}$ of Hs578-T cells expressed significantly less total ERK1/2 and showed a greater dependence on 2,6 deS-NS H, heparin and HS treatments. In contrast the other modified heparin compound, PerS H, showed no effect on decreasing the expression levels of ERK1/2.

In addition, $CD44^{+}/CD24^{-}$ cells treated with HS and modified heparin for different time point in both cell lines expressed significantly less ERK1/2 and showed a greater dependence on FGF2 stimulation; compound treatments alone in unstimulated cells showed undetectable activation of ERK1/2, suggesting that adding HS and modified heparin on cells alone did not activate ERK1/2. Overall, ERK1/2 activation via FGF2 stimulation has been shown to be sensitive to a number of the compounds, but these responses alone could not predict all the altered biological responses noted in the CSC cells. Thus, alteration of activation of ERK1/2 most likely represents one component of a complex system of responses that CSCs make to addition of the compounds.

It is well established that inflammatory signals that come from the tumour microenvironment enhance tumour growth and progression (Bromberg and Wang, 2009, Grivennikov and Karin, 2008). It has been found that IL-6 promotes cell proliferation in prostate cancer *in vitro* (Malinowska et al., 2009) and promotes tumour growth in breast and prostate cancer *in vivo* (Knüpfer and Preiß, 2007, Malinowska et al., 2009). Previous studies reported that inflammatory response pathways have been linked to BCSCs. Of particular interest in this respect is STAT3, one of the common transcription factors, which acts as a key modulator in the inflammatory signaling pathway, leading to cancer when inflammation becomes chronic. STAT3 acts by regulating the expression of inflammatory cytokines including IL-6 that are inflammatory mediators. A growing body of evidence has shown that the IL-6/STAT3 inflammatory cytokine signaling pathway is involved in a wide range of human tumors and impacts cell adhesion and migration. In particular, and most relevant to our mechanistic studies, the IL-6/STAT-3 pathway is recognized as an important signaling pathway in the regulation and maintenance of the $CD44^{+}/CD24^{-}$ BCSC phenotype (Hernandez-Vargas et al., 2011, Xie et al., 2012). A similar link between IL-6 and STAT3 have been demonstrated in the survival of intestinal epithelial cells in colitis-associated cancer and in mammary epithelial cells (Ibrahim et al., 2013). Based on these results, we hypothesized that IL-6 would promote survival of BCSCs via STAT3 and that this signaling axis might be susceptible to HS/heparin treatments.

Indeed we found firstly that the endogenous levels of IL-6 in $CD44^{+}/CD24^{-}$ sorted cells from MDA-MB-231 and Hs578-T BCCs was downregulated upon treatment with HS/heparins compared to untreated cells. Interestingly, PMH treatment significantly upregulated IL-6 expression in Hs578-T cells, and PerS H treatment upregulated IL-6 expression in both MDA-MB-231 and Hs578-T cell lines.

MDA-MB-231 and Hs578-T BCCs reacted rapidly on treatment with HS and modified heparin by increased phosphorylation of STAT3 and also total STAT3 at comparable intensities and kinetics. The phosphorylation and total STAT3 activation could be blocked by low concentrations of 10 ng/ml of PerS H, 2,6 deS-NS H or PMHS in stimulated cells, which presumably competes with cell surface HSPGs for IL-6 binding. Similar concentrations of 2,6 deS-NS H, heparin or PMHS (10 ng/ml)

were found to also inhibit STAT3 phosphorylation in Hs578-T cells, whereas these compounds did not effect total STAT3 expression. In agreement with our findings, it was previously reported that syndecan-1 silencing in MDA-MB-231 BCCs resulted in dysregulation of IL-6-induced NFkB and STAT3 activation (Götte et al., 2007). Our findings showed that exogenous HS and sulphated chemically modified heparin treatments inhibit proinflammatory signaling through downregulation of IL-6 which was linked to reduced constitutive activation of STAT3. These effects of the compounds could be a significant factor in their ability to reduce the $CD44^{+}/CD24^{-}$ sub-population in MDA-MB-231 and Hs578-T BCCs, and also to alteration in their metastatic phenotype. These studies emphasize the importance of HSPGs in underpinning a number of biological processes essential for maintenance of the BC CSC-like cell phenotypes, and the potential to exploit HS and modified heparins to interefere with BC CSCs in novel treatments, perhaps in combination with existing drug treatment regimes.

MAPK/ERK and STAT3 are well known to be activated by various extracellular stimuli such as cytokines, growth factors and hormones. MAPK/ERK and STAT3 signalling are involved in a wide range of cellular processes including proliferation and apoptosis, and inflammation and immunity, respectively (Katz et al., 2007, Kijima et al., 2002, Mebratu and Tesfaigzi, 2009, Zhang et al., 2005). The results from the PathScan intracellular signaling array performed in the current study indicated that ERK1/2 and STAT3 were activated in both MDA-MB-231 and Hs578-T cell lines after stimulation with FGF2, and were altered by additional treatment with HS/heparin derivatives. This suggesting a potential role for these pathways in mediating the effects of the compounds on BCSC phenotype.

Moreover, previous studies have demonstrated that AMPKα signaling has an important role in the regulation of cancer cell invasion and pharmacological activation of AMPK was observed to reduce cancer cell invasion (Fitzgerald et al., 2012). In the present study some chemically modified heparins activated AMPKα phosphorylation in $CD44^{+}/CD24^{-}$ cells from the MDA-MB-231 cell line (although this effect was not observed in Hs578-T cells). Thus, the activation of AMPKα by chemically modified heparins might be part of the mechanism by which they inhibit

the invasive properties of MDA-MB-231 CSCs, and further studies are warranted to investigate the exact role of AMPKα in these effects.

The present study also demonstrated that HS derivatives significantly reduced S6 ribosomal protein phosphorylation levels in $CD44^{+}/CD24^{-}$ cells from MDA-MB-231 and Hs578-T cells. This protein is found downstream of the effector mTOR (a protein that has a pivotal role in cell growth and homeostasis), and predicts cell cycle progression (Ruvinsky and Meyuhas, 2006). Phosphorylation of S6 ribosomal is required in the regulation of mRNA expression during the G1 phase of the cell cycle (Thomas et al., 1979). As anticipated, the phosphorylation level of S6 ribosomal protein was decreased by treatment with heparin derivatives, and the mTOR signaling pathway was inhibited in a similar manner (Figure 5.10). Thus, the findings here revealed for the first time, to the best of our knowledge, that the activation of AMPKα and inhibition of mTOR and S6 ribosomal by HS and chemically modified heparins may play a key role in inhibiting the invasive and cell proliferative capacity of CSCs. Future studies should be performed to investigate the exact roles of AMPKα, S6 ribosomal protein and mTOR signaling in BCSCs, and their responses to treatment of the cells with chemically modified heparins. This could include using chemical inhibitors or activators of these pathways to establish whether rescue or antagonism of the effects of the modified heparins is possible.

HSPGs expression is markedly changed during the tumour transformation and progression, leading to affects on both the PG core proteins and the GAG chains (Raman and Kuberan, 2010). The fine structure of HS can be determined by the expression in cells of HS biosynthetic enzymes, some of which have multiple isoforms; the existence in some specific cases of regulation at translation level or enzymatic catalysis has been noted (Grobe and Esko, 2002, Theocharis et al., 2010). In the present work the expression of genes involved in the biosynthesis of HSPGs has been tested in $CD44^{+}/CD24^{-}$ human BCCs (MDA-MB-231 and Hs578-T) treated with HS/heparin or a selected modified heparin 2,6 deS-NS H, compared to those of untreated cells from the same sub-populations. Previous studies demonstrated that

there are 13 full-time HSPGs encoding genes in human cells. It was found that only syndecan1 was overexpressed in metastatic and non metastatic tumors. In addition, the upregulation of SDC-1 has been previously reported in BC (Löfgren et al., 2007). Further studies reported that SDC-1 expression shifts from epithelial to stromal cells during breast tumour progression, suggesting involvement in the stimulation of tumour growth and angiogenesis (Maeda et al., 2006, Yang et al., 2011). Upregulation of SDC-1 has also been reported in other tumors including, lung, pancreatic and brain cancer, indicating that SDC-1 may play a crucial role in promoting growth factor signaling in cancer cells (Raman and Kuberan, 2010). In contrast, SDC-1 has been found to be a downregulated in various tumours, such as colorectal cancer, suggesting that this HSPG may play a key role as a prognostic marker in a cancer-type-specific manner (Raman and Kuberan, 2010).

In this study, adding HS to $CD44^{+}/CD24^{-}$ cells was found to downregulate the SDC isoforms in BCC lines MDA-MB-231 and Hs578-T cells, compared to untreated cells. In contrast, adding heparin to those cells was found to upregulate the expression of SDCs in MDA-MB-231 and did not significantly affect changes in Hs578-T cells. Selected modified heparin 2,6 deS-NS H showed significant differences on expression of syndecans in both cell lines. Upregulation of SDCs has been previously reported in an estrogen receptor-negative highly proliferative breast carcinoma subtype (Baba et al., 2006). Consistent with this result, cell lines analyzed in this study displayed a claudin-low phenotype, which constitutes a common late stage of breast cancer where tumors have negative levels of estrogen and progesterone receptors.

Members of the GPC group of HSPGs are modulators of cell adhesion and growth factor signaling. Over or lower expression of GPCs has been related to malignant progression (Stigliano et al., 2009). A previous study found that, GPC-3 has negative effect on cell proliferation, and its depletion may contribute to cancer progression (Theocharis et al., 2010). 6 members of the GPC family have been analyzed in this study. PMHS and 2,6 deS-NS H down regulated the GPC group in $CD44^{+}/CD24^{-}$ sub-population sorted from MDA-MB-231 cells; however, PMHS did not affect GPC-3 and 4, whereas 2,6 deS-NS H did not affect on GPC-6, compared to untreated cells. GPC-2 and 3 were downregulated when cells were treated with heparin. In

contrast GPC-4, 5 and 6 showed a significant increase in their expression. PMHS upregulated most of GPC isoforms, whereas only isoform 3 showed a downregulation in $CD44^{+}/CD24^{-}$ sub-population cells sorted from the Hs578-T line. In addition heparin did not affect GPC-3 and 4 at all compared to untreated samples. As for the SDC group, 2,6 deS-NS H treatment showed significant differences on expression of GPC in the CSCs from the Hs578-T cell line.

GAG chain generation requires the action of multiple GTs and regulation of their expression in the golgi apparatus (Esko and Lindahl, 2001). Analysis of biosynthetic enzymes of HS chains (EXT1, 2 and EXTL1, 2, 3) did not show any significant changes with PMHS in the $CD44^{+}/CD24^{-}$ sub-population sorted from the MDA-MB-231 line, whereas a significant increase was shown in Hs578-T cells. Heparin significantly increased these biosynthetic enzymes in MDA-MB-231 and variations in the levels of these enzymes was shown in Hs578-T cells (both increases and decreases). High and low levels of theses enzymes has been observed in both cell lines treated with 2,6 deS-NS H, suggesting that adding PMHS/heparin and the selective modified heparin 2,6 deS-NS H induce regulation of the relative levels of GTs in BCSCs.

Our results showed no significant differences of transcript levels in CSCs. In contrast, NDST3 and 4 are expressed during embryonic development (Grobe and Esko, 2002). In the present study expression of NDSTs was highly detected in $CD44^{+}/CD24^{-}$ sorted cells from Hs578-T cells treated with PMHS, and was significantly decreased in MDA-MB-231 cells. Although no significant changes of NDSTs enzymes was detected in Hs578-T cells with heparin, these enzymes were highly detected in MDA-MB-231 cells. *NDST3* was only detected at low and high levels in both cell lines, making it difficult to draw conclusions.

HS3ST2 gene silencing via methylation has been demonstrated in various type of cancers, including breast tumours (Bui et al., 2010, Miyamoto et al., 2003). The last group of enzymes, which is involved in the modification of HS chain, was downregulated in $CD44^{+}/CD24^{-}$ sorted cells from the MDA-MB-231 line. However, in this study, adding PMHS to MDA-MB-231 cells appeared to upregulate HS3STs in Hs578-T cells. No significant differences were observed in the levels of transcripts

of those enzymes in Hs578-T cells treated with heparin, while a significant increase was shown in MDA-MB-231 cells. HS2ST1, HS6ST1, 2, 3 and HS3ST1, 2, 3A1, 3B1, 4, 5, 6 all displayed significant differences in MDA-MB-231 and Hs578-T cells treated with 2,6 deS-NS H compared to untreated cells. Whilst the implications of 3-O-sulfation decrease in tumors are not yet known, it has been suggested that certain patterns of 3-O-sulfation could impart cancerous phenotypic changes (Raman and Kuberan, 2010).

HS 6-O-endosulfatases are localized at the cell surface. Analysis of expression of both HS 6-O-endosulfatase genes Sulf1 and Sulf2 did not showed significant differences in MDA-MB-231 and Hs578-T cells treated with PMHS/heparin and the selected modified heparin 2,6 deS-NS H. Previous studies showed that both genes were overexpressed in pancreatic cancer (Raman and Kuberan, 2010). With regard to breast cancer, downregulation of sulf1 has been previously reported, while sulf2 has been indicated to be upregulated in some breast cancer cell lines. Another study suggested that alterations in sulfation patterns in tumors may relate to protecting the cancer cell from Natural Killer (NK) recognition (Raman and Kuberan, 2010). Our data here suggests that HS/heparin and chemically modified heparin treatments could potentially be used to modulate HS biosynthesis and thereby the sulfation patterns in BCSCs, and thereby alter their phenotype and susceptibility to biological or therapeutic control.

The expression of HPSE has been reported in various types of human cancer. In addition, its expression was found to be linked with the reduction of patient survival and increased tumor metastasis (Arvatz et al., 2011). Here, adding PMHS to $CD44^{+}/CD24^{-}$ sorted cells from the MDA-MB-231 line produced a significant reduction in the transcription level of HPSE, while heparin increased the HPSE level. No significant effect was observed in cells treated with 2,6 deS-NS H. HS/heparin and 2,6deS-NS-H produced a significant increase in *HPSE* transcripts in $CD44^{+}/CD24^{-}$ sorted cells from Hs578-T cells. Previous study indicated that HPSE2 may regulate the enzymatic activity and signaling properties of HPSE, resulting in an anti-metastatic effect being proposed (Arvatz et al., 2011, Levy-Adam et al., 2010). Analysis of *HPSE2* transcription in both cell lines MDA-MB-231 and Hs578-T cells showed a noticeable increase in response to treatments, suggesting this may have a

beneficial effect on reducing heparanase activity. The upregulation of HPSE in tumours has been widely reported in the literature, although our results show that HS/heparin and selected modified heparin did appear to significantly increase its transcription levels (although the levels of protein could well be controlled by stability of mRNA isoforms). In addition, although, the interaction of HPSE2 with HS has been proposed to have anti-cancer properties, and are downregulated in major types cancer studied, the present study found that the addition of HS/heparin or modified heparin resulted in strong overexpression of HPSE2 in both cell lines (MDA-MB-231 and Hs578-T cells), pointing to this gene as a potentially interesting target for altering the progression of BCSCs.

Overall, analysis of the effect of HS/heparin and selected chemically modified heparin on the differential expression of the genes involved in the HSPG biosynthesis in BCSCs demonstrated that there are significant changes in their transcript levels. Although some variations were detectable (especially in 2,6 deS-NS H treatment in both cell lines MDA-MB-231 and Hs578-T human BCCs), most changes were identified after either PMHS or heparin treatments.

6 General discussion

Breast cancer is the most common cancer leading to death in women. A small subset of tumour cells, called CSCs or tumour-initiating cells (TICs), has been reported to contribute to breast cancer therapy failure, due to chemoresistance (Van Pham et al., 2012). Tumor progression is hypothesized to depend on the CSC theory, which states that CSCs self-renew (produce copies of themselves), some of which then differentiate to produce cancer cells, ultimately re-grow the cancer leading to relapse. These tumorigenic cells (a small fraction of the TICs) are similar to normal stem cells, being capable of self-renewal and differentiation, but the balance between these two processes is highly deregulated, causing tumour formation (Florio, 2011, Girouard and Murphy, 2011). Recently, targeting BCSCs has become a major focus in clinical trials and is considered a promising therapeutic option.

Isolating CSCs for model studies on their properties

Most commonly FACS has been used to separate CSCs from cell lines or tumor tissue, based on the expression of cell-surface markers (Al-Hajj et al., 2003). The first identified and isolated were $CD44^{+}CD24^{-/low}$ tumorigenic cells from breast non-tumourigenic cancer cells in eight of nine patients. (Singh et al., 2004) successfully isolated $CD133^{+}$ brain tumorigenic cells. Following this, by using different surface markers, a wide range of solid tumours such as prostate (Collins et al., 2005), pancreatic (Olempska et al., 2007) and colon (Ricci-Vitiani et al., 2007), cancer initiating cells were isolated successfully. In breast cancer (Al-Hajj et al., 2003) and other experimental studies CSCs have been correlated with behavior such as self-renewal, invasion and resistance to chemo and radio-therapy have also been investigated (Economopoulou et al., 2012, Sheridan et al., 2006). Although several studies investigated the role of CSCs in primary tumour growth, using large amounts of primary cells, or the technical complexity of studying these cells in *vivo*, presents challenge. Thus, alternative model systems such as cell lines need to be developed and exploited to initially understand the mechanisms involved in regulation of CSCs.

Here, CSCs have been successfully identified and isolated from two of the most commonly studied human BCC lines - MDA-MB-231 and Hs578-T. Based on a

combination of the CD44 and CD24 putative markers. It was observed that MDA-MB-231 and Hs578-T cells express significantly higher levels of CD44 and lower levels of CD24 compared to other common BCC lines (MCF-7-A, T47D and ZR-75-1); the percentage of the $CD44^+/CD24^-$ sub-population varied markedly, and in some cases differed compared to previous studies despite using similar methods and techniques (Bensimon et al., 2013, Sheridan et al., 2006), perhaps reflecting different clonal variations in these lines maintained over time in different labs. In addition, although, CD133 has been described as a stemness marker for identification of BCSCs, and the $CD133^+$ phenotype of BCCs associated with tumor-initiating capacity (Collina et al., 2015, Kagara et al., 2012, Wright et al., 2008), we could not observe and expression of the CD133 marker in any of the above studied BCC lines. This suggests that various measurement protocols used in different laboratory environments (eg antibodies), or different cell culture conditions (eg, serum type/source), may lead to lack of direct comparability of results. In addition, due to the different experimental protocols, the CSCs isolated may contain some non-CSC cancer cells, resulting in artifacts and bias for the analysis of CSC characteristics. More over, CD133 may not be restricted to BCSCs.

$CD44^+/CD24^-$ sub-populations isolated from MDA-MB-231 and Hs578-T cells displayed several properties typically seen in CSCs. It was found that the $CD44^+/CD24^-$ cells demonstrated enhanced growth and increased *in vitro* cell viability compared to $CD44^-/CD24^-$. It should be noted that the isolation of the CSC sub-population from cancer cells may affect restrictions of the cell microenvironment from competitor locations, including neighbouring cells and ECM. It is suggested that cell growth in culture has in many aspects much in common with suppressing the immune system, such as accelerated proliferation. Our functional analyses of BCSC characteristics demonstrated that $CD44^+/CD24^-$ cells isolated from MDA-MB-231 and Hs578-T BCCs reveal important novel features of CSCs including increased *in vitro* invasion, migration, adhesion and colony forming ability compared to the respective isolated sub-populations ($CD44^-/CD24^-$, $CD44^-/CD24^+$ and $CD44^+/CD24^+$). In addition, $CD44^+/CD24^-$ cells were less apoptotic and more resistant to chemotherapeutic agents including doxorubicin, tamoxofin and cisplatin compared to the $CD44^-/CD24^-$ subset. These findings indicate that a distinct $CD44^+/CD24^-$ subpopulation represents the putative CSC (or TICs) in BCCs.

Effects of HS/heparins on BCSCs

The experiments here demonstrated clear dose-responsive and structure-dependent effects of adding exogenous HS/heparin or modified heparins on the tumourigenic behaviour of BCSCs. These effects included significant reductions firstly in the actual levels of the $CD44^{+}/CD24^{-}$ sub-populations, and secondly decreases in their tumourigenic properties in various functional assays. Although adding different concentrations of HS/ heparin and chemically modified heparins to MDA-MB-231 and Hs578-T BCCs significantly reduced the $CD44^{+}/CD24^{-}$ sub-populations, effects at some concentrations particularly at lower concentrations of some heparin derivatives (2 deS-NAc H, 6 deS-NAc H and PMH in MDA-MB-231) were to significantly increase the $CD44^{+}$/ $CD24^{-}$ cells. Furthermore, higher concentrations of heparin derivatives (1-100 μg/ml) were apparently ineffective in the Hs578-T cell line, due in part to larger experimental variations. Care in interpretation of the structure-function relationships is also warranted, since the compounds are still heterogenous, being derived from the same PMH starting material (Celsus Laboratories, Cat. No. PH-3005, OH; USA). In previous work each of the modified heparins 1-8 were purified by size exclusion chromatography and treated with ion exchange resin prior to NMR analysis, followed by compositional analysis after digestion with heparinases I, II and III. It was evident that the polysaccharides were not absolutely pure and contained in some cases a low concentration of remaining disaccharide building blocks different from that predicted from the modifications performed (Table 6.1) (Patey et al., 2006). Nevertheless, these changes support the idea that the compounds with markedly differential structural patterns are causing both a phenotypic switch away from the $CD44^{+}/CD24^{-}$ phenotype, and also altering their responses to the tumour microenvironment. In the latter context, and perhaps most importantly in relation to possible future therapeutic opportunities, the compounds reduced the chemoresistance of $CD44^{+}/CD24^{-}$ treated cells (see below).

Table 6.1 Chemically modified heparins purity (Patey et al., 2006).

	Disaccharide standard							
	D1	D2	D3	D4	D5	D6	D7	D8
	ΔUA-GlcNAc	ΔUA-GlcNAc(6S)	ΔUA-GlcNS	ΔUA-GlcNS(6S)	ΔUA(2S)-GlcNS	ΔUA(2S)-GlcNS(6S)	ΔUA(2S)-GlcNAc	ΔUA(2S)-GlcNAc(6S)
P1	6.8	-	3.4	13.4	7.0	67.4	-	2.0
P2	14.2	7	-	-	-	3.5	-	75.3
P3	7.1	-	13.7	79.2	-	-	0	0
P4	14.4	62.9	3.4	19.3	-	-	-	-
P5	15.5	-	43.2	7.0	34.3	-	-	-
P6	55.8	7.7	-	-	-	-	34.8	1.7
P7	19.1	-	79.1	-	-	1.8	-	-
P8	99	-	-	-	-	-	-	1.0

*P1, PMIH; P2, *N*-acetyl*; P3,* UA-2-OH; P4, UA-2-OH, *N*-acetyl; P5, GlcN-6-OH; P6, GlcN-6-OH, *N*-acetyl*; P7,* UA-2-OH, GlcN-6-OH; P8, UA-2-OH, GlcN-6-OH, *N*-acetyl.

Chemoresistance of BCSCs are modified by exogenous heparins

It is known that conventional chemotherapies used at present are initially effective in killing growing differentiated cells and controlling tumor growth. However, these therapies have been observed to fail to kill CSCs (Dean et al., 2005). One explanation for that is that cells have high tumorigenic properties, making them resistant to chemotherapy (Li et al., 2008). A wide range of studies of the resistance of BCSCs to chemotherapy has been reported (Li et al., 2008). Specifically, previous work suggested that $CD44^{+}/CD24^{-/low}$ BCSCs were more resistant to DNA-damaging drugs such as (doxorubicin and cisplatin) than the unsorted cells (Wright et al., 2008). Therefore, the present study tested the effect of chemotherapy drugs (doxorubicin, cisplatin) on unsorted and sorted ($CD44^{+}/CD24^{-/}$ and $CD44^{-}/CD24^{-}$) cells from MDA-MB-231 and Hs578-T BCCs. Apoptosis results showed a significant resistance to both doxorubicin and cisplatin in $CD44^{+}/CD24^{-/}$ sorted cells from MDA-MB-231 and Hs578-T, compared to the unsorted and sorted $CD44^{-}/CD24^{-}$ cells. It should be noted that these are the front-line therapies in most chemotherapies for ER negative breast cancer patients.

The ER antagonist Tamoxifen has been widely used as a hormone therapy for the treatment for breast patients with hormone receptor-positive breast cancer (Bursch et

al., 1996). In contrast, a few studies suggested that, in a dose- and time-dependent manner the tamoxifen agent induces apoptosis in triple-negative breast cancer cells MDA-MB-231 through downregulation of CIP2A/PP2A/p-Akt signaling (Liu et al., 2014a). Therefore, in the present studies the effective dose and treatment time of tamoxifen were initially identified and optimized by flow cytometry on isolated BCSCs and compared with results from $CD44^-/CD24^-$ or parental cells of both BCC lines (MDA-MB-231 and Hs578-T) MCF-7. In contrast to doxorubicin and cisplatin drugs, the tamoxifen experimental results demonstrated that no significant increase of apoptotic cells occurred at low concentrations of tamoxifen (1-100 nM) at different time points 24, 48 and 72 hrs in both MDA-MB-231 and Hs578-T cells. High concentrations of tamoxifen however induced a significant increase in apoptotic cells compared to untreated cells. Interestingly, $CD44^+/CD24^-$ cells from MDA-MB-231 and Hs578-T lines consisted of less apoptotic cells upon tamoxifen treatment compared to $CD44^-/CD24^-$ and parental cells. Our findings are consistent with previous studies demonstrating that BCSCs show a significant resistance to undergo apoptosis in response to current chemo- and hormonal therapies, thus enhancing malignant behavior of tumours.

During the metastasis process, cells alter their adhesion abilities to facilitate migration through the ECM and basement membranes, migrating into distant organs and finally forming metastases after proliferation, as well as promoting angiogenesis (Olson and Sahai, 2009). In order to understand the molecular foundation of tumour cell invasion, migration, adhesion and chemoresistance it is essential to identify molecular systems which underpin these processes, which may then be attractive therapeutic targets for CSCs. There is substantial evidence for the role of heparin and heparin derivatives as anti-metastasis agents with action against cancer-specific mechanisms, including functions of standard heparin/LMWH in inhibiting selectins (Läubli et al., 2009), and for low sulfated modified heparins in inhibiting galectin-3 interactions (Duckworth et al., 2015). As stated before, HS can bind to a wide range of proteins and regulate cell motility, and cell-cell and cell-ECM adhesion, through molecular signaling pathways (Turnbull et al., 2001). In tumours, the expression of HS has a link with tumour development and progression. The studies here have employed *in vitro* BCC cell systems and have helped delineate specific roles for heparin derivatives in BCSC proliferation, invasion, migration, adhesion and chemo-

resistance, identifying multiple roles of HS/heparin and chemically modified heparin in governing these properties of $CD44^+/CD24^-$ isolated cells from MDA-MB-231 and Hs578-T BCC lines. It was noted that HS/heparin and chemically modified heparins, at notably low concentrations (low ng/ml) in most cases, caused a marked inhibition of cell proliferation, invasion, migration and adhesion in $CD44^+/CD24^-$ sorted cells from MDA-MB-231 and Hs578-T human BCCs compared to untreated cells. Importantly, a combination of low concentrations of a number of the HS/heparin and chemically modified heparins was sufficient, with either doxorubicin, cisplatin or tamoxifen, to increase the apoptotic percentage of $CD44^+/CD24^-$ sorted cells from MDA-MB-231 or Hs578T cells compared to cells treated with chemotherapy agent alone. Thus, it is clear that CSCs from BCCs can be sensitized to induction of apoptosis via a number of chemotherapeutic agents if treated with heparin-based compounds, providing potential new opportunities for therapeutic strategies to target CSCs more effectively. Only a single dose of HS/heparins (10ng/ml) was tested in these experiments, based on optimal doses determined for effects on other BCSC properties; thus, in future work it would be useful to undertake more detailed dose response studies on this specific aspect of the effects of HS/modified heparin on inducing chemoresistance, as this would provide valuable information on the likely clinical doses that might be needed. Nevertheless, the low dose needed to obtain these effects is very encouraging, since it would easily be achievable *in vivo*, based on existing pharmacokinetic data showing that 3mg/kg LMWH administration results in peak blood levels of ~3ug/ml (Zhao et al., 2016)

Exploring mechanisms underlying CSC regulation by HS/heparins

CSC markers and drug resistance*:* As mentioned previously, $CD44^+/CD24^-$ BCCs are associated with tumor-initiating properties, enhanced invasiveness and metastasis (Ratajczak et al., 2010) and chemotherapeutic resistance (Pinto et al., 2013). A number of markers linked to these properties have been identified and were studied here. CD44, a well described CSC marker, was (by definition) highly expressed in $CD44^+/CD24^-$ isolated cells from both cell lines. The present study showed lack of constitutive expression of the EpCAM CSC marker in $CD44^+/CD24^-$ and $CD44^-/CD24^-$ sorted cells from parental human BCC lines MDA-MB-231 and Hs578-T. Of note, most other available human BCC lines are identified to be high expressors of

EpCAM protein, yet MDA-MB-231 and Hs578-T cells have low or even no EpCAM expression. The very low expression of EpCAM that was detected in both cell lines is thus similar to that described in most previous reports (Martowicz et al., 2012, Prang et al., 2005). Over-expression of BCRP/ABCG2 is believed to be involved in drug resistance mechanisms (Dean et al., 2005). Consist with this result; ABCG2 was highly expressed in the $CD44^{+}/CD24^{-}$ cells relative to $CD44^{-}/CD24^{-}$ cells in both MDA-MB-231 and Hs578-T human BCCs.

Moreover, the present study took advantage of the $CD44^{+}/CD24^{-}$ sub-populations as BCSC models to demonstrate whether HS/heparin compounds could alter expression of CSC markers and drug resistance genes in BCSCs. The results indicated that some drug resistance genes and stem cell markers are indeed altered in $CD44^{+}/CD24^{-}$ cells. These included firstly downregulation of CD44 expression (consistent with a switch towards a $CD44^{-}/CD24^{-}$ phenotype); and secondly, elevated expression of ABCG2 (which would be consistent with a feedback mechanism responding to inhibition of ABCG2 activity). Inhibition of ATPase activity of ABCG2 has previously been observed for heparin (Chen et al 2014) Future studies to examine the direct effects of the HS and modified heparin compounds on ATPase activity of ABCG2 are now warranted. Overall HS/ heparin and chemically modified heparins have been demonstrated to have pivotal effects on a number of key genes which provide plausible mechanisms for decreasing the $CD44^{+}/CD24^{-}$ sub-population of BCSCs, and potentially increasing their chemosensitivity.

Angiogenic factors: Angiogenesis is known to be involved in tumor development and progression and is controlled by pro-angiogenic and anti-angiogenic factors induced by several cell types in the tumor microenvironment (Bouïs et al., 2006, Saarinen et al., 2010). Angiogenesis requires the activation of endothelial cells by angiogenic factors, from a quiescent state to a migratory, then proliferative and stabilized phenotype; this is induced and controlled by activator and inhibitor molecules, most notably growth factors such as VEGF (Nishida et al., 2006). There is substantial evidence for the role of angiogenesis in BC growth and progression (Boudreau and Myers, 2003, Longatto Filho et al., 2010). The present study demonstrated that BCSCs can produce factors which would be expected to promote angiogenesis; furthermore, the studies established that HS and chemically modified

heparins modulate these factors in human BCSCs. Several pro-angiogenic genes including Ang-1, Ang-2, VEGFA, VEGFB and IL-8 were highly expressed in $CD44^{+}/CD24^{-}$ sub-population cells in comparison to $CD44^{+}/CD24^{-}$ sub-population cells in MDA-MB-231 cells. Human BCC line Hs578-T also showed a significant increased in Ang-1, VEGFB and IL-8. Angiogenesis stimulation by BC cells has been linked to an increase of VEGF production by the tumor cells and by cells within the tumor stroma (Nishida et al., 2006), However, VEGFA and Ang-1 expression levels were significant in $CD44^{+}/CD24^{-}$ cells relative to $CD44^{-}/CD24^{-}$ cells. A number of these markers were observed to be down-regulated by exposure of $CD44^{+}/CD24^{-}$ cells to HS/heparin and modified heparins, indicating that they can modulate this important feature of their tumourigenic phenotype.

In addition, chemokines and their receptors have been demonstrated to be involved in CSC-mediated angiogenic factor production (Liekens et al., 2010). The chemokine receptor CXCR4 has been observed to play a pivotal role in cancer angiogenesis and to be preferentially expressed by glioblastoma stem cells (Ehtesham et al., 2009, Liekens et al., 2010). The present study observed that CXCR4 levels were also significantly higher in $CD44^{+}/CD24^{-}$ cells relative to $CD44^{-}/CD24^{-}$ in both MDA-MB-231 and Hs578-T BCCs. Importantly, CXCR4 was significantly downregulated in cells treated with HS/heparin and chemically modified heparins. Overall, since these compounds differentially affected expression of various angiogenic markers in $CD44^{+}/CD24^{-}$ BCCs, it is clear that endogenous HS contributes significantly to a greater pro-angiogenic potential of BCCs, and represent useful targets for effective anti-angiogenic therapies.

FGF2/ERK1/2 signalling: ERK1/2 is one class of MAPK intracellular signaling cascades implicated in human breast tumors. ERK1/2 signaling pathways were estimated to be involved in approximately 30% of human BCs (Whyte et al., 2009). A survival analysis reported that a higher expression of pERK1/2 in primary tumors impacts metastasis, and a lower expression of pERK1/2 in primary BCs is prognostic for relapse-free survival of patients (Mueller et al., 2000). In addition, the expression of pERK1/2 can impact a patient's response to treatment (McGlynn et al., 2009, Mueller et al., 2000, Santen et al., 2002). Accumulating evidence suggests that FGF2 and cell surface HSPGs interact to induce intracellular signals (Chua et al., 2004).

Since HS and heparin are known to regulate the FGF2/ERK1/2 pathway (Chua et al., 2004), we questioned whether FGF2-stimulated ERK1/2 activation could be modulated by HS/heparin or chemically modified heparin on BCSCs. FGF2 stimulated the ERK1/2 phosphorylation, whereas HS/heparin and chemically modified heparins could decrease both the intensity and duration of ERK1/2 activation in the $CD44^{+}/CD24^{-}$ sub-population from MDA-MB-231 and Hs578-T BCCs. An opposite effect was observed when HS/heparin and chemically modified heparin was used alone, since a significant increase of ERK1/2 phosphorylation level was observed in $CD44^{+}/CD24^{-}$ cells sorted from both MDA-MB-231 and Hs578-T cells. Thus, when BCSCs are undergoing active FGF-stimulated responses via pERK1/2, the compounds could block this activity. Thus, interference with HS/FGF/FGFR interactions could provide an additional mechanism by which this class of compounds suppresses the tumourigenic properties of BCSCs that depend on this signaling axis.

IL-6/STAT3 signalling: Previous results demonstrated that inhibition of IL-6 gene expression reduces proliferation of $CD44^{+}/CD24^{-}$ human BCCs, via reduced activation of STAT3. In addition, the IL-6/JAK2/Stat3 signaling pathway was significantly active in $CD44^{+}/CD24^{-}$ BCCs in comparison to the other cancer cell types (Marotta et al., 2011). Due to the high expression of IL-6 and IL-8 in $CD44^{+}/CD24^{-}$ sub-population (Sheridan et al., 2006) we were interested in whether HS and chemically modified heparins might affect their action in BCSCs. An increasing number of IL cytokines have been found to bind to HS and heparin. The interaction of IL-6 is highly highly pleiotropic, with HS and heparin found to regulate different mechanisms. However, these cytokines may also be released into the circulatory system, possibly bound to GAG-peptide fragments or GAG oligosaccharides (Mummery and Rider, 2000). Thus, HS may play important roles in regulating IL-6 activity. It was found here that HS/heparin and 2,6 deS-NS H significantly reduced IL-6 expression in $CD44^{+}/CD24^{-}$ cells of MDA-MB-231 and Hs578-T human BCCs. Moreover, treatment of $CD44^{+}/CD24^{-}$ cells with HS/heparin and chemically modified heparins attenuated IL-6 signalling measured by inhibition of the phosphorylation of STAT3, in both MDA-MB-231 and Hs578-T cells. This data indicates a clear role for HS in modulating the STAT3/IL-6 signaling pathway in BCSCs properties, and provides an additional important axis for targeting these

cells in therapies using HS/heparin/modified heparins.

Other mechanisms of action: The above described work clearly demonstrated effects of the compounds were exerted in BCSCs via at least 3 signalling pathways, namely FGF2/FGFR and IL-6/Stat3 and VEGF. Since HS is known to be involved in many GF signaling pathways, it was reasonable to hypothesise that multiple additional pathways might be affected, and this could be one of the principle mechanisms of action of the compounds. To explore this possibility some initial experiments using Pathscan ELISA slides were undertaken. These studies firstly confirmed effects via MAPK/ERK1/2 and Stat3, but secondly revealed for the first time effects of this class of compounds on additional pathways including AMPKα, mTOR and S6 ribosomal protein. Since these pathways are known to be linked to important tumourigenic properties of BCSCs, they now provide new targets for more detailed mechanism of action studies in the future to evaluate dose responses and structural selectivity. Overall, the results also provide further evidence that HS, heparin and chemically modified heparins act on BCSC behaviour via modulating (activating or inhibiting) multiple signaling pathways, in a selective structure-dependent manner.

Finally, it has previously been reported that heparin can induce changes in HS biosynthesis (Skaletz-Rorowski et al., 1996) Thus we hypothesized that addition of exogenous HS, heparin and modified heparins might also act via such mechanisms. Initial qRT-PCR analysis indeed revealed significantly altered expression of genes for HSPG core proteins, biosynthetic enzymes, extracellular sulfatases and heparanase. These preliminary results suggest additional mechanisms by which the compounds influence BCSC behaviour, with a complex interplay between endogenous HS production and feedback from responses to exogenous HS and related molecules, which collectively influence cell responses to HS-dependent proteins. Since this data only demonstrates changes in mRNA levels, further work is needed to establish whether changes in protein expression and ultimately HS structure are actually induced. But overall this data suggests that this would be a rich source of interesting new information on dynamic and responsive changes to the "heparanome" that might be crucial for the tumour biology of BSCSs and other cell types.

Future approaches – towards clinical applications?

Although more work is needed to further define the multiple mechanisms of action of HS and chemically modified heparin polysaccharides on BCSCs, and the underlying functions of the endogenous HS in BCSCs, the work presented here revealed a number of different ways in which HS may be involved in the tumourigenic and metastatic properties of BCSCs. Furthermore, these data have opened up a number of avenues for potential exploitation of HS and chemically modified heparin polysaccharides in targeting CSCs for BC treatment. To validate this possibility *in vivo* experiments are now warranted. Firstly to explore whether BC CSCs pre-treated *in vitro* with the compounds are subsequently less tumourigenic/metastatic when tested in *in vivo* mouse models. Secondly, it would be of interest to test administration of the compounds *in vivo*, to investigate whether tumours induced by injection of BCCs express lower levels of CSCs as would be predicted from our studies. And finally to address the question as to whether the administration of the compounds in such models confirms that tumours display reduced tumour forming ability, metastasis and increased chemosensitivity. If successful these studies would pave the way for clinical trials, perhaps initially in triple negative BC patients which are otherwise very difficult to treat with current therapies. In this context it is worth commenting that heparin/LMWH as a class have an exceptionally long history of safe clinical use; furthermore recently developed modified heparins also display notably low toxicity and lack of target anticoagulant activity (Duckworth et al., 2015, Kovacsovics et al., 2015), making them ideal for such clinical applications.

In addition, these studies have shown clearly that stem cells are sensitive to manipulation by the HS/heparin class of compounds, which control a number of important cell regulatory pathways. In the future, it would be invaluable to explore other applications of these compounds to target stem cell functions, for example in enhancing the responses of endogenous stem cells in repair and regeneration of damaged tissues, and in producing specific stem cells for transplantation to treat damage such as spinal cord injury, or for neurodegenerative conditions such as Parkinson's and Alzheimer's disease.

Final Conclusions

To our knowledge, these are the first results clearly demonstrating an association between BCSCs response to chemotherapeutic agents and treatment with HS/heparin and chemically modified heparin polysaccharides. The results elucidated the importance of HS in some molecular signaling pathways underlying critical BCSC properties that confer their enhanced tumourigenic properties, and demonstrated that the levels of BCSC sub-populations, and their resistance to chemotherapeutic agents, can be decreased by HS/heparin compounds, at least *in vitro*. In addition the studies support the view that HSPGs are important regulators of BCSC progression through regulation of cell invasion, migration and adhesion. This work demonstrated that treatment with HS and chemically modified heparin reduces the BCSC pools both in the aggressive triple negative human MDA-MB-231 cell line and in moderately aggressive human Hs578-T cells. This reduced CSC stemness was associated with downregulation of PAR-1/thrombin, FGF2/ERK1/2, and IL-6/STAT3 signaling pathways in triple-negative cells to differentially mediate breast cancer epithelial cell proliferation, invasion, migration and adhesion. Thus HS-dependent functions emerge as a promising supportive target for combined therapeutic approaches to inhibit CSC stemness, potentially preventing relapse compared to conventional therapy

7 References

Abdullah, L. N. & Chow, E. K.-H. (2013). Mechanisms of chemoresistance in cancer stem cells. *Clinical and translational medicine,* 2**,** 1.

Abraham, B. K., Fritz, P., McClellan, M., Hauptvogel, P., Athelogou, M. & Brauch, H. (2005). Prevalence of CD44+/CD24−/low cells in breast cancer may not be associated with clinical outcome but may favor distant metastasis. *Clinical Cancer Research,* 11**,** 1154-1159.

Aikawa, J.-i., Grobe, K., Tsujimoto, M. & Esko, J. D. (2001). Multiple Isozymes of Heparan Sulfate/Heparin GlcNAcN-Deacetylase/GlcN N-Sulfotransferase STRUCTURE AND ACTIVITY OF THE FOURTH MEMBER, NDST4. *Journal of Biological Chemistry,* 276**,** 5876-5882.

Al-Hajj, M., Wicha, M. S., Benito-Hernandez, A., Morrison, S. J. & Clarke, M. F. (2003). Prospective identification of tumorigenic breast cancer cells. *Proceedings of the National Academy of Sciences,* 100**,** 3983-3988.

Arima, Y., Hayashi, N., Hayashi, H., Sasaki, M., Kai, K., Sugihara, E., Abe, E., Yoshida, A., Mikami, S. & Nakamura, S. (2012). Loss of p16 expression is associated with the stem cell characteristics of surface markers and therapeutic resistance in estrogen receptor-negative breast cancer. *International Journal of Cancer,* 130**,** 2568-2579.

Arvatz, G., Shafat, I., Levy-Adam, F., Ilan, N. & Vlodavsky, I. (2011). The heparanase system and tumor metastasis: is heparanase the seed and soil? *Cancer and Metastasis Reviews,* 30**,** 253-268.

Atkinson, R. L., Yang, W. T., Rosen, D. G., Landis, M. D., Wong, H., Lewis, M. T., Creighton, C. J., Sexton, K. R., Hilsenbeck, S. G. & Sahin, A. A. (2013). Cancer stem cell markers are enriched in normal tissue adjacent to triple negative breast cancer and inversely correlated with DNA repair deficiency. *Breast Cancer Research,* 15**,** 1.

Aznar, S., Valerón, P. F., del Rincon, S. V., Pérez, L. F., Perona, R. & Lacal, J. C. (2001). Simultaneous tyrosine and serine phosphorylation of STAT3 transcription factor is involved in Rho A GTPase oncogenic transformation. *Molecular biology of the cell,* 12**,** 3282-3294.

Baba, F., Swartz, K., van Buren, R., Eickhoff, J., Zhang, Y., Wolberg, W. & Friedl, A. (2006). Syndecan-1 and syndecan-4 are overexpressed in an estrogen receptor-negative, highly proliferative breast carcinoma subtype. *Breast cancer research and treatment,* 98**,** 91-98.

Bachelot, T., Ray-Coquard, I., Menetrier-Caux, C., Rastkha, M., Duc, A. & Blay, J. (2003). Prognostic value of serum levels of interleukin 6 and of serum and plasma levels of vascular endothelial growth factor in hormone-refractory metastatic breast cancer patients. *British journal of cancer,* 88**,** 1721-1726.

Bao, S., Wu, Q., Sathornsumetee, S., Hao, Y., Li, Z., Hjelmeland, A. B., Shi, Q., McLendon, R. E., Bigner, D. D. & Rich, J. N. (2006). Stem cell–like glioma cells promote tumor angiogenesis through vascular endothelial growth factor. *Cancer research,* 66**,** 7843-7848.

Barbareschi, M., Maisonneuve, P., Aldovini, D., Cangi, M. G., Pecciarini, L., Angelo Mauri, F., Veronese, S., Caffo, O., Lucenti, A. & Palma, P. D. (2003). High syndecan-1 expression in breast carcinoma is related to an aggressive phenotype and to poorer prognosis. *Cancer,* 98**,** 474-483.

Beauvais, D. M. & Rapraeger, A. C. (2003). Syndecan-1-mediated cell spreading requires signaling by α v β 3 integrins in human breast carcinoma cells. *Experimental cell research,* 286**,** 219-232.

Beckmann, J., Scheitza, S., Wernet, P., Fischer, J. C. & Giebel, B. (2007). Asymmetric cell division within the human hematopoietic stem and progenitor cell compartment: identification of asymmetrically segregating proteins. *Blood,* 109**,** 5494-5501.

Bensimon, J., Altmeyer-Morel, S., Benjelloun, H., Chevillard, S. & Lebeau, J. (2013). CD24−/low stem-like breast cancer marker defines the radiation-resistant cells involved in memorization and transmission of radiation-induced genomic instability. *Oncogene,* 32**,** 251-258.

Bernfield, M., Götte, M., Park, P. W., Reizes, O., Fitzgerald, M. L., Lincecum, J. & Zako, M. (1999). Functions of cell surface heparan sulfate proteoglycans. *Annual review of biochemistry,* 68**,** 729-777.

Bezakova, G. & Ruegg, M. A. (2003). New insights into the roles of agrin. *Nature Reviews Molecular Cell Biology,* 4**,** 295-309.

Biddle, A., Liang, X., Gammon, L., Fazil, B., Harper, L. J., Emich, H., Costea, D. E. & Mackenzie, I. C. (2011). Cancer stem cells in squamous cell carcinoma switch between two distinct phenotypes that are preferentially migratory or proliferative. *Cancer research,* 71**,** 5317-5326.

Bonneh-Barkay, D., Shlissel, M., Berman, B., Shaoul, E., Admon, A., Vlodavsky, I., Carey, D. J., Asundi, V. K., Reich-Slotky, R. & Ron, D. (1997). Identification of glypican as a dual modulator of the biological activity of fibroblast growth factors. *Journal of Biological Chemistry,* 272**,** 12415-12421.

Bonnet, D. & Dick, J. (1997). Human acute myeloid leukemia is organized as a hierarchy that originates from a primitive hematopoietic cell. *Nature medicine,* 3**,** 730-737.

Boudreau, N. & Myers, C. (2003). Breast cancer-induced angiogenesis: multiple mechanisms and the role of the microenvironment. *Breast cancer research,* 5**,** 1.

Bouïs, D., Kusumanto, Y., Meijer, C., Mulder, N. H. & Hospers, G. A. (2006). A review on pro-and anti-angiogenic factors as targets of clinical intervention. *Pharmacological research,* 53**,** 89-103.

Bretz, N., Noske, A., Keller, S., Erbe-Hofmann, N., Schlange, T., Salnikov, A. V., Moldenhauer, G., Kristiansen, G. & Altevogt, P. (2012). CD24 promotes tumor cell invasion by suppressing tissue factor pathway inhibitor-2 (TFPI-2) in a c-Src-dependent fashion. *Clinical & experimental metastasis,* 29**,** 27-38.

Bromberg, J. & Wang, T. C. (2009). Inflammation and cancer: IL-6 and STAT3 complete the link. *Cancer cell,* 15**,** 79-80.

Bui, C., Ouzzine, M., Talhaoui, I., Sharp, S., Prydz, K., Coughtrie, M. W. & Fournel-Gigleux, S. (2010). Epigenetics: methylation-associated repression of heparan sulfate 3-O-sulfotransferase gene expression contributes to the invasive phenotype of H-EMC-SS chondrosarcoma cells. *The FASEB Journal,* 24**,** 436-450.

Bursch, W., Ellinger, A., Kienzl, H., Török, L., Pandey, S., Sikorska, M., Walker, R. & Hermann, R. S. (1996). Active cell death induced by the anti-estrogens tamoxifen and ICI 164 384 in human mammary carcinoma cells (MCF-7) in culture: the role of autophagy. *Carcinogenesis,* 17**,** 1595-1607.

Busse, M., Feta, A., Presto, J., Wilén, M., Grønning, M., Kjellén, L. & Kusche-Gullberg, M. (2007). Contribution of EXT1, EXT2, and EXTL3 to heparan sulfate chain elongation. *Journal of Biological Chemistry,* 282**,** 32802-32810.

Byrne, A. M., Bouchier-Hayes, D. J. & Harmey, J. H. (2005). Angiogenic and cell survival functions of vascular endothelial growth factor (VEGF). *Journal of cellular and molecular medicine,* 9**,** 777-794.

Byrne, G., McDowell, G., Agarawal, R., Sinha, G., Kumar, S. & Bundred, N. (2007). Serum vascular endothelial growth factor in breast cancer. *Anticancer research,* 27**,** 3481-3487.

Cao, L., Zhou, Y., Zhai, B., Liao, J., Xu, W., Zhang, R., Li, J., Zhang, Y., Chen, L. & Qian, H. (2011). Sphere-forming cell subpopulations with cancer stem cell properties in human hepatoma cell lines. *BMC gastroenterology,* 11**,** 71.

Casu, B. & Lindahl, U. (2001). Structure and biological interactions of heparin and heparan sulfate. *Advances in carbohydrate chemistry and biochemistry,* 57**,** 159-206.

Catlow, K., Deakin, J. A., Delehedde, M., Fernig, D., Gallagher, J. T., Pavão, M. & Lyon, M. (2003). Hepatocyte growth factor/scatter factor and its interaction with heparan sulphate and dermatan sulphate. *Biochemical Society Transactions,* 31**,** 352-353.

Chan, W. K., Howe, K., Clegg, J. M., Guimond, S. E., Price, D. J., Turnbull, J. E. & Pratt, T. (2015). 2-O Heparan Sulfate Sulfation by Hs2st Is Required for Erk/Mapk Signalling Activation at the Mid-Gestational Mouse Telencephalic Midline. *PloS one,* 10**,** e0130147.

Charafe-Jauffret, E., Ginestier, C., Monville, F., Finetti, P., Adelaide, J., Cervera, N., Fekairi, S., Xerri, L., Jacquemier, J. & Birnbaum, D. (2006). Gene expression profiling of breast cell lines identifies potential new basal markers. *Oncogene,* 25**,** 2273-2284.

Chen, E., Hermanson, S. & Ekker, S. C. (2004). Syndecan-2 is essential for angiogenic sprouting during zebrafish development. *Blood,* 103**,** 1710-1719.

Chen, W. J. & Abatangelo, G. (1999). Functions of hyaluronan in wound repair. *Wound Repair and Regeneration,* 7**,** 79-89.

Chen, Y., Scully, M., Petralia, G. & Kakkar, A. (2014). Binding and inhibition of drug transport proteins by heparin: a potential drug transporter modulator capable of reducing multidrug resistance in human cancer cells. *Cancer biology & therapy,* 15**,** 135-145.

Chen, Z., Jing, Y., Song, B., Han, Y. & Chu, Y. (2009). Chemically modified heparin inhibits in vitro L-selectin-mediated human ovarian carcinoma cell adhesion. *International Journal of Gynecological Cancer,* 19**,** 540-546.

Cheng, D., Liang, B. & Li, Y. (2015). Serum galectin-3 as a potential marker for gastric cancer. *Medical Science Monitor,* 21**,** 755-760.

Chiang, M.-K. & Flanagan, J. G. (1995). Interactions between the Flk-1 receptor, vascular endothelial growth factor, and cell surface proteoglycan identified with a soluble receptor reagent. *Growth Factors,* 12**,** 1-10.

Chua, C. C., Rahimi, N., Forsten-Williams, K. & Nugent, M. A. (2004). Heparan sulfate proteoglycans function as receptors for fibroblast growth factor-2 activation of extracellular signal–regulated kinases 1 and 2. *Circulation research,* 94**,** 316-323.

Cohen, T., Gitay-Goren, H., Sharon, R., Shibuya, M., Halaban, R., Levi, B. & Neufeld, G. (1995). VEGF121, a vascular endothelial growth factor (VEGF) isoform lacking heparin binding ability, requires cell-surface heparan sulfates

for efficient binding to the VEGF receptors of human melanoma cells. *Journal of Biological Chemistry,* 270**,** 11322-11326.

Cojoc, M., Mäbert, K., Muders, M. H. & Dubrovska, A. A role for cancer stem cells in therapy resistance: cellular and molecular mechanisms. Seminars in cancer biology, 2015. Elsevier, 16-27.

Cojoc, M., Peitzsch, C., Trautmann, F., Polishchuk, L., Telegeev, G. D. & Dubrovska, A. (2013). Emerging targets in cancer management: role of the CXCL12/CXCR4 axis. *Onco Targets Ther,* 6**,** 1347-1361.

Cole, C. L., Hansen, S. U., Barath, M., Rushton, G., Gardiner, J. M., Avizienyte, E. & Jayson, G. C. (2010). Synthetic heparan sulfate oligosaccharides inhibit endothelial cell functions essential for angiogenesis. *PLoS One,* 5**,** e11644.

Collina, F., Di Bonito, M., Li Bergolis, V., De Laurentiis, M., Vitagliano, C., Cerrone, M., Nuzzo, F., Cantile, M. & Botti, G. (2015). Prognostic value of cancer stem cells markers in triple-negative breast cancer. *BioMed research international,* 2015.

Collins, A. T., Berry, P. A., Hyde, C., Stower, M. J. & Maitland, N. J. (2005). Prospective identification of tumorigenic prostate cancer stem cells. *Cancer research,* 65**,** 10946-10951.

Couchman, J. R., Chen, L. & Woods, A. (2001). Syndecans and cell adhesion. *International review of cytology,* 207**,** 113-150.

Croker, A. K., Goodale, D., Chu, J., Postenka, C., Hedley, B. D., Hess, D. A. & Allan, A. L. (2009). High aldehyde dehydrogenase and expression of cancer stem cell markers selects for breast cancer cells with enhanced malignant and metastatic ability. *Journal of cellular and molecular medicine,* 13**,** 2236-2252.

de Beça, F. F., Caetano, P., Gerhard, R., Alvarenga, C. A., Gomes, M., Paredes, J. & Schmitt, F. (2013). Cancer stem cells markers CD44, CD24 and ALDH1 in breast cancer special histological types. *Journal of clinical pathology,* 66**,** 187-191.

Dean, M., Fojo, T. & Bates, S. (2005). Tumour stem cells and drug resistance. *Nature Reviews Cancer,* 5**,** 275-284.

Delehedde, M., Seve, M., Sergeant, N., Wartelle, I., Lyon, M., Rudland, P. S. & Fernig, D. G. (2000). Fibroblast Growth Factor-2 Stimulation of p42/44MAPKPhosphorylation and IκB Degradation Is Regulated by Heparan Sulfate/Heparin in Rat Mammary Fibroblasts. *Journal of Biological Chemistry,* 275**,** 33905-33910.

Dent, S. (2009). The role of VEGF in triple-negative breast cancer: where do we go from here? *Annals of oncology,* 20**,** 1615-1617.

Dick, D. Human acute myeloid leukemia is organized as a hierarchy that originates from a primitive hematopoietic cell.

Dontu, G., Al-Hajj, M., Abdallah, W. M., Clarke, M. F. & Wicha, M. S. (2003). Stem cells in normal breast development and breast cancer. *Cell proliferation,* 36**,** 59-72.

Dou, J. & Gu, N. (2010). Emerging strategies for the identification and targeting of cancer stem cells. *Tumor Biology,* 31**,** 243-253.

Dou, J., Pan, M., Wen, P., Li, Y., Tang, Q., Chu, L., Zhao, F., Jiang, C., Hu, W. & Hu, K. (2007). Isolation and identification of cancer stem-like cells from murine melanoma cell lines.

Dougher, A. M., Wasserstrom, H., Torley, L., Shridaran, L., Westdock, P., Hileman, R. E., Fromm, J. R., Anderberg, R., Lyman, S. & Linhardt, R. J. (1997).

Identification of a heparin binding peptide on the extracellular domain of the KDR VEGF receptor. *Growth Factors,* 14**,** 257-268.

Dowsland, M., Harvey, J., Lennard, T., Kirby, J. & Ali, S. (2003). Chemokines and breast cancer: a gateway to revolutionary targeted cancer treatments? *Current medicinal chemistry,* 10**,** 579-592.

Dreyfuss, J. L., Regatieri, C. V., Jarrouge, T. R., Cavalheiro, R. P., Sampaio, L. O. & Nader, H. B. (2009). Heparan sulfate proteoglycans: structure, protein interactions and cell signaling. *Anais da Academia Brasileira de Ciencias,* 81**,** 409-429.

Duckworth, C. A., Guimond, S. E., Sindrewicz, P., Hughes, A. J., French, N. S., Lian, L.-Y., Yates, E. A., Pritchard, D. M., Rhodes, J. M. & Turnbull, J. E. (2015). Chemically modified, non-anticoagulant heparin derivatives are potent galectin-3 binding inhibitors and inhibit circulating galectin-3-promoted metastasis. *Oncotarget,* 6**,** 23671.

Economopoulou, P., Kaklamani, V. G. & Siziopikou, K. (2012). The role of cancer stem cells in breast cancer initiation and progression: potential cancer stem cell-directed therapies. *The oncologist,* 17**,** 1394-1401.

Ehtesham, M., Mapara, K. Y., Stevenson, C. B. & Thompson, R. C. (2009). CXCR4 mediates the proliferation of glioblastoma progenitor cells. *Cancer letters,* 274**,** 305-312.

Esko, J. D., Kimata, K. & Lindahl, U. (2009). Proteoglycans and sulfated glycosaminoglycans.

Esko, J. D. & Lindahl, U. (2001). Molecular diversity of heparan sulfate. *The Journal of clinical investigation,* 108**,** 169-173.

Essner, J. J., Chen, E. & Ekker, S. C. (2006). Syndecan-2. *The international journal of biochemistry & cell biology,* 38**,** 152-156.

Evanko, S. P., Tammi, M. I., Tammi, R. H. & Wight, T. N. (2007). Hyaluronan-dependent pericellular matrix. *Advanced drug delivery reviews,* 59**,** 1351-1365.

Feyzi, E., Lustig, F., Fager, G., Spillmann, D., Lindahl, U. & Salmivirta, M. (1997). Characterization of heparin and heparan sulfate domains binding to the long splice variant of platelet-derived growth factor A chain. *Journal of Biological Chemistry,* 272**,** 5518-5524.

Fillmore, C. & Kuperwasser, C. (2007). Human breast cancer stem cell markers CD44 and CD24: enriching for cells with functional properties in mice or in man? *Breast Cancer Research,* 9**,** 1.

Fitzgerald, J. P., Nayak, B., Shanmugasundaram, K., Friedrichs, W., Sudarshan, S., Eid, A. A., DeNapoli, T., Parekh, D. J., Gorin, Y. & Block, K. (2012). Nox4 mediates renal cell carcinoma cell invasion through hypoxia-induced interleukin 6-and 8-production. *PloS one,* 7**,** e30712.

Florio, T. (2011). Adult pituitary stem cells: from pituitary plasticity to adenoma development. *Neuroendocrinology,* 94**,** 265-277.

Forsten-Williams, K., Chu, C. L., Fannon, M., Buczek-Thomas, J. A. & Nugent, M. A. (2008). Control of growth factor networks by heparan sulfate proteoglycans. *Annals of biomedical engineering,* 36**,** 2134-2148.

Fouse, S. D. & Costello, J. F. (2013). Cancer stem cells activate STAT3 the EZ way. *Cancer cell,* 23**,** 711-713.

Fromm, J. R., Hileman, R., Caldwell, E., Weiler, J. & Linhardt, R. (1995). Differences in the interaction of heparin with arginine and lysine and the importance of these basic amino acids in the binding of heparin to acidic

fibroblast growth factor. *Archives of biochemistry and biophysics,* 323**,** 279-287.

Funderburgh, J. L. (2000). MINI REVIEW Keratan sulfate: structure, biosynthesis, and function. *Glycobiology,* 10**,** 951-958.

Gandhi, N. S. & Mancera, R. L. (2008). The structure of glycosaminoglycans and their interactions with proteins. *Chemical biology & drug design,* 72**,** 455-482.

Gasparini, G. (2000). Prognostic value of vascular endothelial growth factor in breast cancer. *The oncologist,* 5**,** 37-44.

Gengrinovitch, S., Berman, B., David, G., Witte, L., Neufeld, G. & Ron, D. (1999). Glypican-1 is a VEGF165 binding proteoglycan that acts as an extracellular chaperone for VEGF165. *Journal of Biological Chemistry,* 274**,** 10816-10822.

Ghaffari, P., Mardinoglu, A. & Nielsen, J. (2015). Cancer metabolism: a modeling perspective. *Frontiers in physiology,* 6.

Ghebeh, H., Sleiman, G. M., Manogaran, P. S., Al-Mazrou, A., Barhoush, E., Al-Mohanna, F. H., Tulbah, A., Al-Faqeeh, K. & Adra, C. N. (2013). Profiling of normal and malignant breast tissue show CD44 high/CD24 low phenotype as a predominant stem/progenitor marker when used in combination with Ep-CAM/CD49f markers. *BMC cancer,* 13**,** 1.

Ghuwalewala, S., Ghatak, D., Das, P., Dey, S., Sarkar, S., Alam, N., Panda, C. K. & Roychoudhury, S. (2016). CD44 high CD24 low molecular signature determines the Cancer Stem Cell and EMT phenotype in Oral Squamous Cell Carcinoma. *Stem cell research,* 16**,** 405-417.

Gil, J., Stembalska, A., Pesz, K. A. & Sąsiadek, M. M. (2008). Cancer stem cells: the theory and perspectives in cancer therapy. *Journal of applied genetics,* 49**,** 193-199.

Girouard, S. D. & Murphy, G. F. (2011). Melanoma stem cells: not rare, but well done. *Laboratory investigation,* 91**,** 647-664.

Gitay-Goren, H., Soker, S., Vlodavsky, I. & Neufeld, G. (1992). The binding of vascular endothelial growth factor to its receptors is dependent on cell surface-associated heparin-like molecules. *Journal of Biological Chemistry,* 267**,** 6093-6098.

Gomes, A. M., Stelling, M. P. & Pavão, M. S. (2013). Heparan sulfate and heparanase as modulators of breast cancer progression. *BioMed research international,* 2013.

Gong, C., Yao, H., Liu, Q., Chen, J., Shi, J., Su, F. & Song, E. (2010). Markers of tumor-initiating cells predict chemoresistance in breast cancer. *PloS one,* 5**,** e15630.

Götte, M., Kersting, C., Radke, I., Kiesel, L. & Wülfing, P. (2007). An expression signature of syndecan-1 (CD138), E-cadherin and c-met is associated with factors of angiogenesis and lymphangiogenesis in ductal breast carcinoma in situ. *Breast Cancer Research,* 9**,** 1.

Grant, D., Long, W., Moffat, C. F. & Williamson, F. B. (1989). Infrared spectroscopy of chemically modified heparins. *Biochemical Journal,* 261**,** 1035-1038.

Greco, V. & Guo, S. (2010). Compartmentalized organization: a common and required feature of stem cell niches? *Development,* 137**,** 1586-1594.

Grivennikov, S. & Karin, M. (2008). Autocrine IL-6 signaling: a key event in tumorigenesis? *Cancer cell,* 13**,** 7-9.

Grobe, K. & Esko, J. D. (2002). Regulated Translation of Heparan SulfateN-Acetylglucosamine N-Deacetylase/N-Sulfotransferase Isozymes by Structured 5′-Untranslated Regions and Internal Ribosome Entry Sites. *Journal of Biological Chemistry,* 277**,** 30699-30706.

Guimond, S., Maccarana, M., Olwin, B., Lindahl, U. & Rapraeger, A. (1993). Activating and inhibitory heparin sequences for FGF-2 (basic FGF). Distinct requirements for FGF-1, FGF-2, and FGF-4. *Journal of Biological Chemistry,* 268**,** 23906-23914.

Guimond, S. E. & Turnbull, J. E. (1999). Fibroblast growth factor receptor signalling is dictated by specific heparan sulphate saccharides. *Current Biology,* 9**,** 1343-1346.

Guimond, S. E., Turnbull, J. E. & Yates, E. A. (2006). Engineered Bio-Active Polysaccharides from Heparin. *Macromolecular bioscience,* 6**,** 681-686.

Han, L., Shi, S., Gong, T., Zhang, Z. & Sun, X. (2013). Cancer stem cells: therapeutic implications and perspectives in cancer therapy. *Acta Pharmaceutica Sinica B,* 3**,** 65-75.

Handler, M., Yurchenco, P. D. & Iozzo, R. V. (1997). Developmental expression of perlecan during murine embryogenesis. *Developmental dynamics,* 210**,** 130-145.

Harvey, J. R., Mellor, P., Eldaly, H., Lennard, T. W., Kirby, J. A. & Ali, S. (2007). Inhibition of CXCR4-mediated breast cancer metastasis: a potential role for heparinoids? *Clinical Cancer Research,* 13**,** 1562-1570.

Hecht, I., Hershkoviz, R., Shivtiel, S., Lapidot, T., Cohen, I. R., Lider, O. & Cahalon, L. (2004). Heparin-disaccharide affects T cells: inhibition of NF-κB activation, cell migration, and modulation of intracellular signaling. *Journal of leukocyte biology,* 75**,** 1139-1146.

Hernandez-Vargas, H., Ouzounova, M., Le Calvez-Kelm, F., Lambert, M.-P., McKay-Chopin, S., Tavtigian, S. V., Puisieux, A., Matar, C. & Herceg, Z. (2011). Methylome analysis reveals Jak-STAT pathway deregulation in putative breast cancer stem cells. *Epigenetics,* 6**,** 428-439.

Hicklin, D. J. & Ellis, L. M. (2005). Role of the vascular endothelial growth factor pathway in tumor growth and angiogenesis. *Journal of clinical oncology,* 23**,** 1011-1027.

Holash, J., Maisonpierre, P., Compton, D., Boland, P., Alexander, C., Zagzag, D., Yancopoulos, G. & Wiegand, S. (1999). Vessel cooption, regression, and growth in tumors mediated by angiopoietins and VEGF. *Science,* 284**,** 1994-1998.

Holliday, D. L. & Speirs, V. (2011). Choosing the right cell line for breast cancer research. *Breast Cancer Research,* 13**,** 1.

Hong, I.-S., Lee, H.-Y. & Nam, J.-S. (2015). Cancer stem cells: the 'Achilles heel'of chemo-resistant tumors. *Recent patents on anti-cancer drug discovery,* 10**,** 2-22.

Horowitz, A. & Simons, M. (1998). Phosphorylation of the cytoplasmic tail of syndecan-4 regulates activation of protein kinase Cα. *Journal of Biological Chemistry,* 273**,** 25548-25551.

Hwang-Verslues, W. W., Kuo, W.-H., Chang, P.-H., Pan, C.-C., Wang, H.-H., Tsai, S.-T., Jeng, Y.-M., Shew, J.-Y., Kung, J. T. & Chen, C.-H. (2009). Multiple lineages of human breast cancer stem/progenitor cells identified by profiling with stem cell markers. *PloS one,* 4**,** e8377.

Ibrahim, S. A., Hassan, H., Vilardo, L., Kumar, S. K., Kumar, A. V., Kelsch, R., Schneider, C., Kiesel, L., Eich, H. T. & Zucchi, I. (2013). Syndecan-1 (CD138) modulates triple-negative breast cancer stem cell properties via regulation of LRP-6 and IL-6-mediated STAT3 signaling. *PloS one,* 8**,** e85737.

Ibrahim, S. A., Yip, G. W., Stock, C., Pan, J. W., Neubauer, C., Poeter, M., Pupjalis, D., Koo, C. Y., Kelsch, R. & Schüle, R. (2012). Targeting of syndecan-1 by microRNA miR-10b promotes breast cancer cell motility and invasiveness via a Rho-GTPase-and E-cadherin-dependent mechanism. *International Journal of Cancer,* 131**,** E884-E896.

Iozzo, R. V. (2001). Series Introduction: Heparan sulfate proteoglycans: intricate molecules with intriguing functions. *The Journal of clinical investigation,* 108**,** 165-167.

Iozzo, R. V. (2005). Basement membrane proteoglycans: from cellar to ceiling. *Nature Reviews Molecular Cell Biology,* 6**,** 646-656.

Irie, A., Yates, E. A., Turnbull, J. E. & Holt, C. E. (2002). Specific heparan sulfate structures involved in retinal axon targeting. *Development,* 129**,** 61-70.

Jaggupilli, A. & Elkord, E. (2012). Significance of CD44 and CD24 as cancer stem cell markers: an enduring ambiguity. *Clinical and Developmental Immunology,* 2012.

Jastrebova, N., Vanwildemeersch, M., Rapraeger, A. C., Giménez-Gallego, G., Lindahl, U. & Spillmann, D. (2006). Heparan sulfate-related oligosaccharides in ternary complex formation with fibroblast growth factors 1 and 2 and their receptors. *Journal of Biological Chemistry,* 281**,** 26884-26892.

Jeyapalan, Z., Deng, Z., Shatseva, T., Fang, L., He, C. & Yang, B. B. (2011). Expression of CD44 3′-untranslated region regulates endogenous microRNA functions in tumorigenesis and angiogenesis. *Nucleic acids research,* 39**,** 3026-3041.

Johnson, G. L. & Lapadat, R. (2002). Mitogen-activated protein kinase pathways mediated by ERK, JNK, and p38 protein kinases. *Science,* 298**,** 1911-1912.

Jung, Y.-C., Han, S., Hua, L., Ahn, Y.-H., Cho, H., Lee, C.-J., Lee, H., Cho, Y.-Y., Ryu, J.-H. & Jeon, R. (2016). Kazinol-E is a specific inhibitor of ERK that suppresses the enrichment of a breast cancer stem-like cell population. *Biochemical and biophysical research communications,* 470**,** 294-299.

Kagara, N., Huynh, K. T., Kuo, C., Okano, H., Sim, M. S., Elashoff, D., Chong, K., Giuliano, A. E. & Hoon, D. S. (2012). Epigenetic regulation of cancer stem cell genes in triple-negative breast cancer. *The American journal of pathology,* 181**,** 257-267.

Kaksonen, M., Pavlov, I., Võikar, V., Lauri, S. E., Hienola, A., Riekki, R., Lakso, M., Taira, T. & Rauvala, H. (2002). Syndecan-3-deficient mice exhibit enhanced LTP and impaired hippocampus-dependent memory. *Molecular and Cellular Neuroscience,* 21**,** 158-172.

Kamijo, T. (2012). Role of stemness-related molecules in neuroblastoma. *Pediatric research,* 71**,** 511-515.

Karamboulas, C. & Ailles, L. (2013). Developmental signaling pathways in cancer stem cells of solid tumors. *Biochimica et Biophysica Acta (BBA)-General Subjects,* 1830**,** 2481-2495.

Katz, M., Amit, I. & Yarden, Y. (2007). Regulation of MAPKs by growth factors and receptor tyrosine kinases. *Biochimica et Biophysica Acta (BBA)-Molecular Cell Research,* 1773**,** 1161-1176.

Keysar, S. B. & Jimeno, A. (2010). More than markers: biological significance of cancer stem cell-defining molecules. *Molecular cancer therapeutics,* 9**,** 2450-2457.

Kijima, T., Niwa, H., Steinman, R. A., Drenning, S. D., Gooding, W. E., Wentzel, A. L., Xi, S. & Grandis, J. R. (2002). STAT3 activation abrogates growth factor dependence and contributes to head and neck squamous cell carcinoma tumor growth in vivo. Cell Growth Differ.

Kim, B.-T., Kitagawa, H., Tamura, J.-i., Saito, T., Kusche-Gullberg, M., Lindahl, U. & Sugahara, K. (2001). Human tumor suppressor EXT gene family members EXTL1 and EXTL3 encode α1, 4-N-acetylglucosaminyltransferases that likely are involved in heparan sulfate/heparin biosynthesis. *Proceedings of the National Academy of Sciences,* 98**,** 7176-7181.

Kim, S.-Y., Kang, J. W., Song, X., Kim, B. K., Yoo, Y. D., Kwon, Y. T. & Lee, Y. J. (2013). Role of the IL-6-JAK1-STAT3-Oct-4 pathway in the conversion of non-stem cancer cells into cancer stem-like cells. *Cellular signalling,* 25**,** 961-969.

Kim, Y., Joo, K., Jin, J. & Nam, D. (2009). Cancer stem cells and their mechanism of chemo-radiation resistance. *International journal of stem cells,* 2**,** 109-114.

Kim, Y., Joo, K. M., Jin, J. & Nam, D.-H. Cancer stem cells and their mechanism of chemo-radiation resistance.

Kjellén, L. & Lindahl, U. (1991). Proteoglycans: structures and interactions. *Annual review of biochemistry,* 60**,** 443-475.

Knüpfer, H. & Preiß, R. (2007). Significance of interleukin-6 (IL-6) in breast cancer (review). *Breast cancer research and treatment,* 102**,** 129-135.

Kotiyal, S. & Bhattacharya, S. (2014). Breast cancer stem cells, EMT and therapeutic targets. *Biochemical and biophysical research communications,* 453**,** 112-116.

Kovacsovics, T., Mims, A. S., Salama, M. E., Rao, N., Pantin, J., Deininger, M. W., Kennedy, T. P., Bavisotto, L. M., Boucher, K. M. & Marcus, S. G. O-desulfated heparin and chemotherapy for the treatment of AML. ASCO Annual Meeting Proceedings, 2015. 7053.

Kreuger, J., Jemth, P., Sanders-Lindberg, E., Eliahu, L., Dina, R., Basilico, C., Salmivirta, M. & Lindahl, U. (2005). Fibroblast growth factors share binding sites in heparan sulphate. *Biochemical Journal,* 389**,** 145-150.

Kreuger, J. & Kjellén, L. (2012). Heparan Sulfate Biosynthesis Regulation and Variability. *Journal of Histochemistry & Cytochemistry,* 60**,** 898-907.

Kröger, S. & Schröder, J. E. (2002). Agrin in the developing CNS: new roles for a synapse organizer. *Physiology,* 17**,** 207-212.

Kucia, M., Reca, R., Miekus, K., Wanzeck, J., Wojakowski, W., Janowska-Wieczorek, A., Ratajczak, J. & Ratajczak, M. Z. (2005). Trafficking of Normal Stem Cells and Metastasis of Cancer Stem Cells Involve Similar Mechanisms: Pivotal Role of the SDF-1–CXCR4 Axis. *Stem cells,* 23**,** 879-894.

Kuniyasu, H., Oue, N., Tsutsumi, M., Tahara, E. & Yasui, W. (2001). Heparan sulfate enhances invasion by human colon carcinoma cell lines through expression of CD44 variant exon 3. *Clinical cancer research,* 7**,** 4067-4072.

Kuschert, G. S., Coulin, F., Power, C. A., Proudfoot, A. E., Hubbard, R. E., Hoogewerf, A. J. & Wells, T. N. (1999). Glycosaminoglycans interact selectively with chemokines and modulate receptor binding and cellular responses. *Biochemistry,* 38**,** 12959-12968.

Lapidot, T., Sirard, C., Vormoor, J., Murdoch, B., Hoang, T., Caceres-cortes, J., Minden, M., Paterson, B., Caligiuri, M. & Dick, J. (1994). A Cell Initiating Human Acute Myeloid-Leukemia After Transplantation into SCID Mice. *Nature,* 367**,** 645-648.

Laterra, J., Silbert, J. E. & Culp, L. A. (1983). Cell surface heparan sulfate mediates some adhesive responses to glycosaminoglycan-binding matrices, including fibronectin. *The Journal of cell biology,* 96**,** 112-123.

Läubli, H., Spanaus, K.-S. & Borsig, L. (2009). Selectin-mediated activation of endothelial cells induces expression of CCL5 and promotes metastasis through recruitment of monocytes. *Blood,* 114**,** 4583-4591.

Lee, C.-J., Lee, H. S., Ryu, H. W., Lee, M.-H., Lee, J.-Y., Li, Y., Dong, Z., Lee, H.-K., Oh, S.-R. & Cho, Y.-Y. (2013). Targeting of Magnolin on ERKs inhibits Ras/ERKs/RSK2 signaling-mediated neoplastic cell transformation. *Carcinogenesis***,** bgt306.

Lee, J., Kim, Y. & Kim, W. (2015). The Differential Expression of Cancer Stem Cell Markers CD44, CD24 and ALDH1 in Breast Cancer Histological Types. *Austin J Surg,* 2**,** 1075.

Leivonen, M., Lundin, J., Nordling, S., von Boguslawski, K. & Haglund, C. (2004). Prognostic value of syndecan-1 expression in breast cancer. *Oncology,* 67**,** 11-18.

Lendorf, M. E., Manon-Jensen, T., Kronqvist, P., Multhaupt, H. A. & Couchman, J. R. (2011). Syndecan-1 and syndecan-4 are independent indicators in breast carcinoma. *Journal of Histochemistry & Cytochemistry,* 59**,** 615-629.

Levy-Adam, F., Feld, S., Cohen-Kaplan, V., Shteingauz, A., Gross, M., Arvatz, G., Naroditsky, I., Ilan, N., Doweck, I. & Vlodavsky, I. (2010). Heparanase 2 interacts with heparan sulfate with high affinity and inhibits heparanase activity. *Journal of Biological Chemistry,* 285**,** 28010-28019.

Li, J.-p., Hagner-McWhirter, Å., Kjellén, L., Palgi, J., Jalkanen, M. & Lindahl, U. (1997). Biosynthesis of Heparin/Heparan Sulfate cDNA CLONING AND EXPRESSION OF d-GLUCURONYL C5-EPIMERASE FROM BOVINE LUNG. *Journal of Biological Chemistry,* 272**,** 28158-28163.

Li, X., Lewis, M. T., Huang, J., Gutierrez, C., Osborne, C. K., Wu, M.-F., Hilsenbeck, S. G., Pavlick, A., Zhang, X. & Chamness, G. C. (2008). Intrinsic resistance of tumorigenic breast cancer cells to chemotherapy. *Journal of the National Cancer Institute,* 100**,** 672-679.

Liekens, S., Schols, D. & Hatse, S. (2010). CXCL12-CXCR4 axis in angiogenesis, metastasis and stem cell mobilization. *Current pharmaceutical design,* 16**,** 3903-3920.

Lim, H. C., Multhaupt, H. A. & Couchman, J. R. (2015). Cell surface heparan sulfate proteoglycans control adhesion and invasion of breast carcinoma cells. *Molecular cancer,* 14**,** 1.

Lin, X. (2004). Functions of heparan sulfate proteoglycans in cell signaling during development. *Development,* 131**,** 6009-6021.

Lin, Y. & Wang, F. (2010). FGF signalling in prostate development, tissue homoeostasis and tumorigenesis. *Bioscience reports,* 30**,** 285-291.

Lindahl, U., Kusche-Gullberg, M. & Kjellén, L. (1998). Regulated diversity of heparan sulfate. *Journal of Biological Chemistry,* 273**,** 24979-24982.

Liu, C.-Y., Hung, M.-H., Wang, D.-S., Chu, P.-Y., Su, J.-C., Teng, T.-H., Huang, C.-T., Chao, T.-T., Wang, C.-Y. & Shiau, C.-W. (2014a). Tamoxifen induces apoptosis through cancerous inhibitor of protein phosphatase 2A–dependent

phospho-Akt inactivation in estrogen receptor–negative human breast cancer cells. *Breast Cancer Research,* 16**,** 1.

Liu, H., Lv, L. & Yang, K. (2015). Chemotherapy targeting cancer stem cells. *American Journal of Cancer Research,* 5.

Liu, S., Cong, Y., Wang, D., Sun, Y., Deng, L., Liu, Y., Martin-Trevino, R., Shang, L., McDermott, S. P. & Landis, M. D. (2014b). Breast cancer stem cells transition between epithelial and mesenchymal states reflective of their normal counterparts. *Stem cell reports,* 2**,** 78-91.

Livak, K. J. & Schmittgen, T. D. (2001). Analysis of relative gene expression data using real-time quantitative PCR and the 2− ΔΔCT method. *methods,* 25**,** 402-408.

Lobba, A., Forni, M., Carreira, A. & Sogayar, M. C. (2012). Differential expression of CD90 and CD14 stem cell markers in malignant breast cancer cell lines. *Cytometry Part A,* 81**,** 1084-1091.

Löfgren, L., Sahlin, L., Jiang, S., Von Schoultz, B., Fernstad, R., Skoog, L. & Von Schoultz, E. (2007). Expression of syndecan-1 in paired samples of normal and malignant breast tissue from postmenopausal women. *Anticancer research,* 27**,** 3045-3050.

Longatto Filho, A., Lopes, J. M. & Schmitt, F. C. (2010). Angiogenesis and breast cancer. *Journal of oncology,* 2010.

Loo, B.-M., Kreuger, J., Jalkanen, M., Lindahl, U. & Salmivirta, M. (2001). Binding of heparin/heparan sulfate to fibroblast growth factor receptor 4. *Journal of Biological Chemistry,* 276**,** 16868-16876.

Lu, Z. & Xu, S. (2006). ERK1/2 MAP kinases in cell survival and apoptosis. *IUBMB life,* 58**,** 621-631.

Luker, K. E. & Luker, G. D. (2006). Functions of CXCL12 and CXCR4 in breast cancer. *Cancer letters,* 238**,** 30-41.

Lundin, L., Larsson, H., Kreuger, J., Kanda, S., Lindahl, U., Salmivirta, M. & Claesson-Welsh, L. (2000). Selectively desulfated heparin inhibits fibroblast growth factor-induced mitogenicity and angiogenesis. *Journal of Biological Chemistry,* 275**,** 24653-24660.

Maeda, T., Desouky, J. & Friedl, A. (2006). Syndecan-1 expression by stromal fibroblasts promotes breast carcinoma growth in vivo and stimulates tumor angiogenesis. *Oncogene,* 25**,** 1408-1412.

Maisonpierre, P. C., Suri, C., Jones, P. F., Bartunkova, S., Wiegand, S. J., Radziejewski, C., Compton, D., McClain, J., Aldrich, T. H. & Papadopoulos, N. (1997). Angiopoietin-2, a natural antagonist for Tie2 that disrupts in vivo angiogenesis. *Science,* 277**,** 55-60.

Malinowska, K., Neuwirt, H., Cavarretta, I. T., Bektic, J., Steiner, H., Dietrich, H., Moser, P. L., Fuchs, D., Hobisch, A. & Culig, Z. (2009). Interleukin-6 stimulation of growth of prostate cancer in vitro and in vivo through activation of the androgen receptor. *Endocrine-related cancer,* 16**,** 155-169.

Mani, S. A., Guo, W., Liao, M.-J., Eaton, E. N., Ayyanan, A., Zhou, A. Y., Brooks, M., Reinhard, F., Zhang, C. C. & Shipitsin, M. (2008). The epithelial-mesenchymal transition generates cells with properties of stem cells. *Cell,* 133**,** 704-715.

Mannelli, G. & Gallo, O. (2012). Cancer stem cells hypothesis and stem cells in head and neck cancers. *Cancer treatment reviews,* 38**,** 515-539.

Mao, Q. & Unadkat, J. D. (2015). Role of the breast cancer resistance protein (BCRP/ABCG2) in drug transport—An update. *The AAPS journal,* 17**,** 65-82.

Marneros, A. G. & Olsen, B. R. (2005). Physiological role of collagen XVIII and endostatin. *The FASEB journal,* 19**,** 716-728.

Marotta, L. L., Almendro, V., Marusyk, A., Shipitsin, M., Schemme, J., Walker, S. R., Bloushtain-Qimron, N., Kim, J. J., Choudhury, S. A. & Maruyama, R. (2011). The JAK2/STAT3 signaling pathway is required for growth of CD44+ CD24–stem cell–like breast cancer cells in human tumors. *The Journal of clinical investigation,* 121**,** 2723-2735.

Martowicz, A., Spizzo, G., Gastl, G. & Untergasser, G. (2012). Phenotype-dependent effects of EpCAM expression on growth and invasion of human breast cancer cell lines. *BMC cancer,* 12**,** 1.

Matsuda, K., Maruyama, H., Guo, F., Kleeff, J., Itakura, J., Matsumoto, Y., Lander, A. D. & Korc, M. (2001). Glypican-1 is overexpressed in human breast cancer and modulates the mitogenic effects of multiple heparin-binding growth factors in breast cancer cells. *Cancer research,* 61**,** 5562-5569.

McDermott, S. P. & Wicha, M. S. (2010). Targeting breast cancer stem cells. *Molecular oncology,* 4**,** 404-419.

McGlynn, L. M., Kirkegaard, T., Edwards, J., Tovey, S., Cameron, D., Twelves, C., Bartlett, J. M. & Cooke, T. G. (2009). Ras/Raf-1/MAPK pathway mediates response to tamoxifen but not chemotherapy in breast cancer patients. *Clinical Cancer Research,* 15**,** 1487-1495.

Mebratu, Y. & Tesfaigzi, Y. (2009). How ERK1/2 activation controls cell proliferation and cell death: Is subcellular localization the answer? *Cell cycle,* 8**,** 1168-1175.

Mellor, P., Harvey, J., Murphy, K., Pye, D., O'Boyle, G., Lennard, T., Kirby, J. & Ali, S. (2007). Modulatory effects of heparin and short-length oligosaccharides of heparin on the metastasis and growth of LMD MDA-MB 231 breast cancer cells in vivo. *British journal of cancer,* 97**,** 761-768.

Meyer, M. J., Fleming, J. M., Lin, A. F., Hussnain, S. A., Ginsburg, E. & Vonderhaar, B. K. (2010). CD44posCD49fhiCD133/2hi defines xenograft-initiating cells in estrogen receptor–negative breast cancer. *Cancer research,* 70**,** 4624-4633.

Mi, D., Gao, Y., Zheng, S., Ba, X. & Zeng, X. (2009). Inhibitory effects of chemically modified heparin on the P-selectin-mediated adhesion of breast cancer cells in vitro. *Molecular Medicine Reports,* 2**,** 301-306.

Mittal, S., Sharma, A., Balaji, S. A., Gowda, M. C., Dighe, R. R., Kumar, R. V. & Rangarajan, A. (2014). Coordinate hyperactivation of Notch1 and Ras/MAPK pathways correlates with poor patient survival: novel therapeutic strategy for aggressive breast cancers. *Molecular cancer therapeutics,* 13**,** 3198-3209.

Miyamoto, K., Asada, K., Fukutomi, T., Okochi, E., Yagi, Y., Hasegawa, T., Asahara, T., Sugimura, T. & Ushijima, T. (2003). Methylation-associated silencing of heparan sulfate D-glucosaminyl 3-O-sulfotransferase-2 (3-OST-2) in human breast, colon, lung and pancreatic cancers. *Oncogene,* 22**,** 274-280.

Moon, J. J., Matsumoto, M., Patel, S., Lee, L., Guan, J. L. & Li, S. (2005). Role of cell surface heparan sulfate proteoglycans in endothelial cell migration and mechanotransduction. *Journal of cellular physiology,* 203**,** 166-176.

Mueller, H., Flury, N., Eppenberger-Castori, S., Kueng, W., David, F. & Eppenberger, U. (2000). Potential prognostic value of mitogen-activated

protein kinase activity for disease-free survival of primary breast cancer patients. *International journal of cancer,* 89**,** 384-388.

Mukherjee, S., Mazumdar, M., Chakraborty, S., Manna, A., Saha, S., Khan, P., Bhattacharjee, P., Guha, D., Adhikary, A. & Mukhjerjee, S. (2014). Curcumin inhibits breast cancer stem cell migration by amplifying the E-cadherin/β-catenin negative feedback loop. *Stem cell research & therapy,* 5**,** 1.

Müller, A., Homey, B., Soto, H., Ge, N., Catron, D., Buchanan, M. E., McClanahan, T., Murphy, E., Yuan, W. & Wagner, S. N. (2001). Involvement of chemokine receptors in breast cancer metastasis. *Nature,* 410**,** 50-56.

Mummery, R. S. & Rider, C. C. (2000). Characterization of the heparin-binding properties of IL-6. *The Journal of Immunology,* 165**,** 5671-5679.

Mundhenke, C., Meyer, K., Drew, S. & Friedl, A. (2002). Heparan sulfate proteoglycans as regulators of fibroblast growth factor-2 receptor binding in breast carcinomas. *The American journal of pathology,* 160**,** 185-194.

Mylona, E., Giannopoulou, I., Fasomytakis, E., Nomikos, A., Magkou, C., Bakarakos, P. & Nakopoulou, L. (2008). The clinicopathologic and prognostic significance of CD44+/CD24−/low and CD44−/CD24+ tumor cells in invasive breast carcinomas. *Human pathology,* 39**,** 1096-1102.

Nagano, M., Yamashita, T., Hamada, H., Ohneda, K., Kimura, K.-i., Nakagawa, T., Shibuya, M., Yoshikawa, H. & Ohneda, O. (2007). Identification of functional endothelial progenitor cells suitable for the treatment of ischemic tissue using human umbilical cord blood. *Blood,* 110**,** 151-160.

Natarajan, K., Xie, Y., Baer, M. R. & Ross, D. D. (2012). Role of breast cancer resistance protein (BCRP/ABCG2) in cancer drug resistance. *Biochemical pharmacology,* 83**,** 1084-1103.

Nemeth, K. & Karpati, S. (2014). Identifying the stem cell. *Journal of Investigative Dermatology,* 134**,** 1-5.

Neve, R. M., Chin, K., Fridlyand, J., Yeh, J., Baehner, F. L., Fevr, T., Clark, L., Bayani, N., Coppe, J.-P. & Tong, F. (2006). A collection of breast cancer cell lines for the study of functionally distinct cancer subtypes. *Cancer cell,* 10**,** 515-527.

Nigam, S. K. & Bush, K. T. (2014). Growth factor–heparan sulfate "switches" regulating stages of branching morphogenesis. *Pediatric Nephrology,* 29**,** 727-735.

Nishida, N., Yano, H., Nishida, T., Kamura, T. & Kojiro, M. (2006). Angiogenesis in cancer. *Vascular health and risk management,* 2**,** 213.

Okolicsanyi, R. K., Buffiere, A., Jacinto, J. M., Chacon-Cortes, D., Chambers, S. K., Youl, P. H., Haupt, L. M. & Griffiths, L. R. (2015). Association of heparan sulfate proteoglycans SDC1 and SDC4 polymorphisms with breast cancer in an Australian Caucasian population. *Tumor Biology,* 36**,** 1731-1738.

Okolicsanyi, R. K., van Wijnen, A. J., Cool, S. M., Stein, G. S., Griffiths, L. R. & Haupt, L. M. (2014). Heparan sulfate proteoglycans and human breast cancer epithelial cell tumorigenicity. *Journal of cellular biochemistry,* 115**,** 967-976.

Olempska, M., Eisenach, P. A., Ammerpohl, O., Ungefroren, H., Fandrich, F. & Kalthoff, H. (2007). Detection of tumor stem cell markers in pancreatic carcinoma cell lines. *Hepatobiliary Pancreat Dis Int,* 6**,** 92-97.

Olson, M. F. & Sahai, E. (2009). The actin cytoskeleton in cancer cell motility. *Clinical & experimental metastasis,* 26**,** 273-287.

Olsson, E., Honeth, G., Bendahl, P.-O., Saal, L. H., Gruvberger-Saal, S., Ringnér, M., Vallon-Christersson, J., Jönsson, G., Holm, K. & Lövgren, K. (2011). CD44 isoforms are heterogeneously expressed in breast cancer and correlate with tumor subtypes and cancer stem cell markers. *BMC cancer,* 11**,** 1.

Ornitz, D. M. (2000). FGFs, heparan sulfate and FGFRs: complex interactions essential for development. *Bioessays,* 22**,** 108-112.

Park, P. W., Reizes, O. & Bernfield, M. (2000). Cell surface heparan sulfate proteoglycans: selective regulators of ligand-receptor encounters. *Journal of Biological Chemistry,* 275**,** 29923-29926.

Patey, S. J., Edwards, E. A., Yates, E. A. & Turnbull, J. E. (2006). Heparin derivatives as inhibitors of BACE-1, the Alzheimer's β-secretase, with reduced activity against factor Xa and other proteases. *Journal of medicinal chemistry,* 49**,** 6129-6132.

Perrimon, N. & Bernfield, M. Cellular functions of proteoglycans—an overview. Seminars in cell & developmental biology, 2001. Elsevier, 65-67.

Peters, M., Farias, E., Colombo, L., Filmus, J., Puricelli, L. & de Kier Joffé, E. B. (2003). Inhibition of invasion and metastasis by glypican-3 in a syngeneic breast cancer model. *Breast cancer research and treatment,* 80**,** 221-232.

Pfankuchen, D. B., Stölting, D. P., Schlesinger, M., Royer, H.-D. & Bendas, G. (2015). Low molecular weight heparin tinzaparin antagonizes cisplatin resistance of ovarian cancer cells. *Biochemical pharmacology,* 97**,** 147-157.

Phillips, P. G., Yalcin, M., Cui, H., Abdel-Nabi, H., Sajjad, M., Bernacki, R., Veith, J. & Mousa, S. A. (2011). Increased tumor uptake of chemotherapeutics and improved chemoresponse by novel non-anticoagulant low molecular weight heparin. *Anticancer research,* 31**,** 411-419.

Pietilä, M., Ivaska, J. & Mani, S. (2016). Whom to blame for metastasis, the epithelial–mesenchymal transition or the tumor microenvironment? *Cancer letters*.

Pinto, C. A., Widodo, E., Waltham, M. & Thompson, E. W. (2013). Breast cancer stem cells and epithelial mesenchymal plasticity–implications for chemoresistance. *Cancer letters,* 341**,** 56-62.

Pönighaus, C., Ambrosius, M., Casanova, J. C., Prante, C., Kuhn, J., Esko, J. D., Kleesiek, K. & Götting, C. (2007). Human xylosyltransferase II is involved in the biosynthesis of the uniform tetrasaccharide linkage region in chondroitin sulfate and heparan sulfate proteoglycans. *Journal of Biological Chemistry,* 282**,** 5201-5206.

Ponti, D., Costa, A., Zaffaroni, N., Pratesi, G., Petrangolini, G., Coradini, D., Pilotti, S., Pierotti, M. A. & Daidone, M. G. (2005). Isolation and in vitro propagation of tumorigenic breast cancer cells with stem/progenitor cell properties. *Cancer research,* 65**,** 5506-5511.

Powell, A. K., Ahmed, Y. A., Yates, E. A. & Turnbull, J. E. (2010). Generating heparan sulfate saccharide libraries for glycomics applications. *Nature protocols,* 5**,** 821-833.

Powell, A. K., Fernig, D. G. & Turnbull, J. E. (2002). Fibroblast Growth Factor Receptors 1 and 2 Interact Differently with Heparin/Heparan Sulfate IMPLICATIONS FOR DYNAMIC ASSEMBLY OF A TERNARY SIGNALING COMPLEX. *Journal of Biological Chemistry,* 277**,** 28554-28563.

Powell, A. K., Yates, E. A., Fernig, D. G. & Turnbull, J. E. (2004). Interactions of heparin/heparan sulfate with proteins: appraisal of structural factors and experimental approaches. *Glycobiology,* 14**,** 17R-30R.

Pozzi, V., Sartini, D., Rocchetti, R., Santarelli, A., Rubini, C., Morganti, S., Giuliante, R., Calabrese, S., Di Ruscio, G. & Orlando, F. (2015). Identification and characterization of cancer stem cells from head and neck squamous cell carcinoma cell lines. *Cellular Physiology and Biochemistry,* 36**,** 784-798.

Prabhakaran, P., Hassiotou, F., Blancafort, P. & Filgueira, L. (2013). Cisplatin induces differentiation of breast cancer cells. *Frontiers in oncology,* 3**,** 134.

Prang, N., Preithner, S., Brischwein, K., Göster, P., Wöppel, A., Müller, J., Steiger, C., Peters, M., Baeuerle, P. & Da Silva, A. (2005). Cellular and complement-dependent cytotoxicity of Ep-CAM-specific monoclonal antibody MT201 against breast cancer cell lines. *British journal of cancer,* 92**,** 342-349.

Prat, A., Parker, J. S., Karginova, O., Fan, C., Livasy, C., Herschkowitz, J. I., He, X. & Perou, C. M. (2010). Phenotypic and molecular characterization of the claudin-low intrinsic subtype of breast cancer. *Breast cancer research,* 12**,** 1.

Presto, J., Thuveson, M., Carlsson, P., Busse, M., Wilén, M., Eriksson, I., Kusche-Gullberg, M. & Kjellén, L. (2008). Heparan sulfate biosynthesis enzymes EXT1 and EXT2 affect NDST1 expression and heparan sulfate sulfation. *Proceedings of the National Academy of Sciences,* 105**,** 4751-4756.

Prydz, K. (2015). Determinants of Glycosaminoglycan (GAG) Structure. *Biomolecules,* 5**,** 2003-2022.

Qian, Z., Shen, Q., Yang, X., Qiu, Y. & Zhang, W. (2015). The Role of Extracellular Vesicles: An Epigenetic View of the Cancer Microenvironment.

Qiu, X., Wang, Z., Li, Y., Miao, Y., Ren, Y. & Luan, Y. (2012). Characterization of sphere-forming cells with stem-like properties from the small cell lung cancer cell line H446. *Cancer letters,* 323**,** 161-170.

Rabenstein, D. L. (2002). Heparin and heparan sulfate: structure and function. *Natural product reports,* 19**,** 312-331.

Raman, K. & Kuberan, B. (2010). Chemical tumor biology of heparan sulfate proteoglycans. *Current chemical biology,* 4**,** 20-31.

Raman, R., Sasisekharan, V. & Sasisekharan, R. (2005). Structural insights into biological roles of protein-glycosaminoglycan interactions. *Chemistry & biology,* 12**,** 267-277.

Ratajczak, M., Tarnowski, M., Staniszewska, M., Sroczynski, T. & Banach, B. (2010). Mechanisms of cancer metastasis: involvement of cancer stem cells? *Minerva medica,* 101**,** 179-191.

Reya, T., Morrison, S. J., Clarke, M. F. & Weissman, I. L. (2001). Stem cells, cancer, and cancer stem cells. *nature,* 414**,** 105-111.

Ribatti, D., Nico, B., Ruggieri, S., Tamma, R., Simone, G. & Mangia, A. (2016). Angiogenesis and Antiangiogenesis in Triple-Negative Breast cancer. *Translational oncology,* 9**,** 453-457.

Ricardo, S., Vieira, A. F., Gerhard, R., Leitão, D., Pinto, R., Cameselle-Teijeiro, J. F., Milanezi, F., Schmitt, F. & Paredes, J. (2011). Breast cancer stem cell markers CD44, CD24 and ALDH1: expression distribution within intrinsic molecular subtype. *Journal of clinical pathology***,** jcp. 2011.090456.

Ricci-Vitiani, L., Lombardi, D. G., Pilozzi, E., Biffoni, M., Todaro, M., Peschle, C. & De Maria, R. (2007). Identification and expansion of human colon-cancer-initiating cells. *Nature,* 445**,** 111-115.

Robinson, C. J., Mulloy, B., Gallagher, J. T. & Stringer, S. E. (2006). VEGF165-binding sites within heparan sulfate encompass two highly sulfated domains and can be liberated by K5 lyase. *Journal of Biological Chemistry,* 281**,** 1731-1740.

Roskoski, R. (2012). ERK1/2 MAP kinases: structure, function, and regulation. *Pharmacological research,* 66**,** 105-143.

Rudd, T. R., Uniewicz, K. A., Ori, A., Guimond, S. E., Skidmore, M. A., Gaudesi, D., Xu, R., Turnbull, J. E., Guerrini, M. & Torri, G. (2010). Comparable stabilisation, structural changes and activities can be induced in FGF by a variety of HS and non-GAG analogues: implications for sequence-activity relationships. *Organic & biomolecular chemistry,* 8**,** 5390-5397.

Rugo, H. S. (2012). Inhibiting angiogenesis in breast cancer: the beginning of the end or the end of the beginning? *Journal of Clinical Oncology,* 30**,** 898-901.

Ruhrberg, C., Gerhardt, H., Golding, M., Watson, R., Ioannidou, S., Fujisawa, H., Betsholtz, C. & Shima, D. T. (2002). Spatially restricted patterning cues provided by heparin-binding VEGF-A control blood vessel branching morphogenesis. *Genes & development,* 16**,** 2684-2698.

Ruvinsky, I. & Meyuhas, O. (2006). Ribosomal protein S6 phosphorylation: from protein synthesis to cell size. *Trends in biochemical sciences,* 31**,** 342-348.

Saarinen, N. M., Abrahamsson, A. & Dabrosin, C. (2010). Estrogen-induced angiogenic factors derived from stromal and cancer cells are differently regulated by enterolactone and genistein in human breast cancer in vivo. *International journal of cancer,* 127**,** 737-745.

Sahlberg, S. H., Spiegelberg, D., Glimelius, B., Stenerlöw, B. & Nestor, M. (2014). Evaluation of cancer stem cell markers CD133, CD44, CD24: association with AKT isoforms and radiation resistance in colon cancer cells. *PloS one,* 9**,** e94621.

Samples, J., Willis, M. & Klauber-DeMore, N. (2013). Targeting angiogenesis and the tumor microenvironment. *Surgical oncology clinics of North America,* 22**,** 629-639.

Sanderson, R. D. Heparan sulfate proteoglycans in invasion and metastasis. Seminars in cell & developmental biology, 2001. Elsevier, 89-98.

Santen, R. J., Song, R. X., McPherson, R., Kumar, R., Adam, L., Jeng, M.-H. & Yue, W. (2002). The role of mitogen-activated protein (MAP) kinase in breast cancer. *The Journal of steroid biochemistry and molecular biology,* 80**,** 239-256.

Sarrazin, S., Lamanna, W. C. & Esko, J. D. (2011). Heparan sulfate proteoglycans. *Cold Spring Harbor perspectives in biology,* 3**,** a004952.

Sasisekharan, R., Shriver, Z., Venkataraman, G. & Narayanasami, U. (2002). Roles of heparan-sulphate glycosaminoglycans in cancer. *Nature Reviews Cancer,* 2**,** 521-528.

Schabath, H., Runz, S., Joumaa, S. & Altevogt, P. (2006). CD24 affects CXCR4 function in pre-B lymphocytes and breast carcinoma cells. *Journal of cell science,* 119**,** 314-325.

Scholefield, Z., Yates, E. A., Wayne, G., Amour, A., McDowell, W. & Turnbull, J. E. (2003). Heparan sulfate regulates amyloid precursor protein processing by BACE1, the Alzheimer's β-secretase. *The Journal of cell biology,* 163**,** 97-107.

Sharma, A., Paranjape, A. N., Rangarajan, A. & Dighe, R. R. (2012). A Monoclonal Antibody against Human Notch1 Ligand–Binding Domain Depletes

Subpopulation of Putative Breast Cancer Stem–like Cells. *Molecular cancer therapeutics,* 11**,** 77-86.

Sheridan, C., Kishimoto, H., Fuchs, R. K., Mehrotra, S., Bhat-Nakshatri, P., Turner, C. H., Goulet, R., Badve, S. & Nakshatri, H. (2006). CD44+/CD24-breast cancer cells exhibit enhanced invasive properties: an early step necessary for metastasis. *Breast Cancer Research,* 8**,** 1.

Shteingauz, A., Boyango, I., Naroditsky, I., Hammond, E., Gruber, M., Doweck, I., Ilan, N. & Vlodavsky, I. (2015). Heparanase enhances tumor growth and chemoresistance by promoting autophagy. *Cancer Research,* 75**,** 3946-3957.

Sicchieri, R. D., da Silveira, W. A., Mandarano, L. R. M., de Oliveira, T. M. G., Carrara, H. H. A., Muglia, V. F., de Andrade, J. M. & Tiezzi, D. G. (2015). ABCG2 is a potential marker of tumor-initiating cells in breast cancer. *Tumor Biology,* 36**,** 9233-9243.

Singh, J. K., Farnie, G., Bundred, N. J., Simões, B. M., Shergill, A., Landberg, G., Howell, S. J. & Clarke, R. B. (2013). Targeting CXCR1/2 significantly reduces breast cancer stem cell activity and increases the efficacy of inhibiting HER2 via HER2-dependent and-independent mechanisms. *Clinical cancer research,* 19**,** 643-656.

Singh, S. K., Hawkins, C., Clarke, I. D., Squire, J. A., Bayani, J., Hide, T., Henkelman, R. M., Cusimano, M. D. & Dirks, P. B. (2004). Identification of human brain tumour initiating cells. *nature,* 432**,** 396-401.

Skaletz-Rorowski, A., Schmidt, A., Breithardt, G. & Buddecke, E. (1996). Heparin-induced overexpression of basic fibroblast growth factor, basic fibroblast growth factor receptor, and cell-associated proteoheparan sulfate in cultured coronary smooth muscle cells. *Arteriosclerosis, thrombosis, and vascular biology,* 16**,** 1063-1069.

Skidmore, M. A., Dumax-Vorzet, A. F., Guimond, S. E., Rudd, T. R., Edwards, E. A., Turnbull, J. E., Craig, A. G. & Yates, E. A. (2008). Disruption of rosetting in Plasmodium falciparum malaria with chemically modified heparin and low molecular weight derivatives possessing reduced anticoagulant and other serine protease inhibition activities. *Journal of medicinal chemistry,* 51**,** 1453-1458.

Smith, L., Watson, M. B., O'Kane, S. L., Drew, P. J., Lind, M. J. & Cawkwell, L. (2006). The analysis of doxorubicin resistance in human breast cancer cells using antibody microarrays. *Molecular cancer therapeutics,* 5**,** 2115-2120.

Stepp, M. A., Gibson, H. E., Gala, P. H., Iglesia, D. D. S., Pajoohesh-Ganji, A., Pal-Ghosh, S., Brown, M., Aquino, C., Schwartz, A. M. & Goldberger, O. (2002). Defects in keratinocyte activation during wound healing in the syndecan-1-deficient mouse. *Journal of cell science,* 115**,** 4517-4531.

Stigliano, I. D., Caramelo, J. J., Labriola, C. A., Parodi, A. J. & D'Alessio, C. (2009). Glucosidase II β subunit modulates N-glycan trimming in fission yeasts and mammals. *Molecular biology of the cell,* 20**,** 3974-3984.

Sun, H., Jia, J., Wang, X., Ma, B., Di, L., Song, G. & Ren, J. (2013). CD44+/CD24− breast cancer cells isolated from MCF-7 cultures exhibit enhanced angiogenic properties. *Clinical and Translational Oncology,* 15**,** 46-54.

Sun, S. & Wang, Z. (2010). ALDH high adenoid cystic carcinoma cells display cancer stem cell properties and are responsible for mediating metastasis. *Biochemical and biophysical research communications,* 396**,** 843-848.

Taylor, K. R. & Gallo, R. L. (2006). Glycosaminoglycans and their proteoglycans: host-associated molecular patterns for initiation and modulation of inflammation. *The FASEB Journal,* 20**,** 9-22.

Theocharis, A. D., Skandalis, S. S., Tzanakakis, G. N. & Karamanos, N. K. (2010). Proteoglycans in health and disease: novel roles for proteoglycans in malignancy and their pharmacological targeting. *FEBS journal,* 277**,** 3904-3923.

Thomas, G., Siegmann, M. & Gordon, J. (1979). Multiple phosphorylation of ribosomal protein S6 during transition of quiescent 3T3 cells into early G1, and cellular compartmentalization of the phosphate donor. *Proceedings of the National Academy of Sciences,* 76**,** 3952-3956.

Thompson, E. W., Paik, S., Brünner, N., Sommers, C. L., Zugmaier, G., Clarke, R., Shima, T. B., Torri, J., Donahue, S. & Lippman, M. E. (1992). Association of increased basement membrane invasiveness with absence of estrogen receptor and expression of vimentin in human breast cancer cell lines. *Journal of cellular physiology,* 150**,** 534-544.

Tumova, S., Woods, A. & Couchman, J. R. (2000). Heparan sulfate proteoglycans on the cell surface: versatile coordinators of cellular functions. *The international journal of biochemistry & cell biology,* 32**,** 269-288.

Turnbull, J., Powell, A. & Guimond, S. (2001). Heparan sulfate: decoding a dynamic multifunctional cell regulator. *Trends in cell biology,* 11**,** 75-82.

Valenzuela, D. M., Griffiths, J. A., Rojas, J., Aldrich, T. H., Jones, P. F., Zhou, H., McClain, J., Copeland, N. G., Gilbert, D. J. & Jenkins, N. A. (1999). Angiopoietins 3 and 4: diverging gene counterparts in mice and humans. *Proceedings of the National Academy of Sciences,* 96**,** 1904-1909.

Van Pham, P., Vu, B. T., Pham, D. X., Nguyen, G. D. T., Le, M. H., Phan, N. K., Phan, N. L. C., Van Tran, T., Duong, T. T. & Vuong, T. G. (2012). *Isolation of Breast Cancer Stem Cells by Single-Cell Sorting*, INTECH Open Access Publisher.

Velasco-Velázquez, M. A., Popov, V. M., Lisanti, M. P. & Pestell, R. G. (2011). The role of breast cancer stem cells in metastasis and therapeutic implications. *The American journal of pathology,* 179**,** 2-11.

Wagers, A. J. & Weissman, I. L. (2004). Plasticity of adult stem cells. *Cell,* 116**,** 639-648.

Wang, Y., Zhu, Y., Qiu, F., Zhang, T., Chen, Z., Zheng, S. & Huang, J. (2010). Activation of Akt and MAPK pathways enhances the tumorigenicity of CD133+ primary colon cancer cells. *Carcinogenesis***,** bgq120.

Wardrop, D. & Keeling, D. (2008). The story of the discovery of heparin and warfarin. *British journal of haematology,* 141**,** 757-763.

Wei, M., Tai, G., Gao, Y., Li, N., Huang, B., Zhou, Y., Hao, S. & Zeng, X. (2004). Modified heparin inhibits P-selectin-mediated cell adhesion of human colon carcinoma cells to immobilized platelets under dynamic flow conditions. *Journal of Biological Chemistry,* 279**,** 29202-29210.

Wei, W., Tweardy, D. J., Zhang, M., Zhang, X., Landua, J., Petrovic, I., Bu, W., Roarty, K., Hilsenbeck, S. G. & Rosen, J. M. (2014). STAT3 Signaling Is Activated Preferentially in Tumor-Initiating Cells in Claudin-Low Models of Human Breast Cancer. *Stem cells,* 32**,** 2571-2582.

Whitelock, J. M. & Iozzo, R. V. (2005). Heparan sulfate: a complex polymer charged with biological activity. *Chemical reviews,* 105**,** 2745-2764.

Whyte, J., Bergin, O., Bianchi, A., McNally, S. & Martin, F. (2009). Key signalling nodes in mammary gland development and cancer. Mitogen-activated protein kinase signalling in experimental models of breast cancer progression and in mammary gland development. *Breast Cancer Research,* 11**,** 1.

Wright, M. H., Calcagno, A. M., Salcido, C. D., Carlson, M. D., Ambudkar, S. V. & Varticovski, L. (2008). Brca1 breast tumors contain distinct CD44+/CD24- and CD133+ cells with cancer stem cell characteristics. *Breast Cancer Research,* 10**,** 1.

Wu, T. & Dai, Y. (2016). Tumor microenvironment and therapeutic response. *Cancer letters*.

Würth, R., Bajetto, A., Harrison, J. K. & Barbieri, F. (2015). CXCL12 modulation of CXCR4 and CXCR7 activity in human glioblastoma stem-like cells and regulation of the tumor microenvironment. *Chemokines and Chemokine Receptors in Brain Homeostasis***,** 106.

Xie, G., Yao, Q., Liu, Y., Du, S., Liu, A., Guo, Z., Sun, A., Ruan, J., Chen, L. & Ye, C. (2012). IL-6-induced epithelial-mesenchymal transition promotes the generation of breast cancer stem-like cells analogous to mammosphere cultures. *International journal of oncology,* 40**,** 1171-1179.

Xiong, A., Yang, Z., Shen, Y., Zhou, J. & Shen, Q. (2014). Transcription factor STAT3 as a novel molecular target for cancer prevention. *Cancers,* 6**,** 926-957.

Xu, D., Fuster, M. M., Lawrence, R. & Esko, J. D. (2011). Heparan sulfate regulates VEGF165-and VEGF121-mediated vascular hyperpermeability. *Journal of Biological Chemistry,* 286**,** 737-745.

Xu, D., Xu, H., Ren, Y., Liu, C., Wang, X., Zhang, H. & Lu, P. (2012). Cancer stem cell-related gene periostin: a novel prognostic marker for breast cancer. *PloS one,* 7**,** e46670.

Xu, Y., Liu, Y.-j. & Yu, Q. (2004). Angiopoietin-3 inhibits pulmonary metastasis by inhibiting tumor angiogenesis. *Cancer research,* 64**,** 6119-6126.

Yan, W., Chen, Y., Yao, Y., Zhang, H. & Wang, T. (2013). Increased invasion and tumorigenicity capacity of CD44+/CD24-breast cancer MCF7 cells in vitro and in nude mice. *Cancer cell international,* 13**,** 1.

Yan, Y., Zuo, X. & Wei, D. (2015). Concise review: emerging role of CD44 in cancer stem cells: a promising biomarker and therapeutic target. *Stem Cells Transl Med,* 4**,** 1033-1043.

Yang, N., Mosher, R., Seo, S., Beebe, D. & Friedl, A. (2011). Syndecan-1 in breast cancer stroma fibroblasts regulates extracellular matrix fiber organization and carcinoma cell motility. *The American journal of pathology,* 178**,** 325-335.

Yashiro, M. & Matsuoka, T. (2016). Fibroblast growth factor receptor signaling as therapeutic targets in gastric cancer. *World journal of gastroenterology,* 22**,** 2415.

Yates, E. A., Guimond, S. E. & Turnbull, J. E. (2004). Highly diverse heparan sulfate analogue libraries: providing access to expanded areas of sequence space for bioactivity screening. *Journal of medicinal chemistry,* 47**,** 277-280.

Yates, E. A., Santini, F., Guerrini, M., Naggi, A., Torri, G. & Casu, B. (1996). 1 H and 13 C NMR spectral assignments of the major sequences of twelve systematically modified heparin derivatives. *Carbohydrate Research,* 294**,** 15-27.

Yenigun, V. B., Ozpolat, B. & Kose, G. T. (2013). Response of CD44+/CD24-/low breast cancer stem/progenitor cells to tamoxifen-and doxorubicin-induced autophagy. *International journal of molecular medicine,* 31**,** 1477-1483.

Yuan, J. S., Reed, A., Chen, F. & Stewart Jr, C. N. (2006). Statistical analysis of real-time PCR data. *BMC Bioinformatics,* 7**,** 1-12.

Zhang, S. S.-M., Liu, M.-G., Kano, A., Zhang, C., Fu, X.-Y. & Barnstable, C. J. (2005). STAT3 activation in response to growth factors or cytokines participates in retina precursor proliferation. *Experimental eye research,* 81**,** 103-115.

Zhang, Y., Toy, K. A. & Kleer, C. G. (2012). Metaplastic breast carcinomas are enriched in markers of tumor-initiating cells and epithelial to mesenchymal transition. *Modern Pathology,* 25**,** 178-184.

Zhao, D., Sang, Q. & Cui, H. (2016). Preparation and evaluation a new generation of low molecular weight heparin. *Biomedicine & Pharmacotherapy,* 79**,** 194-200.

Zhao, W., McCallum, S. A., Xiao, Z., Zhang, F. & Linhardt, R. J. (2012). Binding affinities of vascular endothelial growth factor (VEGF) for heparin-derived oligosaccharides. *Bioscience reports,* 32**,** 71-81

8 Appendices

Appendix 1 Primers list

Appendix 1.1 List of the primers and the expected size of Taqman PCR products with these primer pairs

Gene Symbol	Assay ID	Context Sequence	Group	Gene Name
18S	Hs99999901_s1	N/A	Miscellaneous function	Eukaryotic 18S rRNA
ADAM15	Hs00187052_m1	ATTCGCCGGAGGCGGGATGTGGTAA	Cam family adhesion molecule	ADAM metallopeptidase domain 15
ADAMTS4	Hs00192708_m1	GACAATGGCTATGGGCACTGTCTCT	Cam family adhesion molecule	ADAM metallopeptidase with thrombospondin type 1 motif, 4
ADAMTS5	Hs00199841_m1	GGATGATGGCCATGGTAACTGTTTG	Cam family adhesion molecule	ADAM metallopeptidase with thrombospondin type 1 motif, 5
AGRN	Hs00394748_m1	GTTCTGTGTGGAAGATAAACCCGGG	Other receptor	agrin
CHST11	Hs00905281_s1	TAGAAAACGCTCCCTGTATCTTGCT	Other transferase	carbohydrate (chondroitin 4) sulfotransferase 11
CHST15	Hs01031067_m1	GACCCGGAAGCGCTTTGGAATCGTC	Transferase	carbohydrate (N-acetylgalactosamine 4-sulfate 6-O) sulfotransferase 15
EXT1	Hs00609162_m1	TTTCAACAACAGAGGTGGATTTCGC	Glycosyltransferase	exostosin glycosyltransferase 1
EXT2	Hs00181158_m1	CCCTCCTGCTGTGAAGTGGGGCAGC	Glycosyltransferase	exostosin glycosyltransferase 2
EXTL1	Hs00184929_m1	CCTGGACCTGGGCAGACCCAGCGCC	Glycosyltransferase	exostosin-like glycosyltransferase 1
EXTL2	Hs01018237_m1	CTCAGTTTGGCAGCAATTTCCTGAT	Glycosyltransferase	exostosin-like glycosyltransferase 2
EXTL3	Hs00918601_m1	AAGCCCCCCATCAAGGTGACCTCAC	Glycosyltransferase	exostosin-like glycosyltransferase 3
GAPDH	Hs99999905_m1	N/A	Dehydrogenase	glyceraldehyde-3-phosphate dehydrogenase
GLCE	Hs00392011_m1	GTGGGGTTGAAGGTGTGCCATTATC	Epimerase/racemase	glucuronic acid epimerase
GPC1	Hs00892476_m1	GTCCGGAAAGTGGCTCAGGTCCCCC	Carbohydrate kinase	glypican 1
GPC2	Hs00415099_m1	GCAACTATCTGGATGGTCTCCTGAT	Carbohydrate kinase	glypican 2
GPC3	Hs01018936_m1	CAGCCGAAGAAGGGAACTAATTCAG	Carbohydrate kinase	glypican 3
GPC4	Hs00155059_m1	GCAAGGTCTCCGTGGTAAACCCCAC	Carbohydrate kinase	glypican 4
GPC5	Hs00270114_m1	GACAAAAATTATTGGAACAGGTAAA	Carbohydrate kinase	glypican 5
GPC6	Hs00170677_m1	GGACCGGCTGGTCACAGACATAAAA	Carbohydrate kinase	glypican 6
HPSE	Hs00935036_m1	CCTCATCCTCCTGGGTTCTCCAAAG	Glycosidase	heparanase
HPSE2	Hs00222435_m1	CACAAACCACCACAACCACAACTAC	Glycosidase	heparanase 2
HS2ST1	Hs00202138_m1	CTCGAAGCTAGAAAGGGCTATTGCA	Other transferase	heparan sulfate 2-O-sulfotransferase 1
HS3ST1	Hs00245421_s1	GGAGTTCCTGGTGCGCGATGGCAGG	Cadherin	heparan sulfate (glucosamine) 3-O-sulfotransferase 1
HS3ST2	Hs00428644_m1	GGATTGGTACAGGAGCCTGATGCCC	Cadherin	heparan sulfate (glucosamine) 3-O-sulfotransferase 2
HS3ST3A1	Hs00925624_s1	AGCGCTGCCAGACCCTGTCCGGCCC	Cadherin	heparan sulfate (glucosamine) 3-O-sulfotransferase 3A1
HS3ST3B1	Hs00797512_s1	CTCATGCAGCAGCCTCCTTGCAGAT	Cadherin	heparan sulfate (glucosamine) 3-O-sulfotransferase 3B1
HS3ST4	Hs00901124_s1	AGGCTCCTTGCCTGAGTCCTTGAAT	Cadherin	heparan sulfate (glucosamine) 3-O-sulfotransferase 4
HS3ST5	Hs00999394_m1	GAGCTTGGATAGGCTACAACCCATT	Cadherin	heparan sulfate (glucosamine) 3-O-sulfotransferase 5
HS3ST6	Hs03007244_m1	GGTACCGGAGTCTGATGCCCCGAAC	Cadherin	heparan sulfate (glucosamine) 3-O-sulfotransferase 6
HS6ST1	Hs00757137_m1	GCTGCGCACGCCCAGGAAGTTCTAC	Other transferase	heparan sulfate 6-O-sulfotransferase 1
HS6ST2	Hs02925656_m1	CCCATGGCCAGCGTCGGGAACATGG	Other transferase	heparan sulfate 6-O-sulfotransferase 2
HS6ST3	Hs00542178_m1	ACAGCCACACCAGGAATTTCTATTA	Other transferase	heparan sulfate 6-O-sulfotransferase 3
HSPG2	Hs00194179_m1	GGAGACAAGGTGGCGGCCTACGGTG	Carbohydrate kinase	heparan sulfate proteoglycan 2
LRP1	Hs00233856_m1	GCCCCTGAGATTTGTCCACAGAGTA	Other receptor	low density lipoprotein receptor-related protein 1
NDST1	Hs00925442_m1	TGGACTTGGATTCCCGAGCCTTCCT	Cadherin	N-deacetylase/N-sulfotransferase (heparan glucosaminyl) 1
NDST2	Hs00234335_m1	CCCCAGAAAACAGGGACTACAGCTA	Cadherin	N-deacetylase/N-sulfotransferase (heparan glucosaminyl) 2
NDST3	Hs01128584_m1	TGGATTCTGATAGCAGGACATTTCT	Cadherin	N-deacetylase/N-sulfotransferase (heparan glucosaminyl) 3
NDST4	Hs00224024_m1	TGTCAAAGATGTGAAGGCATTACTA	Cadherin	N-deacetylase/N-sulfotransferase (heparan glucosaminyl) 4
RPLP0	Hs99999902_m1	TGTTTCATTGTGGGAGCAGACAATG	Ribosomal protein	ribosomal protein, large, P0
SDC1	Hs00896423_m1	TCAGGTGCAGGTGCTTTGCAAGATA	Membrane-bound signaling molecule	syndecan 1
SDC2	Hs00299807_m1	GTGTCGGCGGAGTCGAGAGCAGAGC	Other cell adhesion molecule	syndecan 2
SDC3	Hs01568665_m1	GCTCGGGCTACTTCGAGCAGGAGTC	Membrane-bound signaling molecule	syndecan 3
SDC4	Hs00161617_m1	GCCGAGTCGATCCGAGAGACTGAGG	Other cell adhesion molecule	syndecan 4
SULF1	Hs00290918_m1	ATGACCTACACAGAGGACAGTTATG	Esterase	sulfatase 1
SULF2	Hs01016476_m1	CTTCTTCCAAATCACTGGGACAACT	Esterase	sulfatase 2
TGFBR3	Hs01114253_m1	TTAGCCACTGCAGGTCCAGAGCCTG	Cytokine receptor	transforming growth factor, beta receptor III
TIMP3	Hs00165949_m1	CTCCGACATCGTGATCCGGGCCAAG	Dna glycosylase	TIMP metallopeptidase inhibitor 3

Appendix 2 Chemosensitivity data

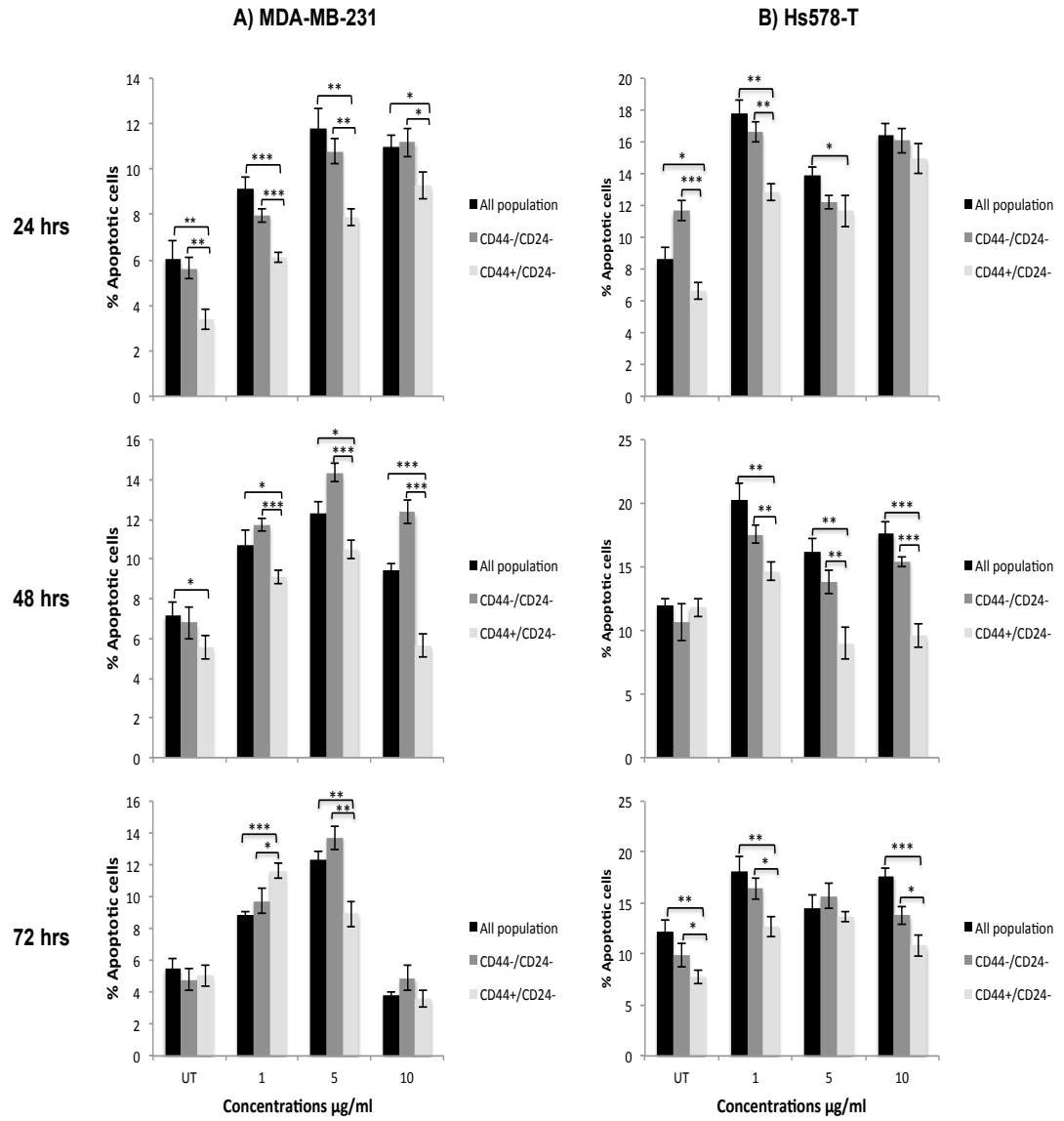

Appendix 2.1 Comparison of chemosensitivity of MDA-MB-231 and Hs578-T unsorted and sorted cells to various concentrations of Doxorubicin. (A) MDA-MB-231 and (B) Hs578-T unsorted and FACS sorted cells were exposed to Dox at increasing concentrations (1, 5, 10 µg/ml) for 24, 48 or 72 hrs. Untreated cells (UT) were used as a control. Apoptotis was measured by Annexin V/PI staining and FACS sorting as described in Methods, and the percentage of early and late apoptotic cells were calculated. All experiments were performed with triplicate cells, and three independent experiments were peformed. Data from one of three representative experiments is shown (mean ± SD, n=2). Data in inset show statistical significance at *= P< 0.05; **= P< 0.01 and ***= P< 0.001 for $CD44^{+}/CD24^{-}$ vs. other respective populations.

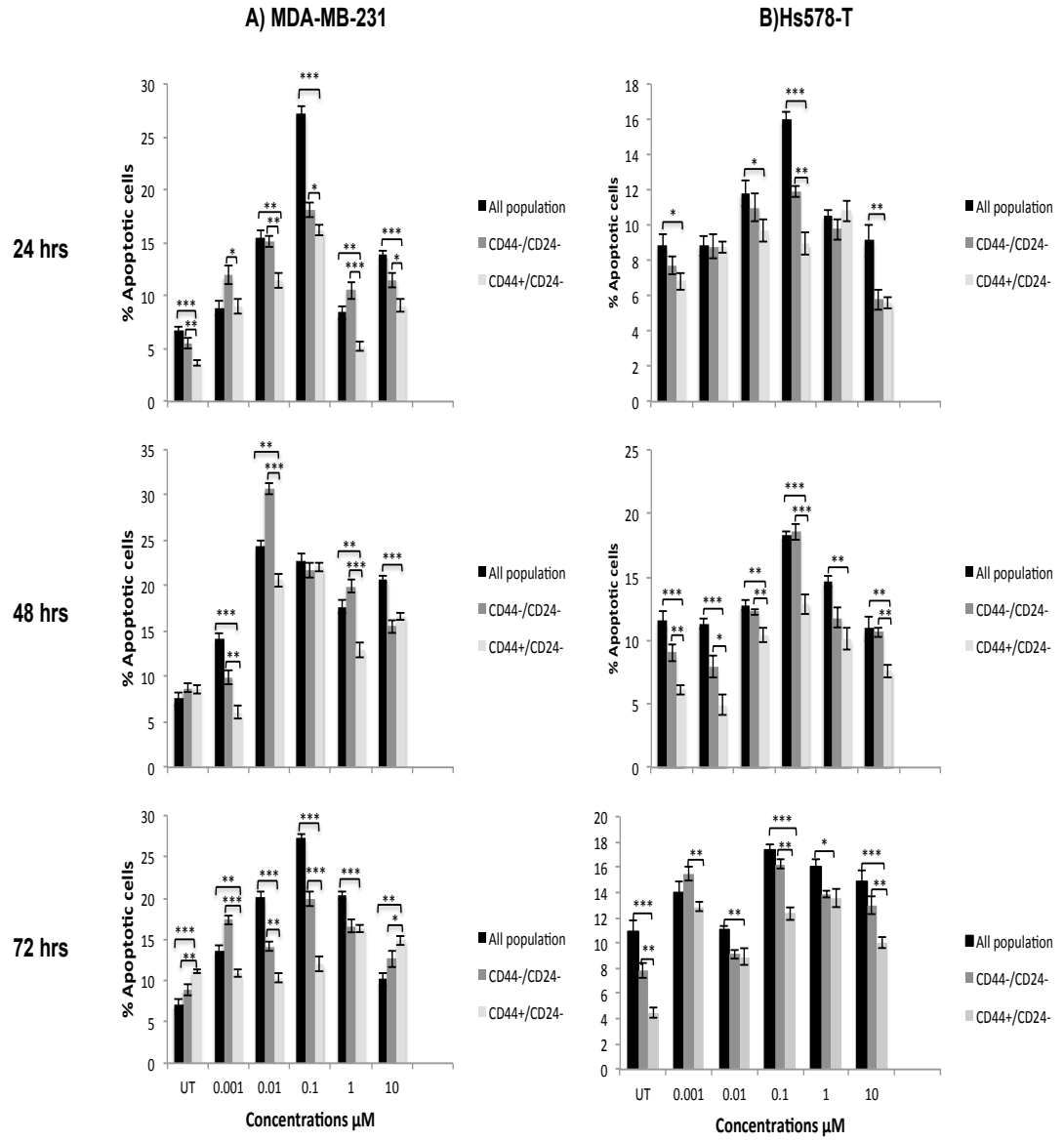

Appendix 2.2 Comparison of chemosensitivity of MDA-MB-231 and Hs578-T unsorted and sorted cells to various concentrations of Cisplatin. (A) MDA-MB-231 and (B) Hs578-T unsorted and FACS sorted cells were exposed to Cis at increasing concentrations (0.001, 0.01, 0.1, 1, 10 µM) for 24, 48 and 72 hrs. Untreated cells (UT) were used as a control. Apoptotis was measured by Annexin V/PI staining and FACS sorting as described in Methods, and the percentage of early and late apoptotic cells calculated. All experiments were performed with triplicate cell, and three independent experiments were peformed. Data from one of three representative experiments is shown (mean ± SD, n=2). Data in inset show statistical significance at *= $P< 0.05$; **= $P< 0.01$ and ***= $P< 0.001$ for $CD44^{+}/CD24^{-}$ vs. other respective populations.

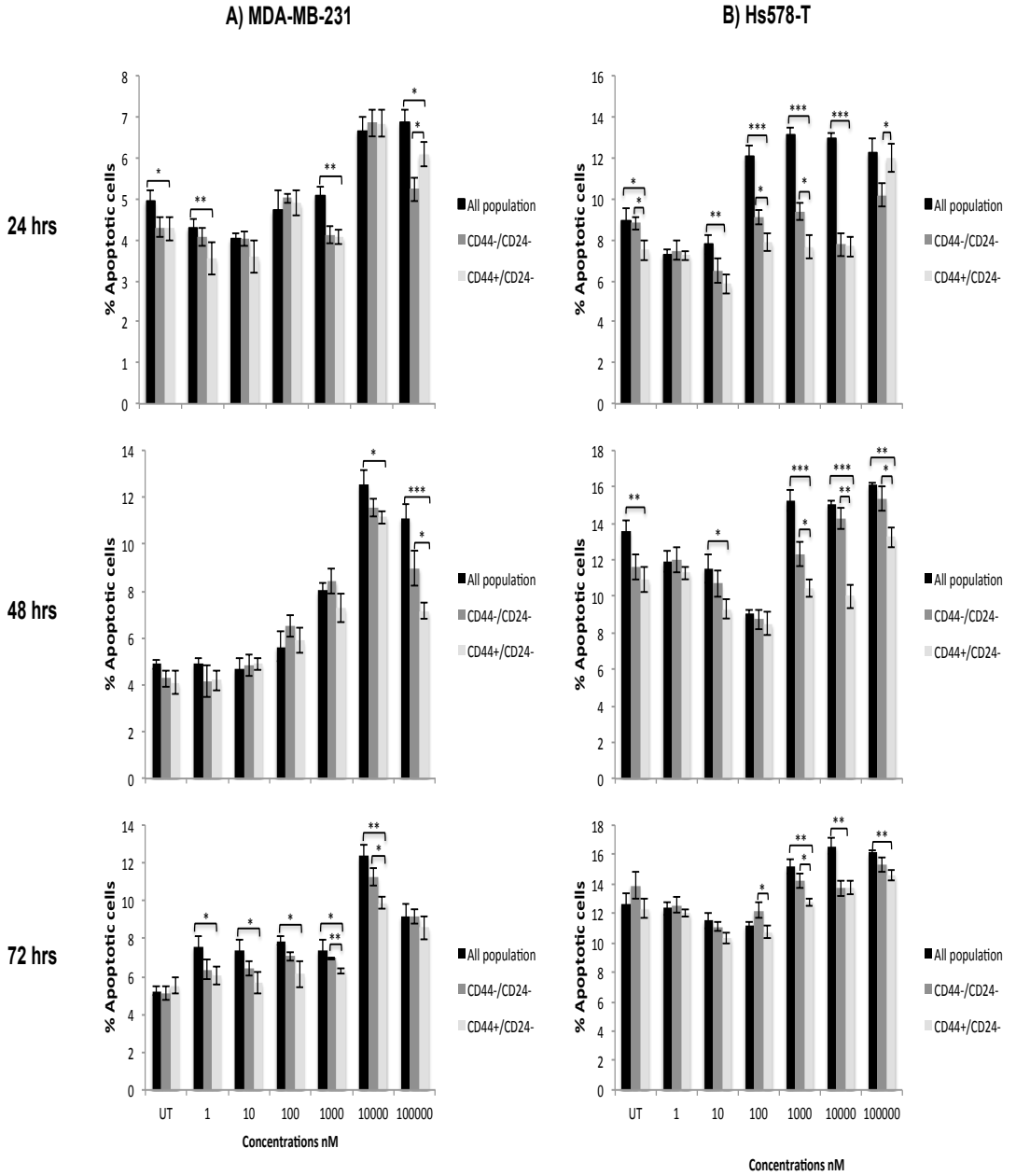

Appendix 2.3 Comparison of chemosensitivity of MDA-MB-231 and Hs578-T unsorted and sorted cells at various concentrations of Tamoxifen. (A) MDA-MB-231 and (B) Hs578-T unsorted and FACS sorted cells were exposed to Tam at increasing concentrations (1, 10, 100, 1000, 10,000, 100,000 nM) for 24, 48 and 72 hrs. Untreated cells (UT) were used as a control. Apoptotis was measured by Annexin V/PI staining and FACS sorting as described in Methods, and the percentage of apoptotic cells calculated. All experiments were performed with triplicate cells, and three independent experiments were peformed. Data from one of three representative experiments is shown (mean ± SD, n=2). Data in inset show statistical significance at *= $P< 0.05$; **= $P< 0.01$ and ***= $P< 0.001$ for $CD44^{+}/CD24^{-}$ vs. other respective populations.

Appendix 3: Flow cytometry data

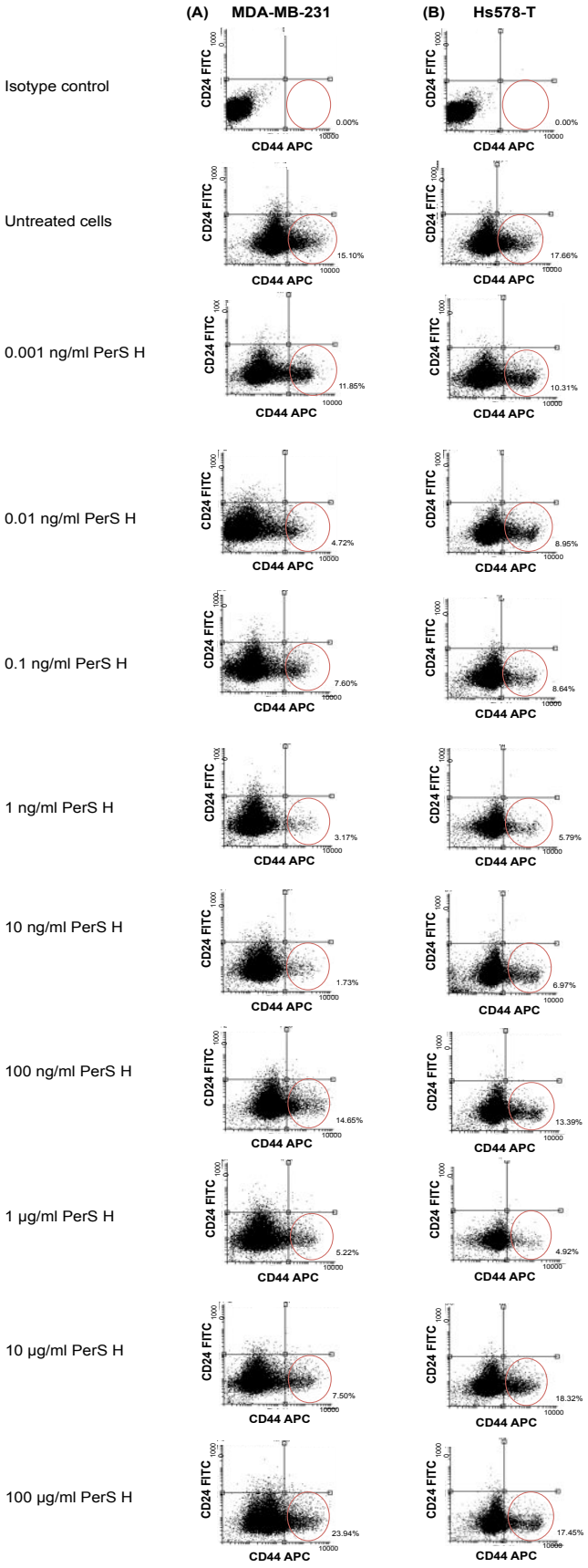

Appendix 3.1 Treatment with porcine mucosal compound 1 (PerS H) reduces the $CD44^+/CD24^-$ subpopulation in BCC lines. Following 48 hrs treatment with perS H at various concentrations, flow cytometry was used to measure the $CD44^+/CD24^-$ subpopulation. MDA-MB-231 (A) and Hs578-T (B) cell lines were maintained in DMEM supplemented with 10% FBS, 10µg/ml insulin, 0.5 µg/ml hydrocortisone and 2 mmol/l L-glutamine, in a humidified atmosphere containing 5% CO_2 at 37°C. Cells were treated with 1, 10, 100 ng/ml, 1,10, 100 µg/ml of PerS H for 48 hrs. 10^5 single-cell suspensions of MDA-MB-231 and Hs578-T were double stained with anti-human CD44 and CD24. Cells in red region corresponding to $CD44^+/CD24^-$ Isotype controls corresponding to MD-MB-231 and Hs578-T cells are shown. Representative data from one of four experiments are shown.

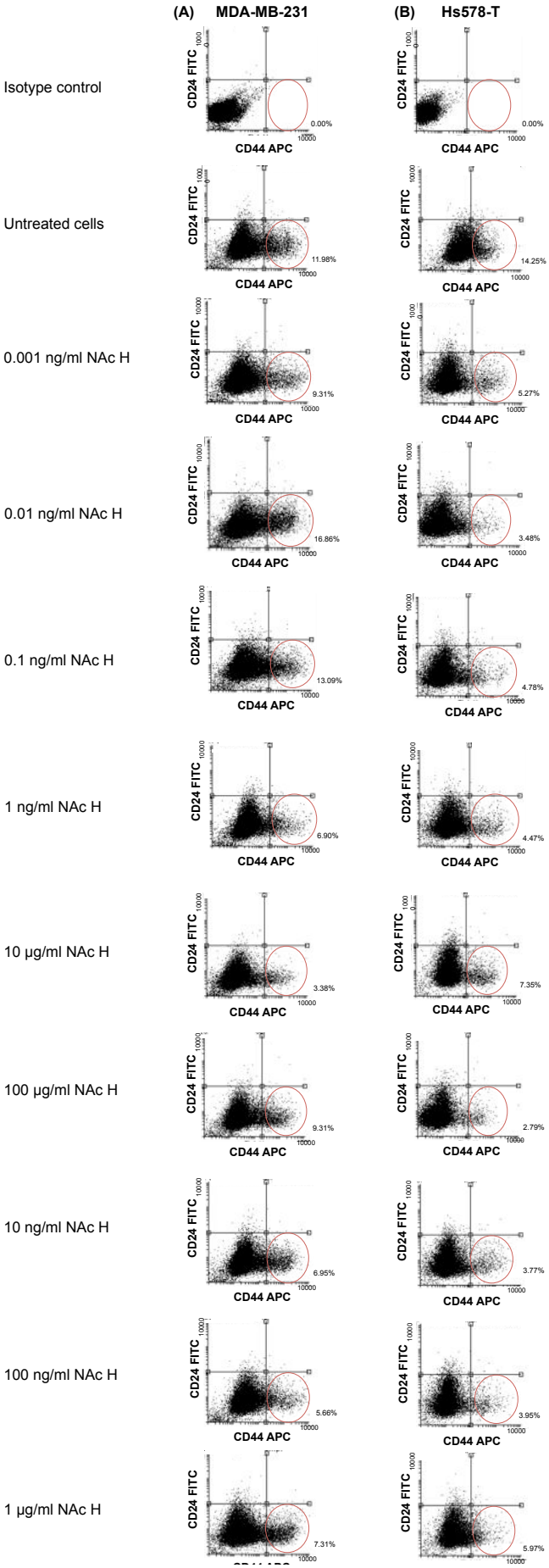

Appendix 3.2 Treatment with compound 2 (NAc H) reduces the $CD44^+/CD24^-$ subpopulation in BCC lines. Following 48 hrs treatment with NAc H at various concentrations, flow cytometry was used to measure the $CD44^+/CD24^-$ subpopulation. MDA-MB-231 (A) and Hs578-T (B) cell lines were maintained in DMEM supplemented with 10% FBS, 10µg/ml insulin, 0.5 µg/ml hydrocortisone and 2 mmol/l L-glutamine, in a humidified atmosphere containing 5% CO_2 at 37°C. Cells were treated with 1, 10, 100 ng/ml, 1,10, 100 µg/ml of NAc H for 48 hrs. 10^5 single-cell suspensions of MDA-MB-231 and Hs578-T were double stained with anti-human CD44 and CD24. Cells in red region corresponding to $CD44^+/CD24^-$ Isotype controls corresponding to MD-MB-231 and Hs578-T cells are shown. Representative data from one of four experiments are shown.

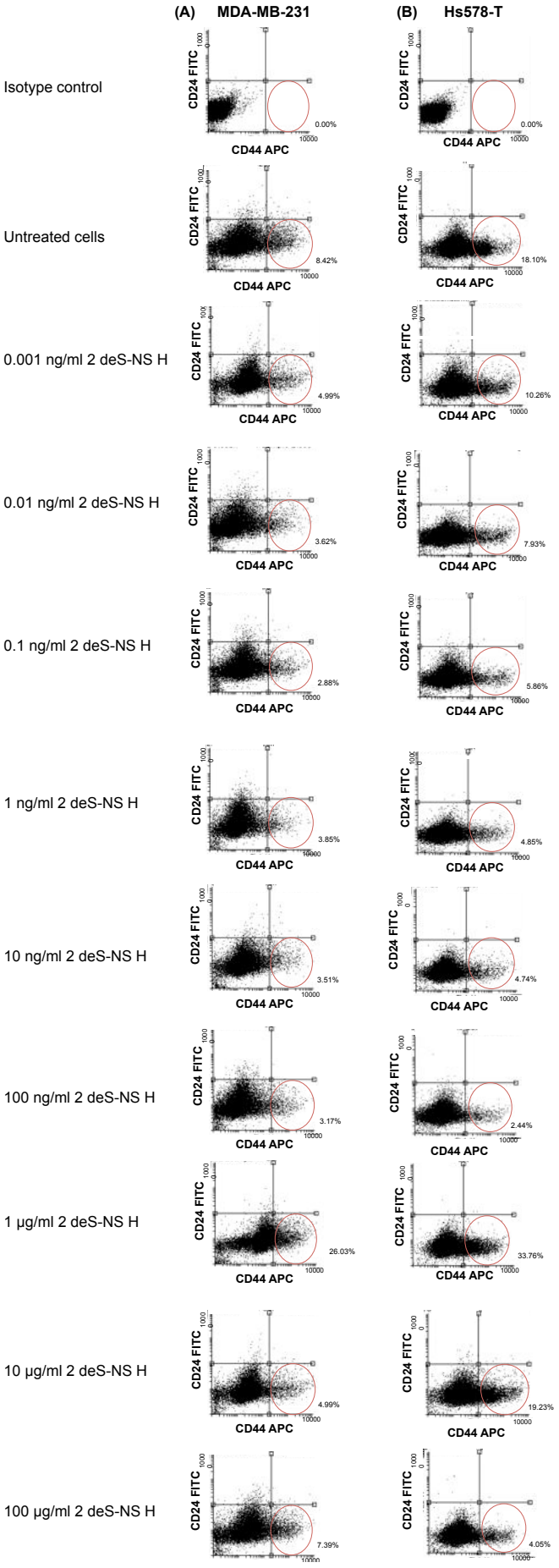

Appendix 3.3 Treatment with compound 3 (2 deS-NS H) reduces the $CD44^+/CD24^-$ subpopulation in BCC lines. Following 48 hrs treatment with 2 deS-NS H at various concentrations, flow cytometry was used to measure the $CD44^+/CD24^-$ subpopulation. MDA-MB-231 (A) and Hs578-T (B) cell lines were maintained in DMEM supplemented with 10% FBS, 10µg/ml insulin, 0.5 µg/ml hydrocortisone and 2 mmol/l L-glutamine, in a humidified atmosphere containing 5% CO_2 at 37°C. Cells were treated with 1, 10, 100 ng/ml, 1,10, 100 µg/ml of 2 deS-NS H for 48 hrs. 10^5 single-cell suspensions of MDA-MB-231 and Hs578-T were double stained with anti-human CD44 and CD24. Cells in red region corresponding to $CD44^+/CD24^-$ Isotype controls corresponding to MD-MB-231 and Hs578-T cells are shown. Representative data from one of four experiments are shown.

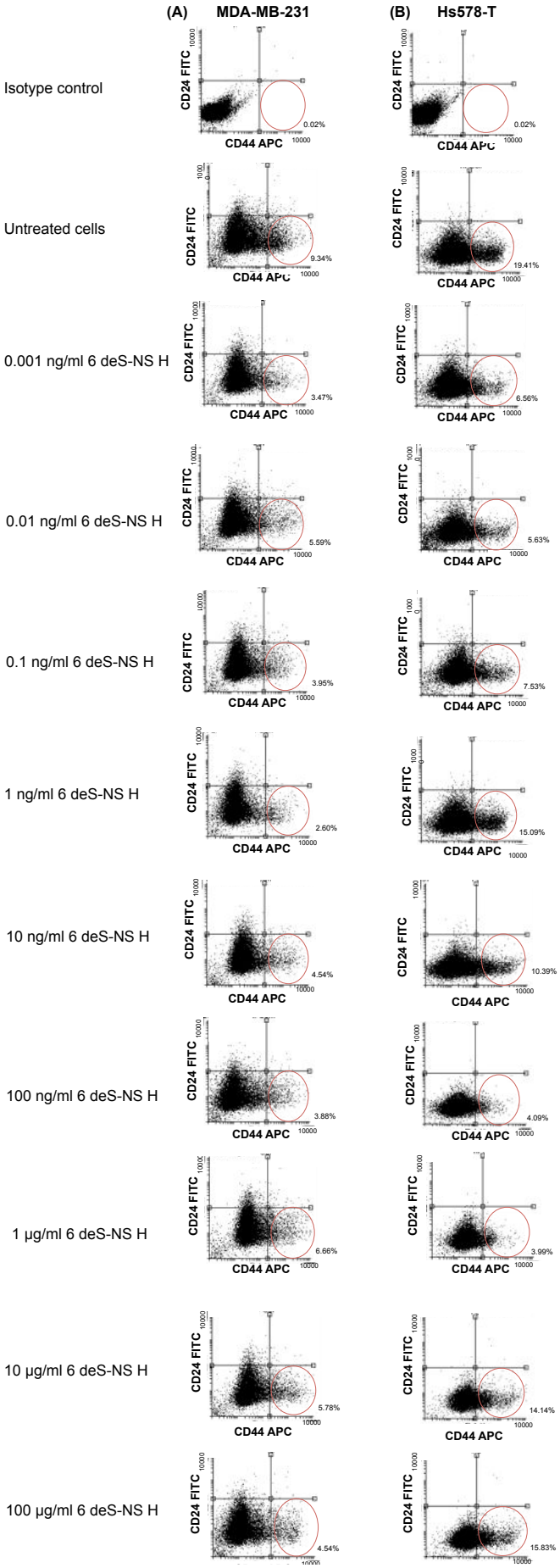

Appendix 3.4 Treatment with compound 4 (6 deS-NS H) reduces the $CD44^+/CD24^-$ subpopulation in BCC lines. Following 48 hrs treatment with 6 deS-NS H at various concentrations, flow cytometry was used to measure the $CD44^+/CD24^-$ subpopulation. MDA-MB-231 (A) and Hs578-T (B) cell lines were maintained in DMEM supplemented with 10% FBS, 10µg/ml insulin, 0.5 µg/ml hydrocortisone and 2 mmol/l L-glutamine, in a humidified atmosphere containing 5% CO_2 at 37°C. Cells were treated with 1, 10, 100 ng/ml, 1,10, 100 µg/ml of 6 deS-NS H for 48 hrs. 10^5 single-cell suspensions of MDA-MB-231 and Hs578-T were double stained with anti-human CD44 and CD24. Cells in red region corresponding to $CD44^+/CD24^-$ Isotype controls corresponding to MD-MB-231 and Hs578-T cells are shown. Representative data from one of four experiments are shown.

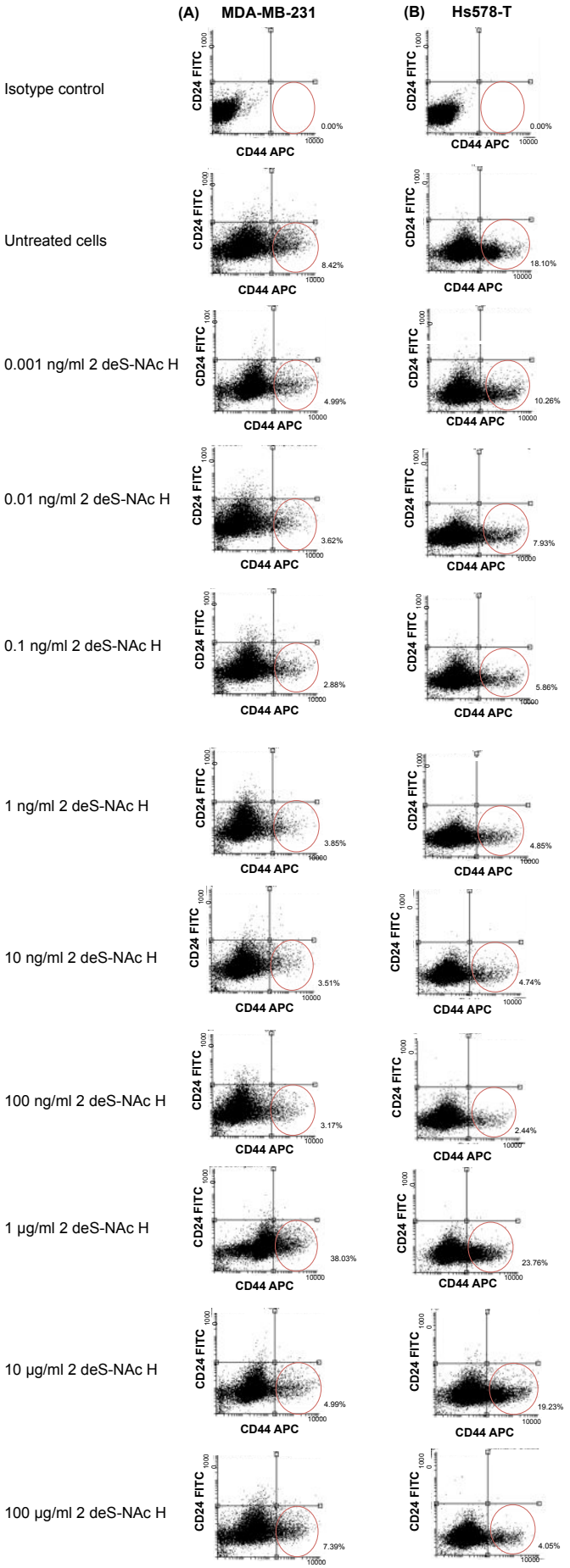

Appendix 3.5 Treatment with compound 5 (2 deS-NAc H) reduces the $CD44^+/CD24^-$ subpopulation in BCC lines. Following 48 hrs treatment with 2 deS-NAc H at various concentrations, flow cytometry was used to measure the $CD44^+/CD24^-$ subpopulation. MDA-MB-231 (A) and Hs578-T (B) cell lines were maintained in DMEM supplemented with 10% FBS, 10µg/ml insulin, 0.5 µg/ml hydrocortisone and 2 mmol/l L-glutamine, in a humidified atmosphere containing 5% CO_2 at 37°C. Cells were treated with 1, 10, 100 ng/ml, 1,10, 100 µg/ml of 2 deS-NAc H for 48 hrs. 10^5 single-cell suspensions of MDA-MB-231 and Hs578-T were double stained with anti-human CD44 and CD24. Cells in red region corresponding to $CD44^+/CD24^-$ Isotype controls corresponding to MD-MB-231 and Hs578-T cells are shown. Representative data from one of four experiments are shown.

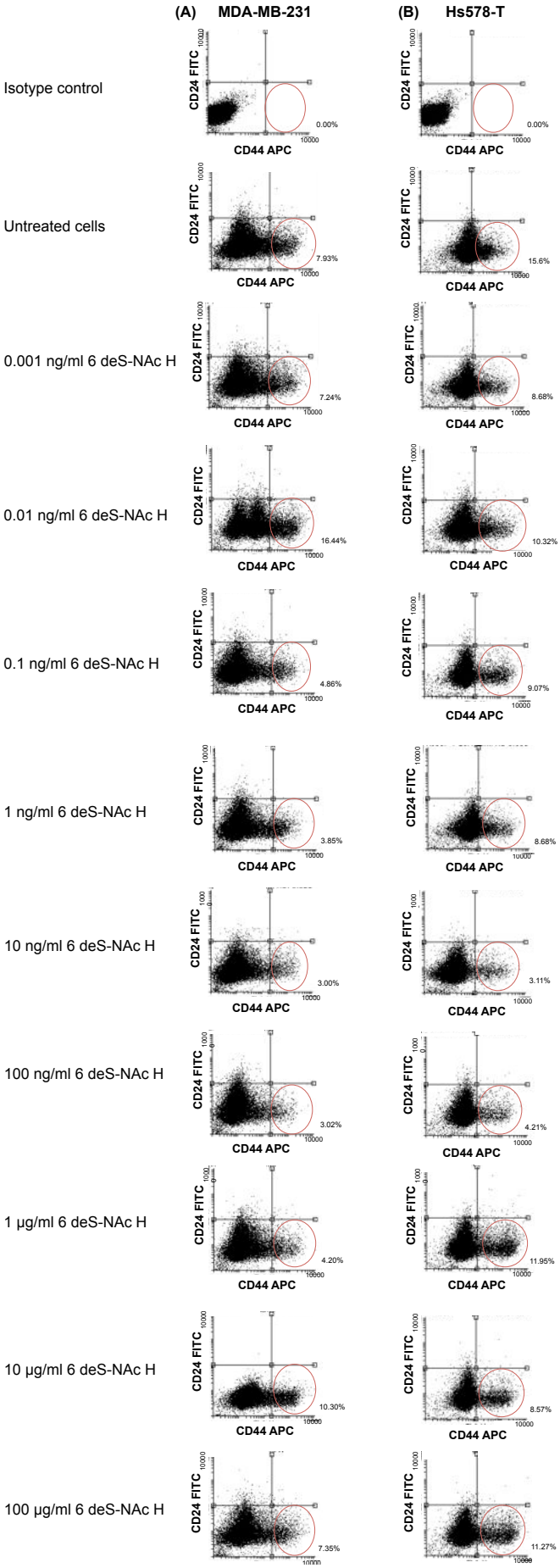

Appendix 3.6 Treatment with compound 6 (6 deS-NAc H) reduces the CD44+/CD24- subpopulation in BCC lines. Following 48 hrs treatment with 6 deS-NAc H at various concentrations, flow cytometry was used to measure the CD44+/CD24- subpopulation. MDA-MB-231 (A) and Hs578-T (B) cell lines were maintained in DMEM supplemented with 10% FBS, 10µg/ml insulin, 0.5 µg/ml hydrocortisone and 2 mmol/l L-glutamine, in a humidified atmosphere containing 5% CO2 at 37oC. Cells were treated with 1, 10, 100 ng/ml, 1,10, 100 µg/ml of 6 deS-NAc H for 48 hrs. 105 single-cell suspensions of MDA-MB-231 and Hs578-T were double stained with anti-human CD44 and CD24. Cells in red region corresponding to CD44+/CD24- Isotype controls corresponding to MD-MB-231 and Hs578-T cells are shown. Representative data from one of four experiments are shown.

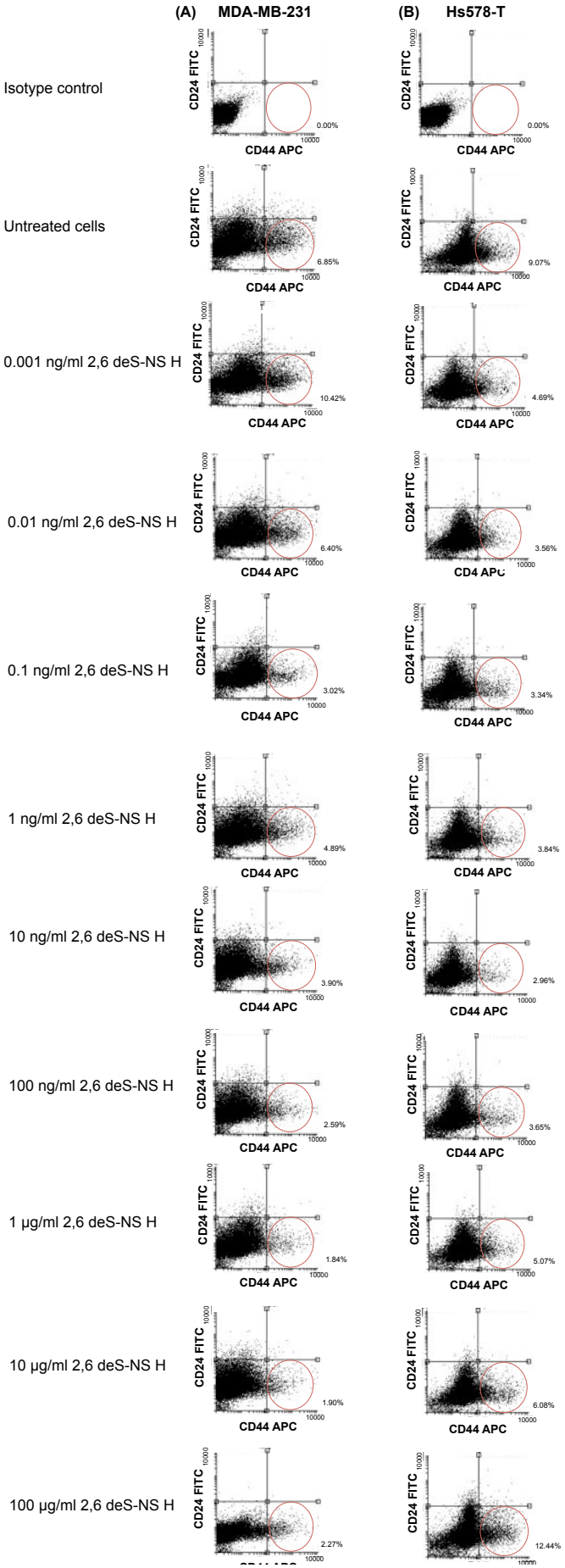

Appendix 3.7 Treatment with compound 7 (2,6 deS-NS H) reduces the $CD44^+/CD24^-$ subpopulation in BCC lines. Following 48 hrs treatment with 2,6 deS-NS H at various concentrations, flow cytometry was used to measure the $CD44^+/CD24^-$ subpopulation. MDA-MB-231 (A) and Hs578-T (B) cell lines were maintained in DMEM supplemented with 10% FBS, 10µg/ml insulin, 0.5 µg/ml hydrocortisone and 2 mmol/l L-glutamine, in a humidified atmosphere containing 5% CO_2 at 37°C. Cells were treated with 1, 10, 100 ng/ml, 1,10, 100 µg/ml of 2,6 deS-NS H for 48 hrs. 10^5 single-cell suspensions of MDA-MB-231 and Hs578-T were double stained with anti-human CD44 and CD24. Cells in red region corresponding to $CD44^+/CD24^-$ Isotype controls corresponding to MD-MB-231 and Hs578-T cells are shown. Representative data from one of four experiments are shown.

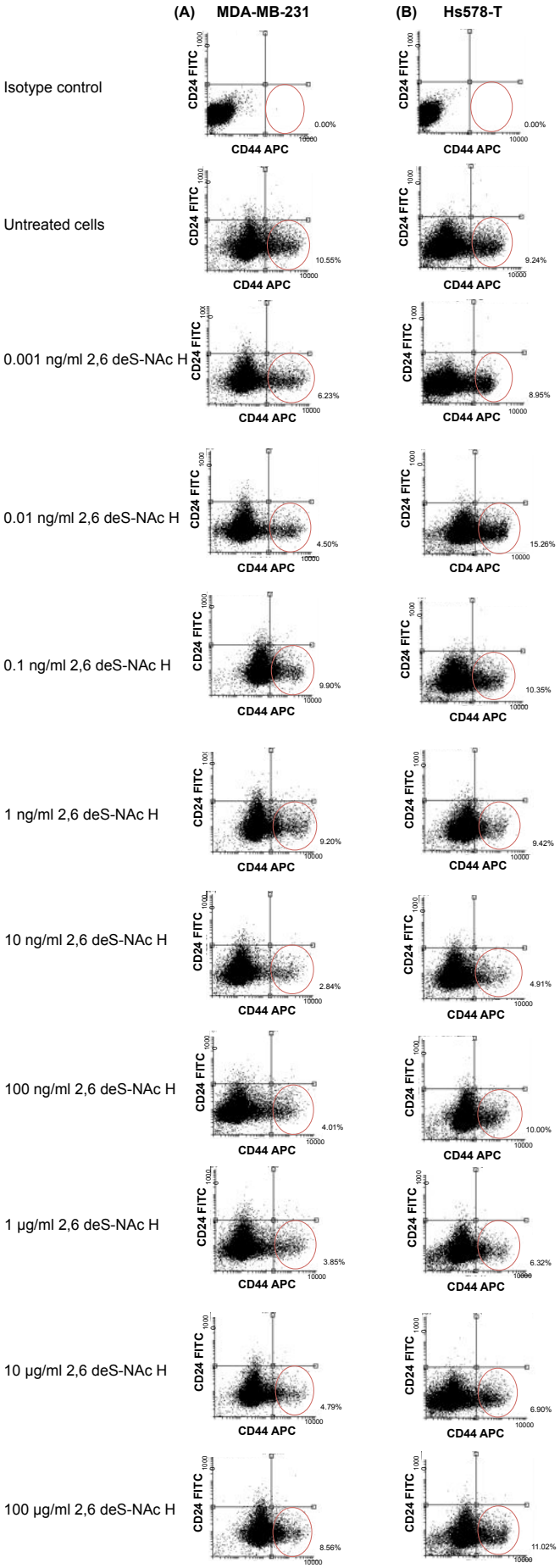

Appendix 3.8 Treatment with compound 8 (2,6 deS-NAc H) reduces the $CD44^+/CD24^-$ subpopulation in BCC lines. Following 48 hrs treatment with 2,6 deS-NAc H at various concentrations, flow cytometry was used to measure the $CD44^+/CD24^-$ subpopulation. MDA-MB-231 (A) and Hs578-T (B) cell lines were maintained in DMEM supplemented with 10% FBS, 10µg/ml insulin, 0.5 µg/ml hydrocortisone and 2 mmol/l L-glutamine, in a humidified atmosphere containing 5% CO_2 at 37°C. Cells were treated with 1, 10, 100 ng/ml, 1,10, 100 µg/ml of 2,6 deS-NAc H for 48 hrs. 10^5 single-cell suspensions of MDA-MB-231 and Hs578-T were double stained with anti-human CD44 and CD24. Cells in red region corresponding to $CD44^+/CD24^-$ Isotype controls corresponding to MD-MB-231 and Hs578-T cells are shown. Representative data from one of four experiments are shown.

Appendix 4: PathScan analysis data

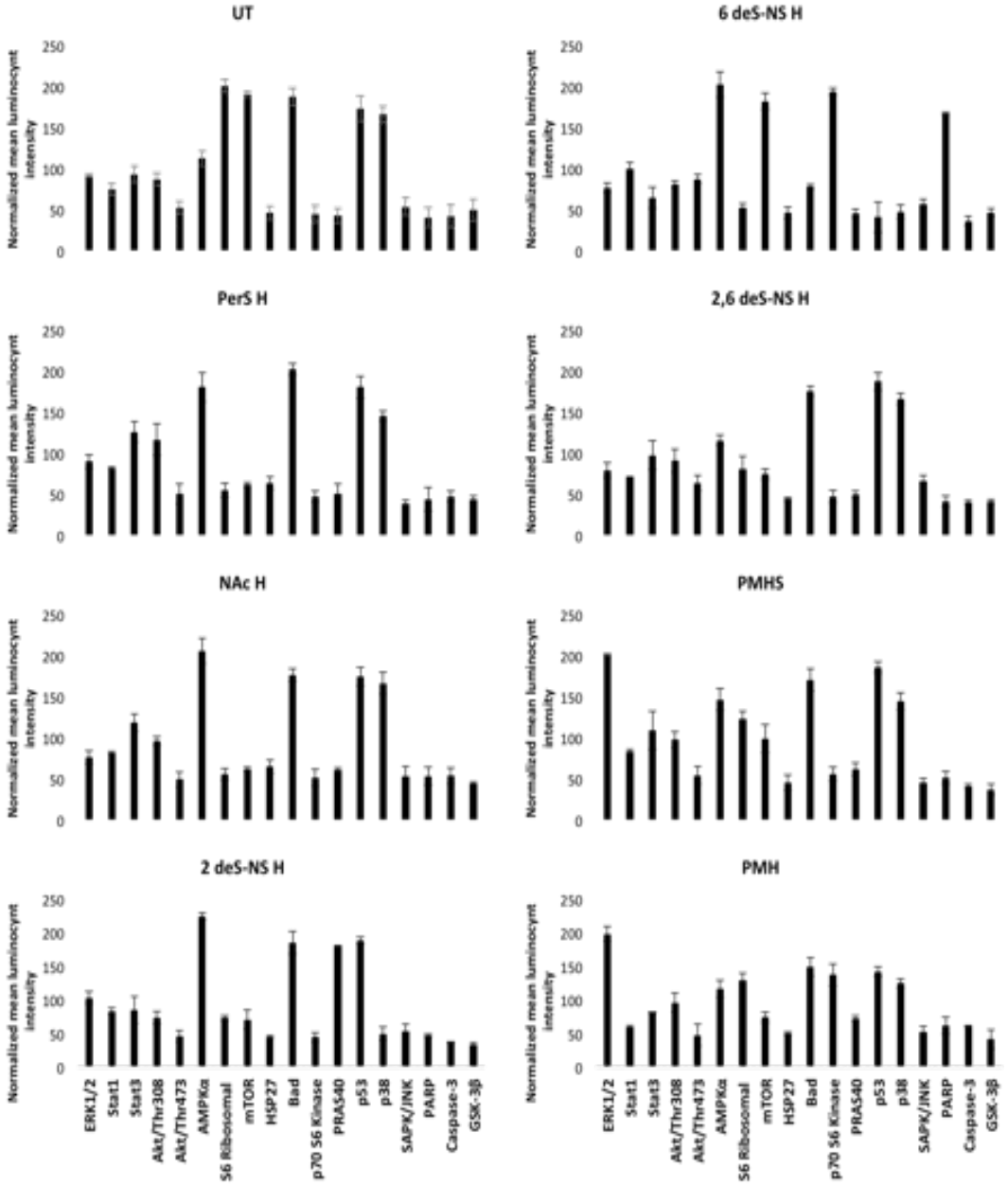

Appendix 4.1 Screening of the phosphorylation of 18 key signaling molecules in CD44^{+}/CD24^{-} sorted cells from MDA-MB-231 BCCs using the PathScan intracellular signaling array. Cells were treated or not with 10 ng/ml of HS derivatives (PerS H, NAc H, 2 deS-NS H, 6 deS-NS H, 2,6 deS-NS H, PMHS and PMH for 48 hrs. Following treatments, cell extracts were prepared and analyzed using the PathScan® intracellular signalling array kit. Treatments revealed changes in the status of various phosphorylated and signaling molecules. The results are representative of two experiments, each run in duplicate. Normalized mean luminescence intensity ± SD.

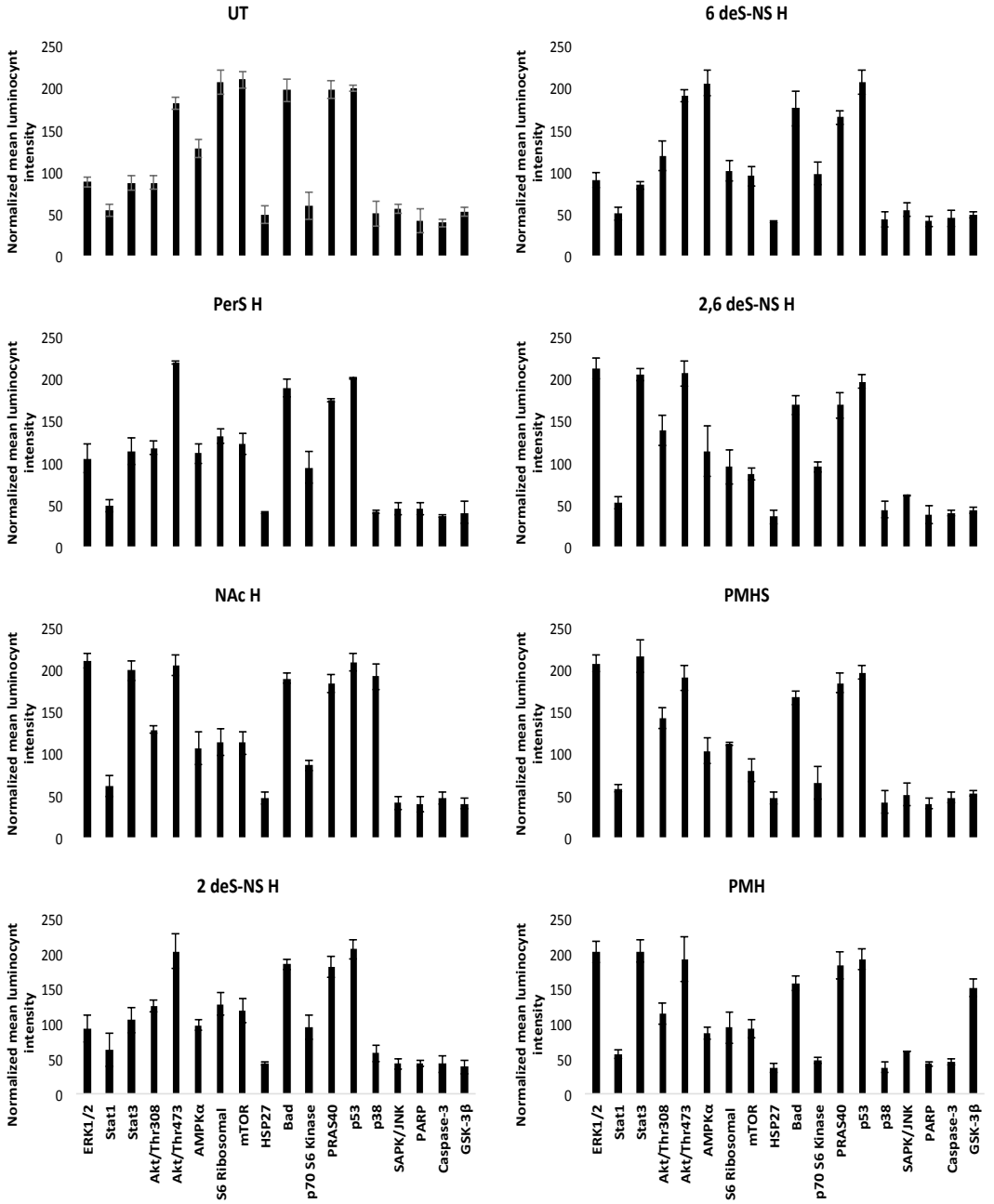

Appendix 4.2 Screening of the phosphorylation of 18 key signaling molecules in CD44^{+}/CD24^{-} sorted cells from Hs578-T BCCs using the PathScan intracellular signaling array. Cells were treated or not with 10 ng/ml of HS derivatives (PerS H, NAc H, 2 deS-NS H, 6 deS-NS H, 2,6 deS-NS H, PMHS and PMH for 48 hrs. Following treatments, cell extracts were prepared and analyzed using the PathScan® intracellular signalling array kit. Treatments revealed changes in the status of various phosphorylated and signaling molecules. The results are representative of two experiments, each run in duplicate. Normalized mean luminescence intensity ± SD.

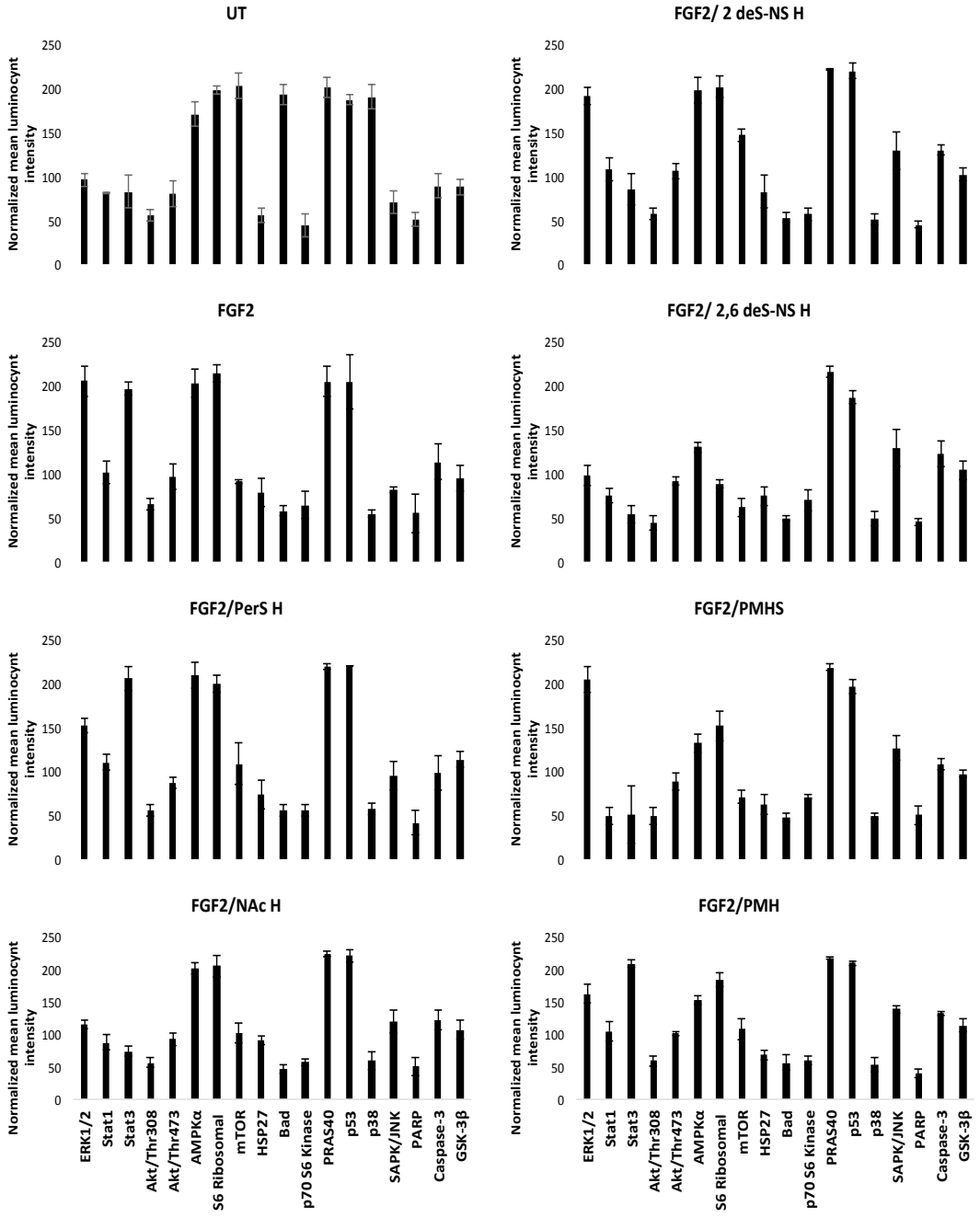

Appendix 4.3 Screening of the phosphorylation of 18 key signaling molecules using the PathScan intracellular signaling array studying the effect of FGF-2/HS or heparin derivatives on CD44^{+}/CD24^{-} sorted cells from MDA-MB-231 BCCs. Cells were stimulated with 20 ng/ml FGF2 and treated or not with 10 ng/ml of HS derivatives (PerS H, NAc H, 2 deS-NS H, 6 deS-NS H, 2,6 deS-NS H, PMHS and PMH) for 60 min. Following treatments, cell extracts were prepared and analyzed using the PathScan® intracellular signalling array kit. Treatments revealed changes in the status of various phosphorylated and signaling molecules. The results are representative of two experiments, each run in duplicate. Normalized mean luminescence intensity ± SD.

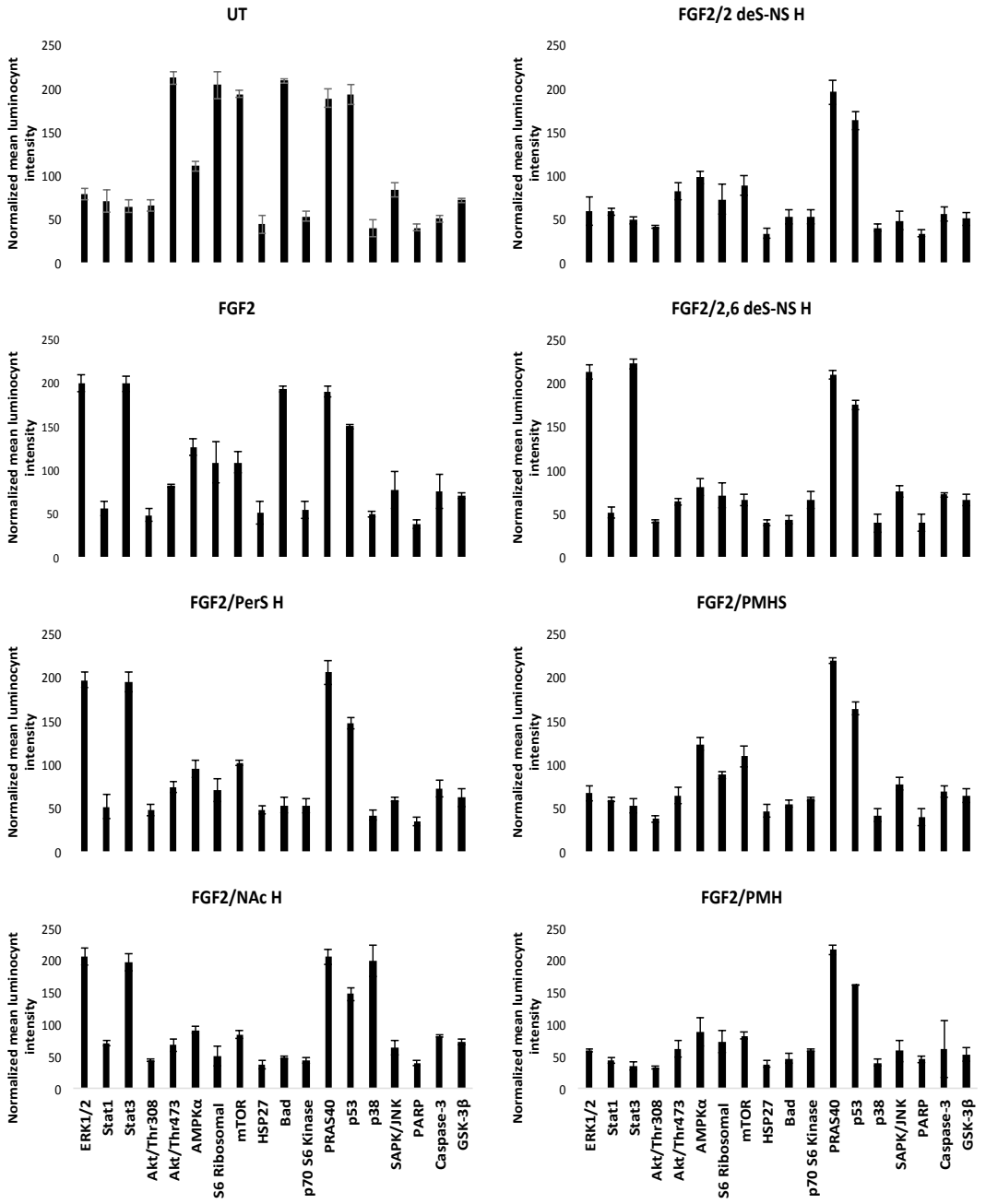

Appendix 4.4 Screening of the phosphorylation of 18 key signaling molecules using the PathScan intracellular signaling array studying the effect of FGF-2/HS or heparin derivatives on CD44^{+}/CD24^{-} sorted cells from Hs578-T BCCs. Cells were stimulated with 20 ng/ml FGF2 and treated or not with 10 ng/ml of HS derivatives (PerS H, NAc H, 2 deS-NS H, 6 deS-NS H, 2,6 deS-NS H, PMHS and PMH) for 60 min. Following treatments, cell extracts were prepared and analyzed using the PathScan® intracellular signalling array kit. Treatments revealed changes in the status of various phosphorylated and signaling molecules. The results are representative of two experiments, each run in duplicate. Normalized mean luminescence intensity ± SD.